69TH FIELD CONFERENCE OF PENNSYLVANIA GEOLOGISTS

Marginalia—Magmatic Arcs and Continental Margins in Delaware and southeastern Pennsylvania

Hosts: Pennsylvania Geological Survey
Delaware Geological Survey
West Chester University

October 7-9, 2004
West Chester, PA

LEGEND

Silurian

- Arden Plutonic Supersuite

Ordovician - Silurian

- Wilmington Complex - Barley Mill Gneiss
- Wilmington Complex - Brandywine Blue Gneiss
- Wilmington Complex - Bringhurst Gabbro
- Wilmington Complex - Christianstead Gneiss
- Wilmington Complex - Faulkland Gneiss
- Wilmington Complex - Iron Hill Gabbro
- Wilmington Complex - Mill Creek Metagabbro
- Wilmington Complex - Montchanin Metagabbro
- Wilmington Complex - Rockford Park Gneiss
- Wilmington Complex - Windy Hills Gneiss
- Wilmington Complex - Confluence Gneiss
- Lima granite

Unknown Age

- pegmatite
- ultramafic rock

Late Proterozoic - Ordovician

- Vintage through Conestoga Formations, undivided
- Antietam and Harpers Formations, undivided
- Chickies Formation
- Octoraro Formation
- Octoraro phyllonite
- Peters Creek Schist
- Peters Creek tectonite
- Peters Creek Schist - variably tectonized
- Chester Park Gneiss
- Type Wissahickon
- Mt. Cuba Wissahickon
- "Glenarm Wissahickon" - Greystone member
- "Glenarm Wissahickon" - Laurels schist
- "Glenarm Wissahickon" - Doe Run schist
- Cockeysville Marble
- Setters Formation
- Setters Formation quartzite
- Setters Formation microcline gneiss
- Baltimore Gneiss - amphibolite grade
- Baltimore Gneiss - granulite grade
- mafic and felsic gneiss
- Kennett Square Amphibolite
- White Clay Creek Amphibolite
- amphibolite (affinity unknown)
- marble
- microcline gneiss

Faults accepted by all field trip leaders

- thrust fault
- high angle fault
- brittle fault

Thrust faults required by Plank and Schenck; disallowed by Blackmer model

Western limit of arc magmatism - a boundary here is favored by Blackmer and Bosbyshell; not drawn by Plank and Schenck

Field Trip Stop (HQ - Field Trip Headquarters)

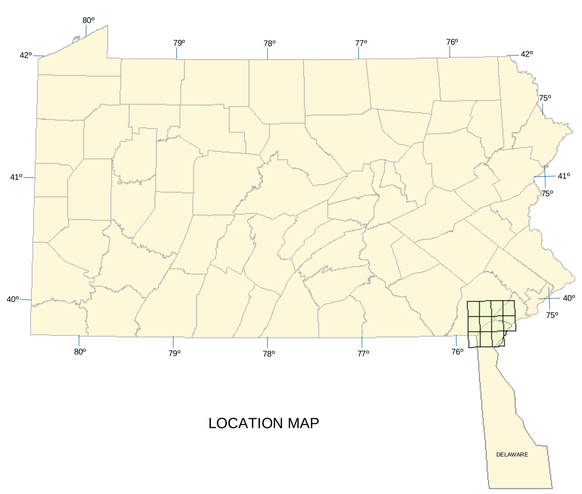

LOCATION MAP

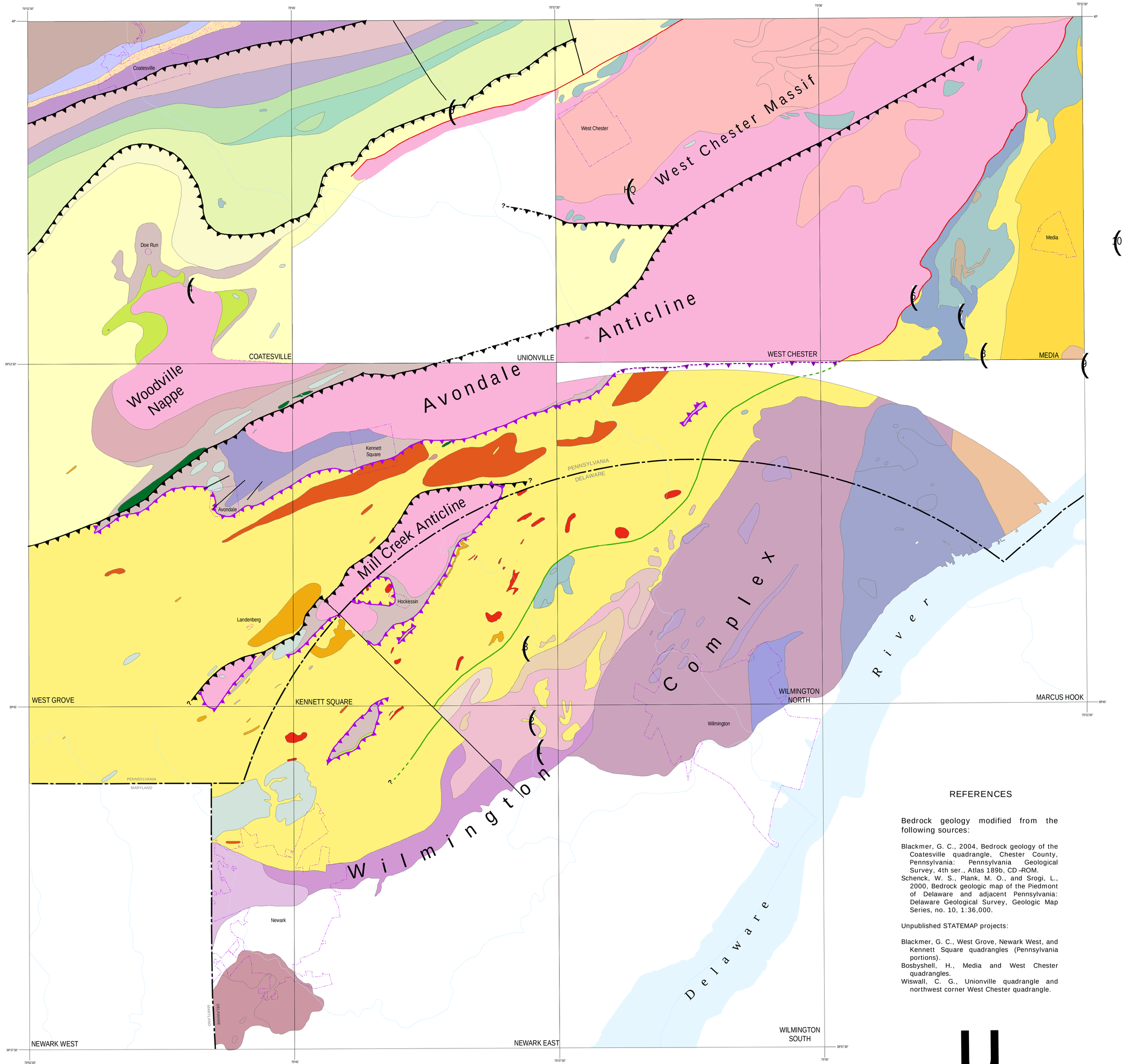

DEPARTMENT OF GEOLOGY AND ASTRONOMY

BEDROCK GEOLOGIC MAP OF SOUTHEASTERN PENNSYLVANIA AND NORTHERN DELAWARE

Compiled by Gale C. Blackmer

Field Conference of Pennsylvania Geologists
October 7-9, 2004

REFERENCES

Bedrock geology modified from the following sources:

Blackmer, G. C., 2004, Bedrock geology of the Coatesville quadrangle, Chester County, Pennsylvania: Pennsylvania Geological Survey, 4th ser., Atlas 189b, CD-ROM.

Schenck, W. S., Plank, M. O., and Srogi, L., 2000, Bedrock geologic map of the Piedmont of Delaware and adjacent Pennsylvania: Delaware Geological Survey, Geologic Map Series, no. 10, 1:36,000.

Unpublished STATEMAP projects:

Blackmer, G. C., West Grove, Newark West, and Kennett Square quadrangles (Pennsylvania portions).

Bosbyshell, H., Media and West Chester quadrangles.

Wiswall, C. G., Unionville quadrangle and northwest corner West Chester quadrangle.

SCALE 1:62,500

UNIVERSAL TRANSVERSE MERCATOR PROJECTION
ZONE 18
1927 NORTH AMERICAN DATUM

1 0 1 2 3 MILES

1 0 1 2 3 4 5 KILOMETERS

Guidebook for the
69TH ANNUAL FIELD CONFERENCE OF PENNSYLVANIA GEOLOGISTS

MARGINALIA – MAGMATIC ARCS AND CONTINENTAL MARGINS IN DELAWARE AND SOUTHEASTERN PENNSYLVANIA

Organizer:
Gale C. Blackmer, Pennsylvania Geological Survey
Editors:
Gale C. Blackmer
LeeAnn Srogi, West Chester University
Field Trip Leaders:
Gale C. Blackmer
Howell Bosbyshell, West Chester University
Margaret O. Plank, Delaware Geological Survey
William S. Schenck, Delaware Geological Survey
C. Gil Wiswall, West Chester University
Additional Contributors:
John H. Barnes, Pennsylvania Geological Survey
Robert C. Smith, II, Pennsylvania Geological Survey

October 7-9, 2004

Hosts: Pennsylvania Geological Survey, Delaware Geological Survey, West Chester University

Headquarters: Holiday Inn, West Chester, PA

Cover: Landscape between Upland and Doe Run, Chester County, Pa. (photo by Gale Blackmer).
Insets: Doe Run schist of the "Glenarm Wissahickon" from an outcrop north of Rt. 82 near Stop 4 (photo by Gale Blackmer); Mt. Cuba Wissahickon from a construction site southeast of Landenberg near the Delaware state line (photo by Gale Blackmer); Type Wissahickon from the type locality along Wissahickon Creek in Philadelphia (photo by Maria Luisa Crawford).

Guidebooks distributed by: Field Conference of Pennsylvania Geologists, Inc.
3240 Schoolhouse Road
Middletown, PA 17057

Frontispiece. Group photo of the 2003 Field Conference of Pennsylvania Geologists at Chimney Rocks Municipal Park (Stop 3)

TABLE OF CONTENTS

page

Frontispiece. 2003 Field Conference of Pennsylvania Geologists group photo
102 years of Wissahickon – An introduction to the 69th Field Conference of Pennsylvania Geologists 1
Marginalia: A tectonic fantasy in five acts 6
The Wissahickon Formation in Delaware 9
Speculation on the tectonic history of the Glenarm Group and associated parts of the Wissahickon Formation 15
White Clay Creek Amphibolite: A Piedmont analog of the Catoctin Metabasalt 28
Bald Friar Metabasalt and Kennett Square Amphibolite: Two Iapetan ocean floor basalts 46
Road Log and Stop Descriptions 70
Day 1
STOP 1. Arc amphibolites southeast of Greenbank Station 71
STOP 2. Mt. Cuba Wissahickon metasediments within the arc at Red Clay Creek and Brandywine Springs Park 73
STOP 3. Wooddale Quarry 75
STOP 4. Fat Chance Farm marble quarry 77
STOP 5. Doe Run schist of the "Glenarm Wissahickon" 80
Day 2
Introduction to Day Two 82
STOP 6. Rosemont shear zone; SEPTA railroad cut, Lenni 90
STOP 7. Confluence Gneiss at Novotni Brothers Paving Company 95
STOP 8. Arc Wissahickon at Pyramid Materials 102
STOP 9. Chester Park Gneiss in Chester Park 108
STOP 10. Wissahickon Formation in Smedley Park 111

List of Illustrations

Inside front cover. Bedrock geologic map of southeastern Pennsylvania and northern Delaware
Figure 1. Bedrock geologic map of potions of the Coatesville, West Grove, Newark West, and Kennett Square 7.5 minute quadrangles 16
2. Equal area plot of 164 poles to S2 17
3. Geologic map of the Woodville Nappe and surrounding area 18
4. Total alkalis v. silica plot of Setters microcline gneiss samples 21
5. Rare earth element patterns for Setters microcline gneiss samples 21
6. Geochemical analyses of Setters microcline gneiss compared to Tibbit Hill trachyte ... 22
7. Geochemical analyses of Setters microcline gneiss compared to potassium-metasomatized tuffs 23
8. Geochemical analyses of Setters microcline gneiss compared to potassium-metasomatized arkose 24
9. Map showing distribution of mafic units by population grouping 30
10. Plots of data from three similar continental initial-rifting tholeiites 34
11. Catoctin Metabasalt compared to the similar combined Sams Creek Metabasalt 39
12. Plots for four groupings of Catoctin Metabasalt *sensu lato* 40
13. Photographs of a slice of an isolated pillow from Bald Friar Metabasalt 47
14. Trace element plots for Bald Friar Metabasalt and Kennett Square Amphibolite 53
15. Amphibolite outcrops along the Wilmington and Western tracks 71
16. Rare earth element and spider diagrams for the Windy Hills and Faulkland gneisses ... 72

17. Felsic gneiss with cummingtonite along the Wilmington and Western tracks 73
18. Outcrop of Mt. Cuba Wissahickon metasediments within the Faulkland Gneiss 74
19. Photographs show back wall of Wooddale Quarry 75
20. Upright folds of amphibolite in the back wall of Wooddale Quarry 76
21. Lime kiln and small marble outcrop near quaary at Stop 4 78
22. Close-up view of the contact of marble and quartzite 79
23. Quartzite-marble contact in the north quarry wall 79
24. Pressure-temperature-deformation-time paths for the Wissahickon Formation 83
25. Schematic representation of deformation and metamorphism in the Wissahickon Formation 84
26. Geologic shaded-relief map of the area near the Rosemont shear zone 90
27. Back scattered electron image of syn-tectonic garnet neoblast in mylonite 91
28. Ca X-ray composition maps and compositional zoning profiles of Wissahickon Formation garnet in the Rosemont shear zone 92
29. Results of thermobarometry near the Rosemont Fault 93
30. Electron microprobe chemical age results for Wissahickon Formation mylonite 94
31. Monazite from pelitic mylonite 94
32. Geologic map showing location of Stops 7 and 7A 95
33. Trace element and igneous rock classification diagrams for rocks from the study area 96
34. REE, trace element, and incompatible/compatible element ratios for boninitic rocks... 97
35. Sketch of possible style of refolding of folds at Stop 7 98
36. Sketch of shear zones in northeast facing quarry wall 99
37. Equal area plots of structural elements at Stop 6 99
38. Photomicrograph of mylonitic rock in shear zone 99
39. Sketch map of first outcrop at Virtual Stop 7A 100
40. Sketch map of second series of outcrops a Stop 7A 100
41. Photograph and sketch of Wissahickon Formation outcrop at King's Mill 101
42. Geologic map showing location of Stop 8 102
43. X-ray composition maps and zoning profiles from garnet in sample from Stop 8 103
44. Estimates of M2 conditions 104
45. TWEEQU 2.02 plot for sample 1303 for the M2 assemblage garnet + biotite + sillimanite + plagioclase + quartz + orthoclase 105
46. Field sketch of refolded F2 isocline showing relationships between different generations of foliation 105
47. Photographs of F3 folds 106
48. Photomicrograph of mm- cm-scale F3 folds of S2, Chester Creek 106
49. Photomicrograph illustrating relative timing of kyanite growth and F3 folding 106
50. Geologic map showing location of Stop 9 108
51. Photographs of Chester Park Gneiss showing inclusions 108
52. Geologic map of Smedley Park showing location of outcrops 110
53. Geochemical classification of Smedley Park Amphibolite 112
54. REE and trace element diagrams comparing Smedley Park amphibolite with back arc basin basalt 112
55. Isograd map of the Crum Creek area, showing andalusite locations 113
56. X-ray composition maps of garnet from samples B22 and KP57 114
57. X-ray composition maps of monazite from sample B22 114
58. Microfiche image of sample B22, Crum Creek 116
59. π-diagram of poles to S5, Crum Creek transect 117

60. Photomicrograph of sample from Smedley Park …….. 117

List of Tables

Table 1. Chemical analyses of Setters Formation microcline gneiss ……. 6
2. Stratigraphic description of the White Clay Creek Amphibolite (WCCA) type section .. 32
3. Medians of selected Trace elements in the White Clay Creek Amphibolite and correlative Catoctin Metabasalt *sensu stricto* analogs ……... 36
4. Selected trace element data to compare with that for the Catoctin Metabasalt *sensu lato* ……. 37
5. Nd isotopic analyses of Catoctin Metabasalt *sensu lato* and Neoproterozoic metabasalt from the Reading Prong ……... 38
6. Apparent stratigraphic section including Bald Friar Metabasalt, Morgan Run Arm, Liberty Reservoir, Maryland ……. 49
7. Medians for selected trace elements in the Bald Friar Metabasalt, Caldwell Group 1b pillow basalts, Liberty Reservoir amphibolites, and Kennett Square Amphibolites .. 50

Appendices

Appendix I. Table 1. Major, minor, and trace element analyses for metabasalt, metadiabase, and amphibolite populations discussed in this report …….. 56
Table 2. Data to assess the precision and accuracy of data in Smith (this volume) and Smith and Barnes (this volume) ……... 68
Appendix II. Explanation of abbreviations and selected terms used in Smith and Barnes (this volume) and Smith (this volume) ……... 69

102 YEARS OF WISSAHICKON – AN INTRODUCTION TO THE 69TH FIELD CONFERENCE OF PENNSYLVANIA GEOLOGISTS

by
Gale C. Blackmer

One look at an outcrop of the Wissahickon Formation tells even the most casual observer that these rocks have had a long and complicated history. The term "Wissahickon Formation" has a history which, although much shorter, is no less complicated than that of the rocks it is used to define. This article is an attempt to summarize how the definition of the Wissahickon Formation as a rock unit has changed over the past 100 years and to provide a preview of the current ideas of the leaders of this Field Conference.

THE FIRST 90 (OR SO) YEARS

The name "Wissahickon gneiss" was first used by Florence Bascom (1902) as a provisional name for the mica gneiss exposed along Wissahickon Creek in Philadelphia. The context for the first use of the name of these Pennsylvania rocks is as a correlative to the mica-gneiss of Cecil County, Maryland. Thus, by default, the unit is originally defined as extending at least from Philadelphia through Delaware and into Maryland. Bascom goes on to state that in Delaware and in Chester County, Pennsylvania (Landenberg area and Doe Run), the Wissahickon conformably overlies marble, which in turn overlies quartzite. She correlates the marble, which she calls limestone, with the Chester Valley limestones (now named Conestoga through Vintage Formations) and assigns it a Cambrian-Silurian age. Bascom also notes that the Wissahickon is in conformable contact with the rocks we now call Octoraro Formation, which she refers to as the Lower Silurian Hudson schist. Because of this stratigraphic position, she assigns a Lower Silurian age to the Wissahickon. As a first illustration of the uncertainties inherent in interpreting these rocks, Bascom also presents an alternative hypothesis: the Wissahickon and its underlying limestone and quartzite may be separated from the known Paleozoic rocks to the north by a thrust fault and could be Precambrian in age. Although she sees no evidence of such a fault, the observation that "eruptive material" is confined to the Wissahickon suggests a time break to her. She concludes with this definitive statement on the age of the Wissahickon: "It is either pre-Cambrian [sic] or Lower Silurian."

The publications of 1905 bring a few changes to the definition of the Wissahickon. Bascom (1905) defines the unit as extending from Trenton into Cecil County, Maryland, having a width of less than one mile at Trenton and expanding to more than 40 miles across at the Maryland border. Mathews (1905) notes the similarities of rocks in the Virginia Piedmont to those in Pennsylvania and Maryland, and proposes extending the Wissahickon as far as southern Virginia. Bascom makes the distinction between the mica schist of the South Valley Hills (now called Octoraro) and the mica gneiss but keeps them both in the Wissahickon. Similarly, Mathews notes the gradual transition from the western phyllite to the "more crystalline" rocks in the east and calls them all Wissahickon. Both authors have moved the age of the Wissahickon to the Ordovician. Bascom (1905) gives us the first detailed description of the Wissahickon rocks. The one sentence summary of this much longer description is "a medium to coarse-grained gneiss, characterized by an excess of mica."

Having extended the Wissahickon from New Jersey to Virginia in 1905, workers now begin to pick apart the Wissahickon. Bascom (in Bascom et al., 1909) removes the mica schist and gives it the name Octoraro. She distinguishes the two units by "the greater metamorphism of the mica gneiss as exhibited in a more coarsely crystalline texture." Because it conformably overlies the Chester

Blakcmer, G. C., 2004, 102 years of Wissahickon – An introduction to the 69th Field Conference of Pennsylvania Geologists, *in* Blackmer, G. C., and Srogi, L., Marginalia – Magmatic arcs and continental margins in Delaware and southeastern Pennsylvania: Guidebook, 69th Annual Field Conference of Pennsylvania Geologists, West Chester, PA, p. 1-5.

Valley limestones, the Octoraro is assigned an Ordovician age. Bascom also returns to the question of the age of the Wissahickon that has been festering for the past seven years. Her new conclusion that the Wissahickon is Precambrian is supported by a number of points which can be summarized as follows: a) intrusive igneous rocks are relatively common in the Wissahickon and are absent in recognized Paleozoic rocks; b) although wherever they are observed together, the mica gneiss overlies the limestone, the structures can be interpreted as overturned synclines, thus allowing the gneiss to be older than the limestone.

Florence Bascom's students, Eleanora Bliss (married name, Knopf) and Anna Jonas (married name, Stose), now make their first contribution to the Wissahickon controversy with the publication of their joint thesis work (Bliss and Jonas, 1916). While holding to the 1909 stratigraphy and age interpretations, they have the Precambrian Wissahickon thrust over the younger rocks on a low-angle, far-traveled overthrust, analogous (according to the authors) to structures in the southern Appalachians, Scotland, and Scandinavia.

Knopf and Jonas (1923) introduce some major changes to the stratigraphic interpretation of the Piedmont rocks. Parts of the Wissahickon gneiss and Octoraro schist are split out to form the newly defined Peters Creek Schist. This new formation is named for exposures along the Susquehanna River, and consists of interbedded micaceous quartzites and chlorite-muscovite schist. The Octoraro schist is demoted from a formation back to a facies of the Wissahickon. They introduce the names oligoclase-mica schist for the southeastern facies of the Wissahickon previously referred to as the mica gneiss, and albite-chlorite schist for the northwestern facies previously designated Octoraro.

Another major contribution of Knopf and Jonas (1923) is the definition of the Glenarm Series. From bottom to top, the Glenarm Series as originally defined includes the Setters Formation, Cockeysville Marble, Wissahickon Formation, Peters Creek Schist, Cardiff Conglomerate, and Peach Bottom Slate. Within the Series, formations are bounded by sedimentary contacts. The Glenarm Series unconformably overlies the Precambrian basement rocks of the Baltimore Gneiss, and is assigned a Precambrian age. This represents the first recognition that the quartzite and marble in the Piedmont (Setters Formation and Cockeysville Marble) are separate units not correlative with the far less metamorphosed Paleozoic limestones and quartzites of the Chester Valley. There is no need for an overthrust fault beneath the Wissahickon, as proposed in 1916, because the Wissahickon is now assumed to be in sedimentary contact with the lower parts of the Glenarm Series.

The 1970's were a period of upheaval in Wissahickon nomenclature in Maryland in Virginia. Pavlides (1974) mapped what was formerly called Wissahickon in Virginia using lithologic units and abandoned the name in Virginia. Crowley (1976) raised the Wissahickon to Group status and identified six new formations within it. Thus, the use of Wissahickon as a formation name was abandoned in Maryland. Since then, even the term Wissahickon Group has fallen into disuse in Maryland, although it has not been formally abandoned.

In Pennsylvania, the stratigraphy of Knopf and Jonas (1923) was maintained intact through the compilation of the Geologic Map of Pennsylvania (Berg et al., 1980). Since then, two significant official changes have been made to the definition of the Wissahickon Formation and its relationship to surrounding units. First, Lyttle and Epstein (1987) reinstated the name Octoraro for the former albite-chlorite schist facies of the Wissahickon, and declared that it is not part of the Wissahickon. Second, Drake (1993) removed the Wissahickon Formation from the Glenarm Group because he interpreted its contact with the lower parts of the Group as a fault. Alcock (1994) also mapped this fault at the base of the Wissahickon in Pennsylvania and Delaware. This is where we begin the story for this Field Conference.

"AND NOW FOR SOMETHING COMPLETELY DIFFERENT…" – THE 2004 FIELD CONFERENCE OF PENNSYLVANIA GEOLOGISTS

The past 10 years have seen a spate of research activity in the Pennsylvania-Delaware Piedmont. Bedrock geologic mapping (inside front cover), geochemical analyses of metabasalts to expand on the work of Smith and Barnes (1994), compositional mapping of garnet to further unravel the metamorphic history, and the application of zircon and monazite geochronology using modern microbeam techniques have given us grist for thinking about the Piedmont in new and different ways. The leaders of this Field Conference have agreed to divide the Wissahickon Formation in Pennsylvania and Delaware into three informal units for the purposes of discussion (inside front cover). The units are divided on the basis of lithology, associations with adjacent rock units (Wilmington Complex, Baltimore Gneiss-Glenarm Group), and to a lesser extent, geochemical and age data. Recognition of divisions within the Wissahickon Formation has allowed us to construct tectonic models that place the individual units in different depositional and tectonic environments. These models refine previous models that proposed differing environments for parts of the Wissahickon (such as Wagner and Srogi, 1987). Still, we do not all agree on a single model and questions remain. The details of the new models are presented in the chapters and stop descriptions of this guidebook. The remainder of this paper will briefly introduce the units, present a general tectonic model, and highlight the differences of opinion about the story.

The Wissahickon Formation, Wilmington Complex, and Glenarm Group are metasedimentary and metaigneous rocks originally deposited or emplaced on the outermost edge of the rifted margin of Laurentia and in an arc-related setting. The Wilmington Complex consists of metavolcanic and metaplutonic remnants of an arc, primarily the forearc region (Stops 1 and 7; see Plank and Schenck, this volume). The Glenarm Group consists of the Setters Formation and Cockeysville Marble, which are metasediments originally deposited unconformably on Baltimore Gneiss (Laurentian continental basement), (Stop 4; see Blackmer, this volume). The three informal units of the Wissahickon Formation are discussed below. The sketch on the inside back cover shows one hypothesis of the tectonic settings of these rocks.

Type Wissahickon (Stop 10)

This unit lies entirely east of the Wilmington Complex and includes the type locality along Wissahickon Creek in Philadelphia's Fairmount Park. These rocks are characterized by well defined interlayering of pelitic (aluminous, mica-rich) and psammitic (quartz-rich) lithologies, which could represent original graded bedding. This layering is characteristic only of this part of the Wissahickon Formation. The Type Wissahickon is associated with neither the Glenarm Group nor arc magmatism, but does include metaigneous amphibolites with compositions similar to modern back-arc basin basalts and within-plate basalts. Bosbyshell speculates that this unit may be younger than the remainder of the Wissahickon Formation, but it must be older than the Silurian age of the intrusive Springfield Granodiorite (J. Aleinikoff, unpublished data).

"Glenarm Wissahickon" (Stop 5)

The term "Glenarm Wissahickon" was first used by Faill (1994) to refer to all of the Wissahickon Formation west of the Wilmington Complex. We have restricted it to the aluminous schist which lies north and west of the Avondale Anticline. The "Glenarm Wissahickon" is in depositional contact with the Glenarm Group and Baltimore Gneiss. West of the Avondale Anticline, its southern boundary is a fault contact with the Mt. Cuba Wissahickon. It includes sparse interlayers of White Clay Creek Amphibolite, which has the geochemical signature of a continental rift basalt (Smith and Barnes, this volume), or within-plate basalt (Plank and Schenck, this volume). Blackmer (this volume) hypothesizes that the Setters Formation and Cockeysville Marble of the Glenarm Group, as well as the "Glenarm Wissahickon", accumulated as sediments in a rift basin floored by

Laurentian continental crust (analogous to the Gulf of Suez) during Late Proterozoic to Cambrian rifting of Laurentia.

Mt. Cuba Wissahickon (Stops 2, 3, 8)

This unit includes a sliver of metasediments on the east side of the Wilmington Complex as well as all of the Wissahickon Formation west of the Wilmington Complex and south of the Avondale Anticline. The rocks are primarily pelitic and psammitic gneisses with interlayers of White Clay Creek Amphibolite and Kennett Square Amphibolite. The White Clay Creek Amphibolite has the geochemical signature of a continental rift basalt (Smith and Barnes, this volume) or of an ocean-island basalt (Plank et al., 2001). The Kennett Square Amphibolite has the geochemical signature of an ocean floor basalt (MORB) (Smith, this volume). Within the Faulkland Gneiss and the Windy Hills Gneiss of the Wilmington Complex, the Mt. Cuba Wissahickon is interlayered with the metaigneous arc rocks.

Plank and Schenck (this volume) hypothesize that the Mt. Cuba Wissahickon is a forearc accretionary complex that is in thrust contact with the Glenarm Group and Baltimore Gneiss. Their model begins in the early Cambrian when sediments eroded off the Laurentian continent were deposited in the Iapetus Ocean. By 480 Ma, an east dipping subduction zone opened in the Iapetus and oceanic crust with a veneer of terrigneous sediments was subducted beneath oceanic crust with a veneer of similar sediments. A volcanic arc formed on the overriding plate and sediments on the subducting plate were accreted to the forearc. Alternatively, the overriding plate may have carried a small microcontinent rifted from Laurentia. This alternative may explain the presence of continental rift basalts (White Clay Creek Amphibolite) within the arc and forearc (Smith and Barnes, this volume). Most of the sediments in the arc basement and the forearc accretionary complex have a Laurentian affinity and are assigned to the Mt. Cuba Wissahickon. Subduction ended around 460 Ma, when the Laurentian margin reached the trench and was back-thrust out of the subduction zone. During this stage the forearc accretionary complex was thrust over a portion of the continental basement and its Glenarm Group cover.

Based on the assumption that association with arc-related rocks versus Laurentian-derived rocks has genetic meaning, Blackmer and Bosbyshell would prefer to draw a boundary at the western limit of arc magmatism in the Mt. Cuba Wissahickon (inside front cover). To the west of such a boundary would be the Mt. Cuba Wissahickon sediments associated with the Glenarm Group and Baltimore Gneiss, possibly deposited in a Late Proterozoic to Cambrian rift basin similar to that described for the "Glenarm Wissahickon." This would fit with Blackmer's field observations that the Mt. Cuba Wissahickon is in depositional contact with the Glenarm Group in Pennsylvania. Separating the rocks associated with the arc also fits better with Bosbyshell's observation that the Mt. Cuba Wissahickon east of the Wilmington Complex is lithologically different from the rocks to the west. Plank and Schenck are reluctant to draw such a boundary because the rocks on either side are essentially indistinguishable in the field.

WHERE DO WE GO FROM HERE?

At first glance, it appears that we have come nearly full circle in our definition of the Wissahickon Formation. The extent of the formation approximates Bascom's original 1902 definition. We can say with some confidence that the age of the Wissahickon is Late Precambrian to Middle Ordovician, a range only slightly smaller than that proposed by Bascom (1902). But a closer look shows that we have a much more detailed framework of mapping, rock relationships, geochemistry, metamorphic history, and ages to use a basis for reasonable tectonic models that agree with plate reconstructions. We know what types of data from which samples will help us test the models. Clearly, though, there is still a lot of work ahead as we refine our picture of stratigraphic and

structural relationships, and continue the search for the ever-elusive reliable depositional age of the Wissahickon.

References

Alcock, J., 1994, The discordant Doe Run thrust: Implications for stratigraphy and structure in the Glenarm Supergroup, southeastern Pennsylvania Piedmont: Geological Society of America Bulletin, v. 106, p. 932-941.

Bascom, F., 1902, The geology of the crystalline rocks of Cecil County: Maryland Geological Survey, Cecil County Report, p. 83-148.

Bascom, F., 1905, Piedmont district of Pennsylvania: Geological Society of America Bulletin, v. 16, p. 289-328.

Bascom, F., Clark, W. B., Darton, N. H., Kummel, H. B., Salisbury, R. D., Miller, B. L., and Knapp, G. N., 1909, Description of the Philadelphia district-Philadelphia Folio: U. S. Geological Survey Geological Atlas of the United States, Folio 162, 24 p. with maps, scale 1:62,500.

Berg, T. M., Edmunds, W. E., Geyer, A. R., Glover, A. D., Hoskins, D. M., MacLachlin, D. B., Root, S. I., Sevon, W. D., and Socolow, A. A., 1980, Geologic map of Pennsylvania: Pennsylvania Topographic and Geologic Survey, Series 4, Map 1.

Bliss, E. F., and Jonas, A. I., 1916, Relation of the Wissahickon mica gneiss to the Shenandoah limestone and the Octoraro schist of the Doe Run and Avondale region, Chester County, Pennsylvania: U.S.G.S. Professional Paper 98, p. 9-34.

Crowley, W. P., 1976, The geology of the crystalline rocks near Baltimore and its bearing on the evolution of the eastern Maryland Piedmont: Maryland Geological Survey Report of Investigations 27, 40 p.

Drake, A. A., 1993, The Soldiers Delight Ultramafite in the Maryland Piedmont: U. S. Geological Survey Bulletin 2076, p. A1-A13.

Knopf, E. B., and Jonas, A. I., 1923, Stratigraphy of the crystalline schists of Pennsylvania and Maryland: American Journal of Science, v. 5, p. 40-62.

Lyttle, P.T. and Epstein, J.B., 1987, Bedrock geologic map of the Newark 2 degrees quadrangle, New York, New Jersey, and Pennsylvania: U.S. Geological Survey Miscellaneous Investigations Series Map, I-1715, 1 sheet, scale 1:250,000

Mathews, E. B., 1905, Correlation of Maryland and Pennsylvania Piedmont formations: Geological Society of America Bulletin, v. 16, p. 329-346.

Pavlides, L., 1974, Age, origin, regional relations, and nomenclature of the Glenarm Series, Central Appalachian Piedmont: a reinterpretation: Discussion: Geological Society of America Bulletin, v. 83, p. 153-155.

Plank, M. O., Srogi, L., Schenck, W. S., and Plank, T. A., 2001, Geochemistry of the mafic rocks, Delaware Piedmont and adjacent Pennsylvania and Maryland: Confirmation of arc affinity: Delaware Geological Survey, Report of Investigations no. 60, 39 p.

Smith, R. C., II, and Barnes, J. H., 1994, Geochemistry and geology of metabasalt in southeastern Pennsylvania and adjacent Maryland, *in* Faill, R.T. and Sevon, W. D., *eds*., Various aspects of Piedmont geology in Lancaster and Chester Counties, Pennsylvania: Annual Field Conference of Pennsylvania Geologists, 59th, Lancaster, PA, Guidebook, p. 45-72.

Wagner, M. E., and Srogi, E. L., 1987, Early Paleozoic metamorphism at two crustal levels and a tectonic model for the Pennsylvania-Delaware Piedmont: Geological Society of America Bulletin, v. 99, p. 113-126.

MARGINALIA: A TECTONIC FANTASY IN FIVE ACTS

by
LeeAnn Srogi

There is a fundamental asymmetry within rocks currently mapped as Wissahickon Formation, in terms of lithologies, associated metasedimentary and metaigneous rocks, and ages of metamorphism and deformation, that provides some basis for tectonic interpretations. Rocks farthest to the west (the "Glenarm Wissahickon") are conformable with the Glenarm Group, and show evidence of deposition before the Ordovician, possibly in basins associated with continental rifting (Blackmer, this volume; Smith, this volume). Moving to the southeast, Blackmer maps a fault contact between the "Glenarm Wissahickon" and the Mt. Cuba Wissahickon, but she proposes essentially similar age and depositional environment for both units. Amphibolites within the Mt. Cuba Wissahickon include those with MORB-like chemistry, and within-plate basalt chemistry (interpreted as continental-rift-related by Smith, this volume, and Blackmer, this volume; or oceanic islands by Plank and Schenck, this volume). The Glenarm Group and Baltimore Gneiss also occur in Delaware, but the Mt. Cuba Wissahickon is mapped in thrust contact rather than conformable contact. Moving farther southeast, the Mt. Cuba Wissahickon is interlayered with and intruded by forearc and arc metaigneous rocks of Ordovician age in the Wilmington Complex. Mt. Cuba Wissahickon of essentially identical compositions, ages, and metamorphic histories occur on the west and east sides of the Wilmington Complex. East of the Wilmington Complex, there is no evidence for the Glenarm Group in the Wissahickon. Moving further east, the Type Wissahickon shows no evidence for Ordovician metamorphism; the major metamorphic event appears to be Devonian in age. In constructing the following tectonic fantasy, we make the assumption that, in most cases, the amphibolites within metasedimentary units have intrusive or stratigraphic original contacts with the sedimentary protoliths. This assumption allows us to associate packages of metasediments and igneous rocks in interpreting original tectonic setting. However, we cannot rule out the possibility that these contacts are tectonic and later in at least some rocks.

ACT I: THE RIFT MARGIN, 600 - 515(?) Ma

Continental rifting along the eastern margin of North America developed during the latest Precambrian - early Cambrian, resulting in the opening of the Iapetus Ocean between Laurentia and Baltica to the southeast and Gondwana to the south. The Glenarm Wissahickon and associated Glenarm Group sediments, as well as the Mt. Cuba Wissahickon, accumulated in a rift basin floored by Laurentian continental crust, where they were associated with early continental rift basalts now called the White Clay Creek Amphibolites (Blackmer, this volume; Smith, this volume). The Kennett Square Amphibolites, which have geochemical compositions similar to MORBs, record the magmatic transition from rift to drift. Alternatively, the Mt. Cuba Wissahickon was originally deposited on the Laurentian slope and rise as Iapetus opened, and the White Clay Creek Amphibolites were oceanic island basalts erupted into Iapetus (Schenck and Plank, this volume).

ACT II: INITIATION OF SUBDUCTION AND THE MAGMATIC ARC, 510-470(?) Ma

By 480 Ma, an east-southeast dipping subduction zone had opened more or less in the middle of the Iapetus Ocean, between Laurentia and Baltica to the southeast. The metaigneous rocks of the Wilmington Complex were formed as volcanics and intrusives in this Ordovician arc. The Rockford Park Gneiss, Faulkland Gneiss, and Windy Hills Gneiss units are consistent with a forearc basin setting. Blakey's reconstructions (http://jan.ucc.nau.edu/~rcb7/global_history.html) show the

Srogi, L., 2004 Marginalia: A tectonic fantasy in five acts, *in* Blackmer, G. C., and Srogi, L., Marginalia – Magmatic arcs and continental margins in Delaware and southeastern Pennsylvania: Guidebook, 69th Annual Field Conference of Pennsylvania Geologists, West Chester, PA, p. 6-8.

subduction zone located between Laurentia and the Iapetan ridge, which lies to the south close to Gondwana. Scotese's reconstructions (http://www.scotese.com/earth.htm) do not seem to show the Iapetan ridge at all. The initiation of subduction in this location would imply that relatively young and hot lithosphere was involved in subduction, and perhaps there was even subduction of the ridge. This would be consistent with the occurrence of mafic igneous rocks with boninite-like compositions in the Rockford Park Gneiss; one hypothesis for the formation of boninitic rocks is subduction of a ridge or young, hot lithosphere. It is notable that there are other boninitic amphibolites of similar age in the Hawley Formation in New England (Kim and Jacobi, 1996). In both the Hawley Formation and the Rockford Park Gneiss, the boninitic rocks are associated with intermediate to felsic igneous rocks; perhaps this is indicating ridge subduction some time after the establishment of the magmatic arc. At least some of the Wissahickon in the Faulkland Gneiss (Schenck and Plank, this volume) and with the Confluence Gneiss (Bosbyshell, 2001) is so intimately associated with the arc rocks that it may have formed the basement to the forearc region, or been deposited with the volcanics in the forearc basin. One area of future investigation is the delineation of the part of the Mt. Cuba Wissahickon that includes older rift/slope/rise sediments tectonically accreted to the accretionary-forearc complex, from the Mt. Cuba Wissahickon that includes sediments directly related to the forearc basin.

ACT III: THE ELUSIVE TACONIC OROGENY, 470 - 440(?) Ma

Direct evidence for an orogenic event in the late Ordovician has become scarce in the Wissahickon and Wilmington Complex, although shelf drowning sequences in the sedimentary record and foreland deformation provide evidence for orogeny at upper crustal and surface levels. Plate reconstructions show the oblique collision of the Taconic arc (which presumably included the Wilmington Complex) with Laurentia beginning as early as 480 Ma in northern New England, and closing from northeast to southwest along the Laurentian margin. The supracrustals of the Rockford Park Gneiss and Faulkland Gneiss which were deposited about 480-470 Ma, were buried to conditions of 500-600 MPa and 700-800°C by about 430 Ma. As suggested by Bosbyshell (2001), the extent of burial suggests more than just arc magmatism and sedimentation. It is possible that, during oblique collision, the magmatic arc overrode its forearc-accretionary complex, accounting for the tectonic burial to depths of 13.5-20 km. However, there is virtually no evidence of mineral growth - zircon or monazite - of late Ordovician age in the Wilmington Complex or Wissahickon to directly date orogeny.

The Type Wissahickon must be Silurian or older in depositional age, because it is intruded by the Silurian Springfield Granodiorite (J. Aleinikoff, personal communication, 2004). However, Bosbyshell (2001) has not found evidence for Ordovician metamorphism in the Type Wissahickon; it seems to have had a different history from the Mt. Cuba and Glenarm Wissahickon, and to not have been metamorphosed significantly by the Taconic orogeny. Perhaps the Type Wissahickon was being deposited southeast of Laurentia, closer to Avalonia or Baltica, at the time of arc-Laurentian collision in late Ordovician time. Input of some continental crustal material is indicated by the relatively siliceous composition of the Type Wissahickon metapelites.

ACT IV: RE-ORGANIZATION OF SUBDUCTION, 435-415 Ma

The Silurian was a time of high-temperature metamorphism and mafic and felsic magmatism in the Pennsylvania-Delaware Piedmont. The locus of highest metamorphic grade is the Brandywine Blue Gneiss in the Wilmington Complex; metamorphic grade decreases west and east of this unit. The Wilmington Complex and Mt. Cuba Wissahickon reached amphibolite to granulite facies conditions (maximum temperatures exceeding 700°C at about 600 MPa), at the time of intrusion of the composite Arden Plutonic Supersuite, the Bringhurst Gabbro, and numerous small mafic dikes and stocks. Silurian mafic igneous rocks have trace element compositions most similar to modern

back-arc basin basalts. These observations led Plank et al. (2001) to suggest an extensional tectonic regime with high mantle heat flow during the Silurian. The Springfield Granodiorite, which intrudes the Type Wissahickon to the east, has a similar Silurian age (J. Aleinikoff, personal communication, 2004), and other granitoid plutons in the region may turn out to be Silurian, as well. Andalusite and sillimanite in the Type Wissahickon could be explained either by overlapping contact metamorphic effects of the Springfield Granodiorite and other intrusions, or by high heat flow at shallow crustal levels in an extensional environment associated with intrusion of granitic and mafic magmas. Different metamorphic pressures in the Type Wissahickon and Wilmington Complex suggest tectonic juxtaposition of these units after the Silurian.

Plate reconstructions for this time period show a west-dipping subduction zone beneath the Laurentian margin, suggesting re-organization of subduction following oblique collision. Perhaps oblique subduction led to slab break-off and the development of an extensional or trans-tensional regime at the locus of the former arc. Alternatively, with the establishment of west-dipping subduction, the Wissahickon and Wilmington Complex could have been in a back-arc position resulting in extension and crustal thinning. In either case, high mantle heat flow and mantle-derived magmatism could have led to partial melting of arc crust and the formation of the granitoid plutons.

Some samples of Type Wissahickon, Mt. Cuba Wissahickon, and Faulkland Gneiss show evidence of deformation and monazite mineral growth at about 415-411 Ma (Bosbyshell, 2001; Aleinikoff, in press). This establishes a maximum age for D3 in the Mt. Cuba Wissahickon and Type Wissahickon, and is interpreted to indicate the onset of renewed plate convergence (Bosbyshell, 2001).

ACT V: OROGENY AGAIN?, 400-360 Ma

In the Mt. Cuba Wissahickon close to the Wilmington Complex, and in the Type Wissahickon, the Silurian high-temperature metamorphism is overprinted by a higher-pressure, lower-temperature metamorphism and deformation at about 380-360 Ma. (Timing of metamorphism and deformation in the western part of the Mt. Cuba Wissahickon and the Glenarm Wissahickon are not yet worked out). Shear zones of this age record down-to-the-southeast motion (Bosbyshell, 2001). These observations would be consistent with another collisional event, tectonic burial of the Wissahickon and Wilmington Complex, metamorphism and deformation during exhumation, possibly associated with gravitational collapse of the orogen. Plate reconstructions show the collision of Avalonia and other peri-Gondwanan fragments with Laurentia during the Devonian, which could account for the metamorphism and deformation in the Pennsylvania-Delaware Piedmont. However, no fragments with a peri-Gondwanan association have been identified in this region. It is possible that these have been eroded away; or that the Piedmont in this region has been moved southward into position along later transcurrent shear zones, leaving Avalonia behind; or that some other tectonic scenario is responsible for the observed Devonian metamorphism and deformation.

References

Aleinikoff, J. N., Schenck, W. S., Plank, M.O., Srogi, L., Fanning, C.M., Kamo, S. J., and Bosbyshell, H., in press, SHRIMP U-PB geochronolgy of igneous and metamorphic events in the Wilmington Complex, Delaware: morphology, zoning, and ages of zircon and monazite, Geological Society of America Bulletin.

Bosbyshell, H., 2001, Thermal evolution of a convergent orogen: Pressure–Temperature–Deformation–Time paths in the central Appalachian Piedmont of Pennsylvania and Delaware: unpublished Ph.D. thesis, Bryn Mawr College, Bryn Mawr, Pa., 233 p.

Kim, J., and Jacobi, R. D., 1996, Geochemistry and tectonic implications of Hawley Formation met-igneous units: American Journal of Science, v. 296, p. 1126-1174.

Plank, M. O., Schenck, W. S., Srogi, L., and Plank, T. A., 2001, Geochemistry of the mafic rocks, Delaware Piedmont and adjacent Pennsylvania and Maryland: Confirmation of arc affinity: Delaware Geological Survey Report of Investigations No. 60, 39 p.

THE WISSAHICKON FORMATION IN DELAWARE

by
Margaret O. Plank and William S. Schenck

INTRODUCTION

Within the central Piedmont of Delaware and Pennsylvania there are currently three "flavors" of Wissahickon (inside front cover). The first is the Type Wissahickon that includes the type section along Wissahickon Creek in Fairmont Park (Bosbyshell, this volume). The second is the Mt. Cuba Wissahickon that includes the metasediments interlayered with the igneous rocks of the Wilmington Complex plus the metasediments that lie west of the Wilmington Complex. Information on this area has been published by the Delaware Geological Survey (Schenck et al., 2000; Plank et al., 2000; Plank et al., 2001). The third unit, the Glenarm Wissahickon includes Wissahickon sediments that lie conformably over the Baltimore Gneiss and Glenarm Group, the Setters Formation and Cockeysville Marble (Blackmer, this volume).

Categorizing these rocks has been difficult due to the high metamorphic grade, intense deformation, and lack of outcrops in a highly populated area. Since most of the variation in the mineral assemblages is due to metamorphism, field evidence is difficult to interpret. Recently, U-Pb geochronologic and geochemical studies of the Wilmington Complex and Wissahickon Formation have provided new data and enabled us to suggest a new model for the geological history of the area.

A DESCRIPTION OF THE WISSAHICKON AND WILMINGTON COMPLEX IN DELAWARE

The Mt. Cuba Wissahickon

The Mt. Cuba Wissahickon in Delaware is an extensive sequence of pelitic and psammitic gneisses and amphibolites that are interlayered with and surround the igneous rocks of the Wilmington Complex. The formation is located within the Wilmington North, Kennett Square, West Grove, Newark West, Newark East, and Marcus Hook 7.5' U. S. Geological Survey Topographic quadrangles. Contacts between the pelitic and psammitic gneisses are gradational while contacts between the gneiss and amphibolites are always sharp. The psammitic rocks are the most abundant. Granitic pegmatites of various sizes, compositions, and ages are ubiquitous; however, the only pegmatite large enough to be mapped occurs north of Newark, Delaware. A linear series of ultramafic pods, now primarily serpentinites and amphibolites, occur in the Mt. Cuba Wissahickon west of the Wilmington Complex. (Berg, 1980; Schenck et al., 2000). The large bodies of amphibolite mapped in the Mt. Cuba Wissahickon south of the Avondale Anticline suggests that the amphibolites are concentrated in that region (Berg, 1980, Blackmer, this volume). This is misleading because the amphibolites are equally abundant in the Mt. Cuba in Delaware, but the layers are normally too small to map (Schenck et al., 2000).

In most cases primary sedimentary structures have been obliterated by metamorphic differentiation, partial melting, and complex folding; however, in a few outcrops the psammitic layers exhibit an inverse grading, which may reflect primary graded bedding. Quartz-rich psammitic layers alternate with biotite-sillimanite rich layers indicating deposition by submarine turbidity currents.

Metamorphism. An obvious feature of the Mt. Cuba Wissahickon in Delaware and Pennsylvania is the amphibolite to granulite grade metamorphism. Apparent differences among outcrops are due primarily to different mineral assemblages resulting from spatial variation in metamorphic grade. The intensity of metamorphism increases toward the Brandywine Blue Gneiss

Plank, M. O., and Schenck, W. S., 2004, The Wissahickon Formation in Delaware, *in* Blackmer, G. C., and Srogi, L., Marginalia – Magmatic arcs and continental margins in Delaware and southeastern Pennsylvania: Guidebook, 69th Annual Field Conference of Pennsylvania Geologists, West Chester, PA, p. 9-14.

of the Wilmington Complex (Wyckoff, 1952; Ward, 1959; Wagner & Srogi, 1987; Srogi, 1988; Plank, 1989; Alcock 1989; Srogi et al., 1993; Bosbyshell et al., 1999).This unit underlies the city of Wilmington, the northeastern suburbs in Brandywine Hundred, and a small area in Pennsylvania (Berg, 1980; Schenck et al., 2000).

The increasing metamorphism can be identified in the field as muscovite disappears and is replaced by the pair orthoclase and sillimanite. This change in mineralogy, often referred to as the second sillimanite isograd, is due to the reaction:

muscovite + quartz = orthoclase + sillimanite + water

Muscovite persists in the metapelites even after the first appearance of orthoclase. This phenomenon is documented in other high-grade metamorphic terranes and is attributed to continuous reactions involving Na and K in muscovite and Na and Ca in plagioclase (Evans and Guidotti, 1966; Tracy, 1978). Metamorphism above the second sillimanite isograd can be identified in the field as garnet replaces biotite (Calem, 1987; Wagner et al., 1991). Garnets in migmatites appear to have grown into zones of biotite and sillimanite, suggestive of the reaction:

sillimanite + biotite + quartz + Na-plagioclase = garnet + Ca-plagioclase + melt

Sillimanite is a key index mineral in the pelitic rocks and is normally present as stringers of fibrolite. In high-grade rocks it also occurs as flattened nodules that vary from ½ to 2 cm in diameter, veins approximately 1/2 cm thick, and fibrous clumps that may be up to 30 cm thick. Owing to its abundance in the Mt. Cuba Wissahickon, and as an indicator of high grade metamorphism, sillimanite was chosen by the Delaware General Assembly as the Delaware state mineral.

Alcock (1989) and Plank (1989) calculated peak temperatures for the Mt. Cuba Wissahickon pelitic rocks that range from 620 ± 50°C west of Newark to 750 ± 50°C east of the Red Clay Creek. Pressures estimated using various geobarometers range from 4 to 7 ± 1 kilobars. The highest metamorphic grade was recorded in pods of pelitic gneiss within the Brandywine Blue Gneiss. Srogi (1988) found evidence for reactions in pelitic rocks that consumed biotite, sillimanite, quartz, and garnet and produced garnet, cordierite, hercynitic spinel, corundum, orthopyroxene, and granitic melt, and calculated peak metamorphic temperatures of 800 ± 50° C and pressures of about 6 kilobars.

Age. Ages of detrital zircons from psammitic gneiss of the Mt. Cuba Wissahickon from Yorklyn, Delaware, range from 735 to 1740 Ma, with most ages between 900 and 1400 Ma. Two major zircon populations occur at about 950 and 1050 Ma. This age distribution suggests the zircons were derived primarily from Middle Proterozoic crystalline basement of Grenvillian age (1.0-1.4 Ga), and that the metasediments of the Mt. Cuba Wissahickon were originally eroded off the ancient Laurentian continent (Aleinikoff, in press).

Monazites from the same outcrop yielded a very precise Concordia Age of 424.9 ± 0.5 Ma. This metamorphic event is labeled M2 by Bosbyshell (2001).

Deformation. Mt. Cuba Wissahickon rocks in the central Piedmont are complexly folded by multiple deformational events. The earliest folding event is preserved in the pelitic and psammitic gneisses as intrafolial folds (D1). The presence of small-scale refolded folds suggests a second event (D2). The dominant event that folded the units into westward verging nappes also folded the compositional layering into isoclinal folds (D3). The axial planes and limbs of the isoclinal folds are parallel and consistently strike between N30°E and N60°E with the most common strike being N40°E. Northeast of the Red Clay Creek most foliations dip steeply to the northwest. Southwest of the creek the foliations dip steeply to the southeast and become shallower to the northwest. The plunge of the folds varies from 0^{o} to 90°. Later folds indicated by the map pattern show broad warps around a northwest-southeast axis (D4). In addition, numerous shear zones and both brittle and ductile faults can be identified.

Geochemistry. Smith and Barnes (1994) collected 23 samples of Wissahickon amphibolites from Pennsylvania and Delaware. Using trace element concentrations they identified two

amphibolite types: type 1 (Kennett Square Amphibolite) with trace elements distinctive of ocean floor basalts (MORBs), and type 2 amphibolites (White Clay Creek Amphibolite) with trace elements typical of within-plate basalts. Geochemical data are reported in Plank et al., 2001.

The Kennett Square Amphibolites lie within the Mt. Cuba Wissahickon in a series of pods that stretch south of and parallel to the Avondale Anticline and in a few random locations in Delaware. Chemically, all samples are ocean floor basalts but are transitional from normal ocean floor basalts in the east to enriched ocean floor basalts in the west. The White Clay Creek Amphibolites were sampled from outcrops along the Creek just above the MD-DE-PA corner. The within-plate geochemistry of the White Clay Creek Amphibolites suggests they may have originated either as continental rift basalts or oceanic island basalts (Smith and Barnes, 1994; Plank et al., 2001). These two types of amphibolites also occur in other areas of Wissahickon. Volkert et al. (1996) found both types in drill cores in the Wissahickon Formation of New Jersey. Bosbyshell (2001) described the Bridgewater Amphibolite in the Wissahickon east of the Wilmington Complex as similar in major and trace element composition to the White Clay Creek Amphibolite. Plank et al. (2001) reported a White Clay Creek Amphibolite within the Faulkland Gneiss. Further study is needed to understand the regional relationships of the various amphibolites.

The Wilmington Complex

In order to understand the Mt. Cuba Wissahickon in Delaware it is necessary to understand the Wilmington Complex as the two units are intimately associated. There are eleven units mapped within the Wilmington Complex (Schenck et al., 2000). Eight of the eleven units are plutons: the Brandywine Blue Gneiss, Christianstead Gneiss, Barley Mill Gneiss, Montchanin Metagabbro, Mill Creek Metagabbro, Bringhurst Gabbro, Iron Hill Gabbro and Arden Plutonic Supersuite. The other three units are metavolcanic or metavolcaniclastic: the Rockford Park Gneiss, the Faulkland Gneiss, and the Windy Hills Gneiss. In most cases, contacts between the Mt. Cuba Wissahickon and the Wilmington Complex are intrusive (Bosbyshell et al., 1999; Plank et al., 2000). Layers and pods of Mt. Cuba Wissahickon are abundant within the Faulkland Gneiss and the Windy Hills Gneiss
The Rockford Park Gneiss is composed of mafic and felsic gneisses that are sharply interlayered on a scale of 6 to10 inches. In Delaware, the Rockford Park Gneiss occurs as screens within the Brandywine Blue Gneiss (Schenck et al., 2000); in Pennsylvania, the Rockford Park Gneiss intrudes the metasediments of the Mt. Cuba Wissahickon (Bosbyshell, 2001). The Brandywine Blue Gneiss is a medium- to coarse-grained, lineated (pinstriped) two-pyroxene gneiss with thin discontinuous mafic layers. In both units intense deformation and metamorphic recrystallization have obscured original igneous features.

The Faulkland Gneiss includes diverse lithologies such as amphibolite, quartz-bearing amphibolite, cummingtonite with amphibolite , and felsic gneiss with minor amounts of biotite, hornblende, or cummingtonite. All of these lithologies are thought to be of volcanic or volcaniclastic origin and are often associated with the metasedimentary rocks of the Mt. Cuba Wissahickon.
The Windy Hills Gneiss is composed of mafic and felsic gneisses of volcanic origin, large bodies of coarse and fine-grained biotite-quartz plagioclase gneiss of possible volcaniclastic origin, and pelitic and psammitic gneisses of the Mt. Cuba Wissahickon. Gradational contacts between the pelitic gneiss and the biotite-quartz-plagioclase gneiss support a volcaniclastic origin for some of the Windy Hills Gneiss.

Geochemistry. Geochemical data on mafic rocks from the Wilmington Complex provide the most convincing evidence to date for its origin as a volcanic arc. The REE patterns and trace element geochemistry of the Rockford Park Gneiss suggests a boninitic affinity. Boninites are distinctive igneous rocks found only in the forearc regions of modern and ancient arcs (Crawford et al., 1989; Taylor, 1992; Kim & Jacobi, 1996). The mafic layers in the Brandywine Blue Gneiss and Faulkland Gneiss have trace element patterns suggestive of volcanic arcs, plot as low-K tholeiites on a SiO_2 vs.

K_2O diagram, and have low TiO_2 concentrations (0.3-1.1%) that are typical of rocks that form in a forearc or frontal arc during the early stages of subduction (Gill, 1981). The Windy Hills samples also have trace element patterns similar to volcanic arcs, but plot as calc-alkaline on a SiO_2 vs. K_2O diagram, and have slightly higher TiO_2 concentrations (Plank et al., 2001).

Age. U-Pb dating of zircons by John Aleinikoff of the U.S. Geological Survey yielded Ordovician crystallization ages between 475 and 482 Ma for felsic meta-igneous rocks in the Brandywine Blue Gneiss, the Rockford Park Gneiss, Faulkland Gneiss and the Windy Hills Gneiss. Based on U-Pb analyses of metamorphic zircon and monazite, amphibolite and granulite grade metamorphism in the Wilmington Complex occurred approximately 50 million years after arc magmatism, between 426 and 432 Ma. This is consistent with the metamorphic age determined on monazites in the Mt. Cuba Wissahickon from Yorklyn, Delaware (Aleinikoff, in press).

In contrast to the other units in the Wilmington Complex, the Faulkland Gneiss recorded at least three other episodes of monazite growth signifying some type of metamorphic event at 447 ± 4, 411 ± 3, and 398 ± 3 Ma (Aleinikoff, in press). Many disequilibrium features, such as halos, coronas, and symplectites, are found in the Faulkland. We do not know why this unit preserved a record of multiple metamorphisms, other than to suggest that a fluid phase, essential for most reactions to proceed, was present in a large fault zone in the Faulkland Gneiss, or that the abundance of Mt. Cuba-type sediments in the Faulkland provided a source for fluids.

Aleinikoff found a large population of detrital zircons within a sample of Windy Hills Gneiss. He found the grains range in age from about 527 to 1933 Ma, with major peaks at about 1.05, 1.15, and 1.22 Ga. Detrital zircons older than about 900 Ma have a similar age distribution as detrital zircons from the Mt. Cuba Wissahickon indicating similar provenances for both samples. The Windy Hills Gneiss and Faulkland Gneiss have often been correlated with the James Run Formation in Maryland (Pickett, 1976; Thompson 1979); however, the age of the Windy Hills and Faulkland Gneiss is reported to be 481 ± 4 Ma (Aleinikoff, in press), and the age of the James Run in Baltimore as 454 ± 5 and 464 ± 5 Ma (Horton et al., 1998). Because of this age difference, we include the Windy Hills and Faulkland Gneiss in the Wilmington Complex. We also suggest, pending age dates, that the adjacent volcanic rocks of Cecil County, Maryland, now mapped as James Run, are probably part of the Wilmington Complex, and their ages should be determined to confirm their association with the James Run or the Wilmington Complex.

FOREARC ACCRETIONARY COMPLEX

A belt of Ordovician volcanics stretches intermittently along the Appalachian mountains from Virginia to Newfoundland. On the basis of Ordovician ages, 475-480 Ma, and arc affinities, the rocks of the Wilmington Complex now exposed in the Central Piedmont of Delaware and Pennsylvania are considered a part of this belt. Originally, the Central Piedmont volcanic arc was hundreds of kilometers wide. Today, after a collision with the ancient North American continent and millions of years of burial, deformation, and erosion only a few telescoped remnants remain of the original arc. Nevertheless, studies of these remnants in Delaware and Pennsylvania allow us to suggest they were part of an Ordovician volcanic arc and specifically they formed in its forearc accretionary complex.

Our model proposes that in the Cambrian, sediments were eroded off the ancient continent of Laurentia and deposited in the Iapetus Ocean. Beginning approximately 480 million years ago an east dipping subduction zone formed in the Iapetus and oceanic crust with a veneer of terrigneous sediments was subducted beneath a slab of oceanic crust with similar sediments. Alternatively the overriding plate may have carried a small microcontinent rifted from Laurentia. This alternative may explain the presence of continental rift basalts within the arc and forearc (Smith and Barnes, this volume), if these are not ocean island basalts. Subsequently, a volcanic arc, now the Wilmington Complex, formed as magma erupted through the overriding plate and sediments on the subducting

plate were scraped off the descending slab and incorporated into an accretionary prism. Thus, most of the sediments that formed the arc basement and the forearc accretionary complex have a Laurentian affinity and are now assigned to the Mt. Cuba Wissahickon.

The Delaware-Pennsylvania forearc accretionary complex resembles a modern forearc which contains a geochemically diverse group of mafic rocks such as boninites, island arc tholeiites, MORBs, transitional MORBs, ocean island basalts, and serpentinites (Fryer et al., 1985; Johnson and Fryer, 1990; Taylor, 1992). In Delaware and Pennsylvania, we also find boninitic rocks (Rockford Park Gneiss), low-K and low-TiO2 island arc tholeiites (Brandywine Blue Gneiss and Faulkland Gneiss), calc-alkaline island arc basalts (Windy Hills Gneiss), MORBs (Kennett Square Amphibolites), within-plate basalts (White Clay Creek Amphibolites), and serpentinites. Kim and Jacobi (1996) found a group of Ordovician, chemically-diverse, mafic rocks in the Hawley Formation in western Massachusetts and also assigned them to a forearc setting.

As the volcanic arc matured the forearc basin probably collected additional sediments eroded off the arc. Subduction ended around 460 Ma when the Laurentian margin stopped up the trench and was back-thrust out of the subduction zone. During this stage we propose that the forearc accretionary complex was thrust over the a portion of the Laurentian continental basement and its Glenarm cover and then folded to form westward verging nappes. Later in the Silurian between 426 and 432 Ma, an intense, pervasive event metamorphosed the entire package of rocks.

Our model for the forearc accretionary complex differs from Blackmer (this volume). Blackmer would prefer to divide the Mt. Cuba Wissahickon into two units: the Mt. Cuba associated with arc rocks and the Mt. Cuba west of the arc that is conformable with the underlying basement and Glenarm Group. Blackmer's proposed boundary occurs in the Mt. Cuba rocks west of the Wilmington Complex. We have found no field evidence to confirm this boundary. Pelitic and psammitic rocks interlayered with White Clay Creek Amphibolites are identical on both sides of the boundary. The textures and mineralogy in the rock units are the same, and there are no structural changes or discontinuities. Based on her mapping in Pennsylvania she finds no evidence for a thrust or other fault contact between Glenarm Group and the Mt. Cuba Wissahickon in Pennsylvania. By contrast, we map the Hockessin-Yorklyn and Landenberg anticlines, cored with continental basement and its Glenarm Group sedimentary cover, in fault contact with the Mt. Cuba Wissahickon (Plank and Schenck, 1997; Schenck et al., 2000). We propose that the forearc accretionary complex was thrust over the Glenarm Group and Laurentian basement in Delaware and adjacent Pennsylvania, although it apparently is conformable with the Glenarm Group farther northwest in Pennsylvania.

References

Alcock, J. E., 1989, Tectonic units in the Pennsylvania-Delaware Piedmont: Evidence from regional metamorphism and structure: Philadelphia, Pennsylvania, University of Pennsylvania, unpublished Ph.D. thesis, 251 p.

Aleinikoff, J. N., Schenck, W. S., Plank, M.O., Srogi, L., Fanning, C.M., Kamo, S. J., and Bosbyshell, H., in press, SHRIMP U-PB geochronolgy of igneous and metamorphic events in the Wilmington Complex, Delaware: morphology, zoning, and ages of zircon and monazite, Geological Society of America Bulletin.

Berg, T. M., 1980, Geologic Map of Pennsylvania: Harrisburg, PA: Pennsylvania Topographic and Geologic Survey, Scale 1:250,000.

Bosbyshell, H., 2001, Thermal evolution of a convergent orogen: Pressure-Temperature- Deformation-Time paths in the central Appalachian Piedmont of Pennsylvania and Delaware: [PhD. thesis]: Bryn Mawr College, Bryn Mawr, Pa., 233 p.

Bosbyshell, H., Crawford, M. L., Srogi, L., 1999, Distribution of overprinting metamorphic mineral assemblages in the Wissahickon group, southeastern Pennsylvania, in, Valentino, D. W. and Gates, A. E., eds., The Mid-Atlantic Piedmont: Tectonic Missing Link of the Appalachians: Boulder, Colorado, Geological Society of America Special Paper 330, p. 41-58.

Calem, J. A., 1987, A petrologic study of migmatites of Brandywine Creek State Park, northern Delaware and implications for the mechanism of migmatization: Philadelphia, Pennsylvania, University of Pennsylvania, unpublished Masters thesis, 111p.

Crawford, A. J., Falloon, T. J., and Green, D. G., 1989, Classification petrogenesis and tectonic setting of boninites, in Crawford, A. J,. editor, Boninites: Unwin Hyman, London, p. 1-49.

Evans, E. J., and Guidotti, C. V., 1966, The sillimanite-potash feldspar isograd in western Maine, U.S.A.: Contributions to Mineralogy and Petrology, v. 12, p. 25-62.

Fryer, P., Ambrose, E. L. and Hussong, D. M., 1985, Origin and emplacement of Mariana forearc seamounts: Geology, v. 13, p. 774-777.

Gill, J. B., 1981, Orogenic andesites and plate tectonics: Springer-Verlag, Berlin, 390 p.

Horton, J. W., Jr., Aleinikoff, J. N., Drake, A. A., Jr., and Fanning, C. J., 1998, Significance of Middle to Late Ordovician volcanic-arc rocks in the central Appalachian Piedmont, Maryland and Virginia: Geological Society of America Abstracts with Programs, v. 30, p. 125.

Johnson, L. E., and Fryer, P., 1990, The first evidence for MORB-like lavas from the outer Mariana forearc: geochemistry, petrography, and tectonic implications: Earth and Planetary Science Letters, v. 100, p. 304-316.

Kim, J., and Jacobi, R. D., 1996, Geochemistry and tectonic implications of Hawley Formation meta-igneous units: American Journal of Science, v. 296, p. 1126-1174.

Plank, M. O., 1989, Metamorphism in the Wissahickon Formation of Delaware and adjacent areas of Maryland and Pennsylvania: Newark, Delaware, University of Delaware, unpublished Masters Thesis, 111 p.

Plank, M. O. and Schenck, W. S., 1997, The Setters Formation in the Pleasant Hill valley, Delaware: metamorphism and structure: Delaware Geological Survey Report of Investigations No. 56, 16 p.

Plank, M. O., Schenck, W. S., and Srogi, L., 2000, Bedrock geology of the Piedmont of Delaware and adjacent Pennsylvania: Delaware Geological Survey Report of Investigations No. 59, 52 p.

Plank, M. O., Schenck, W. S., Srogi, L., and Plank, T. A., 2001, Geochemistry of the mafic rocks, Delaware Piedmont and adjacent Pennsylvania and Maryland: Confirmation of arc affinity: Delaware Geological Survey Report of Investigations No. 60, 39 p.

Schenck, W. S., Plank, M. O., and Srogi, L., 2000, Bedrock geologic map of the Piedmont of Delaware and adjacent Pennsylvania: Delaware Geological Survey Geologic Map Series No. 10, Scale 1:36,000.

Smith, R. C., and Barnes, J. H., 1994, Geochemistry and geology of metabasalt in southeastern Pennsylvania and adjacent Maryland, in, Faill, R. T., and Sevon, W. D. eds., Various aspects of Piedmont geology in Lancaster and Chester Counties, Pennsylvania: Guidebook for the 59th Annual Field Conference of Pennsylvania Geologists, Lancaster, PA, p. 45-72.

Srogi, E. L., 1988, The petrogenesis of the igneous and metamorphic rocks in the Wilmington Complex, Pennsylvania-Delaware Piedmont: Philadelphia, Pennsylvania, University of Pennsylvania, unpublished Ph.D. thesis, 613 p.

Srogi, L., Wagner, M. E., Lutz, T., 1993, Dehydration partial melting and disequilibrium in the granulite-facies Wilmington Complex, Pennsylvania-Delaware Piedmont: American Journal of Science, v. 293, p. 405-462.

Taylor, B., 1992, Rifting and the volcanic-tectonic evolution of the Izu-Bonin-Mariana arc. in Taylor, B., Fujioka, K. et al., Proceedings ODP, Scientific Results, 126: College Station, TX (Ocean Drilling Program), p. 627-651.

Tracy, R. J., 1978, High grade metamorphic reactions and partial melting in pelitic schist, west-central Massachusetts: American Journal of Science, v. 278, p. 150-178.

Volkert, R. A., Drake, A. A., and Sugarman, P. J., 1996, Geology, geochemistry and tectonostratigraphic relations of the crystalline basement beneath the Coastal Plain of New Jersey and contiguous areas: U.S. Geological Survey Professional Paper 1565-B, 48 p.

Wagner, M. E., and Srogi, L., 1987, Early Paleozoic metamorphism at two crustal levels and a tectonic model for the Pennsylvania-Delaware Piedmont: Geological Society of America Bulletin, v. 99, p. 113-126.

Wagner, M. E., Srogi, L., Wiswall, C. G., and Alcock, J. E., 1991, Taconic collision in the Delaware-Pennsylvania Piedmont and implications for subsequence geologic history, in Schultz, A., and Compton-Gooding, E., eds., Geological Evolution of the Eastern United States: Fieldtrip Guidebook, NE-SE Geological Society of America, Virginia Museum of Natural History (VMNH) Guidebook No. 2, 91-119.

Ward, R. F. 1959, Petrology and metamorphism of the Wilmington Complex, Delaware, Pennsylvania, and Maryland: Geological Society of American Bulletin, v. 70, p. 1425-1458.

Wyckoff, D., 1952, Metamorphic facies in the Wissahickon Schist, Philadelphia, Pennsylvania: Geological Society of America Bulletin, v. 63, p. 25-58.

SPECULATION ON THE TECTONIC HISTORY OF THE GLENARM GROUP AND ASSOCIATED PARTS OF THE WISSAHICKON FORMATION

by
Gale C. Blackmer

INTRODUCTION

The interpretation of the Wissahickon Formation has been intimately tied to the Glenarm Group since definition of the latter by Knopf and Jonas (1923). As originally defined, the Glenarm is a sequence of metasediments unconformably overlying Baltimore Gneiss (continental basement) in Maryland and Pennsylvania, comprising from bottom to top: Setters Formation, Cockeysville Marble, Wissahickon Formation, Peters Creek Schist, Cardiff Conglomerate, and Peach Bottom Slate. Higgins (1977) redefined the Glenarm Group to include only those units below the Peters Creek Schist. Drake (1993) further redefined the group to include only the Setters Formation and Cockeysville Marble. This most recent definition of the Glenarm Group will be used throughout this paper. Drake removed the Wissahickon and its equivalents in Maryland because he interpreted the contact of the Wissahickon with the lower parts of the series as a thrust fault. The idea of a thrust fault at the base of the Wissahickon was first proposed by Bliss and Jonas (1916), who abandoned it with their 1923 definition of the Glenarm Group. Alcock (1994) reinstated this low-angle overthrust fault as the contact between the Wissahickon and Baltimore Gneiss-Glenarm Group in Pennsylvania and Delaware. He called the fault the Doe Run thrust, following the usage of Bliss and Jonas (1916).

For the purpose of discussion, the leaders of this Field Conference have agreed to informally subdivide the Wissahickon Formation into three units (inside front cover): Type Wissahickon includes the type locality of the formation in Philadelphia; Mt. Cuba Wissahickon consists of two segments - a relatively thin sliver that lies between Philadelphia Wissahickon to the east and the Wilmington Complex and Rosemont fault to the west, and that part of the Wissahickon Formation that lies west of the Wilmington Complex and south and west of the Avondale anticline; “Glenarm Wissahickon” surrounds the Woodville nappe and lies north of the Avondale anticline. The “Glenarm Wissahickon” is further subdivided into the Doe Run schist and Laurels schist (Blackmer, 2004). Only the Doe Run schist and the Mt. Cuba Wissahickon are in contact with the Glenarm Group. Other parts of the Wissahickon will not be considered in this paper.

The nature of the contact between the Glenarm Group (as defined by Drake (1993) to include only the Setters Formation and Cockeysville Marble) and the Wissahickon has a major role in the interpretation of the origin and history of these rocks. Under the original concept of stratigraphic continuity, the Setters-Cockeysville-Wissahickon series must have been deposited in the same place, and likely represents some sort of oceanic transgression over the edge of a continent. With the addition of the Doe Run thrust, the Setters and Cockeysville remain as transgressive cover rocks over the Baltimore Gneiss, while the Wissahickon might come from anywhere. Plank et al. (2000) and Plank and Schenck (this volume) propose that the Mt. Cuba Wissahickon was deposited on the continental slope and rise of Laurentia, and was later incorporated into the Wilmington Complex forearc and thrust back over the continental margin as later subduction closed the ocean basin.

Recent mapping in the Coatesville, West Grove, Newark West, and Kennett Square 7.5 minute quadrangles in Pennsylvania leads this author to propose yet another hypothesis. The Doe Run schist, and possibly the Mt. Cuba Wissahickon, is in depositional contact with the Glenarm Group, which unconformably overlies Baltimore Gneiss. However, these sediments were deposited under marine conditions in a rift basin rather than on a continental platform. To explore this

Blackmer, G.C., 2004, Speculation on the tectonic history of the Glenarm Group and associated parts of the Wissahickon Formation, *in* Blackmer, G. C., and Srogi, L., Marginalia – Magmatic arcs and continental margins in Delaware and southeastern Pennsylvania: Guidebook, 69th Annual Field Conference of Pennsylvania Geologists, West Chester, PA, p. 15-27

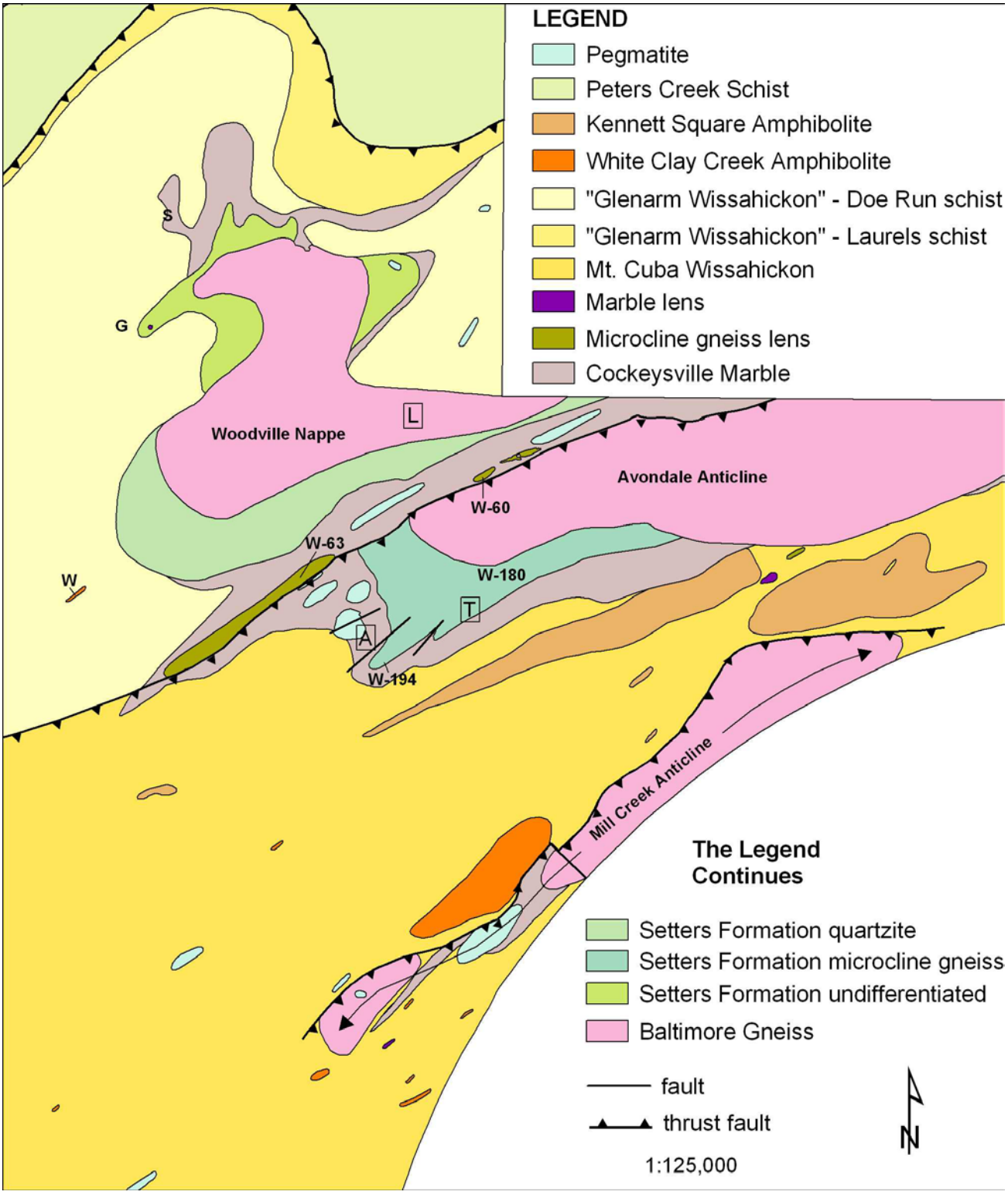

Figure 1. Bedrock geologic map of portions of the Coatesville, West Grove, Newark West, and Kennett Square 7.5 minute quadrangles. Major basement-cored structures are labeled: Woodville Nappe, Avondale Anticline, Mill Creek Anticline. Towns mentioned in text are labeled by letters in boxes: A – Avondale; L – London Grove; T – Toughkenamon. Quarry at Springdell is labeled S. Locations of White Clay Creek Amphibolite samples: G – GREENLAWN2; W – WDCRST2. Locations of Setters microcline gneiss samples: W-60; W-63; W-180; W-194.

possibility, this paper will first examine the nature of the Wissahickon-Glenarm Group contact, and then look at the stratigraphy and geochemistry of the rocks for evidence of their original tectonic setting.

Geologic Setting

The Baltimore Gneiss and Glenarm Group are exposed in four major structures in Chester County, Pennsylvania, three of which are in the area under discussion (figure 1). The West Chester massif lies north of the Avondale anticline, outside of the map area. In the Avondale anticline, Mill Creek anticline, and West Chester massif, basement and cover are raised in anticlines carried on the backs of thrust faults (McKinstry, 1961; Mackin, 1962; Plank et al., 2000). These structures lie within the outcrop area of the Mt. Cuba gneiss unit of the Wissahickon Formation. The Woodville nappe is a distinctly different structure which may be a refolded sheath fold (Blackmer, 2004). It is surrounded by the Doe Run schist unit of the "Glenarm Wissahickon".

The Mt. Cuba Wisahickon is a quartz-plagioclase-biotite gneiss, with or without minor sillimanite, muscovite, and small garnets. The gneiss includes lenses and layers of large-garnet schist with abundant biotite and sillimanite. This unit is described more fully in Plank and Schenck (this volume). The Doe Run schist is a quartz-plagioclase-muscovite-biotite schist with abundant garnet, staurolite, and kyanite. The contact between the Doe Run schist and Mt. Cuba Wissahickon is mapped as an extension of the fault that forms the northern boundary of the Avondale anticline. The original relationship of these units to each other is unclear. They may have been deposited relatively close to each other but in separate subbasins, or they may have been widely separated.

IS THERE A DOE RUN THRUST?

Based on observations in and near the Woodville nappe, Alcock (1994) proposed that the Glenarm Group and the Doe Run schist experienced different structural histories prior to their juxtaposition along the Doe Run thrust. In this model, the major foliation-forming episode in the Glenarm Group was early nappe-style folding prior to emplacement of the Doe Run schist above it on the Doe Run thrust. The Doe Run schist did not experience this nappe folding but brought with it multiple early fabrics. Although fabrics in all units were at least partially reoriented into the regional northeast trend by later folding, the Doe Run schist retained its greater variability in foliation trend.

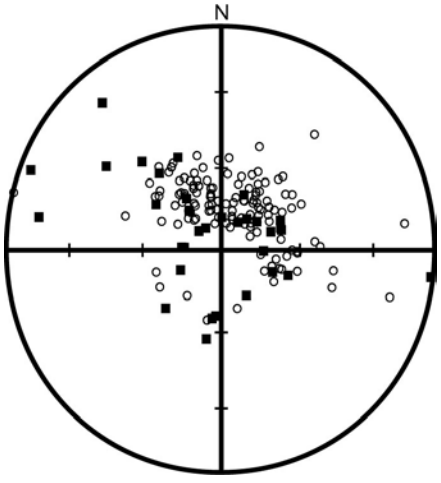

Figure 2. Equal area plot of 164 poles to S2. Symbols: closed squares – Cockeysville Marble and Setters Formation; open circles – "Glenarm Wissahickon".

Thus, one requirement of the Doe Run thrust model is a major structural discontinuity between the Glenarm Group and the Doe Run schist. A second requirement is that the Doe Run schist everywhere overlies the Glenarm Group and Baltimore Gneiss in the Woodville nappe on a low-angle thrust fault which may be locally folded. This section will examine how well these requirements are met.

This investigation found that the structures and structural history are concordant between the Doe Run schist of the Wissahickon Formation and the Glenarm Group. The dominant foliation in all units follows the regional northeast trend, except where it has been affected by later northwest-verging asymmetric folds that are a major influence on the map pattern. In all units, this dominant foliation is the second observable metamorphic foliation. Foliation trends in the "Glenarm Wissahickon" are no more variable than in the Glenarm Group (figure 2). The earliest recognizable foliation in all units is a subvertical compositional layering that strikes nearly north-south. Concordance of even the early structures

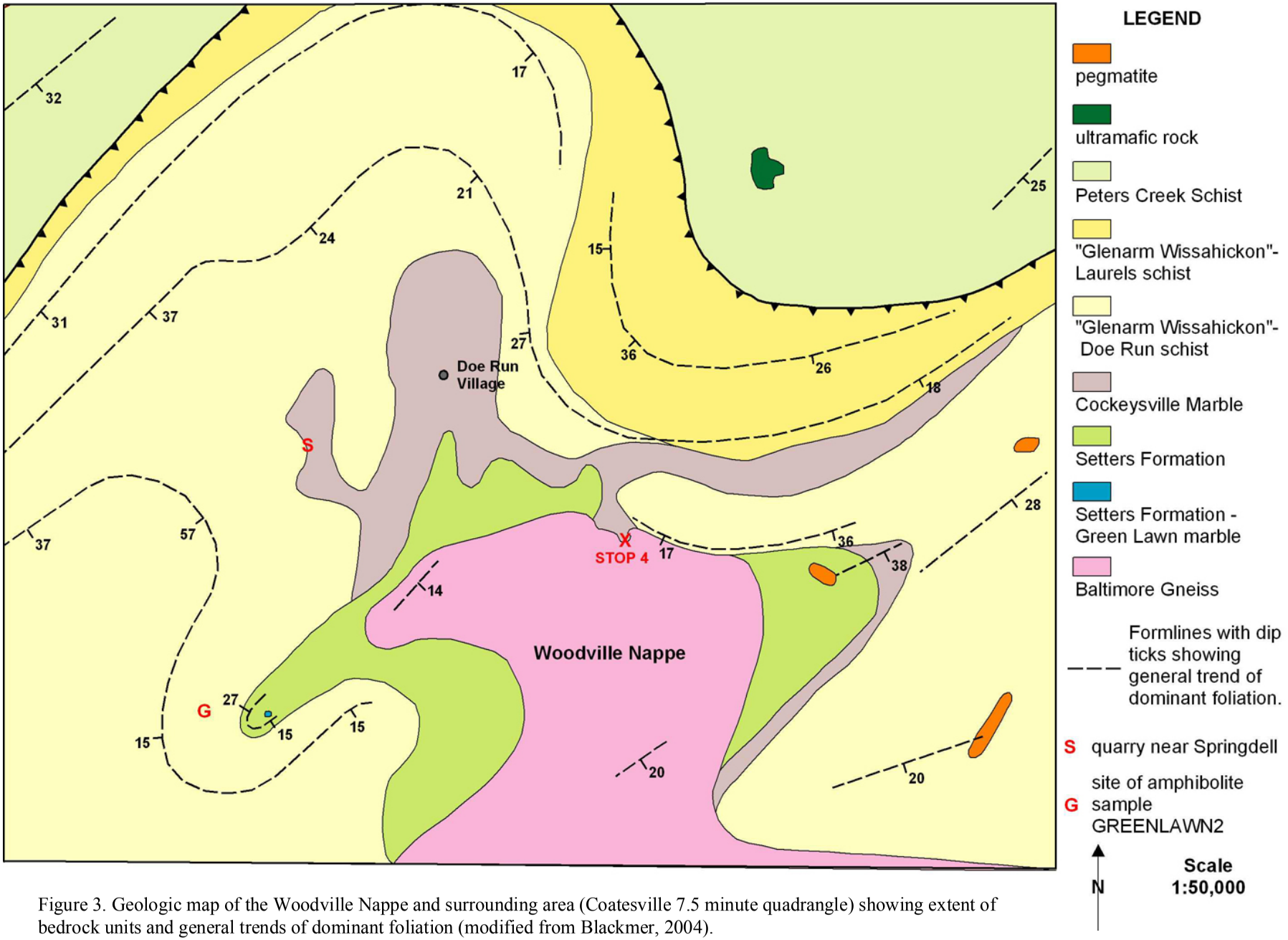

Figure 3. Geologic map of the Woodville Nappe and surrounding area (Coatesville 7.5 minute quadrangle) showing extent of bedrock units and general trends of dominant foliation (modified from Blackmer, 2004).

indicates that the Doe Run schist and Glenarm Group were deformed together throughout their history and not juxtaposed after initial folding. Therefore, there is no need for the Doe Run thrust.

Further evidence for an early contact between the Cockeysville Marble and Doe Run schist comes from a quarry near Springdell (labeled S on figures 1 and 3). Here, marble and schist can be seen complexly infolded at a contact that trends nearly north-south at map scale, parallel to the regional early foliation. At outcrop scale, marble-schist contacts follow the attitude of the early foliation. The dominant foliation cuts across these contacts and partially reorients them, producing folds with axial planes parallel to the dominant foliation. Direct evidence for the nature of this contact – deposition or fault – has been obliterated by subsequent deformation. However, given that the contact pre-dates the observed metamorphic foliations, the simplest assumption is that the marble and schist are a depositional sequence.

The second requirement of the Doe Run thrust model is that the Doe Run schist must always overlie the folded Glenarm Group on a relatively shallowly-dipping contact. One area where this is contradicted is the northeastern boundary of the Woodville nappe. Alcock (1994) shows the Doe Run thrust and its overlying Doe Run schist dipping gently north off the folded Setters and Cockeysville. In fact, the Doe Run schist dips southeast, under the Cockeysville Marble (figure 3; see Stop 4, this volume). Continuing around the eastern side of the nappe, the Doe Run schist and Glenarm Group both retain the southeast dip, such that the schist overlies the Cockeysville on the southeast facing contact. Thus, the Doe Run schist really wraps around the nappe, lying both above and below it. In the absence of a thrust below the Baltimore Gneiss-Glenarm Group fold, for which there is no evidence, the Doe Run schist must be involved in the nappe fold and not overlying it. Blackmer (2004) interprets this structure as the exposed core a sheath fold formed during the same deformation episode as the dominant foliation.

DETAILS OF GLENARM STRATIGRAPHY

The internal stratigraphy of the Setters Formation in Pennsylvania has some distinctive features. In Pennsylvania, three lithologies are found in rocks mapped as Setters. The primary lithology is microcline gneiss consisting of microcline (50-70%), muscovite, biotite, and quartz. Locally, muscovite content is sufficiently high to make the rock a schist. Most of this muscovite is coarse-grained and post-kinematic. The next most common lithology is quartzite having minor microcline, plagioclase, muscovite, and biotite. A layer of biotite-muscovite-quartz schist with large garnet and tourmaline crystals that is perhaps 500 feet thick underlies the hill that extends from southeast of Avondale towards Toughkenamon. The stratigraphic order of these units within the formation is not clear. Except for a single meter-scale layer of microcline gneiss within quartzite south of London Grove, the quartzite and microcline gneiss are found in separate bands. Both occupy the same position between Baltimore Gneiss and Cockeysville Marble. The garnet schist is found only in the location noted above as a layer within microcline gneiss. This is clearly not the same stratigraphy described by Knopf and Jonas (1923) for the Setters Formation in Maryland. There, the Setters consists of a basal biotite-quartz-microcline gneiss with minor calcite overlain by biotite-quartz-feldspar schist with abundant garnets, quartzite with minor muscovite and microcline, and another layer of mica schist. The Pennsylvania Setters bears a much greater similarity to the Setters in Delaware, which varies from feldspathic or micaceous quartzite to feldspathic mica schist or gneiss (Woodruff and Plank, 1995). Either these differences represent a facies change between Maryland and Pennsylvania-Delaware, or the correlation of all of these rocks as the same formation is incorrect.

The Setters microcline gneiss has a sufficiently unusual composition to warrant further investigation. Four samples were collected, trimmed, and sent to ActLabs for crushing, preparation, and chemical analysis (table 1). All samples contained some weathered and iron-stained surfaces even after trimming, so one sample of weathered material was analyzed for comparison. The

composition of W-180-weathered is not significantly different from the composition of W-180, except for the light and middle rare earth elements (REE), which are approximately twice as high in W-180-weathered than in W-180. This may be due to fortuitous inclusion of material in W-180-weathered that is rich in accessory phases, such as apatite, rather than the weathering of the sample. The results suggest that minor weathering and oxidation of iron has not significantly altered the geochemical compositions of the samples.

Table 1. Chemical analyses of Setters Formation microcline gneiss

SAMPLE	SiO_2	TiO_2	Al_2O_3	Fe_2O_3	MnO	MgO	CaO	Na_2O	K_2O	P_2O_5
W-60	72.51	0.897	12.20	3.04	0.021	0.54	0.14	0.59	8.36	0.15
W-63	72.33	0.968	11.64	3.29	0.035	0.94	0.92	0.67	8.17	0.19
W-180	61.76	1.147	17.84	3.46	0.030	0.93	0.40	0.93	12.19	0.11
W-194	73.06	0.747	12.92	2.55	0.010	0.60	0.08	0.55	8.90	0.11
W-180-WEATH	61.85	1.155	17.88	3.56	0.024	0.8	0.24	0.9	12.33	0.09

SAMPLE	Sr	Rb	Cs	Ba	Sc	V	Cr	Co	Ni	Cu
W-60	120	110	1.6	1082	8.44	48	39.2	5	96	96
W-63	106	100	1.7	864	8	47	34.9	7.1	49	49
W-180	211	110	1.1	1078	11.8	78	52.7	19.2	64	64
W-194	122	107	1.5	1171	8.92	46	38.5	3.5	125	125
W-180-WEATH	213	106	1	1102	11.6	76	51.3	9.7	53	53

SAMPLE	Y	Zr	Zn	La	Ce	Nd	Sm	Eu	Tb	Yb
W-60	40	898	39	37.3	76	36	7.48	1.83	0.9	4.6
W-63	45	1018	33	37.7	82	36	7.54	1.81	0.9	4.75
W-180	22	749	37	9.2	18	8	1.87	1.22	0.3	2.86
W-194	29	681	29	34.8	74	31	6.75	1.55	0.7	3.31
W-180-WEATH	26	764	36	18.3	33	17	3.29	1.41	0.6	3

SAMPLE	Lu	Hf	Ta	Pb	Th	U
W-60	0.69	20.3	0.8	16	11.6	4.6
W-63	0.72	22.4	0.8	16	10.7	5.5
W-180	0.43	16.7	1.1	18	8.7	4.1
W-194	0.51	15.1	0.8	17	9.7	3.6
W-180-WEATH	0.45	17.2	0.8	21	8.4	3.4

The most obvious possible parent rocks for the Setters microcline gneiss are a K-feldspar-rich felsic igneous rock (trachyte or syenite) or sedimentary rock (feldspathic sandstone or arkose). On the total alkalis vs. silica diagram (figure 4), three samples plot as rhyolites (W-60, W-63, and W-194), and sample W-180 (and W-180-weathered) plots as a trachyte. A striking feature of the chemical compositions of the Setters microcline gneiss samples is the high to very high K_2O (8-12 weight percent) with very low Na_2O (0.55-0.93 weight percent). This is not found in common trachytes and rhyolites, which typically contain subequal amounts of K_2O and Na_2O. The REE patterns are smoothly varying and consistent with an igneous parent (figure 5); however, a sedimentary parent rock containing mostly K-feldspar and quartz from an igneous source also could display these REE patterns. The positive Eu anomalies in samples W-180 and W-180-weathered are consistent with feldspar accumulation during magma crystallization, while the slight negative Eu

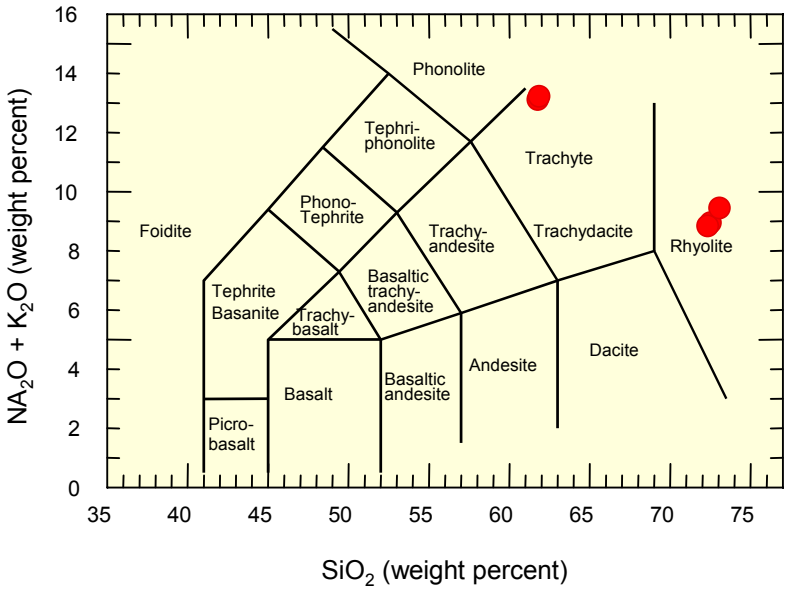

Figure 4. Total alkalis ($Na_2O + K_2O$) v. silica plot of Setters microcline gneiss samples, and the classification of volcanic rocks from Le Bas et al. (1986).

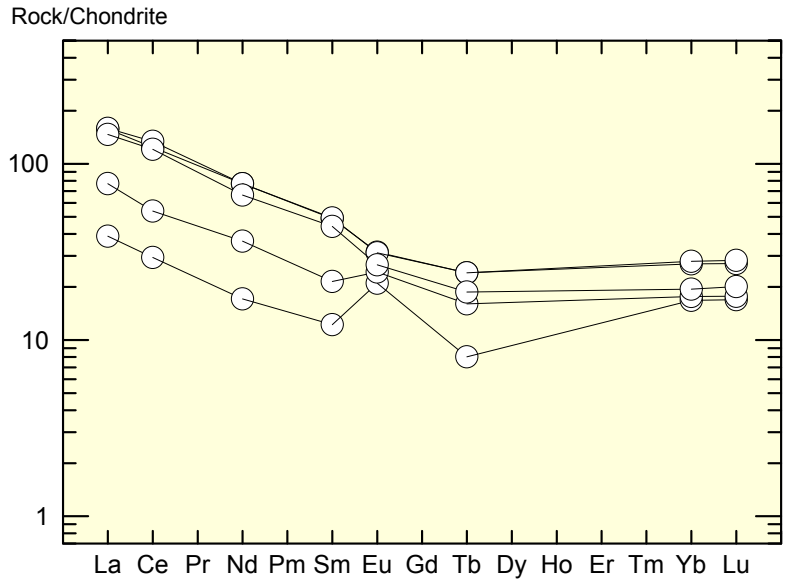

Figure 5. Rare earth element (REE) patterns for Setters microcline gneiss samples. Chondrite values of Sun and McDonough (1989).

anomalies in the other samples are a typical signature of the liquid from which feldspar is fractionating.

In order to obtain a more complete picture of the implications of the geochemistry, the Setters microcline gneiss was compared with both igneous and sedimentary rocks from the published literature. The first criterion for comparison was a good match to the major element chemistry, particularly the high K_2O and very low Na_2O. After this criterion was met, the trace elements were compared. Both volcanic and sedimentary rocks were found to be a good match to the Setters, and in

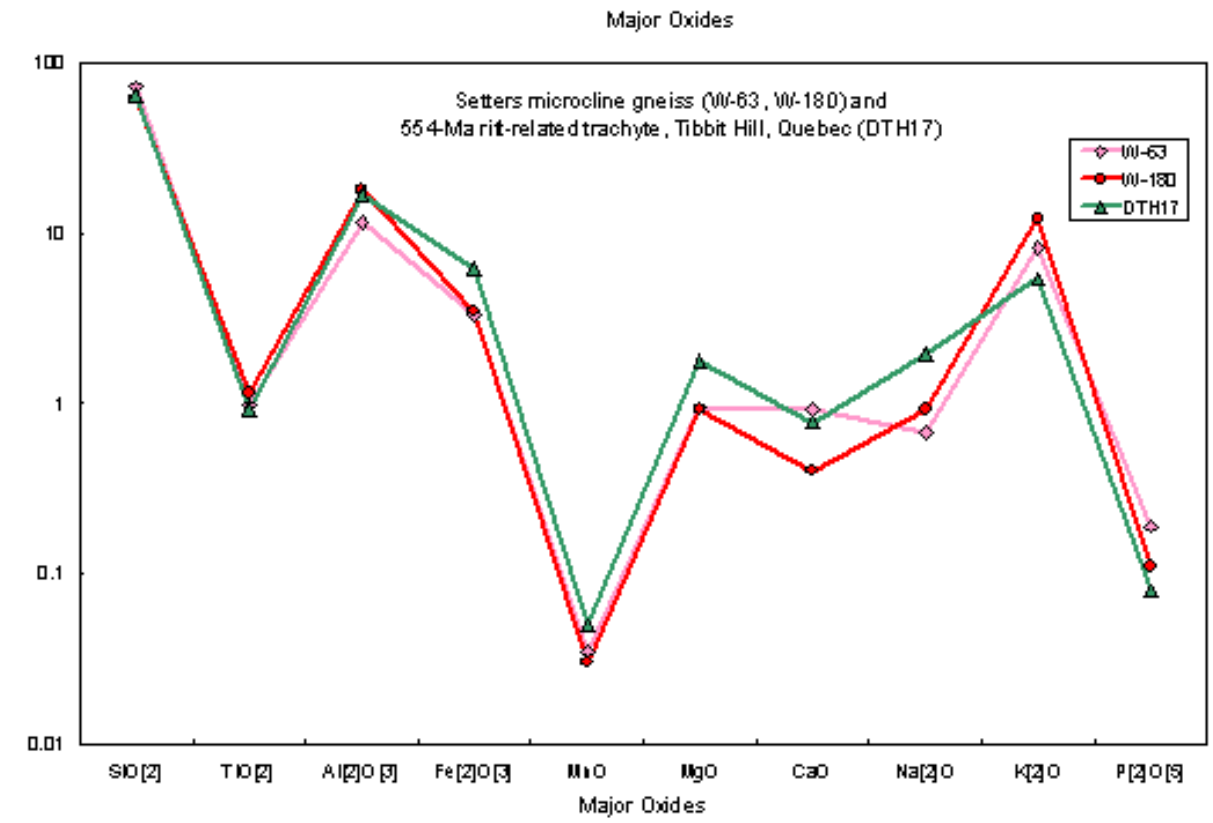

A

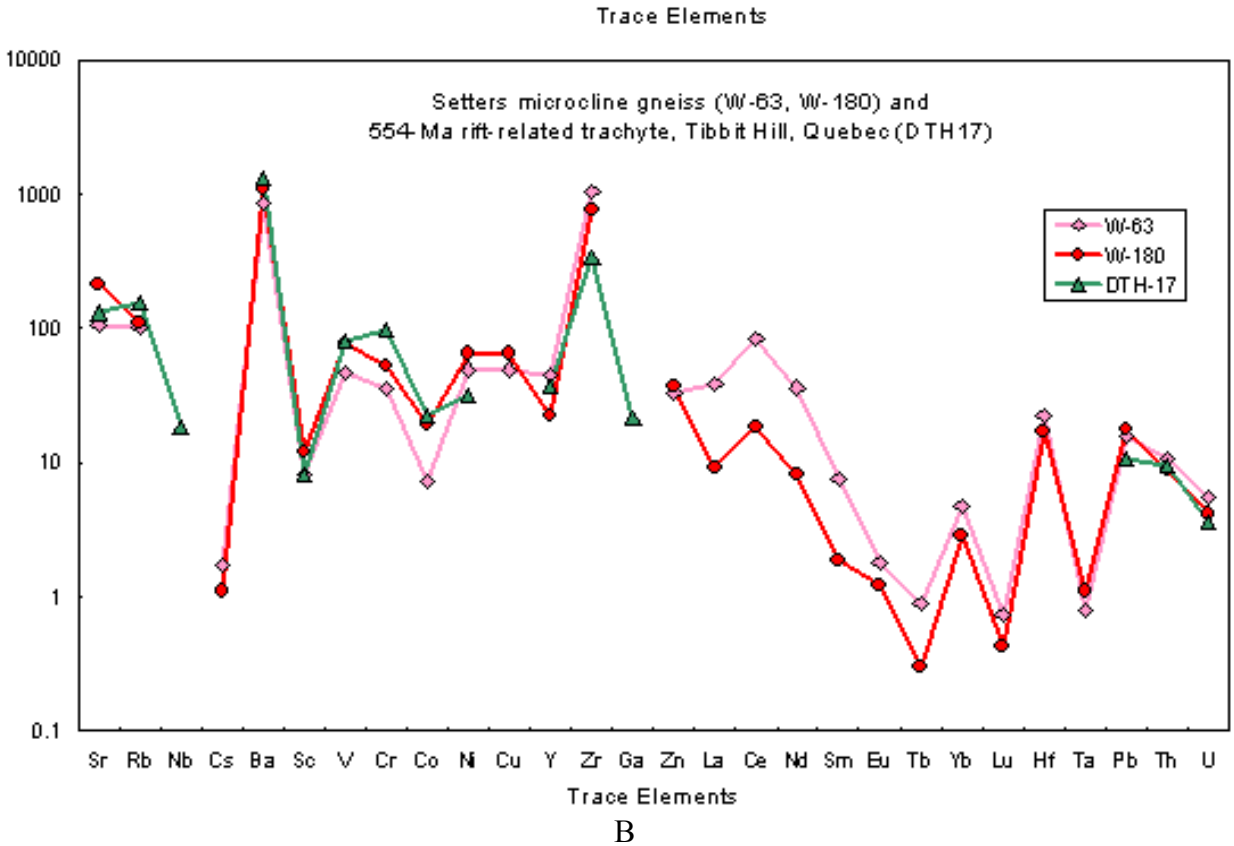

B

Figure 6. Geochemical analyses of Setters microcline gneiss compared to a rift-related trachyte from Tibbit Hill, Quebec (data from Abdel-Rahman and Kumarapeli, 1998). A. Major oxide analyses. B. Trace element analyses.

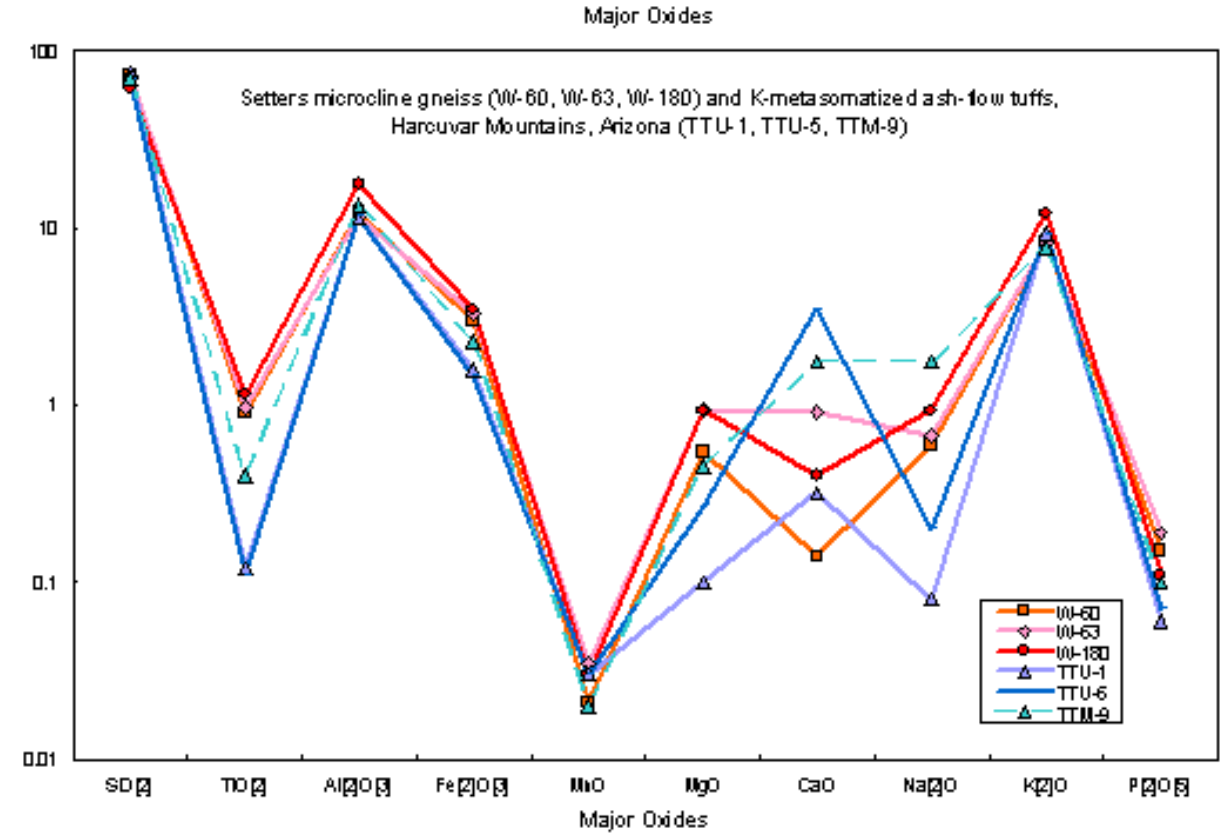

A

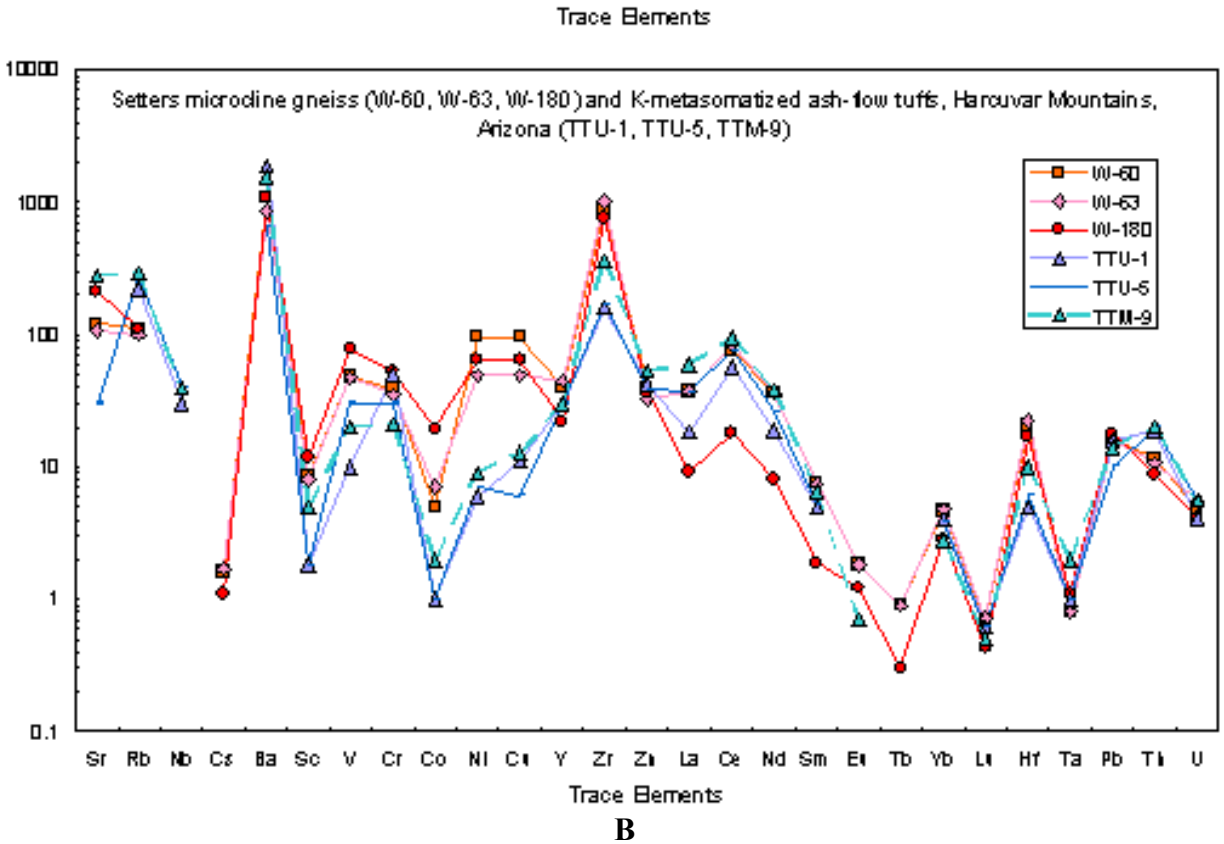

B

Figure 7. Geochemical analyses of Setters microcline gneiss compared to potassium-metasomatized tuffs from the Harcuvar Mountains, Arizona (data from Roddy et al., 1988). A. Major oxide analyses. B. Trace element analyses.

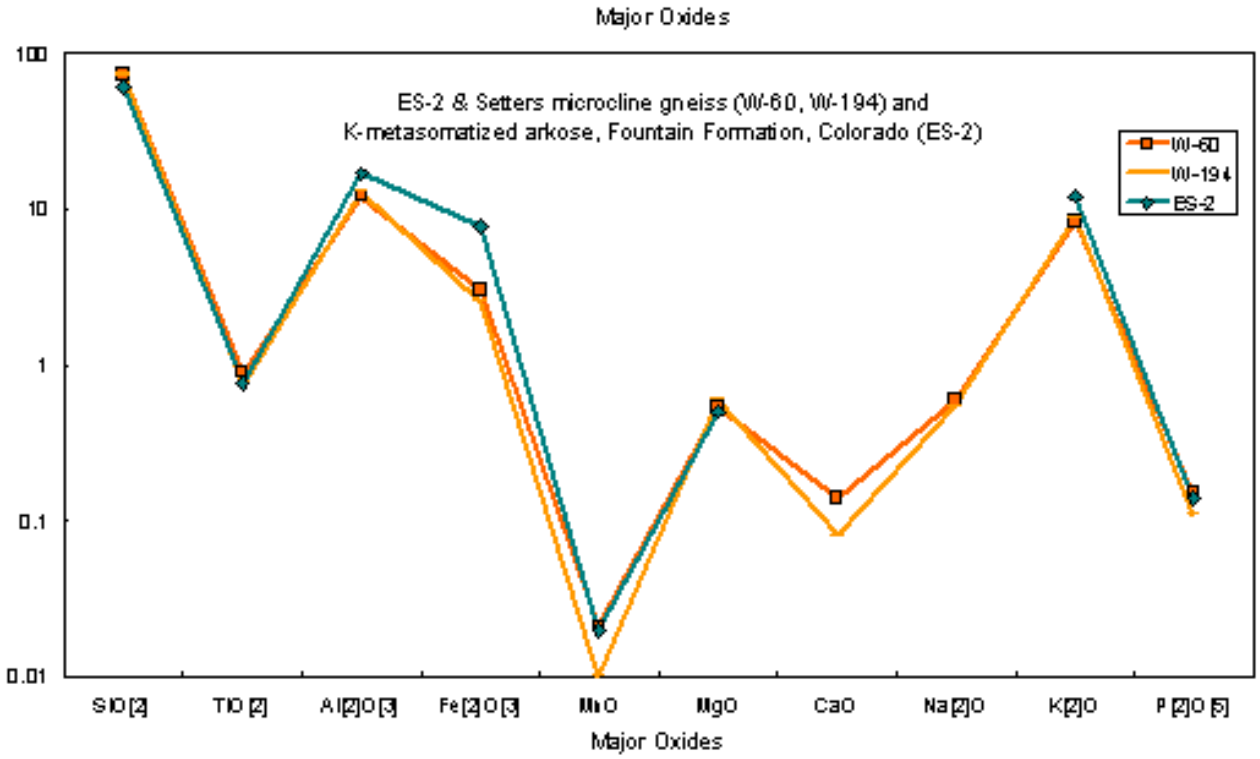

A

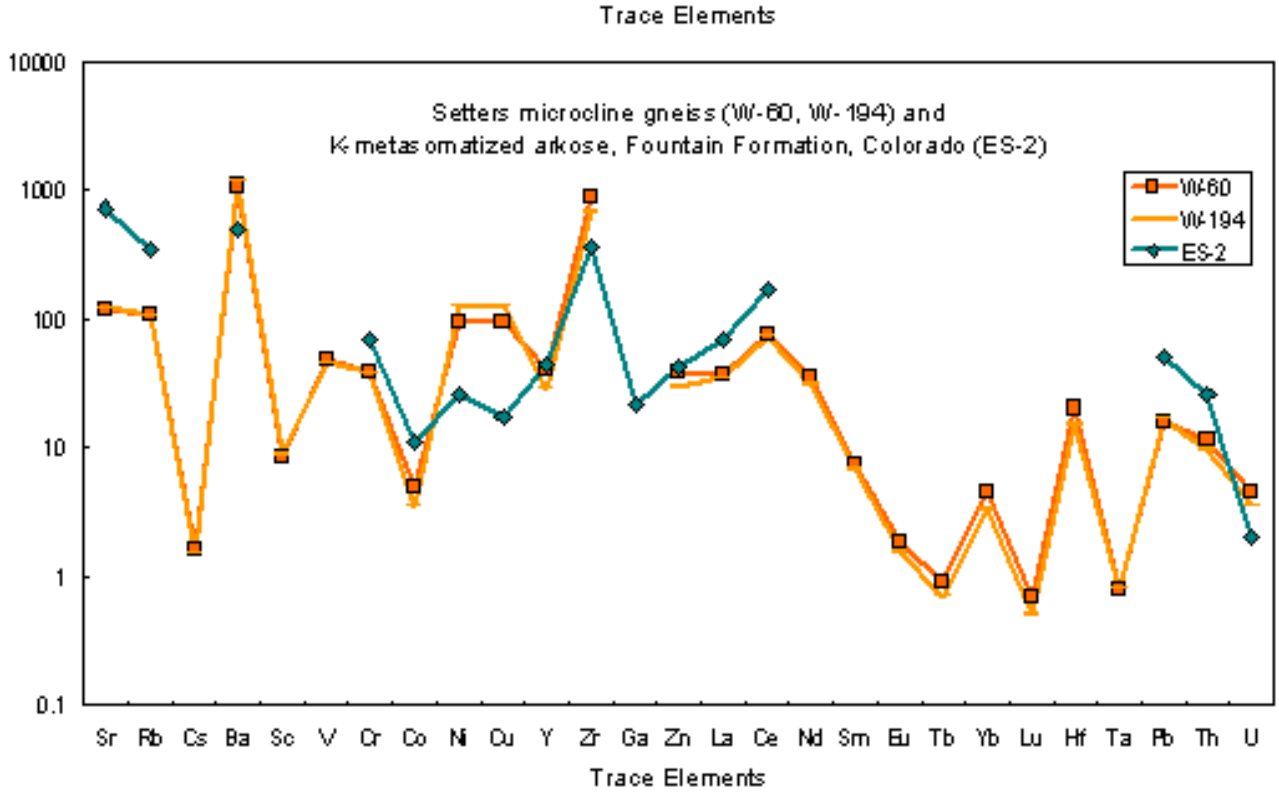

B

Figure 8. Geochemical analyses of Setters microcline gneiss compared to a potassium-metasomatized arkose from the Fountain Formation, Colorado (data from Van de Kamp, 1994). A. Major oxide analyses. B. Trace element analyses.

two of the three examples found, the rocks have been extensively metasomatized to increase the K_2O and remove Na_2O. The best matches are: the 554-Ma, rift-related Tibbit Hill volcanic suite from the Quebec Appalachians (figure 6); Tertiary metasomatized tuffs from the Harcuvar Mountains, Arizona, related to crustal extension (figure 7); and Pennsylvanian-Permian arkoses from the Fountain Formation in Colorado and Utah, deposited as alluvial-fluvial sediments at the time of uplift of the ancestral Rockies and metasomatized during Tertiary crustal extension (figure 8). Although these geochemical analogs do not provide a conclusive parent for the Setters microcline gneiss, their common feature is that they are all related in some way to continental rifting or crustal extension.

The map distribution of Glenarm Group rocks also provides some clues to depositional environment. The traditional model for Glenarm Group stratigraphy has been layer-cake deposition of continentally-derived clastic sediments succeeded by carbonate on a continental platform. In general, the layer-cake model is correct. A reasonable thickness of Setters Formation gneiss, quartzite, and schist overlies Baltimore Gneiss and is in turn overlain by Cockeysville Marble. In places, Setters is not present, either through erosion or non-deposition, and Cockeysville directly overlies Baltimore Gneiss. However, recent mapping has shown that this model breaks down in the details (inside front cover). Lenses of rock identical to Setters microcline gneiss are found within Cockeysville Marble between the Avondale anticline and Woodville nappe. Another lens is found within the Mt. Cuba gneiss south of the Avondale anticline. Meter-scale, Setters-like clastic layers too thin to map are found interlayered with marble in several quarries. There is a lens of marble within the Setters on the west side of the Woodville nappe, and others within the Mt. Cuba gneiss south of the Avondale anticline and near the southwestern end of the Mill Creek anticline. The Cockeysville Marble appears to be interfingered with the Mt. Cuba gneiss, also at the southwestern end of the Mill Creek anticline. The irregularity of this stratigraphy suggests a depositional environment less stable than a continental platform.

GEOCHEMISTRY OF AMPHIBOLITES FROM THE DOE RUN SCHIST OF THE WISSAHICKON FORMATION

The most useful information about the original tectonic setting of the Doe Run schist unit of the Wissahickon Formation comes from the geochemistry of amphibolites which originated as basaltic volcanic layers within the Wissahickon sediments. Two amphibolite samples from the Doe Run schist have been analyzed. These are located immediately west of Green Lawn (sample GREENLAWN2, reported in Plank et al., 2001; Coatesville Quadrangle) and between Jennersville and Chatham (sample WDCRST2, reported in Smith and Barnes, this volume; West Grove Quadrangle). Both of these amphibolites exhibit moderate to high TiO_2 and overall high rare earth element abundances with a negatively sloping pattern. This geochemistry is typical of a group of amphibolites in the Mt. Cuba gneiss of the "Arc" Wissahickon named White Clay Creek Amphibolite by Smith and Barnes (1994) and referred to as Type 2 amphibolites by Plank et al. (2001). Plank et al. (2001) interprets these as ocean-island basalts that may represent seamounts scraped off the subducting slab and incorporated into the forearc sediments. In contrast, Smith and Barnes (2001, written communication) favor an origin involving continental crust, possibly as continental initial rift basalts.

DISCUSSION: A NEW MODEL

Several factors drawn from observations made during recent mapping bear on the tectonic interpretation of the Glenarm Group and the Doe Run schist of the Wissahickon Formation. First, this analysis indicates that the Glenarm Group and the Doe Run schist are stratigraphically continuous. Second, interlayering of marble and microcline gneiss suggests that the Glenarm Group was deposited in a somewhat unstable environment capable of abrupt shifts between clastic and

carbonate sedimentation. Third, the geochemistry of both the Setters microcline gneiss and the Doe Run schist amphibolites opens the possibility of a rift-related environment.

Although none of these factors is conclusive by itself, taken together they suggest that these rocks may represent early marine sediments deposited in an opening continental rift still floored by continental crust, analogous to the Oligocene-Miocene sediments in the Gulf of Suez (Bosworth and McClay, 2001). The Setters Formation represents early clastic sedimentation in the new basin. The microcline gneiss may represent acidic magmas or tuffs generated early in rifting, or sediments derived from igneous rocks in the Baltimore Gneiss, or a combination of these. Carbonates formed as platforms on basement highs or as small reef caps. As the rift grew, the entire area was flooded by the aluminous sediments and interlayered alkalic basalt that became the Doe Run schist of the Wissahickon Formation. Shifting fault blocks within the rift exerted local control on sedimentation and led to the interlayering of carbonate and clastic sediments in response to local changes in water depth and sediment source.

A consideration of the Mt. Cuba Wissahickon

A common feature of the western part of the Mt. Cuba Wissahickon and the Doe Run schist is that they are both presently in contact with the Glenarm Group. Schenck and Plank (this volume) hypothesize that the Mt. Cuba Wissahickon, unlike the Doe Run schist, was part of a forearc accretionary complex. As evidence, they cite interfingering of the easternmost Mt. Cuba Wissahickon with forearc volcanic and plutonic rocks of the Wilmington Complex and the presence of amphibolites representing both slivers of ocean floor (Kennett Square Amphibolite) and the remains of seamounts (White Clay Creek Amphibolite). They further state that the Mt. Cuba Wissahickon contains Grenvillian zircon, indicating that at least some of the clastic sediments were continentally derived, possibly turbidites deposited on the continental slope or rise, subsequently scraped off the subducting plate and incorporated into the forearc. This forearc assemblage would have been thrust over the Glenarm Group on the continental margin as the ocean basin finally closed.

Although this investigation found no structural discontinuity between the Mt. Cuba Wissahickon and the Glenarm Group, there is also no conclusive direct evidence as to the nature of the contact between them. However, if we follow the interpretation of Smith and Barnes (this volume) that the White Clay Creek Amphibolite originated in a continental rift setting, the evidence cited above also lends itself to an origin similar to that of the Doe Run schist. Sediments deposited in a continental rift would necessarily have had a Grenvillian source. The non-random distribution of the two types of amphibolite, one with ocean-floor geochemical signatures and one with continental rift signatures, in broad belts suggests to this author that the volcanics were deposited contemporaneously with the surrounding sediments and not tectonically incorporated at a later time. The sediments might represent a time period spanning initiation of rifting accompanied by within plate magmatism through the transition to sea-floor spreading and production of ocean floor basalt (see also Smith and Barnes, 1994, p. 72-A). A similar geochemical evolution in metabasalts of the Turkey Mountain Member of the Hoosac Formation in Vermont from an alkalic, rift-like composition in the lower parts of the formation to ocean-floor composition in the upper parts has been interpreted as recording progressive rifting and the transition to drift (Ratcliffe and Armstrong, 1999). The Mt. Cuba Wissahickon is sufficiently different from the Doe Run schist in terms of mineralogy and volume of amphibolite to suggest that the two units would have been deposited in different subbasins within the rift. The metamorphic history also indicates that the two units might have originated some distance apart, since the Mt. Cuba Wissahickon is at a higher metamorphic grade and is extensively migmatized. This suggests that even if it did originate in a continental rift, the Mt. Cuba Wissahickon may still have been incorporated into the forearc, allowing the observed interactions with the Wilmington Complex, while the Doe Run schist remained outside the forearc.

Acknowledgements. LeeAnn Srogi and Tracy Ellis (West Chester University) contributed the Setters Formation geochemical analyses and interpretation.

References

Abdel-Rahman, A. M., and Kumarapeli, P. S., 1998, Geochemistry of mantle-related intermediate rocks from the Tibbit Hill volcanic suite, Quebec Appalachians: Mineralogical Magazine, v. 62, p. 487-500.

Alcock, J., 1994, The discordant Doe Run thrust: Implications for stratigraphy and structure in the Glenarm Supergroup, southeastern Pennsylvania Piedmont: Geological Society of America Bulletin, v. 106, p. 932-941.

Blackmer, G. C., 2004, Bedrock geology of the Coatesville Quadrangle, Chester County, Pennsylvania…

Bliss, E. F., and Jonas, A. I., 1916, Relation of the Wissahickon mica gneiss to the Shenandoah limestone and the Octoraro schist of the Doe Run and Avondale region, Chester County, Pennsylvania: U.S.G.S. Professional Paper 98, p. 9-34.

Bosworth, W. and McClay, K.R., 2001, Structural and stratigraphic evolution of the Gulf of Suez rift, Egypt: A synthesis, *in* Ziegler, P., Cavazza, W., Robertson, A.H.F.R., and Crasquin-Soleau, S., eds., Peri-Tethys memoir 6; Peri-Tethyan rift/wrench basins and passive margins, Memoirs du Museum National d'Histoire Naturelle de Paris 186, p. 567-606.

Drake, A. A., 1993, The Soldiers Delight Ultramafite in the Maryland Piedmont: U.S. Geological Survey Bulletin 2076, p. A1-A13.

Higgins, M. W., 1977, Six new members of the James Run Formation, Cecil County, northeastern Maryland, *in* Sohl, N. F. and Wright, W. B., Changes in stratigraphic nomenclature by the U.S. Geological Survey, 1976: U.S. Geological Survey Bulletin 1435-A, p. A122-A127.

Knopf , E. B., and Jonas, A. I., 1923, Stratigraphy of the crystalline schists of Pennsylvania and Maryland: American Journal of Science, v. 5, p. 40-62.

Le Bas, M. J., Le Maitre, R. W., Streckeisen, A., and Zanettin, B., 1986, A chemical classification of volcanic rocks based on the total alkali-silica diagram: Journal of Petrology, v. 27, p. 745-750.

Mackin, J.H., 1962, Structure of the Glenarm Series in Chester County, Pennsylvania: Geological Society of America Bulletin, v. 73, p. 403-410.

McKinstry, H., 1961, Structure of the Glenarm Series in Chester County, Pennsylvania: Geological Society of America Bulletin, v. 72, p. 557-578.

Plank, M. O., Schenck, W. S., and Srogi, L., 2000, Bedrock geology of the Piedmont of Delaware and adjacent Pennsylvania: Delaware Geological Survey, Report of Investigations no. 59, 52 p., 1 pl.

Plank, M. O., Srogi, L., Schenck, W. S., and Plank, T. A., 2001, Geochemistry of the mafic rocks, Delaware Piedmont and adjacent Pennsylvania and Maryland: Confirmation of arc affinity: Delaware Geological Survey, Report of Investigations no. 60, 39 p.

Ratcliffe, N. M., and Armstrong, T. R., 1999, Bedrock geologic map of the West Dover and Jacksonville quadrangles, Windham County, Vermont: USGS Miscellaneous Investigations Series Map I-2552, 1:24,000.

Roddy, M., Reynolds, S., Smith, B., and Ruiz, J., 1988, K-metasomatism and detachment-related mineralization, Harcuvar mountains, Arizona: Geological Society of America Bulletin, v. 100, p. 1627-1639.

Smith, R. C., II, and Barnes, J. H., 1994, Geochemistry and geology of metabasalt in southeastern Pennsylvania and adjacent Maryland, *in* Faill, R.T. and Sevon, W. D., *eds*., Various aspects of Piedmont geology in Lancaster and Chester Counties, Pennsylvania: Annual Field Conference of Pennsylvania Geologists, 59th, Lancaster, PA, Guidebook, p. 45-72.

Sun, S.-S., and McDonough, W.F., 1989, Chemical and isotopic systematics of oceanic basalts: Implications for mantle composition and processes, *in* Saunders, A. D., and Norry, M. J., *eds*., Magmatism in the ocean basins: London, England, Geological Society of London Special Publication 42, p. 313-345.

Van de Kamp, P., 1994, Petrology, geochemistry, provenance, and alteration of Pennsylvanian-Permian arkose, Colorado and Utah: Geological Society of America Bulletin, v. 106, p. 1571-1582.

Woodruff, K. D., and Plank, M. O., 1995, Geology of the Cockeysville Formation, *in* Talley, J. H. *ed.*, Geology and hydrology of the Cockeysville Formation northern New Castle County, Delaware: Delaware Geological Survey, Bulletin No. 19, p. 1-25, 1 pl.

WHITE CLAY CREEK AMPHIBOLITE: A PIEDMONT ANALOG OF THE CATOCTIN METABASALT

by
Robert C. Smith, II and John H. Barnes

Abstract

Analyses of additional samples of the White Clay Creek Amphibolite beyond those studied by Smith and Barnes (1994) in southern Chester County, Pennsylvania, and adjacent Delaware have extended the known geographic limits of the formation and refined its geochemical affinity. It has now been verified in the Bay View, Coatesville, Kennett Square, Newark West, and West Grove 7 ½' quadrangles. Some geochemical correlations are now available from the type locality on White Clay Creek, Pennsylvania, to a principal reference section in the Wilmington and Western Railroad cut, Yorklyn, Delaware. Examination of the relatively large range of compositions, trace element discriminant diagrams, and geologic settings suggests that the White Clay Creek Amphibolite is a continental initial rifting tholeiite. The median composition of the White Clay Creek is similar to the median compositions of the Catoctin Metabasalt of the South Mountain anticlinorium NW of the Tunnel Hill-Jacks Mountain fault system; the Fishing Creek Metabasalt Member of the Sams Creek Formation of Lancaster County; some Sams Creek equivalent metabasalts in southwestern York County; the type and *de facto* reference section Sams Creek Metabasalt of Maryland; the Accomac Metabasalt of York County; and Catoctin Metadiabase dikes in Grenvillian terranes, such as the Womelsdorf outlier, Reading Prong, Honeybrook Upland, and Trenton Prong. This similarity and limited $^{143}Nd/^{144}Nd$ data suggest that all are cogenetic and approximately synchronous. Thus, the White Clay Creek Amphibolite is believed to be of latest Neoproterozoic age as are the others. As such, it should be considered a formation within a mappable continental Laurentian group consisting of it and the host "Wissahickon" and it should make an excellent marker unit to define both the Precambrian-Cambrian boundary and the continental (~Humber-)-oceanic (~Dunnage-equivalent) boundary in the Piedmont of southeastern Pennsylvania and adjacent Delaware.

INTRODUCTION

Some refinement of the affinity of mafic rocks in southeastern Pennsylvania has been achieved since the 1994 Field Conference of Pennsylvania Geologists. In particular, the affinity of the White Clay Creek Amphibolite (WCCA) has been further restricted by additional trace element data and limited Nd isotopic data. Based on these new data, the WCCA appears to have a Late Neoproterozoic age and to extend the Catoctin Metabasalt *sensu lato* farther southeast than previously recognized. Overall, the Catoctin Metabasalt sensu lato is hypothesized to be the result of a transition from rifting to drifting that occurred in fits and starts over a period of millions of years (Smith, 2003).

The White Clay Creek Amphibolite was introduced by Smith and Barnes (1994) as an enigmatic group of 12 mafic bodies in southern Chester County, Pennsylvania, and adjacent Delaware at amphibolite grade metamorphism. They noted that the shape of some of bodies suggested thin flows and that the wide range of TiO_2 content, from 1.66 to 4.75 %, was similar to that of Catoctin Metabasalt, a continental rift basalt of late Neoproterozoic age. However, based on the possibility of associated reef caps, ocean island basalt (OIB) was not ruled out. As a result, they

Smith, II, R. C., and Barnes, J. H., 2004, Whit Clay Creek Amphibolite: A Piedmont analog of the Catoctin Metabasalt, *in* Blackmer, G. C., and Srogi, L., Marginalia – Magmatic arcs and continental margins in Delaware and southeastern Pennsylvania: Guidebook, 69th Annual Field Conference of Pennsylvania Geologists, West Chester, PA, p. 28-45.

did not include WCCA in their conceptual rift-to-drift table (p. 72-A) of "Catoctin group" median trace element analyses. Smith *et al*. (1991, p. 5) had noted that these same probable flows near the Brandywine massifs were not readily distinguishable from Catoctin Metabasalt and that it appeared that magmas of Catoctin affinity were not restricted to the South Mountain anticlinorium. To them, the Catoctin event appeared to be the most underrated geologic event in the Appalachians. Data are now available for 21WCCA bodies sampled by the senior author and the first carbonate reef cap has yet to be found. The locations from which the presently recognized WCCA samples were collected are shown in Figure 9. In general, they seem to define a southwest plunging anticline around the southwest end of the Brandywine massifs. The southeast limb, however, seems to be separated from the south side of the massif by a narrow syncline, presumed to be a folded thrust fault, containing the oceanic Kennett Square Amphibolite bodies.

Because it bears on the age of the WCCA, a note in Smith and Barnes (1994) should be expanded here. Old reports that Catoctin Metadiabase dikes cut the Lower Cambrian Hardyston Formation in the Reading Prong are incorrect. Field examination by the senior author and Sam W. Berkheiser showed that the apparent crosscutting relationship was based on float mapping influenced by topography. By serendipity, they happened to find outcrop in an excavation for a new house showing that the metadiabase dike was not crosscutting.

Shortly after the 1994 Field Conference of Pennsylvania Geologists, it was recognized that median compositions for WCCA are very similar to those for Catoctin metadiabase dikes in Grenvillian terranes and other Catoctin Metabasalt, *sensu lato*, formations. These median data are shown in Table 2, in which the Catoctin has been divided into related subgroups based on immobile trace element content. Relatively complete analyses are included in Appendix I, Table 1 and precision and accuracy are discussed in Appendix I, Table 2.

At the request of Robert R. Jordan, then Delaware State Geologist, the senior author assisted Margaret (Peg) O. Plank and William (Sandy) S. Schenck of the Delaware Geological Survey with two days of field sampling on May 4th and 5th, 2000. On the second day, Peg took the senior author to the Wilmington and Western Railroad cut, Yorklyn, Delaware, which he recognized as containing a section very similar to the White Clay Creek type section (Table 2), Pennsylvania. (That same day Peg showed the senior author serpentinites near Hoopes, Reservoir where he recognized a relatively intact cumulate mafic complex similar to the Baltimore Mafic Complex. Unfortunately, he failed to fully appreciate the fact that he might have crossed Delaware's version of the Baie Verte-Brompton line just after sampling a Catoctin-affinity WCCA outcrop, sampled as WCCMC, which Peg showed him only 1.2 km to the northwest!) Because one or two individual flows can be geochemically correlated from the Wilmington and Western Railroad cut, Yorklyn, Delaware, to the designated type section along White Clay Creek (39^{o} 47'20"N, 75^{o} 48' 09"W), the Yorklyn section (39^{o} 48' 29"N, 75^{o} 40' 16"W) is herein proposed as the principal reference section for the WCCA. (For example, sample WCCMBI 10-20CM (Appendix I, Table 1) from the type section seems to be geochemically paired with sample WCCW+W from the principal reference section.) This field work was followed by sample preparation and commercial analyses obtained by the Pennsylvania Geological Survey.

The present authors provided the Delaware Geological Survey with an unpublished report (updated for them on 2/7/01) on WCCA and 13 analyses from Pennsylvania and 3 from Delaware. Plank *et al.* (2001) combined these with additional data for samples from Delaware and discussed them as "type 2." Since then, the senior author has conducted additional sampling in the Wilmington and Western Railroad cut and at a few localities in Pennsylvania.

Smith (2003) attempted to provide an overview of two stages of Iapetan rifting in eastern North America as it pertains to Pennsylvania.

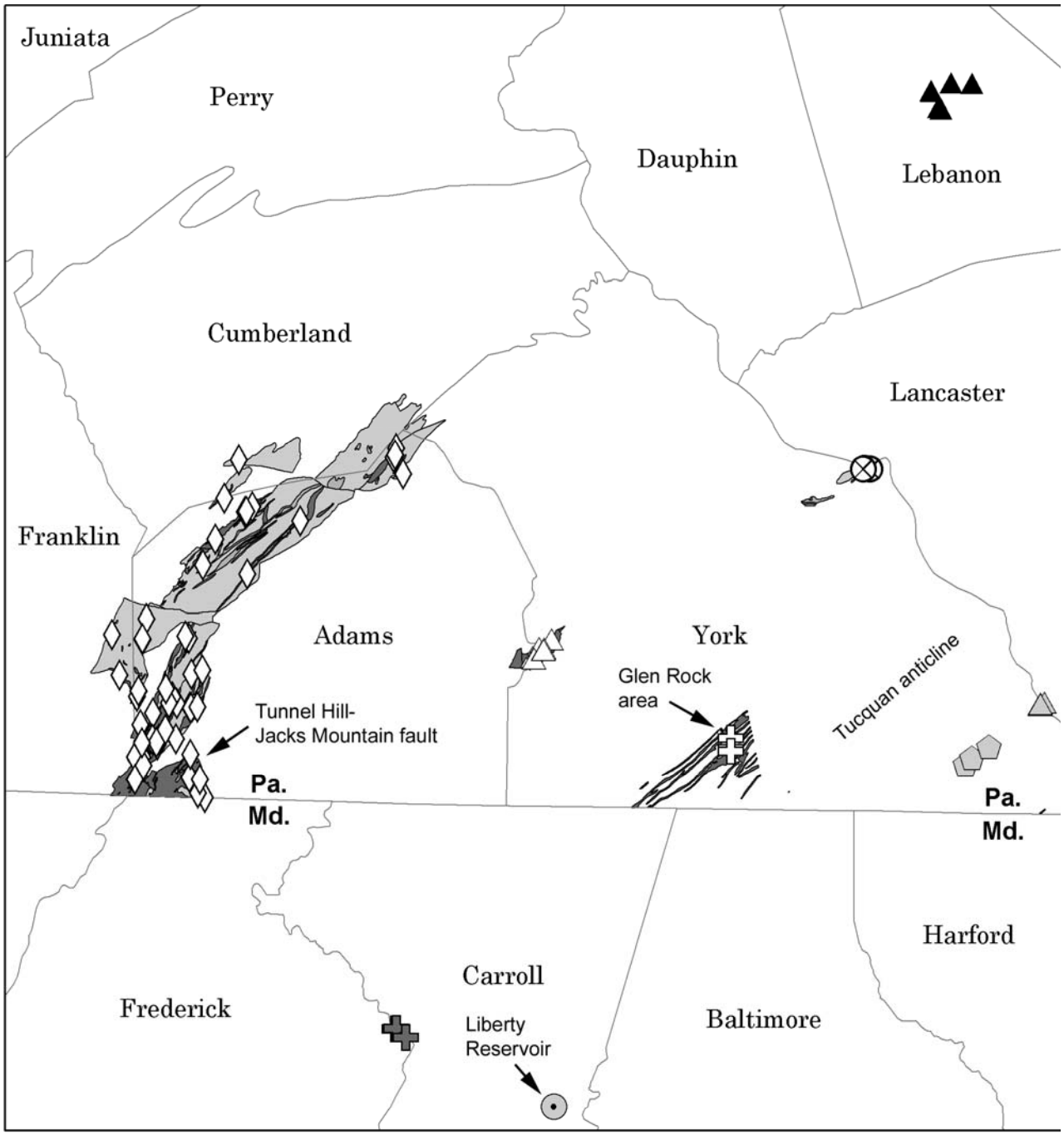

- Accomac Metabasalt
- "Bald Eagle Creek metabasalt"
- Bald Friar Metabasalt
- Catoctin Metabasalt dikes in Grenvillian terrains
- Catoctin Metadiabase
- "Conowingo Creek metabasalt"
- Fishing Creek Metabasalt
- Holtwood Metabasalt
- James Run Metabasalt
- Jonestown Volcanic Complex
- Kennett Square Amphibolite
- "Nottingham County Park amphibolite"
- Pigeon Hills Metabasalt
- Sams Creek Metabasalt–Md.
- Sams Creek Metabasalt–Pa.
- White Clay Creek Amphibolite

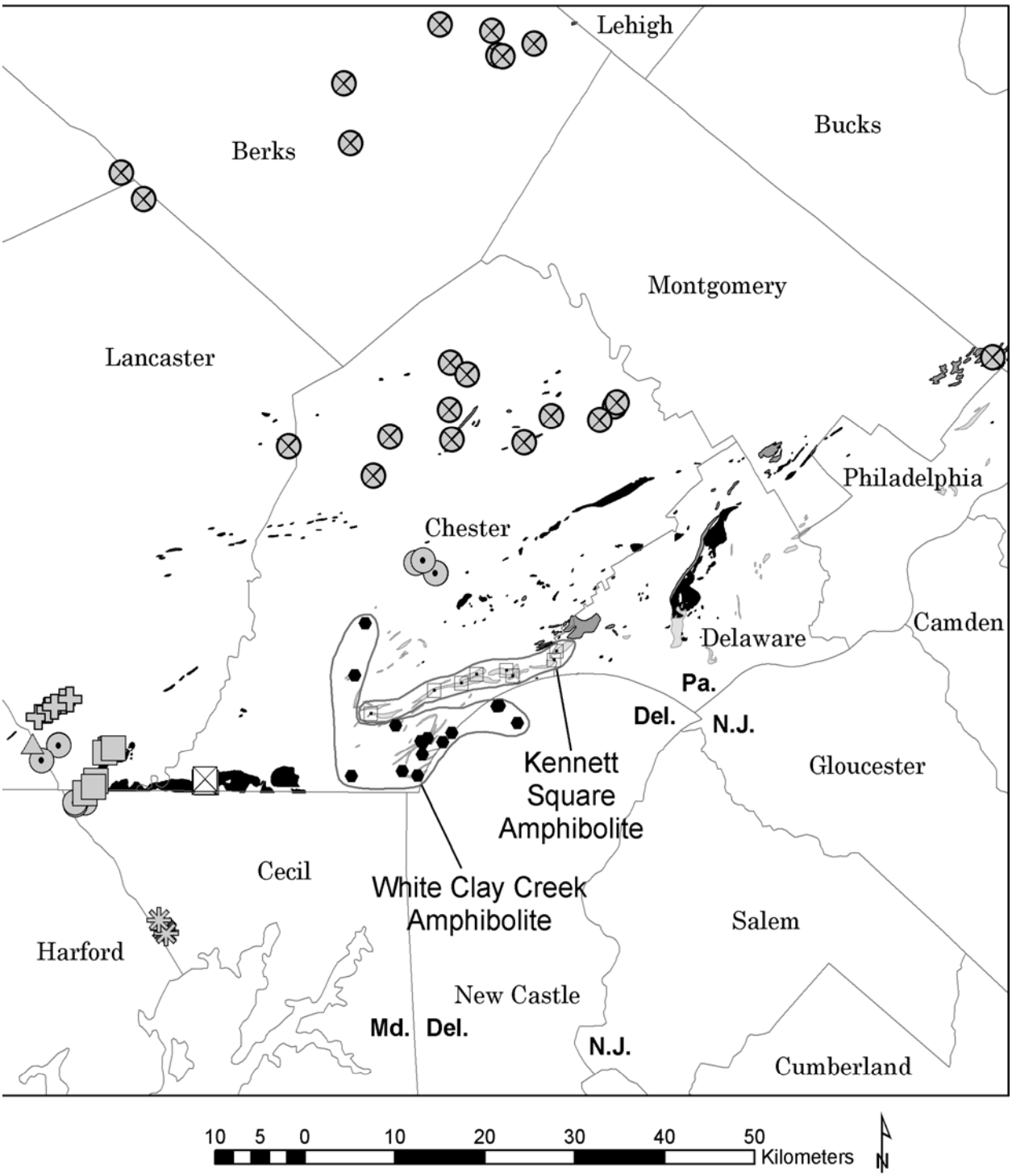

Figure 9. Map showing distribution of mafic units by population groupings. Individual sample locations are provided with the analyses in Appendix I. For clarity, the Catoctin Metabasalt populations on both sides of the Tunnel Hill–Jacks Mountain fault system have been combined. Likewise, the Sams Creek Metabasalt–Pa. is a combination of two populations occurring in a small area. Serpentines in Pennsylvania are shown in solid black. Geologic formation boundaries are from the Digital Bedrock Geologic Map of Pennsylvania (Miles, and others, 2001).

Table 2. Stratigraphic description of the White Clay Creek Amphibolite (WCCA) type section, east bank of Middle Branch of White Clay Creek where it makes a right angle bend from flowing east to south, 0.46 km east of the confluence with Indian Run. These natural outcrops are located 1.35 km northeast of Chesterville, Franklin Township, Chester County, Pa. This is in the West Grove 7 ½' quadrangle at 39° 47' 19"N, 75° 48' 09"W. The description proceeds from the top down.

>4 m-thick dark, medium-fine grained hornblende-plagioclase foliated gneissic WCCA sampled as WCCBMIV 0.5 to 4.5 cm above the base of dark, medium-fine grained hornblende-plagioclase foliated amphibolite. Consists of distinctly bluish-green hornblende and andesine as well as minor opaque oxides, accessory apatite, and trace biotite, zircon, and allanite. Titanite appears to be absent. Chemical analyses for each sample in Appendix I.

1.1 ± 0.2 m metasediment. The lowest 1 cm consists of sheared quartz-biotite-schist and accessory opaque oxides, titanite, some enclosing oxides, allanite, some having partial thin, clear rims of probable epidote, subrounded zircon, and rare schorl. X-ray powder diffraction also suggests possible minor chlorite.

0.5 m-thick medium-grained, dark gray WCCA sampled as WCCMBIII 1.5 to 7.0 cm above the base. This WCCA contains a few 2 mm biotitic patches that could be flattened amygdules. Consists of blue-green hornblende and andesine as well as accessory titanite, opaque oxides, and sparse apatite and biotite.

0.5 m-thick metasediment, possibly tuffaceous.

1.7 m-thick WCCA sampled as WCCMBII 2.5 to 4.5 cm above the base. (The base may be more mafic than the rest of the flow.) Consists of blue-green hornblende and andesine as well as accessory opaque oxides, titanite, apatite, zircon, and rare altered biotite. This 1.7 m-thick WCCA contains a possible metatuff from 0.80 to 0.83 m below the top. It consists of crenulated hornblende-albite-quartz-biotite-schistose gneiss containing accessory opaque oxides, apatite, and rare, zoned allanite. A second possible metatuff from 0.70 to 0.72 m below the top appears to be very similar.

4.5 m-thick micaceous metasediment or metatuff.

0.5 m thick WCCA sampled as a) WCCMBI 10-20CM, a fine- to medium-grained dark greenish black amphibolite from 10 to 20 cm above the base or just above a 2 cm metasediment or metatuff containing allanite-cored euhedral epidote, not unlike that found in the Springfield Granodiorite. This 10-20 cm sample included two 1 mm quartzose layers. Based on thin section examination, this 2 cm layer is a crenulated albite-quartz-biotite schist containing minor hornblende, opaque oxides, allanite-epidote, and trace fluorapatite and zircon. Based on X-ray powder diffraction, it also contains clinochlore and broad peaks at 11.9, 7.2, 3.55 and 3.45 Ångstroms. Also sampled as b) WCCMBI from 1.5 to 6.5 cm above the base. Medium-grained, greenish black amphibolite. Consists of bluish green hornblende and andesine as well as accessory titanite and opaque oxides, trace allanite having epidote rims, and rare biotite. Trace chalcopyrite and pyrite observed in hand sample. An unanalyzed 1-2 cm friable mica zone occurs 7 cm above the base. S_1 and S_o trend N72°W, 30°S.

GEOCHEMISTRY

Median data for selected immobile, incompatible elements for White Clay Creek Amphibolite and related Catoctin populations, *sensu lato*, are presented in Table 3. More complete analyses and latitudes and longitudes are in Appendix I, Table 1. Geochemical data for the various Catoctin Metabasalt *sensu lato* continental rifting populations have a strong commonality, but are extremely distinct from such data for other continental rifts in southeastern Pennsylvania such as the Early Mesozoic (Smith, *et al*., 1975) or older Neoproterozoic rifting (Smith, 2003). For example, see Table 4 containing median trace element data for metabasalts from the next oldest and second youngest periods of continental rifting.

The Catoctin Metabasalt *sensu lato* can be imperfectly divided into two subgroups geographically by the Tunnel Hill-Jacks Mountain (TH-JM) fault system (Fauth, 1978). The TH-JM is located in the southeastern corner of the South Mountain anticlinorium of Pennsylvania and trends NE-SW. Perhaps because of Alleghanian and Mesozoic structural complexities or the spilling over of lavas, this fault system provides only imperfect division of the Catoctin of South Mountain. However, it does help provide an interim geochemical distinction between the two structural units of South Mountain discussed by MacLachlan (1991). Histograms and analyses plotted on a topographic base suggest that natural breaks might divide the Catoctin Metabasalt *sensu stricto* into units containing 1.4-2.2 % TiO_2, 2.2-2.5%, 2.6-3.4%, and >3.7%. Presently

requiring laboratory analyses for recognition, such units do not qualify as formal members, but might help establish a more precise division of the Catoctin Metabasalt in the South Mountain anticlinorium. At present, the relative ages of the potential geochemical units are unknown.

For now, the portion of the Catoctin Metabasalt northwest of the Tunnel Hill-Jacks Mountain fault system (CMNW) consists of those 48 samples believed to be generally located in the metarhyolite-rich main portion of the South Mountain of Adams, Cumberland, and Franklin counties northwest of the fault. It seems to match a subgrouping of the Catoctin *sensu lato* including Catoctin Metadiabase dikes, Accomac Metabasalt, White Clay Creek Amphibolite, and the three subunits of the Sams Creek Metabasalt. CMNW and Accomac Metabasalt are associated with Catoctin Metarhyolite melted from the base of the Grenvillian crust. CMNW does not have a recognized equivalent to the south of Pennsylvania. The abundance of metarhyolite is the basis for various proposals for a triple junction associated with abnormal heat flows in the South Mountain anticlinorium.

The other Catoctin Metabasalt subgrouping, southeast of the fault system (N=6), is associated with sparse metarhyolite and seems have a more easterly trend until cut off by the Mesozoic border, only to reappear on the east side of the Gettysburg Basin as the Pigeon Hills Metabasalt, and then discontinuously as Glen Rock Metabasalt, York County; as Holtwood Metabasalt in the Susquehanna River of Lancaster County; and probably even the Jonestown Volcanic Complex of Lebanon County (Figure 9 and Table 3).

Figure 10 shows updated plots for A. chondrite-normalized rare earths (CNREE), B. Ti-Zr-Y, C. Ti/V, and D. primordial-mantle normalized elements in the WCCA and two geochemically very similar populations in the same subgroup, Catoctin Metadiabase dikes in Grenvillian terrane and Accomac Metabasalt, York County. Figure 10A, CNREE, shows WCCA as a relatively tight, parallel band having a negative slope and generally lacking Eu anomalies. This is consistent with within plate basalts of both oceanic and continental affinity. Plots of Catoctin Metadiabase dikes from four separated Grenvillian terranes are similar, but have a slightly wider geochemical spread. Plots for Accomac Metabasalt are also similar, but have a still larger geochemical spread. As noted by Smith and Barnes (1994), Accomac Metabasalt is a vesicular unit that makes a nice vignette of the Catoctin Metabasalt of the South Mountain Anticlinorium. Ti-Zr-Y plots (Figure 10B) for all three populations plot in the portion of the within plate basalt field slightly toward ocean floor basalts. Stratigraphic superposition at the WCCA type section and a pair of crosscutting Catoctin Metadiabase dikes (samples HUFFM and HUFFC) suggests that TiO_2 content is higher in younger samples. Ti/V plots (Figure 10C) show a wide spread of TiO_2 in particular. For Pennsylvania, this wide spread refutes studies purporting to show a systematic regional pattern for TiO_2 over several states. If the oldest samples were high in TiO_2, then one might hypothesize great depth or small percent initial melting for the older pulses. However, it is the younger magma pulses that seem to be higher in TiO_2. In this case, it is likely that low availability of water and therefore low initial oxygen availability (oxygen fugacity or fO_2) led to late enrichment of TiO_2 in opaque oxides in crustal magma chambers. Primordial-mantle normalized diagrams (Figure 10D) all show similar plots with negative slopes for the immobile, incompatible elements characteristic of continental initial rifting tholeiites (CIRT). For this diagram, Nb (+) anomalies and negative Sm to Y slopes are moderately characteristic of CIRT.

$^{143}Nd/^{144}Nd$ data for WCCA sample WCCMBI 10-20CM and Catoctin Metadiabase dike HNYNW from the Honeybrook Upland (Table 5) are so similar as to suggest that they likely share a source and comparable ages. Data for four other Catoctin Metabasalt *sensu lato* samples are not far off and suggest the probability of similar sources and comparable ages for all six samples. When potential errors in the INAA- and ICP-derived analyses for elemental Nd and Sm used in the epsilon Nd calculations are taken into account, it becomes likely that all six samples have a similar mantle source and age.

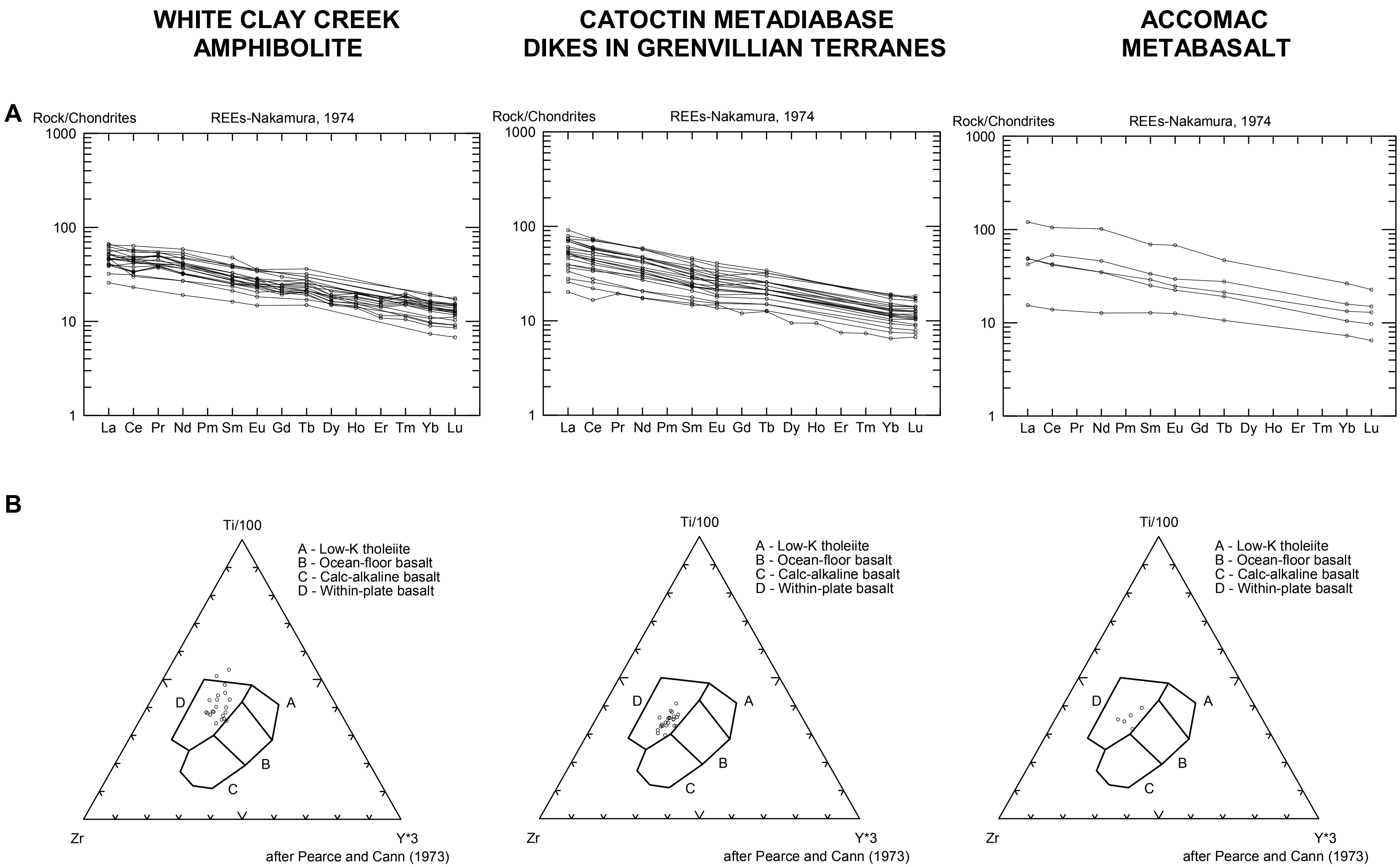
WHITE CLAY CREEK AMPHIBOLITE
CATOCTIN METADIABASE DIKES IN GRENVILLIAN TERRANES
ACCOMAC METABASALT
A
Rock/Chondrites
REEs-Nakamura, 1974
1000
100
10
1
La Ce Pr Nd Pm Sm Eu Gd Tb Dy Ho Er Tm Yb Lu
B
Ti/100
Zr
Y*3
A
B
C
D
A - Low-K tholeiite
B - Ocean-floor basalt
C - Calc-alkaline basalt
D - Within-plate basalt
after Pearce and Cann (1973)

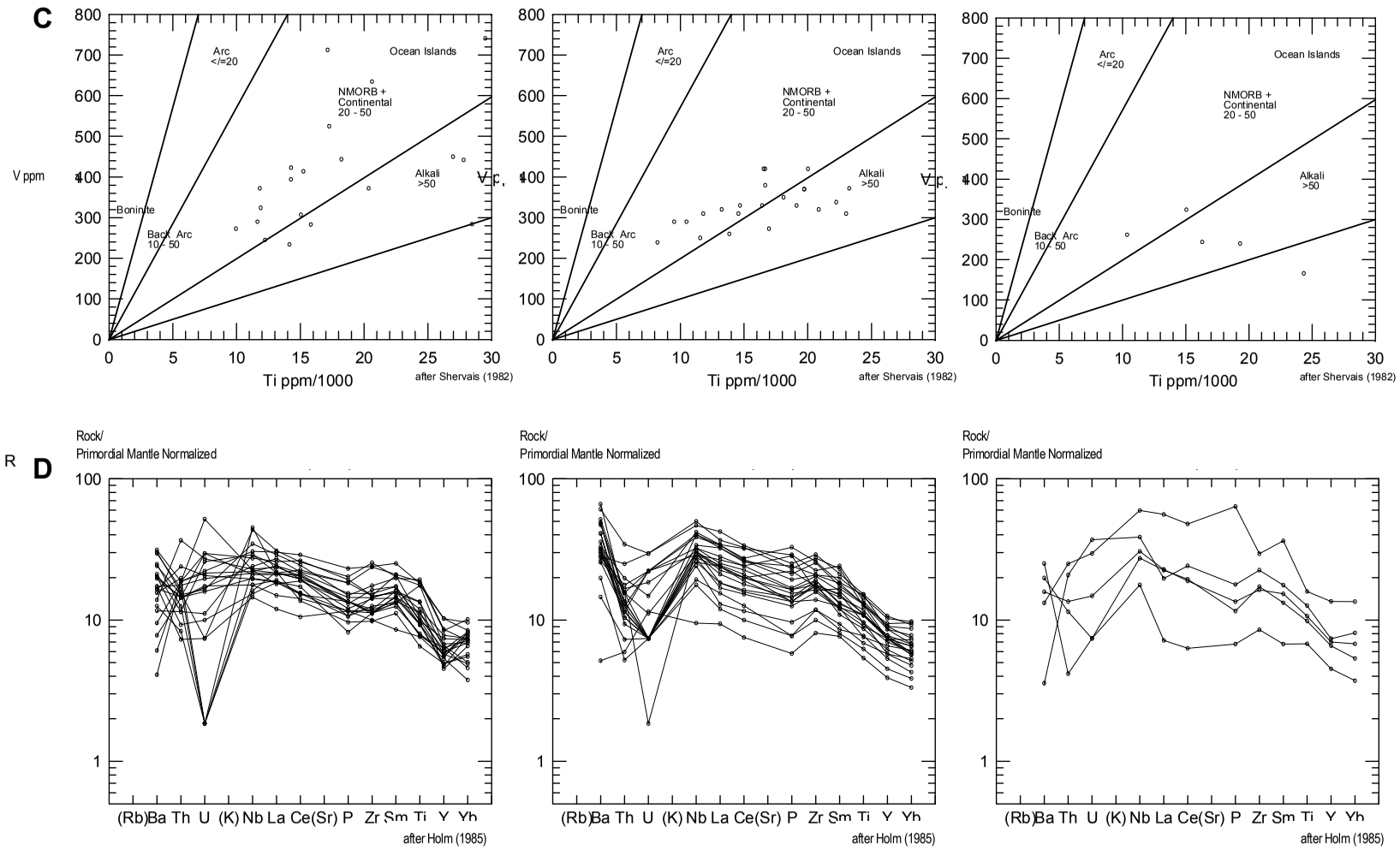

Figure 10. Plots of data from three similar continental initial-rifting tholeiites, White Clay Creek Amphibolite, Catoctin Metadiabase in Grenvillian terrains, and Accomac Metabasalt, showing A. chondrite-normalized rare earth elements, B. Ti–Zr–Y, C. Ti/V, and D. primordial-mantle-normalized elements.

Table 3. Medians of selected trace elements in the White Clay Creek Amphibolite and correlative Catoctin Metabasalt *sensu lato* analogs from southeastern Pennsylvania and adjacent Delaware and Maryland. In general, data in the upper 7 rows, which includes the Catoctin Metabasalt from NW of the Tunnel Hill-Jacks Mountain (TH-JM) fault system, are similar. Those in the lower 5 rows, which include the Catoctin Metabasalt from SE of the same fault system, are also similar. Populations are arranged by decreasing TiO_2, which in this case roughly corresponds to a rift to drift transition. Thus, the populations shown lower in the table may be relatively younger than those near the top. "N" is the number of analyzed samples in each population. The TiO_2 data are listed in percent and others in ppm.

	N	TiO_2	Zr	Hf	Nb	Ta	Th	Ni	V	Y	La	Ce
Catoctin Metadiabase dikes in Grenvillian terrains	23	2.78	210	4.3	19	0.9	1.2	40	330	36	17	38
Accomac Metabasalt, York Co.	5	2.72	190	4.6	19	1	1.3	60	244	32	16	37
White Clay Creek Amphibolite	21	2.64	150	4.1	14	0.9	1.6	66	393	30	15.4	37
Catoctin Metabasalt NW of TH-JM fault	48	2.35	157	3.6	12	0.6	0.7	80	329	36	11.5	29
Sams Creek Metabasalt, York Co.	3	2.02	160	3.5	21	1.1	1.6	160	328	38	16.5	38
Fishing Creek Metabasalt Member of Sams Creek Fm., Lancaster Co.	7	1.94	154	3.6	21	1.1	1.7	96	223	30	14.8	33
Sams Creek Metabasalt, Md., type and reference section	6	1.88	146	3	22	1	1.4	126	306	32	14.2	31
Holtwood Metabasalt, Lanc. Co.	6	1.82	99	2.3	9	0.3	0.4	78	306	28	7.1	18
Glen Rock Metabasalt, York Co.	8	1.82	107	2.6	6	0.4	0.4	104	368	36	7	18
Catoctin Metabasalt SE of TH-JM fault	6	1.74	105	2.4	9	0.4	0.4	110	301	28	6.6	17
Pigeon Hills Metabasalt, Adams and York counties.	6	1.54	96	2	8	0.2	0.2	134	312	28	6.7	16
Jonestown Volcanic Complex, Berks and Lebanon counties	7	1.4	104	2.4	8	0.4	0.8	95	270	32	6.8	18

Figure 11 shows four plots to compare a combined Sams Creek Metabasalt population with Catoctin Metabasalt northwest of the Tunnel Hill-Jacks Mountain fault system (CMNW). The combined Sams Creek Metabasalt consists of the Sams Creek Metabasalt, Maryland, type locality plus reference section (N=7), equivalent Sams Creek Metabasalt, York County (N=3), and Fishing Creek Metabasalt Member of the Sams Creek Formation, Lancaster County (N=7). These three are nearly indistinguishable from one another and, for practical purposes, represent a single population. CNREE plots of the combined Sams Creek Metabasalt (Figure 11A) show a rather tight bundle

Table 4. Selected trace element data to compare with that for the Catoctin Metabasalt *sensu lato* in Table 2. Included here are the next oldest (Neoproterozoic Tunnel Mine Metabasalt and Williams Quarry metabasalt, Smith, 2003) and second youngest (Early Mesozoic Quarryville Diabase, York Haven Diabase, and Rossville Diabase, Smith *et al*., 1975, and present study) continental rift basalts from southeastern Pennsylvania. Data for Quarryville Diabase and York Haven Diabase are from the type localities and that for Rossville is from the principal reference section. Both the upper and lower data blocks are believed to be continental rifting basalts, but contrast sharply with the Catoctin Metabasalt *sensu lato*.

	N	TiO_2	Zr	Hf	Nb	Ta	Th	Ni	V	Y	La	Ce
Tunnel Mine Metabasalt	5	3.70	355	7.6	54	3.5	5.9	191	217	49	61.6	123
Williams Quarry metadiabase	3	3.51	295	5.4	91	5.4	6.6	102	189	44	66.6	132
Quarryville Diabase	1	0.41	59	0.9	4	<.1	0.9	320	160	20	4	9
York Haven Diabase	1	1.12	109	2.1	11	0.3	1.6	73	220	24	8.7	18
Rossville Diabase	1	0.88	77	1.3	7	0.2	1.0	70	254	24	5.2	12

having a moderate negative slope and generally lacking Eu anomalies. CNREE plots for the Catoctin Metabasalt NW of the TH-JM fault system show similar patterns but with the addition of more samples having a lesser slope. Ti-Zr-Y plots for both the combined Sams Creek Metabasalt and the CMNW (Figure 11B) show very similar clusters on the boundary between the within plate basalt and ocean floor basalt fields. Based on these clusters being slightly closer to the oceanic field, it appears the these two populations are more transitional to oceanic than were the WCCA, Catoctin Metadiabase dikes, and Accomac Metabasalt. Ti/V plots for the combined Sams Creek Metabasalt and the CMNW (Figure 11C) are rather similar and exhibit a wide spread compatible with early magmas being reduced and later fractions more oxidized. In this case, the higher TiO_2 magmas were the younger. Primordial mantle normalized diagrams (Figure 11D) have a negative slope consistent with an overall continental rifting environment.

The second major grouping within Catoctin Metabasalt *sensu lato* consists of the Catoctin Metabasalt SE of the TH-JM fault (CMSE) and four similar populations (Table 3). To illustrate relationships in a reasonable number of diagrams, they have been grouped into 1) the Catoctin Metabasalt SE of the Tunnel Hill-Jacks Mountain fault system (N=6) plus the nearly indistinguishable Pigeon Hills Metabasalt from along strike to the east across the Gettysburg Basin (N=6); 2) Glen Rock Metabasalt, York County (N=8), 3); Holtwood Metabasalt from the Susquehanna River, Lancaster County (N=6); and 4) Jonestown Volcanic Complex (N=7) of Lebanon County, Pa. (For those desiring to test the validity of these groupings, data for individual samples are available in Appendix I and for medians with minimal grouping in Table 3.)

Figure 12A shows plots for CNREE for the above groupings. Overall, they are rather similar, having slightly negative slopes and a few rather minor Eu anomalies. In detail, however, two samples of CMSE exhibit subtle light rare earth (LREE) depletion. Somewhat reassuringly, three Pigeon Hills Metabasalt samples from along strike across the Gettysburg Basin to the east also exhibit LREE depletion as do the three Glen Rock Metabasalt samples from the section in the town of Glen Rock, York County, and three from the Jonestown Volcanic Complex. In addition to these similar populations sharing still another attribute, LREE depletion is characteristic of basalts that have at least a moderate oceanic aspect (N-OFB). Thus, using this criterion, the populations

Table 5. Upper block: Nd isotopic analyses of six mafic samples believed to be part of the Catoctin Metabasalt *sensu lato*. From west to east, sample SWPCKS was chosen to represent Catoctin Metabasalt *sensu stricto* from the South Mountain anticlinorium NW of the Tunnel Hill-Jacks Mountain Fault system, ACC48E to represent Accomac Metabasalt of eastern York County, FSHCKOTC to represent the Fishing Creek Member of the Sams Creek Formation of Lancaster County (and likely reflects a minor drifting aspect), FURNCK to represent Catoctin Metadiabase dikes in the Womelsdorf outlier Grenvillian terranes, HNYNW to represent Catoctin Metadiabase in the Honeybrook Upland, and WCCMBI 10-20CM to represent White Clay Creek Amphibolite at the type locality. Lower block: TMMVII and CKWQOTC2 are samples of Neoproterozoic metabasalt from the Reading Prong that likely predate Catoctin Metabasalt *sensu lato* slightly. Data for TMMVII by the Radiogenic Isotopes Laboratory, Ohio State University, as reported by Smith (2003); given is the average of two analyses with total-spiking, isotope dilution determinations of Sm and Nd. All other data by Activation Laboratories Ltd., who reports 3 significant figures for ICP-MS and 2 for INAA. Epsilon Nd is relative to the Chondrite Uniform Reservoir (CHUR) using present-day values of 0.1966 for $^{147}Sm/^{144}Nd$ and 0.512638 for $^{143}Nd/^{144}Nd$, assuming an age of 570 Ma (or 600 Ma for TMMVII, based on actual date

Sample	Nd, ppm	Sm, ppm	$^{143}Nd/^{144}Nd$	+/-2 s	Epsilon Nd assuming an age of 570 Ma.
SWPCKS	20.3	5.40	0.512703	10	+3.9
ACC48E	22.	5.1	0.512599	11	+3.4
FSHCKOTC	18.	5.2	0.512842	12	+5.6
FURNCK	21.	4.7	0.512548	9	+2.7
HNYNW	13.	3.3	0.512680	6	+4.0
WCCBMI 10-20CM	20.3	5.07	0.512661	6	+3.8
TMMVII	68.75	14.5	0.512556	6	+3.7*
CKWQOTC2	59.	9.8	0.512497	5	+4.3

shown in Figure 12 appear to have progressed from pure rifting into a transition to drifting. (The Jonestown Volcanic Complex sample having the highest CNREE, sample BKHLNW2-11, was collected only 2 to 11 cm southeast of the gouge-bearing fault contact with Paleozoic limestone and had calcite-filled vesicles). Figure 12B shows Ti-Zr-Y plots for the same groupings. Overall, they tend to plot near the boundary between the within plate and oceanic fields, but there are subtle differences between populations. Samples from both the CMSE and Pigeon Hills Metabasalt subgroupings plot in both fields and straddle the boundary. Glen Rock Metabasalt samples are mostly in the half of the oceanic field nearest the within plate basalt field. All samples of Holtwood Metabasalt from Holtwood *per se* are within plate basalt but near the oceanic field. Only the geographically isolated COYLK sample from 9 km southeast of Holtwood is oceanic. All Jonestown Volcanic Complex samples plot in the half of the oceanic field nearest the within plate basalt, very similar to Glen Rock Metabasalt. Figure 12C shows a decreasing spread of values as one proceeds farther east geographically from CMSE. Figure 12D shows primordial-mantle normalized data. The plots have some scatter, but tend to have a slight negative slope and positive Nb anomalies. Overall, these four populations have a less negative slope than other Catoctin *sensu lato* and a few samples in three of the populations have normalized La<Ce, somewhat characteristic of N-OFB. The CMSE, Pigeon Hills Metabasalt, Holtwood Metabasalt, and Jonestown Volcanic Complex all seem to have a more distinct drifting aspect than the groups discussed in the two previous figures.

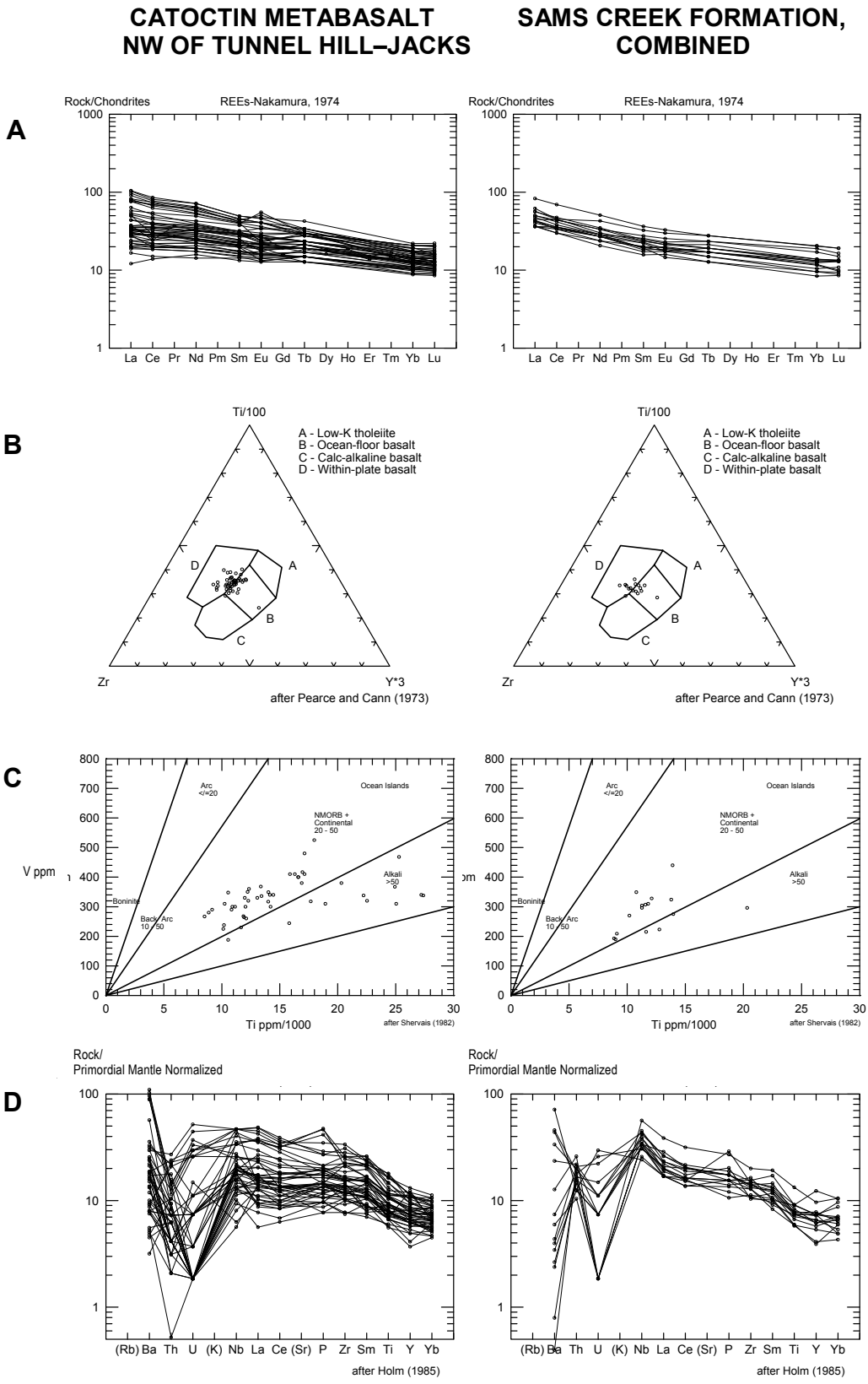

Figure 11. Catoctin Metabasalt NW of the Tunnel Hill–Jacks Mountain fault system compared to the similar combined Sams Creek Metabasalt, which consists of the type and reference section in Frederick County, Md., equivalent metabasalt in York County, and the Fishing Creek Metabasalt member of the Sams Creek in Lancaster County.

A

B

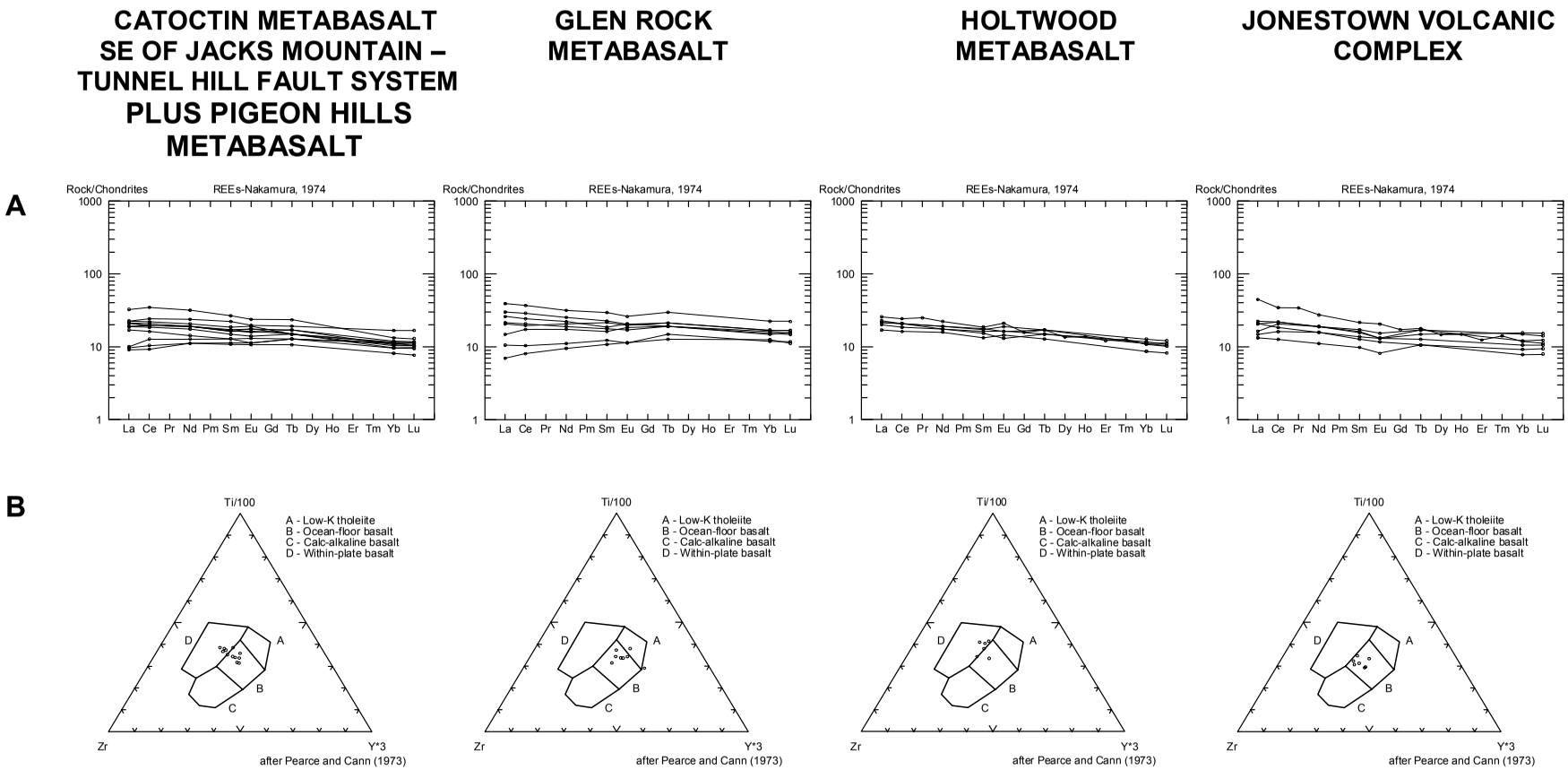
CATOCTIN METABASALT SE OF JACKS MOUNTAIN – TUNNEL HILL FAULT SYSTEM PLUS PIGEON HILLS METABASALT
GLEN ROCK METABASALT
HOLTWOOD METABASALT
JONESTOWN VOLCANIC COMPLEX
Rock/Chondrites
REEs-Nakamura, 1974
1000
100
10
1
La Ce Pr Nd Pm Sm Eu Gd Tb Dy Ho Er Tm Yb Lu
Ti/100
Zr
Y*3
A - Low-K tholeiite
B - Ocean-floor basalt
C - Calc-alkaline basalt
D - Within-plate basalt
after Pearce and Cann (1973)

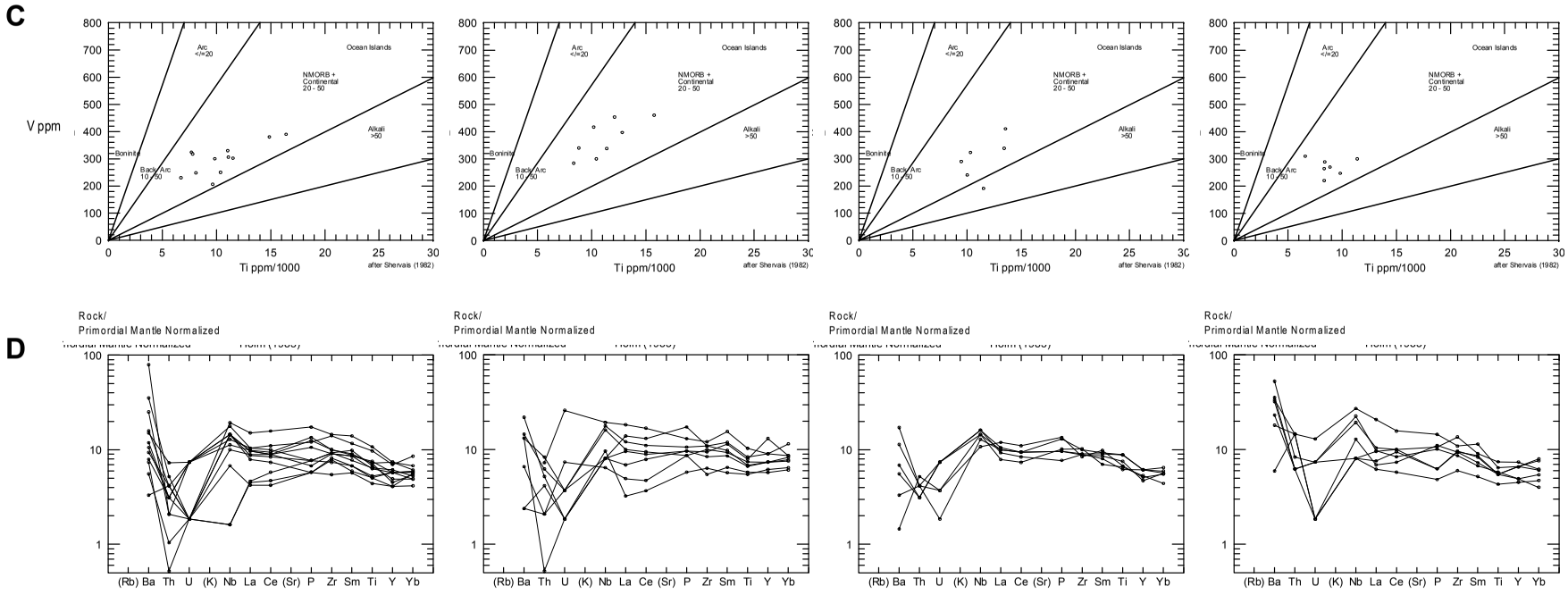

Figure 12. Plots for four groupings of Catoctin Metabasalt *sensu lato*: 1. Catoctin Metabasalt southeast of the Tunnel Mine–Jacks Mountain fault system plus Pigeon Hills Metabasalt along strike to the east. 2. Glen Rock Metabasalt, York County. 3. Holtwood Metabasalt from the Susquehanna River, Lancaster County. 4. Jonestown Volcanic complex, Berks and Lebanon Counties.

No additional work has been done on the poorly defined, informal "Bald Eagle Creek metabasalt" of Smith and Barnes (1994, p. 53 and diagrams in Figure 12). They remain enigmatic, largely because their presently recognized geographic range and host rock outcrops are limited. Most of the traditional diagrams as used above, plus that of Meschede (1986), generally fit alkaline within plate basalt (WPB). However, the primordial mantle normalized diagram of Holm (1985) shows La>Nb, Sm (+), and Y (-) which is distinctive from Catoctin Metabasalt *sensu lato*. Thus, there is presently no convincing evidence to include it in the Catoctin. The unit contains sparse garnet of unknown composition and it cannot presently be ruled out that garnet retained in a deep source has influenced trace-element composition.

No additional work has been done on the James Run Formation along the Susquehanna River, Cecil County, Maryland. A relationship with the Chopawamsic Formation of central Virginia is reasonable, but to date, the James Run Formation has not been recognized in Pennsylvania. Relatively complete analyses and locations for the samples studied are provided in Appendix I, Table 1. Plank *et al.* (2001) discussed these data. A relationship to the lower TiO_2 "older diabase" dikes of Bascom and Stose (1932) cannot be ruled out.

Relatively complete analyses and locations for the sampled "older diabase" dikes of Bascom and Stose (1932) are provided in Appendix I, Table 1. The sampled "older diabase" dikes occur in two somewhat linear ENE-trending belts across the Brandywine massifs. These massifs lack significant indigenous mafic rocks, Lower Cambrian Hardyston or Chickies basal conglomerates, and are not cut by *bona fide* Catoctin Metadiabase dikes. Thus, they are Grenvillian, but not necessarily of Laurentian affinity. (On the "easy come – easy go" assumption, they might represent some of the last Grenvillian crust attached to Laurentia and some of the first to be rifted at ~750 Ma.) It is hypothesized herein, that late in the history of Iapetus the Brandywine massifs were microcontinents inboard of the Wilmington Complex and outboard of the Baltimore Mafic Complex arcs. As suggested by the complex geochemical signature of the "older diabase" dikes, it is possible that the Brandywine massifs overrode subduction zone magmas and a spreading center during the closure of Iapetus. Based on one set of crosscutting dikes (samples BEAU and BEAU2, Appendix I, Table 1), the Brandywine massifs likely overran a backarc spreading center first and then the arc subduction zone magmas themselves. Dike intrusion may have been enhanced by two ENE-trending zones of weakness nearer the thinner edges of the massifs. Samples ARMK2, BEAU, CPSUN, CRUMCK, and RADNOR appear to be various types of island arc tholeiites (IAT) based on Ti-Zr, Ti-V, Cr-Y, and Nb-Zr-Y plots. Samples BEAU2, BALTP, and BALTP2 (Appendix I, Table 1) might be P=E-OFB (enriched or plume ocean-floor basalts), but it cannot be presently ruled out that these three higher TiO_2 dikes were continental rifting basalts.

If the above hypothesis contains some elements of truth, then the Brandywine Massifs overrode the roots of the island arc during the closure of Iapetus and at a time of anomalously high heat flow. This overriding then would likely have been at 430 ± 5Ma, just prior to obduction. Additional corollaries might include 1) that the Brandywine massifs are underlain by ultramafic-bearing mélange in southeast-dipping thrusts, 2) their being overridden by a younger thrust carrying ultramafic-bearing mélange related to the Wilmington Complex, 3) that the Wilmington Complex left an erosional veneer over the top of the Brandywine massifs (such as samples BRANDYB and DILW). Presently, it cannot be ruled out that final placement of the Brandywine massifs was influenced by incipient rifting associated with the ~430-Ma period of widespread crustal thinning and extreme heat flow.

CONCLUSIONS

The Catoctin Metabasalt *sensu lato* is a widespread remnant of Late Neoproterozoic continental initial rifting through early drifting. In Pennsylvania, the initial rifting stage is best

represented by the Catoctin Metabasalt NW of the Tunnel Hill-Jacks Mountain Fault system which contains a range of compositions; the Accomac Metabasalt of York County, the Catoctin Metadiabase dikes cutting Grenvillian terranes; and the White Clay Creek Amphibolite. Their median trace element compositions and limited $^{143}Nd/^{144}Nd$ data simply seem too similar for them to not be related. However, the exact nature of that relationship is not yet certain. Because the Brandywine massifs do not appear to have been cut by Catoctin Metadiabase dikes, the massifs may have been distal from Laurentia during the Late Neoproterozoic, perhaps even on the other side of a then-young seaway. Neodymium isotope data in these mafic units would not be easily reset by variable metamorphism and might further confirm relationships. The probability of matching Catoctin Metarhyolite magmas in the South Mountain anticlinorium and Accomac, York County, further ties the relationship between those two areas and suggest that a bimodal Catoctin veneer likely occurs on basement east from South Mountain to at least the Susquehanna River. Areas still farther east may have been too distant from the main rift-generating heat source to have melted the base of the Grenvillian crust to form rhyolitic magmas. This does not rule out the possibility of metatuffs in sections of WCCA. Saprolites derived from the upper WCCA layers at the type and reference sections seem to be potential candidates for U-Pb isotopic dating of zircons. Preliminary study of heavy minerals indicates that the micaceous partings within the WCCA were not generated strictly by shearing. Their differences in geochemistry across the micaceous zones alone prove this (Appendix I, Table1, samples WCCMBI through WCCMBIV).

One might be able to further assess affinity within Catoctin Metabasalt *sensu lato* with a $^{147}Sm/^{144}Nd$ isochron derived from analyses of carefully selected samples having as great a range of Sm/Nd elemental ratios as available. For this purpose, one might include samples of dubious affinity up to the point of estimating an approximate overall age of those determined therein to be part of a meaningful population. Obviously, such a study would suffer from the limited range of Sm/Nd ratios and the fact that the populations likely represents a transition from rifting to drifting over millions of years rather than a single event.

Sams Creek Metabasalt has been studied in three areas: 1) the type locality and reference section, Maryland, 2) southwestern York County, and 3) as the Fishing Creek Metabasalt Member of the Sams Creek Formation in southwestern Lancaster County. They are so similar geochemically as to suggest one magma pulse over a relatively short time period. They provide the first known stratigraphic and temporal correlation across the Tucquan anticline. All three show a hint of a drifting aspect and can be used as a first approximation of the Precambrian-Cambrian boundary. Detailed mapping by others in the area of type and reference Sams Creek Formation exposures suggests that the formations above and below the Sams Creek Metabasalt might be recognized and utilized in mapping in the Susquehanna River section if the facies changes are not too substantial to prevent field recognition of these sedimentary rocks. Sub-Catoctin units in Virginia, such as the Fauquier, Swift Run, Konnarock, and Robertson River Igneous Suite, should be sought to the northwest of the Fishing Creek Metabasalt in the Susquehanna River section and elsewhere. Median Sams Creek Metabasalt fairly closely matches median CMNW, but the latter includes a range of compositions. For the South Mountain anticlinorium, informal metabasalt units are being worked out by plotting TiO_2 and selected trace-element data on a geologic base.

The Catoctin Metabasalt SE of the Tunnel Hill-Jacks Mountain fault system (CMSE); Pigeon Hills Metabasalt; Glen Rock Metabasalt, southwestern York County; Holtwood Metabasalt of the Susquehanna River, Lancaster County; and Jonestown Volcanic Complex all seem to be closely related geochemically. They appear to have still more of a drift component than the combined Sams Creek Metabasalt, to lack any recognized metarhyolite, and to contain variable evidence of pillows at all but the structurally complex Pigeon Hills area. They are likely the equivalent of the Catoctin Metabasalt of Skyline Drive in Virginia and the Catoctin Mountains of Maryland. (Thus, to geochemists working in Maryland and Virginia, the Sams Creek looks like

Catoctin Metabasalt, whereas, to those working in the CMNW of Pennsylvania, it appears to be a bit evolved toward drifting.) The CMSE and Pigeon Hills Metabasalt provide an excellent stratigraphic marker across the Gettysburg Basin. The match of median Jonestown Volcanic Complex with this grouping is surprising but seems to be too precise to be a coincidence. Where excavated, the JVC appears to be underlain by fault gouge. Likely, it is allochthonous with respect to the Hamburg Group, itself allochthonous. It was probably transported on a low angle thrust fault during the Silurian and then given a free ride during Mesozoic rifting. Reports that the JVC and N-OFB pillow basalts at Stark's Knob, eastern New York, are geochemically related are not supported by the present data. Low La, for example, is one good criterion for N-OFB, but La is 6 times higher in the JVC than in Stark's Knob pillow basalts.

The Brandywine massifs seem to be out-of-place and require further thinking as slightly exotic terrane. Neodymium isotope analyses of "older diabase dikes" might help verify or disprove alternate hypotheses. Drilling in the Brandywine massifs along their margins might help establish their mode of emplacement if ultramafic rocks were to be recognized beneath.

Acknowledgements. Margaret O. Plank took the senior author to the WCCMC outcrop and the Wilmington and Western Railroad cut WCCA section, Delaware. Gale C. Blackmer, Pennsylvania Geological Survey, suggested the new WCCBEC location to the senior author. Sam W. Berkheiser, P.G.S., assisted with the first half of the sampling used in Smith and Barnes (1994) and reused herein. Les T. Chubb assisted with preparing most of the new samples. The authors gratefully acknowledge reviews by Rodger T. Faill, P.G.S.; Art W. Rose, The Pennsylvania State University; and Don U. Wise, University of Massachusetts.

References

Bascom, F. and Stose, G. W., 1932, Coatesville-West Chester folio, Pennsylvania-Delaware, U.S. Geological Survey Atlas of the U.S., Folio 223, 15 p.

Berg, T. M. *et al*., 1980, Geologic map of Pennsylvania, Pennsylvania Geological Survey, 4th ser., Map 1, 1:250,000 scale.

Fauth, J. L., 1978, Geology and mineral resources of the Iron Springs area, Adams and Franklin counties, Pennsylvania, Pennsylvania Geological Survey, 4th ser., Atlas 129c, 72 p.

Flanagan, F. J., 1976, 1972 compilation of data on USGS Standards, U. S. Geological Survey Professional Paper 840, p. 131-183.

Holm, P. E., 1985, The geochemical fingerprints of different tectonomagmatic environments using hygromagmatophile element abundances of tholeiitic basalts and basaltic andesites, Chemical Geology, v. 51, p. 303-323.

Karabinos, P., Morris, D. and Rayner, N., 2004, Silurian tectonism in the western New England Appalachians, Geological Society of America, Abstracts with Programs, v. 36, p. 91.

Meschede, Martin, 1986, A method of discriminating between different types of mid-ocean ridge basalts and continental tholeiites with the Nb-Zr-Y diagram, Chemical Geology, v. 56. p. 207-218.

Miles, C. E., Whitfield, T. G., and others, 2001, Bedrock geology of Pennsylvania, Pennsylvania Geological Survey, 4th ser., scale 1:250,000.

Myers, R. E. and Breitkopf, J. H., 1989, Basalt geochemistry and tectonic settings: a new approach to relative tectonic and magmatic processes, Lithos, v.23, p. 53-62.

Pearce, J. A. and Cann J. R., 1973, Tectonic setting of basic volcanic rocks determined using trace element analysis, Earth and Planetary Science Letters, v. 19, p. 290-300.

Plank, M. O., Srogi, LeeAnn, Schenck, W. S, and Plank, T. A., 2001, Geochemistry of the mafic rocks, Delaware Piedmont and adjacent Pennsylvania and Maryland: confirmation of arc affinity, Delaware Geological Survey, Report of Investigation, No. 60, 39 p.

Shervais, J. W., 1982, Ti-V plots and the petrogenesis of modern and ophiolitic lavas, Earth and Planetary Science Letters, v. 59, p. 101-118.

Smith, II, R. C., 2004, Bald Friar Metabasalt and Kennett Square Amphibolite: two Iapetan ocean floor basalts, 69th Field Conference of Pennsylvania Geologists.

Smith, II, R. C., 2003, Late Neoproterozoic felsite (602.3 +/- 2 Ma) and associated metadiabase dikes in the Reading Prong, Pennsylvania, and rifting of Laurentia, Northeastern Geology and Environmental Sciences, v. 25, no. 3, p. 175-185.

Smith, II, R. C. and Barnes, J. H., 1994, Geochemistry and geology of metabasalt in southeastern Pennsylvania and adjacent Maryland, 59th Field Conference of Pennsylvania Geologists, p. 45-72A.
Smith, II, R. C., Foland, K. A. and Nickelsen, R. P., 2004, The Lower Silurian Clear Spring Volcanic Suite: Sword Mountain Olivine Melilitite (433 +/-3 Ma) and Hanging Rock Tuff/Diatreme, Washington County, Maryland, Geological Society of America, Abstracts with Programs, v. 36, no. 2, p. 71.
Smith, II, R. C., Rose, A. W., and Lanning, R. M., 1975, Geology and geochemistry of Triassic [sic] diabase in southeastern Pennsylvania, Geological Society of America Bulletin, v. 86, p. 943–955.
Trujillo, J. and Sinha, A. K., 2004, Extensional tectonics in collisional orogens: A case study of Early Silurian extension in the central Appalachians associated with the Taconic orogeny, Geological Society of America, Abstracts with Programs, v. 36, no. 2, p. 75.

BALD FRIAR METABASALT AND KENNETT SQUARE AMPHIBOLITE: TWO IAPETAN OCEAN FLOOR BASALTS

by
Robert C. Smith, II

INTRODUCTION

Geologic mapping of the Piedmont of Pennsylvania has largely utilized units defined prior to the development of the plate tectonic paradigm. Widespread acceptance of the pioneer work of Harold Williams in Newfoundland suggests that recognition of terrane boundaries is critical for understanding the geology throughout the Appalachians. One technique to locate such boundaries is to compare the immobile and incompatible trace element contents of mafic volcanic units and compare them to modern, better understood analogs. Such potential affinities can then be combined with traditional field data on the mafics and their host units. Finally, the areal distribution of a given population of mafic rocks can be used to propose new geologic units. This has been attempted and resulted in two first order groupings: One consists of mafic volcanics generated from Catoctin rifting in Laurentia through early drifting. This early grouping is discussed in an accompanying chapter centered on the White Clay Creek Amphibolite. The second grouping consists of pieces of the floor of Iapetus that appear to have formed after the mantle magma source had lost all memory of Catoctin rifting. These were likely docked during the Ordovician and obducted up onto Laurentia during the Silurian. This chapter covers two of the latter such oceanic formations (Bald Friar Metabasalt and Kennett Square Amphibolite) and mentions others that are not yet well defined. The boundary between the two first order groupings is analogous to the Baie Verte-Brompton plate boundary of the northern Appalachians. Unfortunately, the plate boundary is less impressive in Pennsylvania because the original thrust surfaces were later obscured and "repeated" by folding during the Alleghanian (Smith, 1993) and, in places, overprinted by late Alleghanian lateral shearing.

The Bald Friar Metabasalt (BFM) and Kennett Square Amphibolite (KSA) are two mafic units occurring in the general area of the 2004 Field Conference for which some additional data have become available since they were proposed by Smith and Barnes (1994). The KSA is not believed to be directly related to the BFM (Smith and Barnes, 2004).

Host rocks to the BFM at the type locality, Cecil County, Maryland, appear to have been included in the Sykesville Formation (Higgins and Conant, 1986) whereas the host to the southwest at Liberty Reservoir, Carroll County, Maryland, is better exposed and has been mapped as the Morgan Run Formation (Muller et al., 1989). According to Muller et al., the Morgan Run Formation together with the overlying Sykesville Formation constitute the Liberty Complex. The Morgan Run Formation itself consists of pelitic schist and, especially near its base, mafic- and ultramafic-bearing metagraywacke, all derived in an oceanic and trench fill setting. It is the metagraywacke of the Morgan Run Formation that hosts the BFM at Liberty Reservoir. Muller et al. note that the Liberty Complex is underlain by a low angle, folded thrust, similar to the situation noted by Smith (1993) at the Peach Bottom structure. Far to the northeast in Québec, the host to what are likely BFM equivalents is the Caldwell Group (Bédard and Stevenson, 1999).

The Bald Friar Metabasalt was proposed by Smith and Barnes as a formal, field-recognizable and mapable unit. It typically occurs as 2.5 ± 1m-thick fragments in mélange associated with ultramafic fragments of the Baltimore Mafic Complex, locally carbonated to listwaenite or steatized.

Smith, II, R. C., 2004, Bald Friar Metabasalt and Kennett Square Amphibolite: Two Iapetan ocean floor basalts, *in* Blackmer, G. C., and Srogi, L., Marginalia – Magmatic arcs and continental margins in Delaware and southeastern Pennsylvania: Guidebook, 69th Annual Field Conference of Pennsylvania Geologists, West Chester, PA, p. 46-55.

Figure 13. Digital photographs of a slice of an isolated pillow from Bald Friar Metabasalt. Upper photo is of a polished sawn surface. Sample is approximately 19 x 10 cm in size.

Except for pillows (Figure 13), which have partial internal concentric banding, the BFM is typically a laminated, dark green chlorite-actinolite-epidote metabasalt having a notable heft. Chlorite seems to be more abundant than actinolite at the more northwesterly locations such as MORT, MORTNE, TLPPOP, TLPPOP2, and PB1 and actinolite is more abundant at those more to the southeast. Titanite is the most abundant Ti-bearing accessory mineral at most localities, but polymorphs of TiO_2 are abundant at the three BRANDY-series samples (Stop 14, 1994, below).

The type locality for the Bald Friar Metabasalt is herein designated as the four known fragments of BFM exposed in the railroad cut and adjacent areas on the northwest side of Bald Friar, Cecil County, Maryland, in the Conowingo Dam 7½' quadrangle. A stratigraphic section has little meaning in a mélange, but fragments of BFM occur from 550 m WNW of the crest of Bald Friar to 700 m northwest to 450 m slightly north of west. The two most accessible fragments are located in the railroad cut in what was mapped by Higgins and Conant as Sykesville Formation. Sample SYKFM (Appendix I, Table 1) is a greenish gray laminated metabasalt collected from 70 to 80 cm above the base of a 1.6 to 2.05 m-thick slab in the railroad cut that is 14 ± 1 m-long (39º45'24"N, 76º13'05"W). Foliation in the metabasalt trends N77ºE, 47ºS. This sample was collected 33 m NW of sample SYKFM2, 220 m southeast of Mile Post 14 and 550 m northwest of the crest of Bald Friar. Sample SYKFM2 is a greenish, laminated metabasalt containing possible sheared vesicles, from the lower limb of a small chevron fold, the hinge of which trends N10^{o}E. This fragment is 2.5 ± 1 m-thick and exposed for 14 m along the horizontal at track level (39º42'28"N, 76º13'04"W). The sample was collected from a point 7.5 m southeast of where the base is exposed, 530 m WNW of the crest of Bald Friar. Sample BFMZ2 is from a concentrically banded 20x8 cm section through a chlorite-epidote-actinolite pillow. The base of this pillow, which froze in an anomalous orientation of N12ºE, 50ºSE, was left in outcrop for future generations. S_o in this set of outcrops trends N63ºE, 50ºSE. All pillows suggest a right-side-up orientation. This pillow was collected from the middle of a 3.2 ± 0.2 m-thick flow 8 m above water level in the pond and about 9.5 m below the bed containing isolated epidote-bearing pillows. This latter is 95 ± 5 m along the railroad tracks NW of sample SYKFM. Sampled pillow BFMZ2 (39º42'35"N, 76º13'08"W) is located S54ºE of milepost 14 and 0.68 km NW of the crest of Bald Friar. Sample BFMZ1 is a dark green chlorite-epidote-actinolite metabasalt having pahoehoe-like surfaces that trend N61ºE, 63ºSE and that exhibit ropy linear (extrusion?) structures that plunge NE at 84º. (As submarine chill surfaces, this sample was

subjected to "pillow enrichment disease.") Collected from 0.5 m above present water level, 0.5 m above the base of a 2.8 m-thick metabasalt fragment. A well- slickensided fault surface 1.1 m to the east of the sample site trends N78°E, 70°N and contains slickenlines that plunge to the west at 20°. Apparent S_1 in this outcrop trends N75°E, 70°S. This outcrop is located on the SW side of a creekbed and/or eroded talc exploration trench approximately 40 m S50°E of the main hollow at an elevation of about 85 ± 5 m, 0.45 km NNW of the crest of Bald Friar.

Bald Friar Metabasalt was examined at Stops 7 and 14 during the 59th Field Conference of Pennsylvania Geologists. At Stop 14, ultramafic fragments associated with the BFM on the north side of the Peach Bottom structure ranged from an attenuated, 7 cm-wide fragment to a ~2 m-wide talc-magnesite schist zone to a 9.5 m-wide listwaenite and a 1.9 m-wide talc-magnesite schist zone on the south side (Smith, 1994, Figure 73 and Table 13-A and B). At Stop 7, in addition to BFM in both a road cut and railroad cut below, an apparent Mesozoic fault cutting the section in the railroad cut was noted (Figure 61 by R. C. Smith with assistance from R. T. Faill, 1994).

Two new sets of BFM outcrops have been recognized. One chloritic outcrop was reported by Gil Wiswall and Hal Bosbyshell, West Chester University (personal communications, 1994), as occurring north of Mortonville, Chester County, just prior to the 1994 Field Conference. It was since sampled as MORTN has been confirmed to be BFM. Gale Blackmer, Pennsylvania Geological Survey, later found similar outcrops 0.8 km to the northeast. One was sampled as MORTNE and it, too, is BFM based on the analyses included in Appendix I, Table 1. On a weekend visit with his wife to the Mineral Hill area, Carroll County, Maryland, the BFM was recognized by the author in a section (Table 6) on the north shore of the Morgan Run Arm of Liberty Reservoir, Maryland. Samples from there (LRMRA4 and LRMRA6) were found to be BFM. As shown on Figure 9 of Smith and Barnes (2004), the known lateral extent, albeit highly discontinuous, of the BFM is now 143 km. In addition to BFM and serpentinites, the Liberty Reservoir section and area includes presumably related amphibolites. They have not been noted in Pennsylvania and are only informally proposed herein as a working lithodeme until such time as other localities are recognized. Nevertheless, data for selected trace elements are included in Table 7 and relatively complete analyses are presented in Appendix I, Table 1. The amphibolites at Liberty Reservoir might represent fractionated, more slowly cooled intrusive magmas than the BFM.

Smith and Barnes (1994) describe the KSA as a series of amphibolite bodies along the SSE side of the Brandywine massifs. The present, separate bodies may have once been a series of connected basalt flows. It cannot presently be ruled out that some of the limestones in the area were once reefs fringing P=E-OFB (abbreviations explained in Appendix II). Exposure in the area is poor, but Bascom and Stose (1932) did not map any serpentinites with this belt. Metamorphic grade of KSA bodies increases from west to east, but unlike the Brandywine massifs just to the north, they are generally not garnet bearing. Epidote occurs only in sample WICK on the west and hornblende and pyroxene optics change systematically to the east. Sample WICK contains epidote-filled, possible relict amygdules. The map pattern, which Peg Plank has affectionately nicknamed the "snail race" based on the contacts of Berg et al. (1980) and a comment from Sandy Schenck, is permissive of a once-connected series of basalt flows. Limited exposure of contacts and amphibolite facies metamorphism presently restrict interpretation.

The present author and John H. Barnes provided the Delaware Geological Survey with an unpublished report (1994, revised 2001) on KSA that included 7 analyses from Pennsylvania. Plank et al. (2001) combined these with data for samples from Delaware and discussed them as "type 1." Their nomenclature was derived from Volkert et al. (1996).

An additional outcrop of Kennett Square Amphibolite (KSA) was sampled (as encouraged by Gale Blackmer), as LUCKW on the eastern edge of the West Grove 7½' quadrangle. It fits the trend of KSA noted by Smith and Barnes (1994) from N-OFB on the east to P=E-OFB on the west

Table 6. Apparent stratigraphic section including Bald Friar Metabasalt, Morgan Run Arm, Liberty Reservoir, Maryland.

The following is a brief description made 3/26/95 of the apparent stratigraphic section along the northeast shore of Morgan Run Arm of Liberty Reservoir. From the caved shaft at the lakeside dump for Mineral Hill Mine, Sykesville District, Carroll County, Maryland, to the graywacke at the apparent base of the described section is S68 ± 2º W. From this same caved shaft to the center pier for the bridge carrying Maryland Route 32 over Morgan Run Arm is S78 ± 2º W, but this dump from which the bearing was taken does contain magnetite locally. More certainly, the area is 0.45 km ENE of the Maryland Route 32 bridge over Morgan Run. This area is in the Finksburg 7 1/2' quadrangle. The approximate latitude and longitude of the stratigraphic section are 39º26'14"N and 76º55'56"W, respectively. The description proceeds from SE to NW. Bedding appears to roughly parallel foliation, here N32ºE, 62ºSE.

≥17 m thick SE GRAYWACKE UNIT which is crossbedded and contains blue quartz grains up to ~ 1 cm. Graywacke samples were collected 4.1, 3.2, and 2.2 m SE of the NW contact of the graywacke. Graywacke sample 4.1 contains sutured quartz, biotite, muscovite, feldspar porphyroblasts, an unknown having high relief and interference colors such as epidote or zoisite, zircons which are subhedral and partly metamict, and apatite. Graywacke sample 3.2 was collected 18 cm WNW of the apparent pillow and contains sutured quartz, biotite, muscovite, zoisite, euhedral opaque oxides, rounded zircon, and a granular unknown such as titanite having high relief and extremely high interference colors. Graywacke sample 2.2 contains sutured quartz, biotite, muscovite, zoisite (?), euhedral opaque oxides, apatite, and an unknown granular mineral such as titanite.

The ≥ 17 m thick graywacke contains an apparent 60 x 6 cm epidotized metabasalt pillow ~3.2 m SE of the NW contact of the graywacke. In this area at least, the graywacke is crossbedded. The apparent pillow consists of epidote/zoisite-quartz-biotite-granular titanite, minor opaque oxides and rare zircon.

3.4 ± 0.2 m thick AMPHIBOLITE UNIT sampled as LRMRA5 near the middle and LRMRA5A 0.65 ± 0.1 m below the top. The former sample represents 5 cm stratigraphically and the latter sample represents 3 cm stratigraphically. Both samples are gray, fine-grained bluish green amphibole-quartz-epidote-rare barite (?), amphibolite.

1.4 ± 0.1 m thick chlorite-actinolite as a SHEARED UNIT. The protolith to the unit is likely either the amphibolite to the SE or BFM to the NW or both. Sampled as LRMRA8, but unanalyzed, from a 0.20 m channel sample centered 0.5 m below the top and 0.9 m above the base.

16.8 ± 0.5 m thick BALD FRIAR METABASALT UNIT. At spring season water levels, the section consists of a series of well-exposed ribs separated by poorly exposed shear zones. In late summer, at lower water levels, the shear zones may be better exposed at lower elevation.

Sample LRMRA4 was collected 1.5 ± 0.2 m above the base defined as the top of the 1.4 m-thick shear zone. It was collected ~ 1 m above water level as of 3/26/95. From here to the center pier for the Maryland Route 32 bridge over Morgan Run is S77 ± 2ºW. Foliation here trends N32ºE, 66ºSE. Sample LRMRA4 consists of greenish gray, fine-grained, sheared blue actinolite-epidote-chlorite metabasalt containing minor titanite. It represents 6 cm stratigraphically.

Sample LRMRA9 was collected from the NW side of a prominent rib 4.0 ± 0.2 m above LRMRA4 and 8.0 ± 0.5 m below LRMRA6 or 6.5 ± 0.2 m above the base of the metabasalt and 11.3 ± 0.5 m below the top. "S_1" created by limbs of isoclinal folds here trends N36ºE, 74ºSE. The highly deformed sample represents 9 cm stratigraphically.

Sample LRMRA6 was collected ~1.5 m above water level as of 3/26/95 at a point 8.0 ± 0.5 m above LRMRA9 or 3.3 ± 0.2 m below the top of the metabasalt. Sample LRMRA6 consists of greenish, fine-grained, sheared and faulted blue actinolite-epidote-chlorite metabasalt that contains minor titanite. Isoclinal fold hinges near the top of the metabasalt in this area trend N30ºE, 2ºNW.

≥2.4 m thick NW GRAYWACKE UNIT. Bluish quartz augen observed in outcrop. Samples were collected 0.4 and 1.4 m NW of the SE contact. Graywacke sample 1.4 contains sutured quartz, biotite, muscovite, an unknown such as zoisite having high relief and interference colors, and euhedral opaque oxides. Graywacke sample 0.4 m contains sutured quartz, biotite, included garnet, chlorite, apatite, allanite-zoisite, and opaque oxides.

Table 7. Medians for selected trace elements in the Bald Friar Metabasalt (N=14), the potentially correlative Caldwell Group 1b pillow basalts of southeastern Quebec (N variable, Bédard and Stevenson, 1999), the informal Liberty Reservoir amphibolites which are only known to be associated with Bald Friar Metabasalt at that locality (N=5), and Kennett Square Amphibolites (N=8). Possible correlations are suggested only for the BFM and Caldwell Group 1b pillow basalts, but the Liberty Reservoir amphibolite may be cogenetic with the associated BFM.

	TiO_2	Zr	Hf	Nb	Ta	Th	Ni	V	Y	La	Ce
Bald Friar Metabasalt	1.24	80	1.9	3.	<0.1	0.3	102	256	30	2.5	9
Caldwell Group, 1b (mean)	1.24	68	1.7	2.5	_	0.3	69	386	29	2.8	7
Liberty Reservoir amphibolite	1.20	95	2.2	4.	0.2	1.1	67	264	27	5.9	16
Kennett Square Amphibolite	1.10	66	1.5	4.	0.4	0.3	90	275	24	4.2	11

(Figure 9 of Smith and Barnes, 2004). Hal Bosbyshell reported that the KSA population appears to continue to the east of the Rosemont fault. Indeed it might, but an attempt to sample the suggested outcrop did not yield sufficient homogenous mafic material. However, H. Bosbyshell did collect and analyze a sample which he interprets as KSA.

GEOCHEMISTRY

Data for selected elements in the Bald Friar Metabasalt and Kennett Square Amphibolite are presented in Table 7. More complete analyses and latitudes and longitudes are in Appendix I, Table 1. Figure 14 shows updated plots for A. chondrite normalized rare earths, B. Ti-Zr-Y, C. Nb-Zr-Y, D. Ti/V, and E. primordial mantle normalized elements.

BFM plots (Figure 14) for chondrite normalized rare earths (CN REE) show a rather tight bundle having a depleted LREE characteristic of N-OFB. Sample BFMZ represents a flow top having extrusion surfaces and has suffered from “pillow enrichment disease,” a condition resulting from dissolution of glass but not immobile trace elements. BFM plots in a tight cluster for OFB on a Ti-Zr-Y diagram and as either volcanic arc or “MORB” basalts on Nb-Zr-Y plots. On a Ti/V plot, the points fall in a field for “N-MORB” plus continental basalts, but close enough to the origin to fit back arc basalts. Primordial mantle normalized data plot with a positive slope characteristic of OFB. In addition to the diagrams shown, the Nb-normalized spidergram of Myers and Breitkopf (1989) shows all samples as having a positive slope, nicely confirming the N-OFB vs. P-OFB = E-OFB aspect. Taken together, these plots best fit with back arc basin OFB, sometimes known as BABBs (Back Arc Basin Basalts).

Even though the BFM is remarkably uniform, it might be possible to recognize four pulses, initially using the TiO_2 data provided in Appendix I. Doing so yields four possible pulses containing the following samples from "oldest to youngest": 1) LRMRA4-MORTNE-PB1, 2) BFMZ2-MORTN, 3) BRANDYN-SYKFM-BRANDY-SYKFM2, and 4) BRANDYSE-LRMRA6-TLPPOP-TLPPOP2. As noted elsewhere, sample BFMZ-1 has suffered from pillow enrichment disease on an extrusion surface.

Field observations can be combined with geochemical data to further refine the provenance. Most importantly, where exposure is adequate, the BFM can be seen to be fragments in a mélange that are typically near ultramafic fragments of the Baltimore Mafic Complex ranging from centimeters to kilometers in size. This suggests that age data for the BMC (Sinha et al., 1997 and Smith and Barnes, in review) may be relevant to the age of BFM fragments, but of course, not the

disparate mélange matrix which may include a component from continental Laurentia. Affinity might best be established with $^{143}Nd/^{144}Nd$ studies of carefully collected pairs of BFM and mélange matrix samples.

Based on the compositions of included chromites, the BMC likely represents the roots of an island arc complex (Smith and Barnes, in review). Based on the Co-Cu-Fe-Au deposits drilled by Noranda Mining Company Ltd. at Mineral Hill in the Sykesville District (Candela et al., 1989) other occurrences of BFM might be mineralized. Indeed, the geologic situation at the Peach Bottom structure, York and Lancaster counties, Pennsylvania, a serpentinite-bearing mélange in fault contact with slate, is similar to that at the Mother Lode Au District, California. Candela et al. (1989) note that the mineralization they observed in the area of Liberty Reservoir occurs on the chlorite-actinolite facies contact of the blackwall (Sanford, 1982) between the ultramafic fragments and more pelitic host rock. (Some Cu-Co-Au mineralization observed in dump samples by the author was also associated with ultramafics that were partly carbonated to listwaenites or steatized.) Based on a very high Cu+Zn/Pb ratio of the ore, Candela et al. note that the ore solutions probably only contacted ultramafic oceanic lithologies. Metabasalt is a good potential source for Zn and the early Zn mineralization in the Liberty Reservoir area suggests that some BFM may have been involved.

A bed of well-preserved BFM pillows indicates that the BFM was extruded into a subaqueous environment. The noted dark green color, high density, laminated character, and common association with nearby ultramafics, makes the BFM an excellent marker for the now-folded and sheared mélange associated with the BMC. Steatitization of associated ultramafic fragments appears to have reduced the competence of the mélange similar to the situation near the northern terminus of the obducted Dunnage zone at Baie Verte, Newfoundland. In the Piedmont of Pennsylvania, the mélange nicely traces the Silurian obduction zone (Smith and Barnes, in review), even where folded, such as across the Peach Bottom fold (Smith, 1993) and along lateral, Alleghanian shear zones elsewhere.

For KSA, parameters such as TiO_2, Zr, Hf, and La tend to increase from east to west (Figure 9 of Smith and Barnes, 2004), suggesting that the source magma evolved as one might expect in an active tectonic environment. Enrichment of La shows best on the CN REE diagram (Figure 14A). La/Ce, Zr, Hf, and TiO_2 show depletion to the east, characteristic of N-OFB, and generally increase to the west (data and locations in Appendix I), which is consistent with P=E-OFB. Figure 12E of Smith and Barnes (1989) in Smith and Barnes (1994) yields similar conclusions: Two N-OFB on the east, two transitional T-OFB in the middle, and four P=E-OFB on the west. Ti-Zr-Y plots (Figure 14B) for KSA yield an open cluster in the OFB field. Nb-Zr-Y plots (Figure 14C) for KSA yield an open grouping in or near the field for N-type "MORB" and volcanic arc basalt. The Ti/V plot (Figure 14D) shows a grouping permissive of a back arc setting. The mantle normalized diagram (Figure 14E) shows the two different types of OFB via Nb and LREE in particular. KSA may have formed in a similar, but different back arc setting from the BFM. However, definitive evidence has not yet been recognized. The lack of strong negative Nb and Ta anomalies in particular show that it is not a subduction-related arc basalt. As shown by Taylor and Martinez (2003), lower TiO_2, La, and Nb back arc basalts (such as CHFD and BRANDY2 on the east end of the KSA "snail race") may be more proximal to the arc and be derived from higher percentages of melting due to higher water contents.

No additional work has been done on the poorly defined, informal "Conowingo Creek metabasalt" of Smith and Barnes (1994, p. 64). As noted by Smith and Barnes (1994), it occurs in ultramafic-bearing mélange overlooking Conowingo Creek and its tributaries in southern Lancaster County. The CONJSE-series samples (Appendix I, Table 1) contain variable evidence of pillow textures. The CNREE plots show "steer horn" patterns suggestive of boninites which, in turn, suggest a forearc environment. The reader is referred to the above reference for a discussion of

BALD FRIAR

KENNETT SQUARE

A

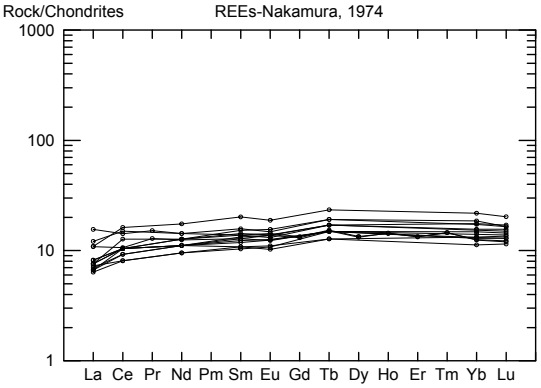

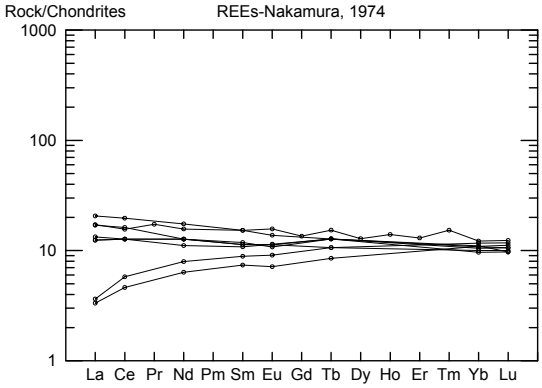

B

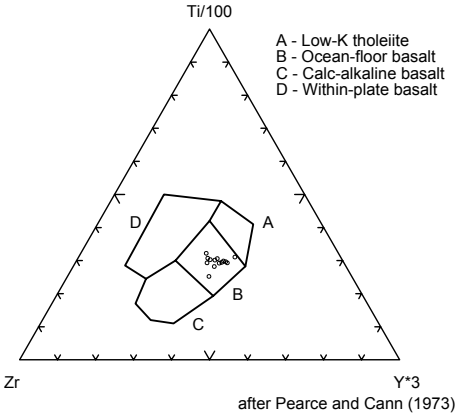

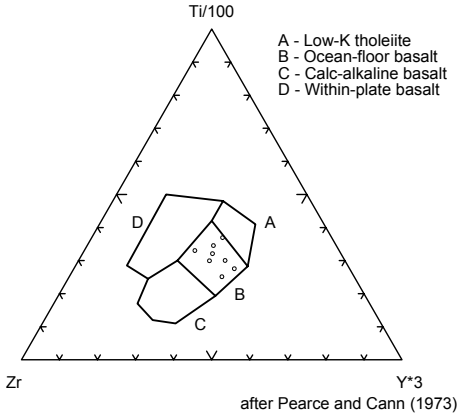

C

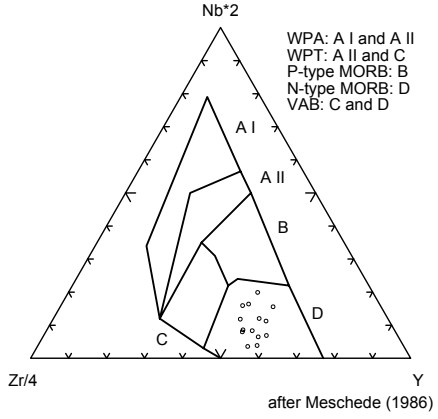

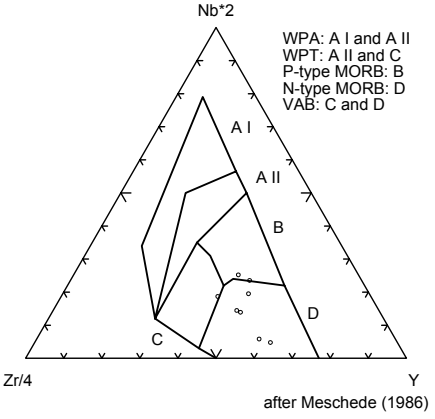

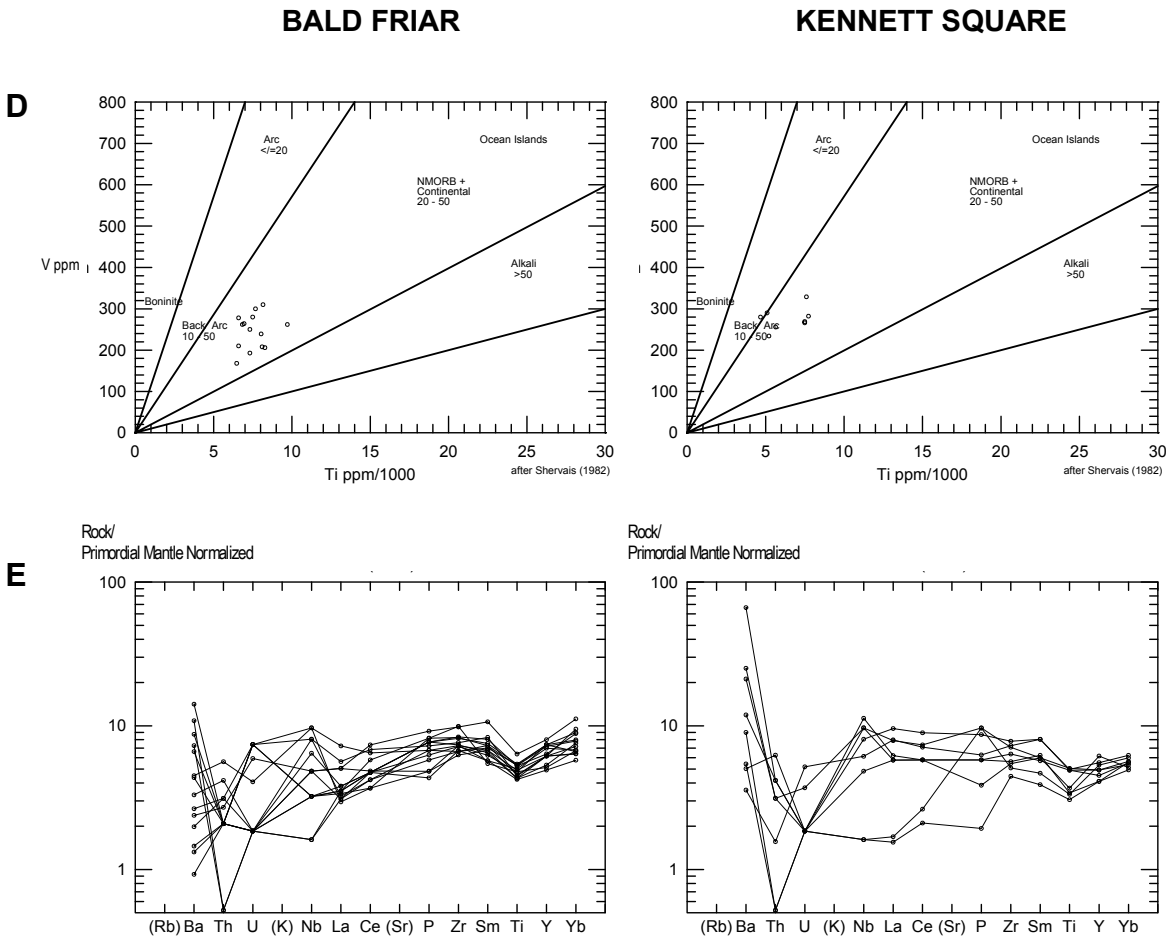

Figure 14. Trace element plots for Bald Friar Metabasalt and Kennett Square Amphibolite. The former is most compatible with an N-OFB in a back arc setting and the latter in a N-OFB transitional to P=E-OFB in a similar setting.

their association with the BMC, boninitic character, nearly exclusive association of boninites with the forearc portion of island arcs (Crawford et al., 1989, p. 38 and 43), and well-documented occurrences of similar boninites in the Thetford, Québec, ophiolite mélange and *de facto* ophiolite type locality, Troodos, Cyprus.

During field work in the Baltimore Mafic Complex for the report "Geology of Nottingham County Park" (Smith and Barnes, 1998), dense, fine- to medium-grained columnar amphibolite dikelets were found to be cutting serpentinite. These have been grouped as informal, poorly understood "Nottingham County Park amphibolite." Relatively complete data are included in Appendix I. On most tectonomagmatic diagrams they generally fall outside established fields, a common characteristic of cumulate plutons. This tends to be confirmed by the CN REE plots, which have distinct positive Eu anomalies, characteristic of plagioclase accumulation.

CONCLUSIONS

The Bald Friar Metabasalt is a back arc basin basalt (BABB), chemically similar to N-OFB, from the floor of the Iapetus Ocean. It occurs in tectonic mélange containing ultramafic clasts likely derived from the Baltimore Mafic Complex. Where it is not tectonically attenuated, it and associated ultramafic fragments, and steatized and carbonated fragments derived therefrom, make

an excellent marker for the Morgan Run Formation of the Liberty Complex. The work of Candela et al. (1989) indirectly suggests that detrital chromite might make a suitable marker in sheared formations. Because of the excellent exposure at Liberty Reservoir during water drawdowns, it is suggested that the well-described Morgan Run Formation (Muller et al., 1989) be considered for extension into York, Lancaster, and Chester counties, Pennsylvania. With some caution, such a tectonostratigraphic unit could likely be used to map the low-angle Baie Verte-Brompton equivalent obduction thrust fault over the Brandywine massifs, especially along their margins where it was later sheared. It might also prove useful in many other areas of the Piedmont of southeastern Pennsylvania where its appearance is repeated by folding.

The association of BFM with an island arc complex does not make it an island arc basalt. The lack of negative Nb and Ta anomalies on mantle-normalized diagrams in particular clearly shows this. The fact that fragments of BFM fell into sediments derived from a continent does not make it a continental basalt. All that is required for this association is that the closure of Iapetus transport oceanic material toward a continent. The fact that the BFM is associated with ultramafics at early stages (Candela et al., 1989) clearly shows that it would be quite misleading to consider it part of Catoctin rifting as opposed to generation of the oceanic floor of Iapetus.

Thus, the Baltimore Mafic Complex was a sub-arc portion of the floor of Iapetus, the Bald Friar Metabasalt an initially somewhat distal portion of the back arc now found with the BMC in mélange, and the informal Conowingo Creek Metabasalt a forearc boninitic basalt.

Kennett Square Amphibolite was part of the floor of Iapetus derived from a spreading center having its lower TiO_2, La, and Nb end to the east, suggesting that the Wilmington Complex is more likely to have been the source than the Baltimore Mafic Complex. As noted by Smith and Barnes (1994, p.69), amphibolite samples BRANDYB and DILW, which have an apparent affinity to the Wilmington Complex, are found very close to the east end of the "snail race." They were likely obducted onto the Brandywine massifs during the Silurian. This obduction likely left an attenuated, garnet-free veneer of arc-related granites, amphibolites, and ultramafic over much of the otherwise garnet-bearing Brandywine massifs, not to mention in the higher angle shear zone along the margins. (These shears are likely the result of obduction of the same mélange folded during the Alleghanian and laterally sheared during the late Alleghanian. That they became shear zones is likely due to steatitization of ultramafic clasts in the original mélange.) This obduction likely occurred after the widespread, rift-related thermal pulse associated with the 432.6-Ma Sword Mountain Olivine Melilitite (Smith, Foland, and Nickelsen, 2004) of the extreme northern part of the Ridge and Valley, Maryland, the related 424 ± 20 Ma Beemerville Igneous Complex of northwestern New Jersey, and the 442 ± 7 Ma baddeleyite-bearing refractory oxides in the Baltimore Mafic Complex, Lancaster County, Pennsylvania (Smith and Barnes, in review). The full range of this Silurian extensional event is still being evaluated, but likely includes the Beckett Quarry volcanic arc granite on the margin of the Connecticut Valley trough. Karabinos (2004) related the Beckett Quarry granite to an extensional environment and dated it at 432 ± 3 Ma using $^{206}Pb/^{238}U$ dating of zircons. To the south, Trujillo and Sinha (2004) document similar such dates in mantle-derived gabbros to diorites in an extensional setting at several localities in Virginia.

Acknowledgements. In addition to coauthoring the article for the 59th Field Conference of Pennsylvania Geologists upon which the present update is based, John H. Barnes continued to assist with data management as the author conducted additional field studies. His assistance with the present figures is also gratefully acknowledged. L. T. Chubb, Pennsylvania Geological Survey, assisted with preparing most of the new samples. John Barnes and Rodger T. Faill, P.G.S., Art W. Rose, The Pennsylvania State University, and Don U. Wise, University of Massachusetts, reviewed the present article. Two new Bald Friar Metabasalt localities were provided by Gale Blackmer, P.G. S., and Hal Bosbyshell and C. Gil Wiswall, West Chester University.

References

Bascom, F. and Stose, G. W., 1932, Coatesville-West Chester folio, Pennsylvania-Delaware, U.S. Geological Survey Atlas of the U.S., Folio 223, 15 p.

Bédard, J. H. and Stevenson, Ross, 1999, The Caldwell Group lavas of southeastern Quebec: MORB-like tholeiites associated with the opening of Iapetus Ocean, Canadian Journal of Earth Sciences, v. 36, p. 999-1019.

Berg, T. M. et al., 1980, Geologic map of Pennsylvania, Pennsylvania Geological Survey, Map 1, 1:250,000 scale.

Candela, P. A., Wyllie, A. G., and Burke, T. M., 1989, Genesis of ultramafic rock-associated Fe-Cu-Co-Zn-Ni deposits of the Sykesville District, Maryland Piedmont, Economic Geology, v. 84, p. 663-675.

Crawford, A. J., Falloon, T. J., and Green, D. H., 1989, Classification, petrogenesis and tectonic setting of boninites, Chapter 1 in Boninites, A. J. Crawford, ed., Unwin Hyman.

Higgins, M. W. and Conant, L. C., 1986, Geologic map of Cecil County, Maryland Geological Survey, 1 sheet, 1:62,500 scale.

Holm, P. E., 1985, The geochemical fingerprints of different tectonomagmatic environments using hygromagmatophile element abundances of tholeiitic basalts and basaltic andesites, Chemical Geology, v. 51, p. 303-323.

Karabinos, P., Morris, D. and Rayner, N., 2004, Silurian tectonism in the western New England Appalachians, Geological Society of America, Abstracts with Programs,

Meschede, Martin, 1986, A method of discriminating between different types of mid-ocean ridge basalts and continental tholeiites with the Nb-Zr-Y diagram, Chemical Geology, v. 56. p. 207-218.

Muller, P. D., Candela, P. A., and Wyllie, A. G., 1989, Liberty Complex; Polygenic mélange in the central Maryland Piedmont, Geological Society of America, Special Paper 228, p. 113-134.

Myers, R. E. and Breitkopf, J. H., 1989, Basalt geochemistry and tectonic settings: a new approach to relative tectonic and magmatic processes, Lithos, v. 23, p. 53-62.

Pearce, J. A. and Cann J. R., 1973, Tectonic setting of basic volcanic rocks determined using trace element analysis, Earth and Planetary Science Letters, v. 19, p. 290-300.

Plank, M.O., Srogi, LeeAnn, Schenck, W.S, and Plank, T.A., 2001, Geochemistry of the mafic rocks, Delaware Piedmont and adjacent Pennsylvania and Maryland: confirmation of arc affinity, Delaware Geological Survey, Report of Investigation, No. 60, 39 p.

Shervais, J. W., 1982, Ti-V plots and the petrogenesis of modern and ophiolitic lavas, Earth and Planetary Science Letters, v. 59, p. 101-118.

Sinha, A. K., Hanan, H. B. and Wayne, D. M., 1997, Igneous and metamorphic U-Pb zircon ages from the Baltimore Mafic Complex, Maryland Piedmont, Geological Society of America Memoir 191, p. 275-286.

Smith, II, R. C., 1993, Tell-tale talcs-Chemical Clues to unravel the Earth's secrets, Pennsylvania Geology, v. 24, no. 1, p. 2-6.

Smith, II, R.C. and Barnes, J. H., 2004, White Clay Creek Amphibolite: a Piedmont analog of the Catoctin Metabasalt, 69th Field Conference of Pennsylvania Geologists.

Smith, II, R. C. and Barnes, J. H., 1998, Geology of Nottingham County Park, Pennsylvania Geological Survey, Open File Report 98-12.

Smith, II, R. C. and Barnes, J. H., 1994, Geochemistry and geology of metabasalt in southeastern Pennsylvania and adjacent Maryland, 59th Field Conference of Pennsylvania Geologists, p. 45-72A.

Smith, II, R. C., Foland, K. A. and Nickelsen, R. P., 2004, The Lower Silurian Clear Spring Volcanic Suite: Sword Mountain Olivine Melilitite (433 ± 3 Ma) and Hanging Rock Tuff/Diatreme, Washington County, Maryland, Geological Society of America, Abstracts with Programs, v. 36, no. 2, p. 71.

Taylor, Brian and Martinez, Fernando, 2003, Back-arc basin basalt systematics, Earth and Planetary Science Letters, v. 210, p. 481-497.

Trujillo, J. and Sinha, A. K., 2004, Extensional tectonics in collisional orogens: A case study of Early Silurian extension in the central Appalachians associated with the Taconic orogeny, Geological Society of America, Abstracts with programs, v. 36, no. 2, p. 75.

Volkert, R. A., Drake, A. A., and Sugarman, P. J., 1996, Geology, geochemistry, and tectonostratigraphic relations in the crystalline basement beneath the coastal plain of New Jersey and contiguous areas; U. S. Geological Survey Professional Paper 1565-B. 48 p.

Appendix I

Table 1. Major, minor, and trace element analyses for metabasalt, metadiabase, and amphibolite populations discussed in this report.

SAMPLE NAME	Major and minor elements: SiO_2%	Al_2O_3%	Fe_2O_3%	CaO%	MgO%	Na_2O%	K_2O%	TiO_2%	MnO%	P_2O_5%	Ba ppm	Sr ppm	Zr ppm	LOI%	TOTAL%	Trace elements Ag	As	Au	Be
Accomac																			
ACC330E	46.43	13.94	15.49	5.19	5.01	4.97	0.32	4.06	0.35	1.32	100	70	324	2.55	99.61	<0.1	<1	<0.002	<1
ACCOM	52.17	13.52	15.16	5.00	1.87	7.14	0.29	3.22	0.07	0.37	27	108	248	<0.01	98.84		<1	<0.005	<1
ACCPU	46.75	15.43	12.06	6.51	6.73	4.49	0.42	2.72	0.28	0.28	120	220	180	3.09	98.76	<0.1	1	<0.002	<1
ACC 48E	46.45	14.28	14.23	7.96	6.34	4.02	0.34	2.51	0.23	0.24	150	230	190	3.06	99.64	<0.1	<1	0.002	4
ACC180E	48.70	15.77	11.54	9.19	4.68	4.33	0.78	1.73	0.13	0.14	190	210	94	1.81	98.79	<0.1	1	<0.002	2
Bald Eagle																			
BLDEAGSW	46.13	13.24	17.43	7.57	5.56	3.63	0.09	4.27	0.22	0.65	22	275	261	0.54	99.34	<0.4	3	0.049	<2
BLDEAG2	47.65	15.00	15.55	8.27	4.89	2.62	0.60	3.32	0.19	0.44	154	267	195	1.45	99.98	0.5	<1	0.003	<2
BLDEAG	47.48	15.48	15.36	8.20	4.94	3.40	0.84	3.10	0.20	0.44	324	230	177	0.34	99.76	0.7	<1	<0.002	3
WOODB	48.09	15.37	15.91	5.95	6.56	1.33	0.06	3.03	0.27	0.34	31	429	169	3.82	100.73	<0.4	2	<0.002	2
Bald Friar																			
BFMZ1	45.10	14.73	13.44	15.16	5.22	1.47	0.16	1.62	0.19	0.19	33	220	108	1.33	98.61	<0.4	4	0.004	<2
TLPPOP2	43.42	12.52	11.56	12.24	5.85	2.53	<0.02	1.38	0.17	0.16	10	260	90	9.79	99.63	<0.1	5	<0.002	<1
TLPPOP	47.75	14.05	11.99	12.67	5.06	0.84	0.23	1.36	0.15	0.12	11	344	73	5.24	99.51	<2	5	<0.002	<1
LRMRA6	44.37	15.43	10.31	16.70	7.75	0.93	0.08	1.35	0.21	0.17	7	197	91	1.79	99.07	<0.4	2	0.004	<2
BRANDYSE	49.19	15.67	12.24	10.95	5.60	2.21	0.38	1.34	0.20	0.16	55	154	92	1.11	99.04	<0.4	2	<0.002	<2
SYKFM2	47.22	14.57	11.41	14.04	5.34	2.15	0.44	1.28	0.18	0.10	50	230	80	2.66	99.38	<0.1	3	<0.002	2
BRANDY	47.38	16.54	11.25	12.21	6.27	2.14	0.62	1.25	0.20	0.14	82	279	80	1.81	99.79	0.1	<1	0.006	1
SYKFM	44.88	15.75	11.91	15.05	5.21	2.23	0.40	1.22	0.22	0.17	107	201	109	2.42	99.50	<2	3	<0.002	<1
BRANDYN	47.56	16.59	10.60	11.05	5.53	2.95	0.36	1.22	0.16	0.13	66	198	79	3.17	99.31	<0.4	<1	<0.002	<2
MORTN	44.62	13.74	10.25	11.11	6.05	2.88	0.26	1.16	0.17	0.14	34	144	73	9.80	100.17	<0.3	<1	0.011	<1
BFMZ2	44.22	15.90	12.01	17.69	5.98	1.03	0.05	1.14	0.20	0.15	25	338	84	1.39	99.76	<0.4	14	0.003	<2
PB1	46.20	17.12	11.93	10.98	4.30	3.17	0.03	1.10	0.19	0.16	15	433	81	4.61	99.78	<0.4	5	<0.002	<2
MORTNE	50.52	15.44	10.30	11.01	6.30	2.81	0.10	1.10	0.14	0.10	18	136	69	2.33	100.15	<0.3	<1	<0.002	<1
LRMRA4	46.10	14.66	9.17	13.92	10.70	1.55	0.17	1.08	0.22	0.09	20	128	74	1.78	99.43	<0.4	2	0.003	<2
Catoctin dikes in Grenvillian terrains																			
PATPK	50.06	12.06	16.10	8.20	3.92	2.62	1.64	3.88	0.24	0.52	460	240	320	1.34	100.52	0.1	<1	0.003	2
ANT RESV	48.79	12.71	15.61	8.20	4.27	2.70	1.63	3.84	0.24	0.68	357	303	286	1.17	99.96	<2	<1	<0.002	<1
BROOKM	48.47	11.88	17.11	8.45	4.54	2.47	0.54	3.71	0.35	0.40	210	280	230	0.94	98.86	<0.1	<1	0.002	<1
HSTR	48.02	12.92	15.78	8.77	4.46	3.05	0.86	3.48	0.24	0.60	250	312	247	1.18	99.35	0.1	1	0.007	1
LS3	49.17	12.50	17.00	8.77	4.67	2.65	1.04	3.34	0.24	0.44	390	340	280	0.39	100.20	<0.1	<1	0.002	6
TOPFND	46.99	13.46	14.57	9.09	5.70	2.35	1.56	3.29	0.23	0.59	366	422	178	1.76	99.70	<2	<1	<0.002	<1
LS2	45.14	13.27	15.64	7.97	5.46	3.05	1.46	3.29	0.21	0.50	500	380	230	2.12	98.10	<0.1	<1	<0.002	5
HUFFC	49.08	12.42	16.67	8.51	4.31	2.52	0.62	3.19	0.24	0.48	213	280	302	1.53	99.56	0.1	<1	0.003	<1
ISHMTN	45.70	13.41	14.87	9.32	6.00	2.55	1.56	3.02	0.22	0.46	370	360	190	1.73	98.85	<0.1	<1	<0.002	5
PH152	49.99	13.64	13.27	9.54	5.67	3.24	0.49	2.83	0.19	0.34	242	318	196	1.72	100.91	<0.4	<1	0.003	<2
D-266	47.57	13.61	14.54	10.93	5.38	2.18	0.70	2.78	0.22	0.35	311	315	225	1.09	99.45	<2	1	<0.002	<1
UWC	46.90	12.76	16.03	10.01	5.47	2.59	0.66	2.78	0.24	0.30	230	280	210	0.80	98.55	<0.1	<1	0.003	5
DV	45.95	13.00	16.19	10.22	5.51	2.20	0.76	2.76	0.23	0.30	240	280	190	1.30	98.46	<0.1	<1	0.004	5
LYDRY	45.59	13.50	14.06	9.88	5.48	2.44	0.82	2.74	0.23	0.34	220	440	210	2.53	97.60	<0.1	<1	<0.002	5
LUD COR	49.40	13.69	14.74	9.73	5.38	2.73	0.72	2.45	0.23	0.28	198	308	153	0.81	100.24	<2	<1	<0.002	<1
HUFFM	48.10	13.53	14.06	9.72	5.48	2.32	0.76	2.43	0.21	0.28	232	379	193	1.53	98.44	0.1	<1	<0.002	<1
STP FA	46.53	14.35	14.59	10.42	5.62	2.44	0.73	2.31	0.21	0.26	194	269	174	0.89	98.42	<2	<2	<0.002	4
ELBNW	49.33	13.69	14.15	10.25	5.73	2.76	0.72	2.21	0.21	0.28	230	330	200	0.96	100.29	<0.1	<1	0.003	4
HNYNW	48.85	13.54	13.48	11.04	6.31	2.57	0.44	1.97	0.21	0.20	110	300	130	1.48	100.09	<0.1	<1	<0.002	3

Appendix I

Table 1. Major, minor, and trace element analyses for metabasalt, metadiabase, and amphibolite populations discussed in this report.

	Major and minor elements:															Trace elements			
SAMPLE NAME	SiO_2%	Al_2O_3%	Fe_2O_3%	CaO%	MgO%	Na_2O%	K_2O%	TiO_2%	MnO%	P_2O_5%	Ba ppm	Sr ppm	Zr ppm	LOI%	TOTAL%	Ag	As	Au	Be
FURNCK	48.66	15.41	12.17	9.56	5.18	3.03	1.46	1.93	0.19	0.32	310	390	180	2.21	100.12	<0.1	<1	<0.002	3
HNY82	49.60	16.27	11.58	10.32	5.20	2.71	0.72	1.75	0.17	0.16	270	310	130	1.07	99.55	<0.1	<1	0.003	3
MRCK	49.29	14.89	12.05	11.95	6.74	2.24	0.36	1.59	0.18	0.16	150	250	110	0.91	100.35	<0.1	<1	0.007	2
HPD	48.74	14.49	11.21	11.47	8.00	2.58	0.06	1.37	0.16	0.12	39	270	89	1.97	100.16	<0.3	<1	0.016	<1
Conowingo																			
CONJSEIII	37.44	11.69	23.63	14.29	4.60	0.39	0.08	5.13	0.29	0.79	39	557	188	1.15	99.48	<0.4	12	<0.002	4
LEO	41.14	16.47	19.12	9.67	7.28	0.90	0.10	2.13	0.34	0.34	24	255	59	3.27	100.78	<0.4	12	0.006	<2
PLGRV	42.00	16.96	15.66	8.72	8.88	0.94	0.16	1.34	0.26	0.36	40	232	136	3.92	99.18	<0.4	10	<0.002	<2
CONJSEII	41.57	17.57	16.06	7.38	9.05	1.20	0.15	1.34	0.33	0.11	344	242	75	5.19	99.96	<0.4	5	<0.002	<2
WAKES	43.18	13.92	14.74	7.14	11.86	0.58	0.12	0.98	0.28	0.40	40	144	86	4.70	97.88	<0.4	6	<0.002	2
CONJSE	43.04	14.52	15.58	7.30	12.42	0.22	0.08	0.94	0.22	0.04	20	260	41	4.90	99.26	<0.4	2	0.024	<2
APPLE	45.73	17.72	13.00	11.20	7.65	1.14	0.12	0.83	0.19	0.04	28	190	37	0.55	98.16	<0.4	<1	0.022	<2
PLGRVS	45.59	11.47	14.72	5.03	15.70	0.38	0.04	0.64	0.27	0.15	72	16	56	5.22	99.22	<0.4	8	0.003	<2
Fishing Creek																			
FSHCKT	34.72	18.07	17.49	12.75	7.53	0.70	0.26	3.39	0.24	0.56	96	363	220	4.89	100.59	<0.4	3	<0.002	<2
FSHCKOTC	45.40	14.83	13.67	7.41	7.76	3.38	0.27	2.33	0.18	0.29	45	203	163	3.56	99.07	<0.4	2	0.004	<2
FSHCKFG	46.37	15.54	11.74	7.20	7.77	3.99	0.12	2.24	0.16	0.38	50	180	150	3.66	99.17	<0.1	1	<0.002	<1
FSHCKFGIII	45.83	15.90	12.10	7.32	7.82	4.05	0.12	2.15	0.16	0.36	101	196	168	3.45	99.24	<0.4	2	<0.002	<2
FSHCKFGIV	46.74	16.12	11.94	7.12	8.11	4.08	0.12	2.13	0.17	0.39	33	196	166	3.64	100.56	<0.4	2	0.003	<2
FSHCKFGV	47.07	16.04	10.47	7.18	8.53	4.07	0.15	2.11	0.16	0.33	31	184	163	3.64	99.75	<0.3	2	0.003	<1
FSHCKFGII	46.47	16.29	11.94	7.28	8.18	4.08	0.16	2.09	0.17	0.38	50	197	150	3.69	100.75	<0.1	2	<0.002	1
FSHCKRR	42.52	16.02	10.74	13.48	4.74	3.20	0.20	1.94	0.12	0.36	56	150	154	4.20	97.54	0.4	<1	<0.002	<2
FSHCKQ	46.56	16.28	10.90	6.44	9.31	3.65	0.14	1.70	0.13	0.25	<10	227	118	3.84	99.25	<2	<1	0.011	<1
FSHCKINT	45.95	15.56	9.95	9.53	7.37	3.24	0.01	1.52	0.15	0.22	18	354	124	5.80	99.31	<0.4	3	<0.002	<2
FSHCKMON	42.24	13.94	9.59	14.58	5.03	3.49	0.94	1.48	0.17	0.42	254	289	114	7.41	99.28	<0.3	1	0.004	1
Holtwood																			
HLTWCOL	44.52	16.09	15.51	9.10	5.21	3.37	0.30	2.26	0.18	0.27	42	265	110	1.72	98.57	<2	5	<0.002	<1
HLTWM	48.61	13.41	14.30	8.24	5.55	4.59	0.38	2.24	0.13	0.20	130	200	100	1.79	99.44	<0.1	4	0.002	<1
HLTWNE	47.32	13.53	14.09	8.59	4.80	4.63	0.38	1.92	0.16	0.20	86	203	97	4.13	99.75	<0.4	3	<0.002	<2
HLTWTN	43.04	16.10	12.19	9.47	5.41	4.20	<0.01	1.72	0.13	0.28	11	341	93	7.62	100.17	<0.3	4	<0.002	<1
HLTWBASE	47.16	16.80	11.51	11.09	5.44	2.08	0.13	1.67	0.18	0.21	52	258	113	4.01	100.35	<2	4	<0.002	2
COYLK	48.23	15.16	11.36	10.77	5.85	2.03	0.23	1.58	0.17	0.16	25	265	98	4.41	99.99	<2	2	<0.002	<1
Group IV of Plank																			
CB12-C 43506	47.14	15.94	11.67	11.47	8.41	2.54	0.69	0.81	0.19	0.05	35	97	43	0.76	99.65	0.4	<1	<2	<1
JRBEWH*	48.89	15.98	8.43	11.66	8.32	2.60	0.86	0.76	0.20	0.06	96	127	42	1.14	98.89	<0.3	<1	<2	<1
WCCTP*	47.03	15.18	10.12	16.28	7.36	1.64	0.29	0.66	0.17	0.08	185	99	54	0.57	99.39	<0.3	<1	<2	4
James Run																			
JRFM C	53.27	13.02	16.45	7.22	3.29	3.25	0.42	2.16	0.28	0.62	70	140	97	0.90	100.88	<0.1	<1	<0.002	2
JRGFAS	60.21	14.56	9.96	5.44	2.38	5.25	0.16	1.48	0.17	0.30	46	208	246	0.41	100.32	0.3	<1	0.014	<2
JRGFA	58.95	12.89	11.64	6.43	2.41	3.48	0.34	1.45	0.22	0.34	90	160	180	0.58	98.75	<0.1	<1	<0.002	3
JRFM V	66.24	13.56	5.48	3.54	2.26	5.42	0.52	1.20	0.08	0.24	160	140	166	0.86	99.42	<0.1	<1	<0.002	<2
JRS	56.84	15.64	11.70	4.86	3.54	4.98	0.72	0.84	0.20	0.08	220	80	59	1.34	100.78	<0.1	<1	<0.002	<2
Jonestown Volcanics																			
BKHLM	46.57	16.28	11.26	9.07	7.95	2.81	0.64	1.90	0.18	0.22	270	230	150	3.63	100.50	0.2	<1	0.002	<2
BKHLNW2-11	40.54	12.67	9.98	13.41	6.41	3.57	0.50	1.64	0.18	0.30	254	199	120	11.27	100.46	<0.3	<1	<0.002	<1
BKHL	47.90	15.20	10.62	13.64	4.06	3.14	0.93	1.48	0.17	0.21	175	269	95	2.42	99.83	<2	1	<0.002	<1

Appendix I

Table 1. Major, minor, and trace element analyses for metabasalt, metadiabase, and amphibolite populations discussed in this report.

	Major and minor elements:															Trace elements			
SAMPLE NAME	SiO_2%	Al_2O_3%	Fe_2O_3%	CaO%	MgO%	Na_2O%	K_2O%	TiO_2%	MnO%	P_2O_5%	Ba ppm	Sr ppm	Zr ppm	LOI%	TOTAL%	Ag	As	Au	Be
BKHLV	50.91	13.80	9.40	14.49	2.97	2.12	0.10	1.39	0.16	0.23	244	45	103	5.32	100.89	<0.4	2	0.003	<2
KENB	50.63	13.72	13.70	5.90	7.55	4.64	0.06	1.39	0.21	0.13	45	150	106	2.93	100.86	<0.4	14	0.003	<2
PA 72	50.47	14.36	11.07	9.30	6.36	2.15	1.38	1.10	0.19	0.10	399	244	66	2.14	98.70	<2	4	0.004	<1
Kennett Square																			
LUCK	47.93	14.08	11.92	11.52	8.40	2.59	0.50	1.29	0.20	0.08	190	160	60	0.60	99.12	<0.1	<1	0.002	<1
LUCKW	48.40	14.69	12.70	11.11	7.33	1.79	0.18	1.27	0.19	0.13	27	135	80	1.73	99.61	<0.3	<1	0.003	<1
KS	48.99	15.18	11.07	9.46	7.62	4.42	0.32	1.25	0.17	0.12	160	90	70	0.38	98.96	<0.1	<1	0.008	<1
WICK	43.89	15.54	12.00	14.57	7.14	2.03	0.38	1.25	0.16	0.18	38	198	86	0.59	97.71	<0.3	<1	0.004	<1
ROSE	46.80	14.09	10.73	18.65	6.71	1.72	0.60	0.94	0.24	0.20	502	192	78	0.05	100.72	0.8	<1	0.005	<2
BRNTML	46.65	15.55	10.51	12.65	8.47	2.72	0.62	0.87	0.18	0.12	90	128	62	0.70	99.05	<0.3	<1	0.009	<1
CHFD	46.24	14.26	10.64	15.32	7.61	1.85	0.20	0.85	0.17	0.20	41	81	56	0.76	98.10	<0.1	<1	0.003	<1
BRANDY2	47.03	14.75	11.12	14.43	8.12	2.41	0.50	0.78	0.19	0.04	68	107	49	0.68	100.06	<0.1	1	0.004	<1
Liberty Reservoir																			
LRMRA3	46.52	16.19	14.42	14.08	4.98	0.76	0.19	1.41	0.22	0.17	39	298	105	1.78	100.73	<0.4	2	0.003	<2
LRMRA5A	50.51	13.73	13.28	10.60	6.24	1.98	0.25	1.24	0.20	0.13	63	187	66	1.26	99.50	<0.3	2	<0.002	<1
LRMRA5	51.43	14.23	12.90	10.49	6.46	2.22	0.27	1.20	0.20	0.12	76	159	92	1.20	100.73	<0.4	<1	0.004	<2
LRMRA9	46.89	14.54	8.75	13.70	10.04	1.91	0.25	0.92	0.21	0.10	26	195	97	1.98	99.36	<0.3	1	<0.002	<1
LRMRA2	50.52	14.05	10.20	11.07	10.23	1.73	0.17	0.66	0.18	0.05	24	109	51	1.73	100.59	<0.4	<1	0.005	<2
Nottingham County Park																			
NCPAVH4.74	38.66	14.33	20.92	11.42	8.20	1.92	0.56	2.05	0.26	0.14	62	50	16	0.52	98.97	<0.3	2	<0.002	<1
NCPKIRK6	38.74	13.50	22.22	10.88	8.52	2.80	0.42	1.78	0.32	0.02	21	34	16	0.65	99.84	<0.3	<1	<0.002	3
NCPNN	41.12	14.10	16.82	13.11	8.51	2.27	0.43	1.28	0.20	<0.01	242	106	15	1.23	99.07	<0.3	<1	<0.002	<1
"Older diabase"																			
BALTP2	50.50	12.76	17.48	8.65	4.57	2.19	0.04	3.52	0.24	0.44	13	194	275	<0.01	99.70	0.4	<1	0.002	<1
BALTP	50.43	12.95	16.65	8.65	4.37	3.03	0.16	3.42	0.24	0.46	110	236	275	<0.01	100.24	0.1	<1	0.004	2
BEAU2	51.25	12.23	16.51	8.86	4.36	2.48	1.04	3.19	0.24	0.36	350	310	220	<0.01	100.13	<0.1	<1	<0.002	<1
BALTP3	49.64	14.75	12.96	9.91	5.30	3.19	0.66	2.18	0.20	0.30	186	86	144	0.23	99.32	<0.3	<1	0.006	<1
BAYARD	49.50	12.61	16.39	9.22	4.64	2.63	0.62	1.63	0.25	0.29	280	180	134	0.83	98.59	<0.3	<1	<0.002	<1
ARMK2	48.33	15.46	11.92	10.98	7.67	3.10	0.38	0.96	0.19	0.22	117	119	84	1.20	100.40	<0.3	<1	0.004	<1
CPSUN	50.09	16.20	11.40	11.09	7.87	2.13	0.40	0.81	0.18	0.12	210	200	81	0.21	100.50	<0.1	<1	<0.002	<1
CRUMCK	48.40	15.66	12.31	11.64	7.86	2.60	0.16	0.74	0.20	0.06	60	100	46	0.23	99.87	<0.1	<1	0.008	<1
BEAU	47.72	16.75	11.97	11.16	7.69	2.71	0.19	0.59	0.20	0.09	66	106	43	0.70	99.80	<2	<1	0.005	<1
RADNOR	47.43	15.92	11.12	11.06	8.51	2.48	0.28	0.59	0.18	0.12	142	142	67	0.65	98.35	<0.3	<1	0.003	<1
Pigeon Hills																			
PIGHL	34.01	20.72	17.77	1.15	14.36	0.53	0.81	2.48	0.21	0.25	114	88	155	7.66	99.99		2	<0.005	<1
PIGHL2	49.60	16.13	12.05	3.32	8.54	1.27	0.08	1.85	0.16	0.28	90	270	110	5.27	98.57	<0.1	<1	<0.002	1
PIGHL888	39.70	15.11	13.03	10.02	5.62	1.14	0.36	1.73	0.19	0.16	190	110	102	12.25	99.32	<0.1	<1	<0.002	1
PIGHL3	46.20	16.34	11.77	11.59	7.22	0.90	0.02	1.35	0.20	0.12	80	580	90	4.14	99.85	<0.1	1	<0.002	<1
PIGHL5	43.56	16.04	12.48	11.06	8.38	2.08	0.08	1.30	0.20	0.12	42	62	86	2.52	97.82	0.6	<1	0.004	<2
PIGHL4	46.32	16.02	12.34	9.42	8.38	1.64	0.12	1.28	0.20	0.16	56	42	81	2.04	97.94	0.5	2	0.004	<2
Sams Creek																			
GLENRK	48.32	15.24	16.05	4.18	5.54	3.22	0.10	2.63	0.26	0.27	<10	58	133	3.27	99.02	<2	2	<0.002	<1
DISEQ	34.90	20.30	16.98	14.58	5.80	0.12	1.12	2.32	0.28	0.32	346	550	170	0.80	97.52	1.5	2	0.002	<2
SC340NE	46.76	15.84	12.62	9.08	6.54	2.60	0.04	2.30	0.16	0.32	20	300	180	3.70	99.92	<0.1	<2	<0.002	<2
PCSC4	42.64	14.32	15.86	11.44	8.12	1.44	0.56	2.14	0.30	0.36	166	278	120	0.86	98.00	1	30	0.018	<2
PA616	52.16	13.82	12.94	6.60	6.96	3.04	0.04	2.02	0.20	0.20	18	102	104	0.74	98.70	0.4	<1	0.006	<2

Appendix I

Table 1. Major, minor, and trace element analyses for metabasalt, metadiabase, and amphibolite populations discussed in this report.

	Major and minor elements:															Trace elements			
SAMPLE NAME	SiO_2%	Al_2O_3%	Fe_2O_3%	CaO%	MgO%	Na_2O%	K_2O%	TiO_2%	MnO%	P_2O_5%	Ba ppm	Sr ppm	Zr ppm	LOI%	TOTAL%	Ag	As	Au	Be
PCSC3	44.44	15.50	13.02	6.34	10.54	2.60	<0.04	2.02	0.18	0.36	6	206	145	3.18	98.20	0.5	2	0.003	<2
PCSC	39.86	17.54	14.50	14.27	4.71	2.20	0.56	1.97	0.27	0.60	540	280	160	3.45	99.93	<0.1	3	0.002	3
SC240NE	45.99	16.45	11.96	9.53	7.84	2.85	0.06	1.93	0.20	0.36	3	396	155	3.34	100.52	0.8	<1	0.002	<2
GLENM	47.01	14.08	13.90	10.93	6.47	2.58	0.24	1.90	0.19	0.18	110	590	110	2.54	100.02	<0.1	13	<0.002	<1
SCTYPE	47.28	16.28	11.12	11.04	6.16	2.76	0.56	1.88	0.16	0.36	178	502	151	2.66	100.26	1.3	<1	0.007	<2
SC 40NE	46.91	17.30	10.33	10.32	6.93	2.48	0.08	1.88	0.16	0.32	30	547	141	3.40	100.10	0.8	2	0.005	<2
SC440NE	44.52	16.60	11.42	11.98	7.20	2.14	0.80	1.80	0.18	0.32	332	402	118	2.52	99.68	0.7	<1	<0.002	<2
SCQ	49.26	15.53	12.08	8.08	5.96	4.16	0.16	1.74	0.18	0.22	100	260	120	2.58	99.95	<0.1	6	0.002	<1
GLENT	45.68	15.16	14.54	9.56	7.38	2.94	0.08	1.70	0.22	0.20	18	394	93	2.84	100.32	0.7	3	0.003	<2
SC144NE	43.77	16.20	11.18	10.03	9.67	1.80	0.10	1.50	0.21	0.28	26	379	141	4.78	99.48	<2	<2	<0.002	3
GLENN	44.56	13.27	13.92	8.03	9.73	3.00	0.14	1.47	0.20	0.18	50	140	60	3.69	98.18	<0.1	2	<0.002	<1
GLENS	47.51	15.01	11.72	10.22	7.60	3.10	0.08	1.39	0.17	0.12	100	160	70	3.35	100.25	<0.1	<1	<0.002	<1
White Clay Creek																			
NEWARKRD	45.83	11.54	19.63	9.19	5.37	1.43	0.65	4.92	0.23	0.31	183	258	193	0.40	99.49	<0.3	2	<0.002	2
WCCMBIV	45.79	13.70	16.83	7.95	4.91	2.77	0.63	4.75	0.20	0.38	118	494	261	0.49	98.40	<0.4	<1	0.003	<2
YRKLYN	47.13	11.86	18.14	9.33	5.00	2.36	0.78	4.64	0.26	0.48	237	242	264	0.35	100.32	<0.3	<1	0.003	<1
LANS	46.64	12.13	17.67	8.59	4.51	1.95	0.58	4.50	0.24	0.42	230	260	280	0.37	97.60	<0.1	<1	<0.002	7
WDCRST2	43.14	11.73	21.55	9.87	6.17	1.65	0.48	4.49	0.21	0.22	153	275	138	0.81	100.30	<0.3	<1	0.005	<1
WCCW	43.88	12.74	19.04	10.40	6.52	1.82	0.48	3.44	0.20	0.28	126	264	131	0.50	99.28	0.6	<1	0.003	2
WCCBEC	48.04	14.31	14.89	10.24	6.34	1.00	0.43	3.40	0.33	0.38	59	415	163	1.04	100.39	<0.3	<1	<0.002	<1
LANM	47.67	11.62	15.44	10.93	6.54	2.00	0.44	3.04	0.19	0.22	160	280	160	0.75	98.86	<0.1	1	<0.002	<1
WCCMBI	47.02	13.48	18.36	9.72	5.52	1.50	0.76	2.88	0.24	0.28	72	136	125	0.52	100.28	<0.4	<1	0.008	2
GREENLAWN2	46.86	12.95	18.66	9.14	5.18	1.59	0.45	2.86	0.22	0.24	154	228	130	1.72	99.87	<0.3	<1	0.008	2
WCCMBIII	48.24	14.70	14.64	9.70	5.80	2.60	0.56	2.64	0.18	0.40	46	398	164	0.68	100.12	0.5	<1	<0.002	2
WCCW+WA	50.11	13.55	16.48	8.51	5.07	2.15	0.51	2.54	0.23	0.32	31	341	169	0.39	99.92	<0.3	<1	<0.002	1
WCCMC	51.21	14.07	13.17	8.91	6.26	2.33	0.49	2.51	0.17	0.27	105	344	180	0.45	99.84	0.4	<1	<2	2
WCCN2	48.54	13.82	16.84	9.60	6.00	1.30	0.68	2.38	0.22	0.28	224	304	122	0.58	100.22	<0.4	<1	<0.002	2
WCCW+WC	48.91	13.57	16.25	9.11	5.89	1.54	0.36	2.38	0.24	0.30	131	299	158	0.74	99.35	<0.3	<1	<0.002	1
WCCMBII	47.23	16.92	13.01	10.50	5.88	2.22	0.58	2.36	0.19	0.25	88	450	156	0.47	99.61	<0.4	<1	<0.002	<2
MP 5	48.39	14.71	12.59	11.01	7.19	2.35	0.32	2.04	0.17	0.24	95	369	124	0.58	99.59	1	<1	0.007	<1
WCCMBI 10-20CM	49.64	13.78	14.31	9.66	6.25	2.13	0.65	1.98	0.20	0.28	124	314	126	0.75	99.63	<0.3	<1	<2	<1
WCCW+W	49.78	14.54	13.88	10.28	6.00	1.74	0.50	1.97	0.21	0.17	149	456	124	0.47	99.54	<0.3	<1	<2	1
LANN	48.14	14.08	11.81	11.32	7.37	2.36	0.40	1.94	0.17	0.24	130	310	110	0.82	98.64	<0.1	<1	<0.002	3
WCC	49.53	14.49	13.31	9.90	6.42	2.27	0.50	1.66	0.19	0.20	188	313	108	0.65	99.14	<0.3	<1	0.005	<1

Appendix I

Table 1. Major, minor, and trace element analyses for metabasalt, metadiabase, and amphibolite populations discussed in this report.

SAMPLE NAME	Bi	Br	Cd	Co	Cr	Cs	Cu	F	Ga	Ge	Hf	Ir	Pb	Mo	Nb	Ni	Rb	Sb	Sc	Se	Sn	Ta	Th	Tl	U
Accomac																									
ACC330E	<100	<0.5		31	2.9	<0.2	130				9.4	<0.001	<50	<2	37	<10	10	<0.1	29	<0.6		1.8	2.4		0.8
ACCOM	<3	<0.5	<5	23	22	<0.5	40				5.8	<0.001	<5	<2	24	50	<10	0.2	34	<3	<5	1.0	2.0		1.0
ACCPU	<100	<0.5		54	120	<0.2	25				4.6	<0.001	<50	<2	19	60	10	0.1	35	<0.5		1.0	1.3		0.4
ACC 48E	<200	<0.5		43	96	<0.2	60				3.9	<0.001	<100	<2	17	60	13	0.1	31	<0.5		0.7	1.1		<0.5
ACC180E	<100	<0.5		37	180	0.3	10				2.0	<1	<50	<2	11	190	20	0.1	24	<0.5		0.4	0.4		<0.5
Bald Eagle																									
BLDEAGSW	<5	<0.5	0.6	72	125	<0.2	72				6.5	<0.001	7	<2	30	84	<10	0.2	33	<0.5		1.7	2.9		0.6
BLDEAG2	<5	<0.5	<0.5	48	185	1.9	40				5.2	<0.001	15	<2	23	54	44	0.3	28	<0.5		1.3	2.3		0.4
BLDEAG	<5	<0.5	<0.5	52	190	1.1	45				5.6	<0.001	<5	<2	21	51	41	0.2	31	<0.5		1.6	2.4		0.7
WOODB	<5	<0.5	<0.5	58	170	<0.2	89				5.2	<0.001	20	<2	25	77	15	1.5	31	<0.5		1.6	2.4		1.0
Bald Friar																									
BFMZ1	<5	<0.5	<0.5	42	295	<0.2	37				2.8	<0.001	<5	<2	3	110	10	1.0	41	<0.5		<0.1	0.2		<0.1
TLPPOP2	<100	<0.5		46	200	<0.2	85				2.2	<0.001	<50	<2	4	100	<10	1.0	40	<0.5		<0.1	0.2		<0.1
TLPPOP	<3	<0.5	<5	37	220	<0.2	40				2.1	<0.001	14	<2	5	85	<10	1.8	33	<0.5	<5	<0.1	0.2		<0.5
LRMRA6	<5	<0.5	0.6	35	353	<0.2	23				2.0	<0.001	14	<2	2	71	<10	0.4	39	<0.5		<0.1	0.2		<0.1
BRANDYSE	<5	<0.5	<0.5	46	390	<0.2	46				2.1	<0.001	<5	<2	<2	124	<10	0.3	41	<0.5		<0.1	<0.1		<0.1
SYKFM2	<100	<0.5		35	210	0.6	40				1.6	<0.001	<50	<2	2	80	13	0.7	32	<0.5		0.2	0.2		<0.5
BRANDY		<0.5		44	260	<0.2	65				1.8	<0.001	<5	<2	<2	90	19	0.6	38	<0.5		0.1	<0.1		<0.1
SYKFM	<100	<0.5		33	180	0.9	45				1.6	<0.001		<2	6	70	15	0.8	31	<0.5		<0.1	0.2		<0.5
BRANDYN	<5	<0.5	<0.5	42	290	<0.2	39				1.6	<0.001	<5	<2	3	84	<10	0.6	37	<0.5		<0.1	0.2		<0.1
MORTN	<2	<0.5	<0.3	43.3	457	0.5	63		15	0.9	2.0	<0.002	3	<2	6	123	11	0.7	38.5	<0.5	<1	0.4	0.5	0.1	0.1
BFMZ2	<5	<0.5	<0.5	37	258	<0.2	11				2.0	<0.001	<5	<2	5	111	10	1.5	38	<0.5		0.2	0.4		<0.1
PB1	<5	<0.5	0.6	51	411	<0.2	89				1.8	<0.001	7	<2	2	129	<10	1.0	40	<0.5		<0.1	0.3		<0.1
MORTNE	<2	<0.5	<0.3	44.3	448	<0.1	49		16	1.7	1.9	<0.002	<3	<2	3	117	3	0.3	41.3	<0.5	<1	0.2	0.3	<0.05	0.2
LRMRA4	<5	<0.5	0.7	38	402	<0.2	66				1.6	<0.001	9	<2	2	105	11	0.3	32	<0.5		0.2	0.3		0.2
Catoctin dikes in Grenvillian terrains																									
PATPK	<200	1		36	14	0.5	180				7.1	<0.001	<100	<2	29	<20	28	0.3	31	<0.5		1.3	3.3		0.8
ANT RESV	<3	<0.5	<5	32	11	<0.2	45				5.6	<0.001	<5	<2	24	<50	28	<0.1	22	<0.5	<5	1.1	1.5		0.6
BROOKM	<100	<0.5		52	39	<0.2	230				6.1	<0.001	100	<2	25	20	12	0.1	38	<0.5		1.2	1.7		0.6
HSTR		<0.5		41	86	<0.2	35				6.3	<0.001	<5	<2	26	20	15	<0.1	29	0.6		1.8	1.9		0.4
LS3	<100	<0.5		39	33	0.3	140				5.5	<0.001	<50	<2	25	40	24	<0.1	27	<0.5		1.1	1.5		<0.5
TOPFND	<3	<0.5	<5	35	71	0.4	60				4.1	<0.001	<5	<2	18	53	34	<0.1	25	<0.5	<5	1.0	1.2		0.6
LS2	<100	<0.5		40	29	0.7	55				5.2	<0.001	<50	<2	21	30	29	0.1	26	<0.5		1.1	1.3		<0.5
HUFFC		<0.5		44	73	0.3	150				6.9	<0.001	<5	<2	31	40	11	0.1	27	0.6		1.9	2.4		0.8
ISHMTN	<100	<0.5		40	53	<0.2	65				3.8	<0.001	<50	<2	17	50	26	<0.1	26	<0.5		0.7	1.1		<0.5
PH152	<5	<0.5	1.7	43	100	<0.2	125				4.3	<0.001	5	<2	20	34	13	<0.1	30	<0.5		1.2	1.5		<0.1
D-266	<3	<0.5	<5	38	39	<0.2	65				5.2	<0.001	6	<2	20	<50	<10	<0.1	27	<0.5	5	0.8	1.1		0.6
UWC	<100	0.5		43	46	0.3	230				4.3	<0.001	<50	<2	18	50	10	<0.1	32	<0.5		0.9	1.1		<0.5
DV	<100	<0.5		42	46	<0.2	240				4.1	<0.001	<50	<2	19	40	16	<0.1	29	<0.5		0.7	1.0		<0.5
LYDRY	<100	<0.5		38	42	<0.2	160				4.6	<0.001	<50	<2	19	40	19	<0.1	23	<0.5		0.8	1.2		<0.5
LUD COR	<3	<0.5	<5	41	16	<0.3	130				3.7	<0.001	7	<2	19	<50	13	<0.1	28	<0.5	<5	0.8	1.6		0.5
HUFFM		<0.5		44	100	<0.2	140				4.6	<0.001	<5	<2	18	70	<10	<0.1	29	<0.5		1.2	1.5		0.3
STP FA	<100	<0.5		43	89	<0.2	510				3.7	<0.001		<2	17	93	13	<0.1	29	<0.5		0.7	1.1		<0.5
ELBNW	<100	<0.5		41	18	<0.2	120				3.4	<0.001	<50	<2	16	50	17	<0.1	26	<0.5		0.7	1.3		<0.5
HNYNW	<100	<0.5		42	33	<0.2	110				2.8	<0.001	<50	<2	15	50	11	<0.1	27	<0.5		0.5	0.7		<0.5

Appendix I

Table 1. Major, minor, and trace element analyses for metabasalt, metadiabase, and amphibolite populations discussed in this report.

SAMPLE NAME	Bi	Br	Cd	Co	Cr	Cs	Cu	F	Ga	Ge	Hf	Ir	Pb	Mo	Nb	Ni	Rb	Sb	Sc	Se	Sn	Ta	Th	Tl	U
FURNCK	<100	<0.5		36	85	0.3	65				4.0	<0.001	<50	<2	16	40	38	<0.1	24	<0.5		0.8	0.9		<0.5
HNY82	<100	<0.5		33	90	0.4	120				3.1	<0.001	<50	<2	12	60	17	<0.1	24	<0.5		0.6	1.0		<0.5
MRCK	<100	<0.5		46	170	0.6	130				2.4	<0.001	<50	<2	11	70	<10	<0.1	29	<0.5		0.4	0.5		<0.5
HPD	<0.1	<0.5	<0.3	45.3	345	0.4	62	233	17	1.3	2.1	<0.002	<3	<2	5.9	49	3	<0.1	38.6	<0.5	<1	0.68	0.57	0.05	0.31
Conowingo																									
CONJSEIII	<5	<0.5	0.6	51	70	<0.2	187				5.2	<0.001	<5	<2	28	44	<10	0.4	53	1.3		1.5	<0.1		<0.1
LEO	<5	<0.5	1.3	62	159	<0.2	229				1.2	<0.001	7	<2	9	65	<10	0.5	49	<0.5		<0.1	0.3		<0.1
PLGRV	<5	<0.5	<0.5	57	420	0.8	124				5.0	<0.001	<5	<2	8	114	<10	0.5	46	<0.5		<0.1	<0.1		<0.1
CONJSEII	<5	<0.5	0.5	54	470	<0.2	41				1.6	<0.001	<5	<2	9	150	<10	0.4	47	<0.5		0.4	<0.1		<0.1
WAKES	<5	<0.5	<0.5	64	460	0.7	98				2.7	<0.001	<5	<2	8	139	<10	0.3	49	<0.5		0.2	<0.1		<0.1
CONJSE	<5	<0.5	<0.5	72	910	<0.2	350				0.8	<0.001	<5	<2	5	221	<10	0.3	36	<0.5		0.3	<0.1		<0.1
APPLE	<5	<0.5	<0.5	51	175	<0.2	33				0.5	<0.001	<5	<2	4	39	<10	<0.1	48	<0.5		<0.1	<0.1		<0.1
PLGRVS	<5	<0.5	<0.5	68	960	<0.2	59				0.9	<0.001	<5	<2	<2	266	<10	0.4	40	<0.5		<0.1	<0.1		<0.1
Fishing Creek																									
FSHCKT	<5	<0.5	1.2	73	239	<0.2	65				5.0	<0.001	10	<2	35	96	<10	0.2	50	<0.5		1.8	2.5		<0.1
FSHCKOTC	<5	<0.5	<0.5	44	92	1.5	59				3.4	<0.001	<5	<2	16	54	<10	0.1	39	0.8		0.7	1.0		<0.1
FSHCKFG	<100	<0.5		42	170	0.3	85				3.6	<0.001	<50	<2	30	50	<10	0.2	40	<0.5		1.4	2.2		0.8
FSHCKFGIII	<5	<0.5	<0.5	39	170	<0.2	71				3.4	<0.001	<5	<2	28	63	<10	0.2	36	<0.5		1.6	2.0		0.6
FSHCKFGIV	<5	<0.5	<0.5	40	191	<0.2	73				3.6	<0.001	12	<2	27	46	<10	0.1	38	<0.5		1.6	2.0		0.6
FSHCKFGV	<2	<0.5	<0.3	41	191	0.2	75		18	0.7	3.6	<0.001	4	<2	27	57	3	<0.1	39.3	<0.5	1	1.94	2.5	<0.05	
0.61																									
FSHCKFGII		<0.5		40	190	0.4	95				3.3	<0.001	<5	<2	28	90	10	0.2	35	1.0		1.6	2.2		0.6
FSHCKRR	<5	<0.5	<0.5	49	280	1.2	24				3.8	<0.001	<5	<2	19	99	<10	0.3	44	<0.5		1.1	1.7		0.7
FSHCKQ	<3	<0.5	<5	39	290	<0.2	75				3.6	<0.001	<5	<2	15	140	<10	0.3	34	<0.7	<5	1.0	1.2	0.8	
FSHCKINT	<5	<0.5	<0.5	41	165	<0.2	58				2.6	<0.001	<5	<2	21	94	<10	0.2	50	<0.5		1.1	1.6		0.4
FSHCKMON	<5	<0.5	<0.5	35	180	1.2	80				2.4	<0.001	5	<2	24	110	27	0.4	26	<0.5		1.8	1.9		0.3
Holtwood																									
HLTWCOL	<3	<0.5	<5	51	190	<0.2	40				2.6	<0.001	5	<2	10	100	14	0.4	38	<0.5	<5	<0.1	0.3	<0.5	
HLTWM	<100	<0.5		58	230	3.1	15				2.5	<0.001	<50	<2	9	80	14	0.9	52	<0.5		0.3	0.4		<0.2
HLTWNE	<5	<0.5	<0.5	44	180	2.0	4				2.1	<0.001	14	<2	8	75	<10	0.5	40	<0.5		0.4	0.4		<0.1
HLTWTN	3	<0.5	1.1	92	310	0.1	133		19	1.2	2.6	<0.002	<3	<1	6.7	80	<1	0.9	40.2	<0.5	1	0.5	0.5	<0.05	0.1
HLTWBASE	<100	<0.5		30	110	0.5	90				1.8	<0.001		<2	9	60	<10	0.5	30	<0.5		<0.1	0.3		<0.5
COYLK	<3	<0.5	<5	27	110	<0.2	50				2.1	<0.001	6	<2	10	<50	<10	0.3	32	<0.5	<5	<0.4	0.4	<0.5	
Group IV of Plank																									
CB12-C 43506	<2	<0.5	<0.3	55.4	458	<0.2	208		14	1.0	1	<2	<3	<2	<0.2	105	5	<0.1	51.7	<0.5	1	0.08	1.53	<0.05	0.17
JRBEWH*	<2	<0.5	<0.3	42	391	0.4	7		15	0.9	1.0	<2	540	<2	2.1	82	16	<0.1	42	<0.5	<1	0.1	0.8	0.1	0.2
WCCTP*	<2	<0.5	0.3	47.5	460	0.1	61		7	<0.5	1.0	<2	12	<2	2.6	82	4	<0.1	45.6	<0.5	<1	0.0	0.1	<0.5	0.1
James Run																									
JRFM C	<100	<0.5		15	3.4	<0.2	50				2.4	<0.001	<50	<2	6	<10	<10	<0.1	33	<0.5		0.2	0.6		<0.5
JRGFAS	<5	<0.5	0.5	14	140	0.4	14				5.9	<0.001	16	<2	11	10	<10	<0.1	21	<0.5		0.7	6.0		1.3
JRGFA	<100	<0.5		17	3	<0.2	15				4.4	<0.001	<50	<2	<2	<10	10	<0.1	21	<0.5		0.5	3.6		0.8
JRFM V	<200	<0.5		9.1	0.7	0.3	<10				4.0	<0.001	<100	<2	10	<20	16	<0.1	19	<0.5		0.5	3.9		1.2
JRS	<200	<0.5		26	2.7	0.3	10				1.3	<0.001	<100	<2	5	<20	20	<0.1	30	<0.5		<0.1	1.1		<0.5
Jonestown Volcanics																									
BKHLM	<200	<0.5		43	370	0.8	70				2.7	<0.001	<100	<2	12	220	13	<0.1	36	<0.5		0.4	0.6		<0.5
BKHLNW2-11	<0.1	<0.5	<0.3	39.7	276	0.6	51	500	15	1.1	2.5	<0.002	<3	<2	16.9	109	8	<0.1	28.7	<0.5	14	1.19	1.40	0.05	0.35
BKHL	<3	<0.5	<5	39	530	0.7	60				2.0	<0.001	7	<2	14	190	16	<0.1	26	<0.5	<5	0.5	0.6	<0.5	
BHBACH	<5	<0.5	<0.5	46	92	1.0	131				2.6	<0.001	5	<2	5	47	16	0.1	46	<0.5		0.5	1.4		<0.1

Appendix I

Table 1. Major, minor, and trace element analyses for metabasalt, metadiabase, and amphibolite populations discussed in this report.

SAMPLE NAME	Bi	Br	Cd	Co	Cr	Cs	Cu	F	Ga	Ge	Hf	Ir	Pb	Mo	Nb	Ni	Rb	Sb	Sc	Se	Sn	Ta	Th	Tl	U
BKHLV	<5	<0.5	0.6	26	283	0.9	34				2.0	<0.001	7	<2	8	92	<10	<0.1	27	<0.5		0.3	0.6		<0.1
KENB	<5	<0.5	<0.5	45	91	0.5	133				2.4	<0.001	5	<2	5	53	<10	0.4	46	<0.5		<0.1	1.4		<0.1
PA 72	<3	<0.5	<5	36	220	0.4	140				1.6	<0.001	<5	<2	5	95	18	0.2	36	<0.5	<5	<0.1	0.8	<0.5	
Kennett Square																									
LUCK	<100	<0.5		51	330	<0.2	160				1.4	<0.001	<50	<2	6	90	10	<0.1	50	0.9		0.2	0.3		<0.2
LUCKW	<2	<0.5	<0.3	47.9	317	<0.1	110		17	1.5	2.1	<0.002	<3	<2	3.8	84	2	0.2	46.9	<0.5	1	0.26	0.15	<0.05	0.14
KS	<100	<0.5		49	240	<0.2	440				1.6	<0.001	<50	<2	7	90	23	0.7	38	<0.5		0.4	0.3		<0.1
WICK	<5	<0.5	<0.5	53	280	1.0	1				1.9	<0.001	<5	<2	5	171	<10	0.3	34	<0.5		0.7	0.6		<0.1
ROSE	<5	<0.5	<0.5	42	320	0.5	86				1.6	<0.001	<5	<2	6	129	11	0.1	32	<0.5		0.4	0.4		<0.1
BRNTML	<5	<0.5	0.6	46	340	<0.2	23				1.3	<0.001	<5	<2	3	126	<10	<0.1	38	<0.5		0.6	0.4		<0.1
CHFD		<0.5		41	330	<0.2	110				1.2	<0.001	<5	<2	<2	80	<10	<0.1	45	<0.5		0.1	<0.1		<0.1
BRANDY2		<0.5		48	310	<0.2	250				1.0	<0.001	<5	<2	<2	90	<10	<0.1	45	<0.5		0.4	<0.1		<0.1
Liberty Reservoir																									
LRMRA3	<5	<0.5	1.2	36	128	<0.2	69				2.4	<0.001	8	<2	6	48	<10	0.4	45	<0.5		0.3	1.5		0.3
LRMRA5A	<2	<0.5	<0.3	41.9	232	<0.1	130		19	1.9	2.9	<0.002	15	<2	4.4	67	4	0.2	46	<0.5	3	0.25	1.63	0.09	0.42
LRMRA5	<5	<0.5	0.8	42	179	<0.2	117				2.2	<0.001	13	<2	4	62	13	0.2	46	<0.5		0.6	1.1		<0.1
LRMRA9	<2	<0.5	<0.3	37.5	362	<0.1	35		15	1.5	1.7	<0.002	5	<2	0.4	133	5	0.3	32.8	<0.5	<1	0.05	0.22	<0.05	0.11
LRMRA2	<5	<0.5	0.6	45	539	<0.2	85				1.1	<0.001	10	<2	3	148	<10	0.2	42	<0.5		<0.1	0.6		<0.1
Nottingham County Park																									
NCPAVH4.74	<2	<0.5	<0.3	61	55.4	0.21	22		8	0.6	0.2	<0.001	7	1	1	89	4	<0.1	66	<0.5	<1	<0.01	<0.05	<0.5	0.02
NCPKIRK6	4	<0.5	<0.3	61	62.3	0.1	57		18	1.2	0.3	<0.001	<3	<1	3	35	2	0.2	72.1	<0.5	2	0.02	<0.05	<0.2	0.04
NCPNN	3	<0.5	<0.3	65	51.6	0.6	205		14	0.9	0.2	<0.001	<3	1	1	33	12	<0.1	62.4	<0.5	2	<0.01	<0.05	<0.5	0.03
"Older diabase"																									
BALTP2		<0.5		40	210	<0.2	170				6.1	<0.001	<5	<2	31	80	<10	<0.1	29	<0.5		1.6	3.3		0.6
BALTP		<0.5		42	130	<0.2	70				6.8	<0.001	<5	<2	28	70	<10	0.2	31	<0.5		1.7	0.8		0.4
BEAU2	<100	<0.5		41	15	<0.2	70				5.0	<0.001	<50	<2	27	20	18	<0.1	32	<0.5		1.2	1.5		0.5
BALTP3	<5	<0.5	1	41	150	<0.2	37				3.7	<0.001	12	<2	5	61	<10	0.1	40	1.5		0.6	0.6		<0.1
BAYARD	<0.1	<0.5	1.0	49	156	<0.1	76	446	15	1.4	3.3	<0.002	4	<2	7.2	29	10	<0.1	41.9	1.5	<1	0.2	1.49	0.09	0.41
ARMK2	<5	<0.5	0.5	44	480	<0.2	79				1.5	<0.001	<5	<2	4	160	16	<0.1	35	<0.5		<0.1	0.4		<0.1
CPSUN	<100	<0.5		42	150	<0.2	30				1.5	<1	<50	<2	6	80	<10	<0.1	30	<0.5		<0.1	0.6		<0.5
CRUMCK	<100	<0.5		51	100	0.3	65				0.7	<0.001	<50	<2	3	110	<10	<0.1	44	<0.5		<0.1	<0.1		<0.1
BEAU	<100	<0.5		49	94	<0.2	25				0.8	<0.001		<2	4	180	<10	<0.1	40	<0.5		<0.1	<0.1		<0.5
RADNOR	<5	<0.5	<0.5	48	400	<0.2	54				1.3	<0.001	<5	<2	<2	234	13	<0.1	35	<0.5		0.6	0.4		<0.1
Pigeon Hills																									
PIGHL	<3	<0.5	<5	74	405	<0.5	20				3.8	<0.001	<5	<2	11	220	<10	0.2	53	<3	<5	1.0	0.7	<0.5	
PIGHL2	<100	<0.5		50	230	<0.2	5				2.5	<1	<50	<2	7	130	<10	<0.1	30	<0.5		<0.1	0.3		<0.5
PIGHL888	<100	<0.5		54	240	<0.2	20				2.2	<1	<50	<2	8	130	<10	0.1	26	<0.5		0.2	0.2		<0.5
PIGHL3	<100	<0.5		47	130	<0.2	105				1.9	<1	<50	<2	9	120	<10	<0.1	30	<0.5		0.3	0.3		<0.5
PIGHL5	<5	<0.5	<0.5	52	150	<0.2	142				1.5	<0.001	<5	<2	<2	151	<10	<0.1	36	<0.5		<0.1	0.1		<0.1
PIGHL4	<5	<0.5	<0.5	54	190	<0.2	385				1.7	<0.001	9	<2	<2	138	<10	<0.1	35	<0.5		0.2	<0.1		<0.1
Sams Creek																									
GLENRK	<3	<0.5	<5	43	130	<0.2	85				4.6	<0.001	12	<2	12	190	<10	0.5	48	<0.8	<5	<0.2	0.7	0.7	
DISEQ	<5	<0.5	1	65	1100	1.2	13				3.9	<0.001	32	<2	21	314	31	0.7	42	<0.5		1.1	1.8		<0.1
SC340NE	<200	<0.5		37	180	<0.2	<10				3.3	<0.001	<100	<2	24	80	<10	<0.1	29	<0.5		1.1	1.4		<0.5
PCSC4	<5	<0.5	<0.5	54	340	<0.2	97				3.3	<0.001	8	<2	5	97	18	0.3	43	<0.5		0.5	0.5		<0.1
PA616	<5	<0.5	<0.5	33	90	<0.2	65				2.5	0.001	<5	<2	5	36	11	0.3	62	<0.5		0.4	0.4		<0.1

Appendix I

Table 1. Major, minor, and trace element analyses for metabasalt, metadiabase, and amphibolite populations discussed in this report.

SAMPLE NAME	Bi	Br	Cd	Co	Cr	Cs	Cu	F	Ga	Ge	Hf	Ir	Pb	Mo	Nb	Ni	Rb	Sb	Sc	Se	Sn	Ta	Th	Tl	U
PCSC3	<5	<0.5	<0.5	51	350	<0.2	82				3.5	<0.001	5	<2	21	148	<10	0.3	30	0.6		1.4	1.6		<0.1
PCSC	<100	<0.5		59	430	<0.2	40				3.0	<0.001	<50	<2	22	160	16	0.5	35	<0.5		0.8	1.2		<0.5
SC240NE	<5	<0.5	0.5	44	350	<0.2	3				3.3	<0.001	15	<2	26	144	12	<0.1	31	<0.5		1.4	2.0		0.2
GLENM	<100	<0.5		39	230	0.8	150				2.8	<0.001	<50	<2	10	80	12	0.3	42	<0.5		0.4	0.6		<0.2
SCTYPE	<5	<0.5	<0.5	40	230	<0.2	30				3.1	<0.001	8	2	28	78	<10	<0.1	31	<0.5		1.5	2.1		0.3
SC 40NE	<5	<0.5	0.5	41	240	<0.2	5				3.0	<0.001	10	<2	21	107	<10	<0.1	30	<0.5		1.0	1.4		<0.1
SC440NE	<5	<0.5	<0.5	44	390	<0.2	58				2.4	<0.001	6	<2	19	157	17	<0.1	35	<0.5		0.9	1.5		0.3
SCQ	<100	<0.5		32	220	<0.2	80				2.8	<0.001	50	<2	11	70	<10	1.2	46	<0.5		0.5	0.8		<0.2
GLENT	<5	<0.5	<0.5	43	300	0.3	141				2.3	<0.001	<5	<2	5	112	<10	0.3	41	<0.5		0.3	0.2		0.1
SC144NE	<100	<0.5		43	420	<0.2	180				2.6	<0.001		<2	20	210	<10	<0.1	25	<0.5		0.9	1.2		<0.5
GLENN	<100	<0.5		61	540	<0.2	150				1.8	<0.001	<50	<2	4	360	<10	0.1	38	<0.5		0.2	0.2		<0.5
GLENS	<100	<0.5		48	300	<0.2	110				1.6	<0.001	<50	<2	6	140	<10	0.2	40	<0.5		0.1	<0.1		<0.1
White Clay Creek																									
NEWARKRD	0.1	<0.5	0.8	65	130	<0.1	367	895	20	1.7	5.2	<0.002	15	<2	21.5	55	5	0.3	40.9	1.6	3	1.07	1.45	0.11	0.44
WCCMBIV	<5	<0.5	<0.5	54	80	<0.2	30				6.7	<0.001	11	<2	28	41	<10	<0.1	36	<0.5		1.2	1.9		<0.1
YRKLYN	<5	<0.5	<0.5	52	70	<0.2	90				7.1	<0.001	<5	<2	19	25	20	<0.1	33	0.9		1.6	1.8		0.6
LANS	<100	<0.5		45	1.9	<0.2	280				6.6	<0.001	<50	<2	27	20	<10	<0.1	30	<0.5		1.1	1.5		<0.5
WDCRST2	<0.1	<0.5	<0.3	72.1	48.2	<0.1	336	300	21	1.4	3.4	<0.002	<3	<2	9.5	80	7	<0.1	40.7	<0.5	2	0.88	0.89	<0.05	0.27
WCCW	<5	<0.5	<0.5	77	70	<0.2	246				4.7	<0.001	<5	<2	13	131	16	0.1	44	<0.5		0.6	1.4		0.8
WCCBEC	0.4	<0.5	<0.3	50.2	257	0.2	17	800	19	2.3	3.7	<0.002	<3	<2	14.9	89	7	0.1	31.3	<0.5	7	1.32	1.38	0.06	0.46
LANM	<100	<0.5		53	4.8	<0.2	245				4.3	<0.001	<50	<2	18	80	14	0.1	46	<0.5		0.9	1.1		0.7
WCCMBI	<5	<0.5	<0.5	65	85	0.6	131				3.9	<0.001	<5	<2	14	54	<10	<0.1	51	<0.5		0.7	1.8		1.4
GREENLAWN2	<2	<0.5	<0.3	56	110	0.2	127		19	1.5	3.0	<0.002	27	2	11	56	10	<0.1	51	<0.5	1	0.8	1.4	<0.05	0.5
WCCMBIII	<5	<0.5	<0.5	51	200	<0.2	26				5.2	<0.001	<5	<2	17	69	<10	<0.1	39	<0.5		0.9	1.8		0.8
WCCW+WA	<2	<0.5	<0.3	51.1	195	0.1	70.5		22	2.3	4.8	<0.002	9	<2	13.7	32	3	<0.1	41.5	<0.5	6	0.93	1.8	0.09	0.58
WCCMC	<2	<0.5	0.4	48.1	159	<0.2	26		19	1.4	4.8	<2	<3	<2	14.2	110	3	<0.1	28.7	<0.5	2	1.21	3.52	<0.05	0.73
WCCN2	<5	<0.5	<0.5	67	180	<0.2	152				4.1	<0.001	<5	<2	14	66	12	0.2	52	<0.5		1.2	1.6		<0.1
WCCW+WC	<2	<0.5	<0.3	52.1	95.6	<0.1	89		21	1.8	4.3	<0.002	8	<2	13.3	48	2	0.1	38.6	<0.5	2	0.87	1.69	<0.05	0.53
WCCMBII	<5	<0.5	0.6	45	170	<0.2	28				3.7	<0.001	5	<2	18	111	14	<0.1	28	<0.5		0.4	1.1		0.3
MP 5	<5	<0.5	<0.5	49	240	<0.2	149				3.0	<0.001	7	<2	11	209	<10	<0.1	27	1.3		1.0	0.8		<0.1
WCCMBI 10-20CM	<2	<0.5	0.8	49.2	121	<0.2	37		19	1.2	3.2	<2	<3	2	12.1	57	5	<0.1	38.1	<0.5	2	0.99	2.30	<0.05	0.56
WCCW+W	<2	<0.5	1	50.3	171	<0.1	99		23	1.4	3.6	<2	9	<2	12.2	44	3	<0.1	46.6	<0.5	1	0.8	1.4	<0.5	0.4
LANN	<100	<0.5		41	240	<0.2	120				2.7	<0.001	<50	<2	9	130	11	<0.1	28	<0.5		0.3	0.7		<0.5
WCC	<5	<0.5	<0.5	50	140	<0.2	99				2.8	<0.001	10	<2	10	85	<10	<0.1	34	<0.5		0.7	1.2		<0.1

Appendix I

Table 1. Major, minor, and trace element analyses for metabasalt, metadiabase, and amphibolite populations discussed in this report.

					Rare-earth elements:														
SAMPLE NAME	V	W	Y	Zn	La	Ce	Pr	Nd	Sm	Eu	Gd	Tb	Dy	Ho	Er	Tm	Yb	Lu	Latitude	Longitude
Accomac																				
ACC330E	166	<1	66	225	39.7	91		64	14.0	5.24		2.2					5.81	0.77	40°02'39"N	76°33'51"W
ACCOM	240	<1	36	40	14	46		29	6.8	2.27		1.3					3.49	0.51	40°02'38"N	76°33'56"W
ACCPU	244	<1	34	185	16.2	36		22	5.9	1.90		1.0					2.92	0.44	40°02'39"N	76°33'50"W
ACC 48E	324	<1	32	60	16	37		22	5.1	1.72		0.9					2.30	0.33	40°02'38"N	76°33'26"W
ACC180E	262	<1	22	70	5.1	12		8	2.6	0.97		0.5					1.60	0.22	40°02'38"N	76°33'55"W
Bald Eagle																				
BLDEAGSW	310	<1	49	159	35.1	83		49	10.0	3.53		1.8					4.95	0.67	39°46'02"N	76°25'56"W
BLDEAG2	268	<1	31	92	35.1	70		44	8.0	2.77		1.2					3.05	0.43	39°46'25"N	76°25'27"W
BLDEAG	273	<1	28	89	32.3	78		40	8.5	2.92		1.2					3.06	0.43	39°46'25"N	76°25'27"W
WOODB	227	<1	33	177	36.9	73		44	9.8	3.36		1.6					3.72	0.50	39°47'04"N	76°24'14"W
Bald Friar																				
BFMZ1	262	<1	39	70	3.6	14		11	4.1	1.45		1.1					4.80	0.69	39°42'36"N	76°12'20"W
TLPPOP2	206	<1	36	75	2.7	9		8	2.9	1.07		0.8					3.86	0.58	39°45'57"N	76°14'27"W
TLPPOP	310	<1	36	67	2.3	8		7	2.7	1.06		0.8					3.43	0.53	39°45'56"N	76°14'26"W
LRMRA6	208	<1	35	57	2.5	11		8	2.8	1.01		0.8					3.37	0.51	39°26'15"N	76°55'57"W
BRANDYSE	239	<1	31	71	2.5	9		8	3.1	1.20		0.9					3.80	0.56	39°56'14"N	76°45'09"W
SYKFM2	300	<1	34	75	2.4	7		6	2.2	0.85		0.6					2.92	0.46	39°42'28"N	76°13'04"W
BRANDY	280	<1	30	65	2.2	8		7	2.6	0.95		0.7					3.09	0.47	39°56'13"N	76°45'10"W
SYKFM	250	<1	36	59	2.1	7		6	2.1	0.83		0.7					2.84	0.44	39°42'29"N	76°13'04"W
BRANDYN	193	<1	25	67	2.2	9		7	2.4	0.96		0.7					2.89	0.44	39°56'14"N	76°45'10"W
MORTN	264	0.7	30	70	5.14	12.3	1.7	9	2.8	1.10	3.69	0.7	4.6	1.0	3.0	0.4	2.76	0.42	39°56'49"N	76°46'43"W
BFMZ2	262	2	30	52	4.0	13		9	3.2	1.14		0.9					4.08	0.56	39°42'35"N	76°13'08"W
PB1	210	<1	26	87	2.5	9		7	2.5	0.97		0.7					3.26	0.49	39°45'02"N	76°15'45"W
MORTNE	278	0.7	30	72	3.58	9.21	1.44	7.86	2.6	1.06	3.61	0.7	4.5	1.0	3.0	0.4	2.74	0.41	39°56'58"N	76°46'10"W
LRMRA4	168	<1	24	77	2.7	9		7	2.2	0.79		0.6					2.48	0.39	39°26'15"N	76°55'57"W
Catoctin dikes in Grenvillian terrains																				
PATPK	372	<1	52	160	30	64		36	8.2	2.30		1.5					3.98	0.62	40°05'45"N	75°44'11"W
ANT RESV	310	<1	42	81	24	52		30	7.1	2.49		1.2					2.93	0.46	40°21'15"N	75°52'09"W
BROOKM	338	<1	50	160	23	50		29	7.7	2.65		1.4					4.20	0.59	40°06'02"N	75°31'15"W
HSTR	320	<1	44	170	24.3	61		37	9.3	3.13		1.6					3.74	0.55	40°08'30"N	75°44'09"W
LS3	420	<1	44	160	24	51		29	6.7	2.15		1.2					3.20	0.48	40°26'29"N	75°40'36"W
TOPFND	370	<1	36	77	19	46		26	6.4	2.15		1.1					2.80	0.42	40°27'55"N	75°41'07"W
LS2	370	<1	42	110	23	49		29	7.0	2.28		1.2					3.36	0.48	40°26'26"N	75°40'13"W
HUFFC	330	<1	46	190	26.1	62		36	8.9	2.89		1.5					4.11	0.58	40°27'10"N	75°37'46"W
ISHMTN	350	<1	36	110	17	38		22	5.6	2.02		1.0					2.45	0.35	40°24'45"N	75°52'42"W
PH152	273	<1	36	66	17.9	43		27	5.8	1.89		1.0					3.11	0.48	40°06'16"N	75°31'04"W
D-266	380	<1	36	82	20	46		27	6.2	1.82		1.2					2.82	0.43	40°17'51"N	76°08'21"W
UWC	420	<1	38	120	15	34		20	5.0	1.80		1.0					2.90	0.43	40°03'52"N	75°38'20"W
DV	420	<1	38	120	13	31		18	4.7	1.60		0.9					2.50	0.37	40°05'13"N	75°32'26"W
LYDRY	330	<1	36	110	16	38		22	5.1	1.67		0.9					2.56	0.36	40°28'15"N	75°45'12"W
LUD COR	330	<1	28	84	17	36		20	4.8	1.45		0.9					2.29	0.35	40°07'50"N	75°42'51"W
HUFFM	310	<1	34	70	17.3	40		23	5.9	2.02		1.0					2.57	0.40	40°27'10"N	75°37'46"W
STP FA	260	<1	36	98	12	29		19	4.6	1.66		0.9					2.45	0.35	40°08'57"N	75°01'38"W
ELBNW	320	<1	30	100	13	30		17	4.2	1.38		0.8					2.20	0.31	40°05'26"N	75°36'14"W
HNYNW	310	<1	26	95	9.2	22		13	3.3	1.17		0.7					1.84	0.27	40°03'32"N	75°56'47"W

Appendix I

Table 1. Major, minor, and trace element analyses for metabasalt, metadiabase, and amphibolite populations discussed in this report.

					Rare-earth elements:														
SAMPLE NAME	V	W	Y	Zn	La	Ce	Pr	Nd	Sm	Eu	Gd	Tb	Dy	Ho	Er	Tm	Yb	Lu	Latitude	Longitude
FURNCK	250	<1	32	110	17	38		21	4.7	1.66		0.9					2.63	0.38	40°19'22"N	76°10'10"W
HNY82	290	<1	28	90	11	24		13	3.6	1.21		0.7					2.05	0.30	40°04'09"N	75°48'50"W
MRCK	290	<1	22	90	8.5	19		11	3.1	1.05		0.6					1.66	0.25	40°04'00"N	75°43'59"W
HPD	239	<1	19	177	6.67	14.3	2.17	10.9	2.95	1.14	3.30	0.59	3.25	0.66	1.68	0.220	1.43	0.228	40°01'51.8"N	75°50'07.8"W
Conowingo																				
CONJSEIII	408	<1	49	101	16.5	52		44	11.0	3.27		2.0					4.73	0.66	39°45'42"N	76°10'25"W
LEO	360	<1	20	160	8.2	21		12	2.9	1.17		0.6					2.34	0.37	39°43'08"N	76°12'20"W
PLGRV	267	<1	12	144	14.3	32		17	3.3	1.39		0.6					2.12	0.31	39°43'51"N	76°11'30"W
CONJSEII	206	<1	6	143	9.9	20		9	1.5	1.08		0.3					1.86	0.29	39°45'45"N	76°10'16"W
WAKES	205	<1	18	142	16.4	38		21	4.7	1.28		0.8					2.93	0.43	39°45'32"N	76°10'49"W
CONJSE	554	<1	5	95	4.8	10		4	0.7	0.69		0.1					1.34	0.20	39°45'47"N	76°10'11"W
APPLE	339	<1	3	80	3.8	10		6	1.5	0.63		0.4					1.12	0.16	39°42'04"N	75°48'04"W
PLGRVS	149	<1	6	107	6.4	15		7	1.4	0.67		0.4					1.72	0.26	39°43'31"N	76°11'41"W
Fishing Creek																				
FSHCKT	296	<1	47	154	27.4	60		32	7.4	2.53		1.3					4.52	0.65	39°47'58"N	76°15'17"W
FSHCKOTC	275	<1	36	82	12	31		18	5.2	1.77		1.1					3.75	0.51	39°48'30"N	76°14'09"W
FSHCKFG	240	<1	34	70	19.5	42		22	4.9	1.71		1.0					3.09	0.46	39°47'56"N	76°15'23"W
FSHCKFGIII	230	3	28	75	19.7	41		21	4.8	1.68		0.8					2.86	0.39	39°47'56"N	76°15'23"W
FSHCKFGIV	223	<1	30	74	18.5	41		22	5	1.71		0.9					3.05	0.45	39°47'56"N	76°15'23"W
FSHCKFGV	299	<0.5	35	87	20.9	43.2	5.07	23.2	5.39	1.97	5.84	1.0	5.9	1.2	3.3	0.5	3.02	0.44	39°47'56"N	76°15'23"W
FSHCKFGII	310	<1	32	80	17.5	40		24	4.9	1.57		0.9					2.95	0.42	39°47'56"N	76°15'23"W
FSHCKRR	215	<1	35	71	14.8	38		21	5.6	1.96		1.1					4.15	0.56	39°47'34"N	76°16'04"W
FSHCKQ	270	<1	28	120	12	29		17	4.5	1.35		0.9					2.92	0.45	39°48'00"N	76°15'15"W
FSHCKINT	209	<1	19	53	13.3	30		17	4.0	1.35		0.8					2.55	0.33	39°48'37"N	76°13'38"W
FSHCKMON	193	<1	20	69	15.8	33		18	3.9	1.12		0.6					1.85	0.29	39°48'10"N	76°14'49"W
Holtwood																				
HLTWCOL	410	<1	30	78	7.5	18		12	3.6	1.24		0.8					2.43	0.38	39°49'28"N	76°20'27"W
HLTWM	338	<1	30	110	7.1	18		12	3.5	1.45		0.8					2.79	0.41	39°49'29"N	76°20'26"W
HLTWNE	191	<1	23	76	7.1	18		11	3.3	1.26		0.7					2.42	0.35	39°49'32"N	76°20'26"W
HLTWTN	323	<0.5	25	79	8.5	21	2.8	14	3.8	1.62	4.36	0.8	4.7	1.0	2.7	0.4	2.38	0.35	39°49'36.5"N	76°20'09.1"W
HLTWBASE	240	<1	26	66	5.6	14		10	2.7	1.11		0.6					1.90	0.28	39°49'31"N	76°20'26"W
COYLK	290	<1	30	52	6.6	16		11	3.1	1.00		0.7					2.57	0.37	39°45'59"N	76°16'28"W
Group IV of Plank																				
CB12-C 43506	211	<1	24	139	1.01	3.05	0.58	3.70	1.64	0.738	2.68	0.54	3.53	0.79	2.58	0.371	2.63	0.393	39°44'54"N	75°43'58"W
JRBEWH*	233	0.9	21	70	4.79	9.62	1.39	6.49	1.9	0.80	2.36	0.5	3.0	0.6	1.9	0.3	1.83	0.28	39°41'32"N	75°43'29"W
WCCTP*	260	<0.5	25	46	0.87	2.76	0.51	3.21	1.4	0.62	2.10	0.5	3.2	0.7	2.2	0.3	2.17	0.33	39°44'20"N	75°45'02"W
James Run																				
JRFM C	76	<1	52	35	6.5	18		14	4.6	1.60		1.2					4.18	0.66	39°35'08"N	76°05'54"W
JRGFAS	117	<1	64	120	24.3	55		29	7.1	1.88		1.4					5.86	0.88	39°35'20"N	76°06'09"W
JRGFA	110	<1	48	90	14	34		19	4.9	1.47		1.2					4.30	0.68	39°35'21"N	76°06'10"W
JRFM V	120	<1	40	<10	17	37		18	4.4	1.18		1.0					3.60	0.58	39°35'03"N	76°05'54"W
JRS	288	<1	24	60	3	6		4	1.5	0.54		0.4					1.76	0.28	39°35'49"N	76°06'27"W
Jonestown Volcanics																				
BKHLM	300	<1	36	50	7.4	19		12	3.5	1.18		0.8					2.67	0.42	40°24'02"N	76°29'17"W
BKHLNW2-11	247	<1	32	65	14.8	29.9	3.84	17.3	4.40	1.58	4.73	0.84	5.05	1.04	2.79	0.425	2.61	0.381	40°24'06"N	76°29'20"W
BKHL	270	<1	24	40	6.9	16		10	2.6	0.90		0.5					1.72	0.27	40°24'33"N	76°27'50"W
BHBACH	289	<1	32	92	6.8	19		12	3.3	1.01		0.7					3.43	0.52	40°23'10"N	76°28'45"W

Appendix I

Table 1. Major, minor, and trace element analyses for metabasalt, metadiabase, and amphibolite populations discussed in this report.

					Rare-earth elements:														
SAMPLE NAME	V	W	Y	Zn	La	Ce	Pr	Nd	Sm	Eu	Gd	Tb	Dy	Ho	Er	Tm	Yb	Lu	Latitude	Longitude
BKHLV	220	<1	24	58	4.9	14		10	2.8	1.01		0.6					2.33	0.36	40°24'02"N	76°29'17"W
KENB	264	<1	32	78	5.4	18		12	3.2	1.02		0.8					3.29	0.48	40°24'32"N	76°26'16"W
PA 72	310	<1	22	60	4.4	11		7	2.0	0.63		0.5					2.03	0.32	40°23'04"N	76°28'33"W
Kennett Square																				
LUCK	282	<1	24	65	4.1	11		8	2.3	0.87		0.6					2.31	0.36	39°49'50"N	75°43'03"W
LUCKW	329	<1	27	76	5.67	13.5	1.94	9.89	3.1	1.21	3.73	0.72	4.40	0.98	2.93	0.459	2.68	0.42	39°49'23"N	75°45'10"W
KS	266	<1	24	110	4.4	11		7	2.2	0.88		0.6					2.43	0.33	39°50'21"N	75°41'52"W
WICK	269	<1	22	91	6.8	17		11	3.1	1.06		0.6					2.38	0.36	39°48'00"N	75°50'05"W
ROSE	256	<1	30	71	5.6	14		8	2.3	0.87		0.5					2.20	0.34	39°50'35"N	75°39'32"W
BRNTML	234	<1	20	71	4.1	11		8	2.4	0.83		0.6					2.12	0.33	39°50'16"N	75°39'04"W
CHFD	290	<1	26	50	1.2	5		5	1.8	0.70		0.5					2.57	0.40	39°51'44"N	75°35'40"W
BRANDY2	280	<1	20	45	1.1	4		4	1.5	0.55		0.4					2.40	0.38	39°51'12"N	75°35'50"W
Liberty Reservoir																				
LRMRA3	346	5	33	69	8.7	21		13	3.4	1.11		0.8					3.65	0.58	39°24'10"N	76°53'08"W
LRMRA5A	365	<1	19	91	7.33	16	2.4	11.3	3.49	1.2	4.28	0.81	5.05	1.13	3.37	0.539	3.27	0.506	39°26'13.5"N	76°55'54.5"W
LRMRA5	264	<1	27	87	5.9	16		11	2.9	0.83		0.7					2.98	0.44	39°26'14"N	76°55'56"W
LRMRA9	180	<1	28	65	2.2	6.58	1.08	6.1	2.24	0.88	2.93	0.6	3.73	0.86	2.58	0.401	2.39	0.37	39°26'14.5"N	76°55'55.5"W
LRMRA2	171	<1	15	70	3.0	9		6	1.5	0.48		0.4					1.68	0.25	39°23'35"N	76°52'46"W
Nottingham County Park																				
NCPAVH4.74	649	<0.5	14	94	1.7	2	0.4	2	0.8	0.46	1.22	0.2	1.5	0.3	1.0	0.1	0.86	0.13	39°43'50"N	76°02'52"W
NCPKIRK6	756	<0.5	16	92	0.8	2	0.32	2	1.0	0.80	1.57	0.3	2.2	0.5	1.4	0.2	1.32	0.20	39°43'51"N	76°03'04"W
NCPNN	660	0.8	12	60	0.4	1	0.18	1	0.5	0.38	0.90	0.2	1.2	0.3	0.8	0.1	0.69	0.11	39°44'01"N	76°03'00"W
"Older diabase"																				
BALTP2	380	<1	52	140	26.1	57		32	7.9	2.22		1.4					3.61	0.54	39°53'21"N	75°30'50"W
BALTP	370	4	50	160	13.5	38		27	6.9	1.99		1.6					4.34	0.61	39°53'21"N	75°30'41"W
BEAU2	332	<1	46	130	20.5	45		24	6.0	2.04		1.2					3.53	0.53	40°01'22"N	75°25'46"W
BALTP3	335	<1	44	131	14.4	37		23	6.4	1.70		1.4					4.35	0.65	39°52'15"N	75°36'07"W
BAYARD	412	<0.5	46	117	15.1	33.7	4.18	20.0	5.42	1.58	6.73	1.22	7.63	1.65	5.28	0.79	4.83	0.78	39°51'15"N	75°40'37.4"W
ARMK2	214	<1	28	82	5.1	13		8	2.5	0.85		0.6					2.80	0.46	40°03'47"N	75°18'24"W
CPSUN	244	<1	24	100	6.7	14		8	1.9	0.65		0.4					1.84	0.29	39°54'18"N	75°31'27"W
CRUMCK	246	<1	24	65	1.1	3		3	1.0	0.48		0.3					2.19	0.36	40°00'33"N	75°28'02"W
BEAU	200	<1	20	38	1	3		2	0.9	0.46		0.3					1.80	0.29	40°01'22"N	75°25'46"W
RADNOR	227	<1	20	90	5.2	13		8	2.0	0.70		0.5					2.12	0.32	40°02'06"N	75°22'22"W
Pigeon Hills																				
PIGHL	380	<1	34	220	7.4	21		15	4.5	1.52		0.9					3.68	0.57	39°51'39"N	76°58'15"W
PIGHL2	306	<1	36	110	7	18		12	3.4	1.22		0.8					2.63	0.40	39°52'10"N	76°57'47"W
PIGHL888	250	<1	24	130	7.4	19		13	3.8	1.47		0.7					2.12	0.33	39°52'40"N	76°56'52"W
PIGHL3	248	<1	28	95	5.6	14		9	2.6	0.87		0.6					2.10	0.32	39°51'33"N	76°58'09"W
PIGHL5	317	<1	28	89	3.2	9		7	2.3	0.86		0.6					2.51	0.39	39°52'09"N	76°57'24"W
PIGHL4	324	<1	20	92	3.3	11		8	2.6	1.00		0.6					2.42	0.37	39°52'04"N	76°57'27"W
Sams Creek																				
GLENRK	460	<1	44	130	13	32		20	6.0	2.01		1.4					4.95	0.76	39°46'14"N	76°42'56"W
DISEQ	440	<1	60	109	20.4	39		27	6.6	2.30		1.3					4.47	0.65	39°46'41"N	76°43'23"W
SC340NE	324	<1	36	50	14	31		17	3.9	1.54		0.8					2.91	0.44	39°30'28"N	77°07'49"W
PCSC4	397	<1	44	136	9.9	25		16	4.6	1.57		1.0					3.72	0.57	39°47'40"N	76°44'00"W
PA616	454	<1	64	79	6.8	17		13	4.4	1.52		1.0					3.70	0.57	39°46'13"N	76°42'43"W

Appendix I

Table 1. Major, minor, and trace element analyses for metabasalt, metadiabase, and amphibolite populations discussed in this report.

					Rare-earth elements:														
SAMPLE NAME	V	W	Y	Zn	La	Ce	Pr	Nd	Sm	Eu	Gd	Tb	Dy	Ho	Er	Tm	Yb	Lu	Latitude	Longitude
PCSC3	328	<1	36	111	16.5	38		21	4.8	1.64		1.0					3.04	0.46	39°47'17"N	76°43'24"W
PCSC	310	<1	38	100	14	29		15	4.1	1.49		0.8					2.73	0.44	39°46'33"N	76°43'22"W
SC240NE	307	<1	30	102	18.7	39		19	4.8	1.63		0.9					2.84	0.44	39°30'28"N	77°07'47"W
GLENM	338	<1	36	90	7.1	18		12	3.6	1.31		0.9					3.57	0.52	39°47'36"N	76°43'47"W
SCTYPE	304	<1	32	77	16.6	36		18	4.6	1.46		0.8					2.61	0.34	39°30'00"N	77°07'01"W
SC 40NE	296	<1	36	87	12.2	26		15	3.5	1.34		0.7					2.10	0.30	39°30'27"N	77°07'50"W
SC440NE	349	<1	32	81	14.3	31		17	3.7	1.43		0.7					2.30	0.37	39°30'29"N	77°07'45"W
SCQ	300	<1	36	70	8.6	21		14	3.8	1.60		0.9					3.36	0.50	39°47'03"N	76°45'09"W
GLENT	417	<1	36	94	4.9	15		11	3.3	1.42		0.9					3.26	0.54	39°47'38"N	76°43'49"W
SC144NE	190	<1	26	68	12	26		13	3.2	1.23		0.6					2.11	0.32	39°30'27"N	77°07'51"W
GLENN	340	<1	28	90	3.5	9		7	2.5	0.87		0.7					2.62	0.40	39°47'36"N	76°43'49"W
GLENS	284	<1	30	65	2.3	7		6	2.2	0.88		0.6					2.77	0.38	39°47'36"N	76°43'46"W
White Clay Creek																				
NEWARKRD	741	<0.5	42	142	20.6	46.6	6.09	29.4	7.62	2.63	8.25	1.30	7.15	1.37	3.92	0.54	3.08	0.45	39°46'23"N	75°44'27.5"W
WCCMBIV	284	<1	41	120	15.3	43		30	8.1	2.64		1.5					4.35	0.58	39°47'19"N	75°48'09"W
YRKLYN	442	<1	50	222	21.5	55		37	9.7	2.74		1.7					4.14	0.60	39°48'32"N	75°40'05"W
LANS	450	<1	50	150	22	49		32	7.8	2.75		1.4					3.64	0.52	39°46'21"N	75°46'03"W
WDCRST2	1044	<1	32	145	13.1	29.2	4.16	20.0	5.08	1.79	5.55	0.90	5.19	1.03	2.59	0.344	2.16	0.311	39°50'13"N	75°51'24"W
WCCW	635	<1	22	134	14.9	40		26	6.2	2.03		1.3					2.82	0.40	39°44'38"N	75°47'37"W
WCCBEC	372	<1	31	108	19.4	41.7	5.64	26.0	6.00	2.15	5.84	0.93	5.12	0.98	2.44	0.315	1.97	0.293	39°44'20"N	75°51'34"W
LANM	444	<1	38	130	17.3	37		25	6.2	2.20		1.2					3.19	0.44	39°46'36"N	75°45'40"W
WCCMBI	525	<1	28	123	15.3	39		23	5.6	1.82		1.1					3.45	0.51	39°47'20"N	75°48'09"W
GREENLAWN2	713	0.6	33	129	13.6	29.6	4.27	20.6	5.3	1.85	6.00	1.0	5.9	1.2	3.4	0.5	2.97	0.43	39°53'16"N	75°50'37"W
WCCMBIII	283	<1	30	102	18.4	50		34	8.0	2.73		1.4					3.55	0.50	39°47'20"N	75°48'09"W
WCCW+WA	414	<1	27	103	17.2	40.9	5.57	25.7	6.64	2.18	6.69	1.15	6.54	1.39	3.96	0.595	3.51	0.523	39°48'29"N	75°40'16.5"W
WCCMC	307	3	36	162	16.8	39.1	5.66	26.5	6.66	2.18	6.75	1.20	6.51	1.26	3.62	0.481	3.12	0.413	39°47'32"N	75°38'40"W
WCCN2	423	<1	23	124	12.8	36		25	5.7	1.87		1.2					3.32	0.47	39°45'38"N	75°46'04"W
WCCW+WC	394	<1	27	137	15.2	37.4	5.09	23.7	6.18	1.99	6.24	1.07	6.13	1.29	3.67	0.558	3.33	0.493	39°48'29"N	75°40'15.5"W
WCCMBII	234	<1	24	101	15.4	37		23	5.5	1.93		1.0					2.46	0.35	39°47'20"N	75°48'09"W
MP 5	245	<1	28	101	10.6	27		17	4.8	1.58		1.0					2.11	0.31	39°46'55"N	75°43'47"W
WCCMBI 10-20CM	324	<1	31	167	13.1	28.8	4.38	20.3	5.07	1.72	5.33	0.97	5.55	1.10	3.30	0.461	3.09	0.434	39°47'20"N	75°48'09"W
WCCW+W	372	0.8	29	80	13.3	32.7	4.41	20.3	5.1	1.85	5.57	1.0	5.6	1.1	3.2	0.4	2.96	0.42	39°48'29"N	75°40'16"W
LANN	290	<1	26	85	8.5	20		12	3.3	1.14		0.7					1.62	0.23	39°46'26"N	75°46'11"W
WCC	273	<1	24	102	15.6	26		17	4.3	1.41		0.8					2.37	0.38	39°44'24"N	75°46'25"W

Appendix I, Table 2. Data to assess the precision and accuracy of data in Smith (2004) and this report .

Smith and Barnes (1994, p. 53) used U.S. Geological Survey reference sample BCR-1, run as a blind unknown by Activation Laboratories Ltd. (Actlabs), to assess accuracy, and three adjacent slices of a block of Fishing Creek Metabasalt separately prepared and run with separate batches to assess precision. (This sample contains 1 mm hard opaque oxides and is likely less homogenous than most samples.) Precision in this case is the sum of analytical error, sample preparation error, and a minimum estimate of sampling error. The present studies utilized U.S. Geological Survey reference W-1, also run as a blind unknown by Actlabs, to assess accuracy. The results suggest that "Father" Flanagan's **recommended** values for SiO_2, Al_2O_3, total Fe as Fe_2O_3, CaO, TiO_2 and Zr err on the high side. The next two adjacent slabs of Fishing Creek Metabasalt were analyzed in separate batches to assess precision. The results of the analyses of the slabs are presented in the last table. Since 1994, Actlabs has reduced its use of INAA in favor of ICP-MS on a fusion. Though the data presented here cannot demonstrate it, this seems to have improved detection limits and probably accuracy and precision.

U.S. Geological Survey Reference Sample W-1
Major and Minor Oxides in percent

	SiO_2	Al_2O_3	Fe_2O_3	MnO	MgO	CaO	Na_2O	K_2O	TiO_2	P_2O_5
Actlabs (Present study)	52.08	14.60	10.92	0.167	6.60	10.80	2.20	0.64	1.057	0.13
Flanagan (1976)	52.64	15.00	11.09	0.17	6.62	10.96	2.15	0.64	1.07	0.14
Smith (1973)	51.85	14.55	10.82	0.18	6.49	10.90	2.0	0.62	1.05	0.14

Selected Trace Elements in ppm

	Zr	Hf	Nb	Ta	Th	U	Ni	V	Y	La	Ce	Ba
Actlabs (Present study)	99 90	2.9	8.0	0.45	2.17	.55	71	262	22	12.2	27.3	161
Flanagan (1976)	105	2.67	9.5	0.50	2.42	.58	76	264	25	9.8	23	160
Smith (1973)	94	-	11.2	-	-	-	78.5	300	20	-	-	167

Fishing Creek Metabasalt
Selected Trace Elements in ppm

	TiO_2	Zr	Hf	Nb	Ta	Th	U	Ni	V	Y	La	Ce	Ba
FSHCKFG	2.24	150	3.6	30	1.4	2.2	0.8	50	240	34	19.5	42	50
FSHCKFGII	2.09	150	3.3	28	1.6	2.2	0.6	90	310	32	17.5	40	50
FSHCKFGIII	2.15	168	3.4	28	1.6	2.0	0.6	63	230	28	19.7	41	101
FSHCHFGIV	2.11	132	3.6	27	1.6	2.0	0.6	46	223	30	18.5	41	33
FSHCHFGV	2.11	163	3.6	27	1.9	2.5	0.6	57	299	35	20.9	43	31

Appendix II

Explanation of abbreviations and selected terms used in Smith and Barnes (this volume) and Smith (this volume)

BABB: **B**ack-**a**rc **b**asin **b**asalt. Presumably formed at a spreading center in the back-arc region of a destructive plate margin and, except for volatiles, may be indistinguishable from MORB.

E-OFB = P-OFB ≈ E-MORB = P-MORB: **E**nriched or **p**lume **o**cean-**f**loor **b**asalts. As used herein, does not assume that all spreading centers are located at **m**id-**o**cean **r**idges. Our experience suggests that spreading centers are not readily divided on the basis of abundances of nonvolatile elements. Therefore, we prefer the more inclusive "OFB."

HREE: **H**eavy chondrite-normalized **r**are-**e**arth **e**lements. Generally Er, Tm, Yb, and Lu.

IAT: **I**sland-**a**rc **t**holeiite. Presumably associated with destructive plate margins. As used by some, would include the series that evolve from LKT to calc-alkaline to alkaline to shoshonite.

IREE: **I**ntermediate chondrite-normalized **r**are-**e**arth **e**lements. Generally Sm, Gd, Tb, Dy, and Ho.

IRT: Continental **i**nitial-**r**ifting **t**holeiites. In our experience, may be transitional from continental to ocean-floor (OFB). Also a part of the New York subway system.

LKT: **L**ow-**K** (potassium) **t**holeiite. Presumably an early stage of island-arc development associated with a destructive plate margin.

LREE: **L**ight chondrite-normalized **r**are-**e**arth **e**lements. Generally La, Ce, Nd, and Pr.

N-OFB ≈ N-MORB: **N**ormal **o**cean-**f**loor **b**asalt. The former abbreviation does not, unlike the latter, assume that all spreading centers are located at **m**id-**o**cean **r**idges.

OFB: **O**cean-**f**loor **b**asalt. Does not assume that all spreading centers are located at mid-ocean ridges. Back-arc and possibly other environments could yield similar basalts.

OFT: **O**cean-**f**loor **t**holeiite. This term appears to be intended as an equivalent to N-MORB, but without the implied unique genesis at a mid-ocean ridge spreading center.

OIT = OIB: **O**cean-**i**sland **t**holeiite = **o**cean-**i**sland **b**asalt. Presumably formed within oceanic plates.

OTL: **O**ut-**t**o-**l**unch basalts. Presumably includes those subjected to intense hydrothermal alteration.

"Steerhorn": A chondrite-normalized rare-earth plot in which the intermediate-atomic-number rare-earth elements are depleted relative to light and heavy rare-earths. For volcanic rocks, generally considered to be diagnostic of boninites.

T—MORB ≈ T—OFB: **T**ransitional **m**id-**o**cean **r**idge **b**asalt = **t**ransitional **o**cean-**f**loor **b**asalt. The transition presumably is from N (**n**ormal) to P=E (**p**lume = **e**nriched) basalt.

VAB: **V**olcanic-**a**rc **b**asalts associated with a destructive plate margin. Presumably includes a range of K_2O contents.

WPB: **W**ithin-**p**late **b**asalts. From either continental or oceanic plates. "WP" is used as an adjective to refer to the same environment.

From Smith, II, R. C., and Barnes, J. H., 1994, Geochemistry and geology of metabasalt in southeastern Pennsylvania and adjacent Maryland, in Faill, R. T., and Sevon, W. D., eds., Various aspects of Piedmont geology in Lancaster and Chester counties, Pennsylvania, 59th Field Conference of Pennsylvania Geologists Guidebook, p. 51.

ROAD LOG AND STOP DESCRIPTIONS

DAY 1

Mileage Int.	Mileage Cum.	Description
0.0	0.0	Depart hotel parking lot. Turn RIGHT out of parking lot on Stanton Avenue. Continue about 50 feet to stop sign. Since it is illegal to turn left here, we must turn right and then turn around. Turn RIGHT onto US 322 Business – High Street. Stay to the left; do NOT exit onto US 202 North. Then move to right lane.
0.2	0.2	First traffic light. Turn RIGHT into Parkway Center, make a U-turn, and return to the same traffic light. Get into left lane.
0.1	0.3	Turn LEFT onto 322 Business – High Street, which becomes US 202 South, heading toward Wilmington, DE. Stay to the left; do NOT exit onto US 202 North.
1.7	2.0	Intersection of US 202 South and PA Rt. 926 (Street Road). Note house the northwest corner (near right corner) built of serpentinite. This is the same serpentinite used for the external facing stone for many buildings in West Chester, West Chester University, and the University of Pennsylvania in Philadelphia. This serpentinite is unusual. Most in the area have too many closely-spaced fractures to be quarried for dimension stone. The quarry is located to the west along Rt. 926, and is now a private swim club.
3.1	5.1	Intersection of US 202 South with US 1 (Baltimore Pike); traffic light. Continue straight on US 202.
3.0	8.1	Delaware State Line. The contact of the Mt. Cuba Wissahickon with the Brandywine Blue Gneiss (Wilmington Complex) is under the Brandywine Town Center on the left. Tons of Brandywine Blue Gneiss were blasted out during construction of the large lakes on the property and stockpiled behind the shopping center.
4.0	12.1	Turn RIGHT onto DE Rt. 141 South at Astra Zeneca.
1.0	13.1	Pass Alfred I. duPont Children's Hospital and Nemours Estate on the left. You might catch a glimpse of the estate house through the large ironwork gates. The story goes that the glass on top of the walls is from champagne bottles from the wedding of Alfred and his second wife. Alfred had a bit of a falling out with the rest of the family, and put the glass on the walls to discourage access to his house.
1.0	14.1	Pass DuPont Experimental Station on the left. Turn RIGHT to cross Brandywine Creek on the J.H. Tyler McConnell Bridge. The stone buildings along the creek and up the hill are part of the original DuPont Company black powder mills. Yes, this is where it all began. It is now the Hagley Museum.
0.5	14.6	St. Joseph's on the Brandywine church on the corner of Rt. 100 was built by the duPont family for the Hagley mill workers.
0.4	15.0	Outcrops of Brandywine Blue Gneiss (Wilmington Complex) on the left. This rock is a locally popular building stone, and has given its name to Wilmington's minor league baseball team – the Wilmington Blue Rocks.
0.8	15.8	Continue through intersection with Rt. 48 (Lancaster Pike).
0.9	16.7	Turn RIGHT on Rt. 34 (Faulkland Road).
0.7	17.4	Turn LEFT on Centerville Road.
0.6	18.0	Turn RIGHT on Greenbank Road, immediately before underpass.
0.5	18.5	Turn LEFT into parking lot for Greenbank Station, Wilmington and Western Railroad. Field Conference attendees will ride the Wilmington and Western Railroad to Stops 1 and 2. Stop 1 is along the tracks, easily accessible only from the train.

STOP 1. ARC AMPHIBOLITES SOUTHEAST OF GREENBANK STATION
Leaders: Sandy Schenck and Peg Plank

South of the Greenbank Station, between the station house and the Fall Line, metamorphosed igneous rocks are exposed along the railroad track (figure 15). These rocks are excellent exposures of amphibolites in the Windy Hills Gneiss unit in the Wilmington Complex. The rocks are broken by numerous fractures (joints) and are round on the surface. These features are the result of expansion and weathering as the overlying rocks are removed by erosion. The round surface that forms as the outer weathered layer peels off into curved sheets is called exfoliation and is a distinguishing characteristic of the weathered metamorphosed igneous rocks.

Figure 15. Amphibolite with characteristic island arc geochemistry crops out along the Wilmington and Western Railroad tracks east of the Greenbank Station.

If you look closely at the rocks, you will see that the individual mineral grains in the rocks are large enough to be identified with the naked eye. The minerals are black, sparkling amphiboles, dull black pyroxenes, and opaque white feldspars. Look carefully at the rock and you will see the individual grains of amphibole occur as tiny elongate prisms that are aligned with their long directions parallel to one another. The alignment of these grains indicates these rocks were compressed while they were soft and hot. Old fractures that formed while the rocks were buried are now filled with white quartz. These quartz-filled fractures are either folded into tight folds or stretched into thin veins. The folds and veins also indicate compression in soft rocks. "Bright eyes," which are small black grains of magnetite surrounded by halos of white feldspar, are sprinkled throughout the outcrop. This texture is a retrograde texture common in the Windy Hills Gneiss and Faulkland Gneiss units of the Wilmington Complex.

Rock cores taken about ½ mile northeast of this outcrop near Prices Corner contain metasediments (biotite gneisses) of the Mt. Cuba Wissahickon that demonstrate the intimate association of this Windy Hills unit with the metasediments of the forearc accretionary complex. Although these are only shown in core samples, there are places further to the southwest in this unit where exposures exist and are available to look at if anyone is interested.

Rare earth element (REE) signatures of the mafic rocks in the Windy Hills and Faulkland gneisses are similar to modern arc mafic volcanics. Below are REE diagrams and Thompson spider diagrams comparing these rocks to those of the Honshu Arc (figure 16). The sample from these amphibolites is called HAVEG and is shown as a closed diamond in the right hand diagrams for Windy Hills Gneiss. The Honshu Arc is shown as the asterisk in all of the diagrams.

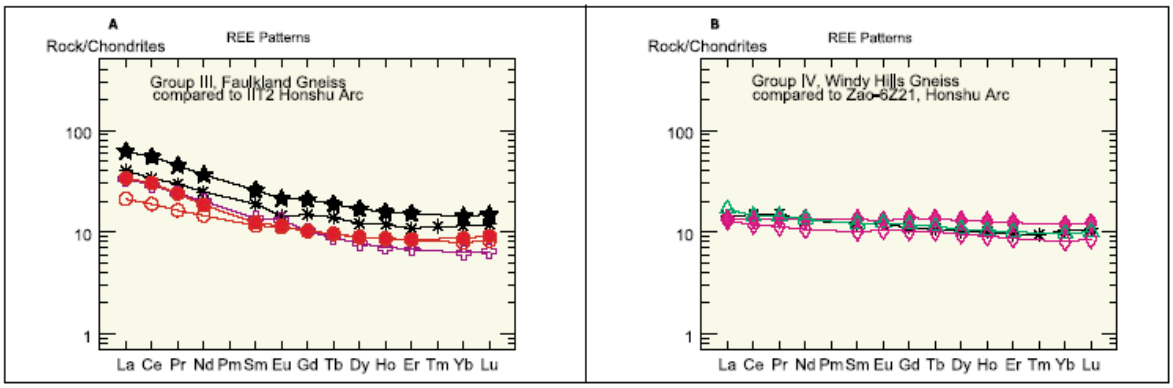

REE patterns for groups III and IV. Chondrite values proposed by Sun and McDonough (1989). A. Group III samples are from the Faulkland Gneiss; compared to IIT2 Takahara volcano, Honshu Arc. B. Group IV samples are from Windy Hills Gneiss; compared to 6Z21 Zao volcano Honshu Arc.
Symbols: closed star, PACKARD; open plus sign, BSP; open circle, HYDE; closed circle, HAGLEY; open triangle, WINDY; open diamond, GREEN; closed diamond, HAVEG. Asterisk is symbol for Takahara volcano, IIT2 and Zao volcano, 6Z21 from the Honshu Arc (Gust et al., 1997).

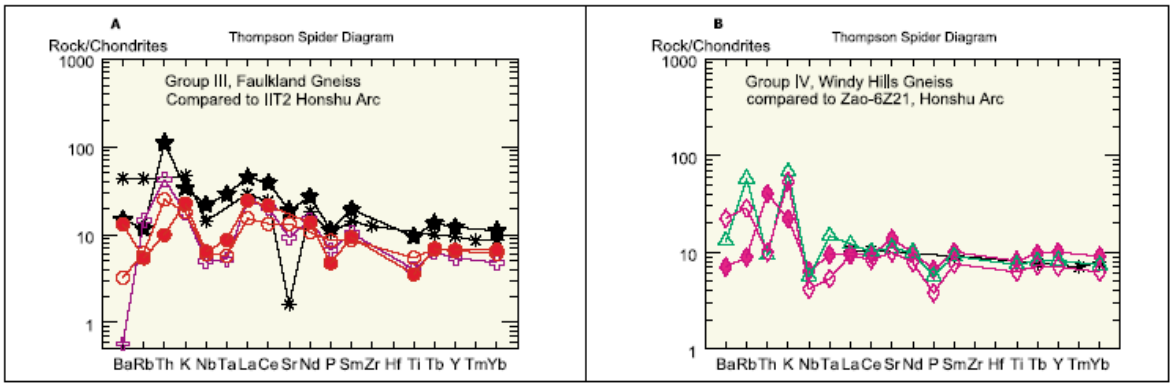

Spider diagrams for groups III and IV using element order and normalizing values of Thompson, 1982.
A. Group III; B. Group VI.
Symbols are same as in Figure 11.

Figure 16. Rare earth element pattern and spider diagrams for the Windy Hills and Faulkland gneisses of the Wilmington Complex.

Just down the tracks towards the highway overpass there is an exposure of felsic gneiss. This felsic gneiss contains quartz, plagioclase, hornblende, and laths of cummingtonite and minor biotite. The cummingtonite is another retrograde mineral that forms a texture common in the Windy Hills and Faulkland gneisses that is reminiscent of snowflakes or feathers (figure 17).

The amphibolites were once volcanic igneous rocks, possibly ash falls, lava flows, or intrusive dikes or sills in the active volcanic island arc. The felsic gneiss was possible a volcaniclastic or ash fall. Any original igneous textures that formed in these rocks have been erased.

Field Conference attendees will reboard the train and continue to Stop 2 at Brandywine Springs Park. Buses will drive from Greenbank Station to the park, following directions below.

Figure 17. Felsic gneiss with cummingtonite (Wilmington Complex) located along the Wilmington and Western Railroad tracks near the overpass of Rt. 2 (Kirkwood Highway).

		Leave Greenbank Station, turning LEFT onto Greenbank Road.
0.1	18.6	Turn RIGHT on Rt. 41.
0.7	19.3	Turn RIGHT on Faulkland Road (Rt. 34).
0.1	19.4	Turn RIGHT into parking lot at Brandywine Springs Park. Park at far end of lot. Field trip attendees will walk up the hill and across the playing fields to rejoin the buses.

STOP 2. MT. CUBA WISSAHICKON METASEDIMENTS WITHIN THE ARC AT RED CLAY CREEK & BRANDYWINE SPRINGS PARK

Leaders: Sandy Schenck and Peg Plank

On the way to and in Brandywine Springs Park (Stop 2), you will notice there are many large round boulders in the stream bed and along the stream banks. These boulders are gneisses and amphibolites, and if you could see them up close, you would find that many of them are spotted with large olive-green grains of poikiloblastic pyroxene, a mineral commonly found in the high-grade metamorphic rocks of the Faulkland Gneiss of the Wilmington Complex.

The hills that enclose both the Red Clay Creek and its tributary Hyde Run are riddled with fresh water springs. The springs occur at the contacts between rock units and are probably abundant here because of the interlayering of rock units (gneisses, schists, amphibolites, and pegmatites) in these hills. Early in this century the Kiamensi Bottling Company bottled and sold fresh spring water from these springs. The bottling company made use of the Wilmington and Western Railroad for shipping during the last part of the 19th century and the early part of the 20th century. The most famous spring located in Brandywine Springs Park spewed brown water charged with iron. Renowned in the nineteenth century for its health restoring qualities, this spring attracted the very wealthy from Philadelphia and Baltimore. A grand hotel was built on the hill above Hyde Run to house the guests, who walked twice each day to the spring to drink the foul tasting water. After a disastrous fire destroyed the hotel, enthusiasm for the spa waned. In 1886 the area was restored as an amusement park, complete with rides, picnic areas, and a trolley.

Today Brandywine Springs is still a park operated by New Castle County, but without the attraction of mineral springs or amusements. Within the park, mineral collectors have found large boulders of sillimanite. Sillimanite is a common mineral in highly metamorphosed rocks, but its occurrence as large boulders of coarse fibrous crystals is extremely rare. Because of these unusual boulders, sillimanite was chosen by Delaware's General Assembly as the state mineral.

The rocks exposed here and elsewhere within the park are Mt. Cuba Wissahickon metasediments within the Faulkland Gneiss. Here amongst the mafic and felsic metavolcanic and metavolcaniclastic gneisses we can see the intimate association of the island arc volcanics and ocean basin sediments in the forearc accretionary complex. Many interesting and odd disequilibrium retrograde metamorphic textures can be found in these rocks including but not limited to: bright eyes (magnetite with halos of plagioclase and quartz), garnet with halos (garnet bright eyes?), cummingtonite laths and sprays, poikiloblastic orthopyroxene in black amphibolite (like leopard spots), gabbroic pegmatite, and large chunks to boulders of sillimanite. If there is time and if you care to wander down towards the trestle and the gravel bars along the creek, you can find many of these textures in hand sized cobbles. They make great paperweights and conversation pieces!

The Delaware State Mineral
Sillimanite (Al_2SiO_5) was named for Benjamin Silliman, the founder of Yale University's geology department. It is a common mineral in aluminum-rich rocks that have been buried and heated to temperatures greater than 1,100°F. The metamorphic event that produced the sillimanite at Brandywine Springs occurred hundreds of millions of years ago during an early phase of mountain building in the Appalachian Range.

The boulders of sillimanite may have formed in the schists near the contact with the pyroxene-bearing gneisses, but no one has found a boulder of sillimanite imbedded in bedrock, so we are not sure precisely how or where these boulders formed at Brandywine Springs.

Exposed in the "cave" outcrop (figure 18) is Mt. Cuba Wissahickon composed of highly deformed pelitic gneiss overlying a pyroxene bearing quartzite. The difference in deformation between the pelitic gneiss and the quartzite demonstrates the difference in competence the two rock types maintained during the deformational events. The pelitic layer has taken up most of the strain while the quartzite deformed in broad open folds This quartzite is so dense that single boulder of it rings like a bell when hit with a rock hammer. We have informally given this rock the name "the rock that rings." This rock locally also contains many small, lavender pyrope garnets. If one were to gold pan in the Red Clay Creek nearby, you would not find any gold, but your pan bottom would be bright lavender-purple with these tiny garnets!

Figure 18. Outcrop of Mt. Cuba Wissahickon metasediments within the Faulkland Gneiss unit of the Wilmington Complex in Brandywine Springs Park.

Field trip attendees walk up the hill and across the field to rejoin the buses in the parking lot. Leave Stop 2. Exit parking lot, turning RIGHT onto Faulkland Road.

1.0	20.4	Turn LEFT onto Centerville Road.
1.1	21.5	Cross Rt. 48 (Lancaster Pike). The large development on the left, called Stonewold, is underlain by Barley Mill Gneiss, a composite pluton in the Wilmington Complex. The Barley Mill Gneiss intrudes both the Faulkland Gneiss and the Mt. Cuba Wissahickon. Igneous zircons recovered from a sample collected during construction of Stonewold yielded SHRIMP (Sensitive High Resolution Ion Microprobe) U-Pb ages of 470 +/- 9 Ma.
0.5	22.0	Turn LEFT on Barley Mill Road.

0.8 22.8 Hoopes Reservoir, the supplemental water supply for the city of Wilmington, is on the right. The road here parallels Red Clay Creek. Approximately 0.4 miles to the left, down the creek in the railroad cut at Wooddale, an outcrop of Barley Mill Gneiss contains large xenoliths of Mt. Cuba Wissahickon, providing clear evidence of an intrusive contact.

0.4 23.2 Cross the bridge over Red Clay Creek and immediately turn LEFT into Spring Valley. Buses will discharge passengers here and park back at . Walk along the railroad track on the left to 101 Tumblerock Road (Peg Plank's house). This is the Wilmington and Western rail line, once again. We would have ridden the train but at least three bridges and several lengths of tracks between Stop 2 and here were destroyed last fall by the remnants of a tropical storm that hit the week before Hurricane Isabelle.

STOP 3 AND LUNCH. WOODDALE QUARRY
Leaders: Peg Plank and Sandy Schenck

Figure 19. Photographs show back wall of Wooddale quarry in the fall when the leaves are off the trees.

This is one of four inactive quarries located in the Red Clay Creek Valley near the community of Wooddale. The two large quarries (including Stop 3) north of Wooddale expose rocks of the Mt. Cuba Wissahickon. When in full operation around the turn of the century, the rock was used by the B&O Railroad to supply crushed stone for railroad ballast. The quarries were last used in 1932 when they supplied stone for Hoopes Reservoir Dam. After completing the reservoir, local residents feared that continuous blasting might damage the dam's foundations so the quarries were closed. In the 1960's the land north of Wooddale was sold and houses were built in the two large quarries. The stone used to build the houses is from these quarries. The quarry visited at stop 3 is one of the largest quarries in Delaware with the back wall rising approximately 50 meters (160 feet) above the quarry floor (figure 19).

The Mt. Cuba Wissahickon lithologies exposed in this quarry are pelitic gneiss, psammitic gneiss, amphibolite, and a variety of pegmatites. The association of gneisses and pegmatites defines the rock as a migmatite (figure 20). The rocks are sharply folded and units are sometimes jumbled due to the intrusion of pegmatites. Layering strikes consistently N35°E to N40°E, the axial planes of upright folds dip slightly to the NW, and the fold axes plunge S60°W.

The psammitic gneiss is indistinctly foliated and contains the assemblage biotite, plagioclase, and quartz with/without garnet. The pelitic gneiss contains garnet, sillimanite, orthoclase, biotite, quartz, and plagioclase. Contacts between the units are gradational and the above assemblages are considered end members in a continuous series.

The amphibolite is weakly layered, but contacts with the pelitic and psammitic gneisses are sharp. The amphibolites are composed of sub-equal amounts of green-brown hornblende and plagioclase. Chemical analyses identify the amphibolites as White Clay Creek Amphibolites.

Figure 20. Upright folds in amphibolite on the back wall of Wooddale Quarry. Light rock on the left of the fold is a granitic pegmatite.

The two small quarries located south of Wooddale expose a unit composed of diorite, tonalite and trondhjemite mapped as the Barley Mill Pluton. The intrusive contact between the Mt. Cuba Wissahickon and the Barley Mill is approximately 450 meters southeast of this quarry. A few ductile shear zones mark the contact.

Migmatites are composites of metamorphic and igneous rocks. The unaltered metamorphic rock is called the paleosome and the newly formed igneous rock is called the neosome. The neosome can be separated into a restite and a leucosome. In this quarry the leucosomes are granitic rocks formed by metamorphic differentiation, anatexis or partial melting, and intrusion of granitic magma. The difference between anatexis and intrusion of magma is a matter of distance. How far must a melt migrate to become intrusive? All these processes have been effective in the formation of these migmatites and can easily be recognized. Metamorphic differentiation is responsible for the thin gneissic layering in the paleosome. These leucosomes contain primarily orthoclase, plagioclase and quartz. The coarser pegmatites, either anatectic or intrusive, contain lower grade assemblages: microcline, muscovite, plagioclase, and quartz. Anatectic pegmatites are often associated with restites that are coarse-grained layers and stringers of biotite, sillimanite, and garnet.

Metamorphic temperatures and pressures were estimated using thermometers based on the Fe-Mg exchange between garnet and biotite and barometers based on garnet-plagioclase-sillimanite-quartz equilibria. Results found peak temperatures in the quarry reached 700 +/-50 C at pressures of 4 +/-1 kilobars (Plank, 1989).

		Walk back along the railroad track to meet the buses at the entrance to the development. Exit Spring Valley, turning RIGHT on Barley Mill Road.
1.2	24.4	Turn RIGHT on Centerville Road.
0.5	24.9	Turn RIGHT (west) onto Rt. 48 (Lancaster Pike).
0.6	25.5	Cross Red Clay Creek. The contact between the Wilmington Complex and Mt. Cuba Wissahickon is in this valley.

2.0	27.5	Merge with Rt. 41 (Newport-Gap Pike). Continue on Rt. 41 toward Hockessin.
1.2	28.7	You are at the top of the hill looking down into the Hockessin valley, which is floored by Cockeysville Marble. The hill on the other side of the valley is underlain by 1.2 billion year old Baltimore Gneiss.
0.6	29.3	Continue on Rt. 41 through intersection with Yorklyn Road. Gale Blackmer's field accommodations, generously provided by her parents at no cost to the Commonwealth, are down Yorklyn Road and up the hill.
1.1	30.4	Pennsylvania State Line.
1.8	32.2	Brittany Hills development on the right – outcrops of Mt. Cuba Wissahickon and some impressive pegmatite were exposed during construction.
0.4	32.6	Turn RIGHT on Newark Road.
1.7	34.3	Intersection with Old Baltimore Pike. Continue on Newark Road. You have just crossed a narrow valley of Cockeysville Marble. The hill in front of you is underlain by Setters Formation. A number of quarries along Old Baltimore Pike in this hill produced "Avondale Stone", a locally popular building stone. One operator down the road to the left is still actively quarrying.
0.2	34.5	Slumpy outcrops of Setters Formation along the roadside.
0.8	35.3	Intersection with US 1. Continue on Newark Road. This is approximately the contact between Setters Formation and Baltimore Gneiss in the core of the Avondale anticline.
0.4	35.7	There is a tiny outcrop of serpentinite under the sign for Line Road. This is still Baltimore Gneiss. The valley ahead is underlain by Cockeysville Marble on the other side of a fault contact.
0.8	36.5	Outcrops of Setters Formation quartzite on both sides of the road going up the hill.
0.3	36.8	Contact with Baltimore Gneiss in the core of the Woodville nappe is about at the intersection with Spencer Road.
0.2	37.0	Intersection with Rt. 926. Continue on Newark Road.
0.3	37.3	Outcrops of Baltimore Gneiss in the roadbanks.
0.6	37.9	Saprolitic outcrops of "Glenarm Wissahickon", Doe Run schist.
0.3	38.2	Intersection with Rt. 842. Continue on Newark Road.
1.2	39.4	Turn LEFT on Rt. 82. The hill on the right is underlain by Doe Run schist. The valley on the left is over Cockeysville Marble.
0.9	40.3	Buses pull over in graveled area at end of hill. Disembark and gather at the end of the parking area down the hill to walk to Stop 4. We will cross the road *en masse*. THIS IS A DANGEROUS ROAD. PEOPLE DRIVE WAY TOO FAST AND THEY CAN'T SEE YOU OVER THE HILL. Cross the road and proceed to the left, back up the hill along the fence. Note the large pile of rocks under a telephone pole partway up the hill. These are excellent examples of Doe Run schist, "chunky" with garnet, staurolite, and tourmaline. You may see kyanite if you are lucky. Continue to the gate at the top of the hill. Proceed through the gate and along the track. Cross the wooden bridge and gather near the old stone house. We will talk here for a moment before proceeding along the track, around the hill and into the quarry.

STOP 4. FAT CHANCE FARM MARBLE QUARRY
Leader: Gale Blackmer

The Big Picture: The marble and feldspathic quartzite exposed in the Fat Chance Farm quarry are identified as Cockeysville Marble and Setters Formation, respectively. The Setters Formation is defined as quartzite and schist that lie stratigraphically above Baltimore Gneiss and below

Cockeysville Marble. The Cockeysville, by definition, lies stratigraphically above Setters or, where Setters is absent, directly above Baltimore Gneiss. At Fat Chance Farm, the sequence of units suggests the overturned limb of an anticline or nappe. Baltimore Gneiss is exposed in the hill west of the quarry at an elevation higher than the quarry floor; because the contacts and foliations dip southwest, the gneiss projects above the quarry. With quartzite above marble in the quarry wall, this makes a sequence of (structural top to bottom) Baltimore Gneiss-Setters-Cockeysville. The gneiss at Fat Chance Farm is at about the center of the northern edge of a large body of gneiss that extends south for about 4.5 km. It is likely that the quarry sits at the leading edge of a map-scale nappe whose upright upper limb has been eroded away.

And what of the Wissahickon? Either it stratigraphically overlies the Cockeysville (Knopf and Jonas, 1923), or it is thrust over top of nappe folds of the other units on a low-angle fault plane called the Doe Run thrust (Bliss and Jonas, 1916; Alcock, 1994). Garnet-staurolite-kyanite schist belonging to the Doe Run unit of the "Glenarm Wissahickon" crops out in the hill across Rt. 82 from the quarry, adjacent to the parking area. Foliation strikes northeast and dips southeast (see figure 3, this volume). Therefore, the Doe Run schist must dip under the Cockeysville Marble exposed in the quarry. This geometry argues against the Doe Run thrust, which would drape the Doe Run schist over the gneiss-cored nappe on a low-angle fault plane.

Although the sequence Baltimore Gneiss – Setters – Cockeysville – Wissahickon works here in the quarry, a look outside the quarry shows that the stratigraphy is more complex. The Setters exposed in the quarry appears to be laterally isolated. Both Cockeysville and Setters pinch out to the east against Wissahickon, which is in direct contact with the Baltimore Gneiss about 100 meters northeast of the quarry. Immediately west of the quarry, Cockeysville is in direct contact with Baltimore Gneiss. Because the gneiss projects so closely above the top of the quarry, this lens of Setters must be quite thin as well as limited in lateral extent. In a smaller quarry northeast in the same hill, metaclastic rocks identical to Setters are interlayered with marble near the top of the outcrops but at a lower elevation than the Setters contact in "our" quarry (we will not visit this quarry due to access issues). A cm-scale layer of the same metaclastic rocks is visible in the small marble outcrop near the lime kiln that we walk past on the way into the quarry (figure 21). And so the question: is what we see in the quarry really Setters Formation, or is it a layer of Setters-like metaclastic rocks within the Cockeysville? Similar complexities are found at localities in adjacent quadrangles (see figure 1, this volume). Lenses of marble are found within the Setters and Wissahickon formations. Lenses of metaclastic rocks identical to Setters are found within the Cockeysville and Wissahickon. The answer may not mean much to the gross interpretation of this locality, but it does have broader implications for regional stratigraphy, and thus the definition and interpretation of these rock units.

Figure 21. Hillside near quarry at Stop 4 with the remnants of a lime kiln in the foreground (dark area) and small marble outcrop at the crest of the hill in the background. The barely visible dark horizon in the outcrop is a layer of metaclastic rock.

***In the quarry*:** Enter the quarry using the upper entrance, in the southwest corner. The primary rock remaining in the highwalls, and the "quarry" of the quarrymen, is marble. The marble here has too many impurities to be useful for much other than agricultural lime. You can see quartz and phlogopite with your eye or handlens. Microcline is also present. The layering visible in places around the quarry is due to variation in the amount of impurities present, which causes color and

textural differences. Note how easily the marble disaggregates when weathered, making it a poor building stone. Walk along the east wall (to your right) to get a look at the marble.

Figure 22. Close-up view of the contact of marble (light-colored rock below) and quartzite.

Continue along the wall into the southeast corner, and climb up the debris slope to the highwall. About 6-7 feet above the soil is the contact of the marble with feldspathic quartzite (figure 22). The quartzite is the darker, slabby rock. For a closer look, access to pieces in the debris is easier and safer. The quartzite consists of generally fine-grained quartz, muscovite, and microcline with larger microcline porphyroclasts and accessory tourmaline. The grain size is a product of mylonitization. Foliation in the quartzite is due to aligned muscovite and compositional layering. The foliation here dips to the southwest at a shallow angle. The ground surface dips at a steeper angle, such that the quartzite thins and is cut out before it reaches the quarry entrance.

Climb back down to ground level and follow the path around the north (highest) wall for a good look at the marble and a good view of the contact, now well above your head (figure 23). Quartzite forms the upper 6-10 feet of this wall. The foliation in this wall dips to the northeast. An open arch with a nearly north-south trending axis passes through the quarry to produce the change in dip. These localized open folds are common late-stage structures in this area.

Figure 23. The pronounced break near the top of the north quarry wall is the quartzite-marble contact (quartzite is the darker rock overlying marble). This photo was taken in 1998, when there was significantly less vegetative overgrowth.

Leave Stop 4 by turning RIGHT out of parking area and continuing north on Rt. 82.

0.4	40.7	On the left is the entrance to Fat Chance Farm, our hosts for Stop 4.
0.6	41.3	The prominent hill on the left is underlain by Setters Formation. The valley on both sides of the road is in Cockeysville Marble.
0.3	41.6	Intersection with Rt. 841, locally known as “Blow Horn”. The stop sign was added only about 5 years ago. Previously, the owners of the barn which blocks the line of sight around the curve painted the words “blow horn” on the barn as a suggested method for drivers to announce their presence.
0.2	41.8	The grove of trees on the left surrounds a marble quarry. In this area, marble was quarried by the farmers for use as agricultural lime. Many quarries (including this one) had a kiln adjacent for burning the marble to produce lime. This quarry is at the western limit of the marble. The hill which extends behind this quarry and across the road ahead is underlain by Doe Run schist.
0.3	42.1	Another marble quarry on the right behind the house at the corner of Dupont Road.
1.2	43.3	Crummy outcrop of Doe Run schist in the left roadbank.
0.3	43.6	Look for emus in the pasture on the right.

0.5	44.1	Cross the contact with the Peters Creek Schist just before Rt. 82 bears right at the church.
0.6	44.7	4-way stop sign; turn RIGHT onto Strasburg Road.
2.7	47.4	Continue on Strasburg Road. Doe Run Church Road enters from the right. Outcrops between here and Brandywine Creek are Peters Creek Schist.
0.8	48.2	Cross West Branch Brandywine Creek at Mortonville. There are more outcrops of Peters Creek leaving the stream valley.
3.6	51.8	Outcrop of Baltimore Gneiss in small borrow pit on the right.
0.9	52.7	Intersection with Rt. 162 and Telegraph Road. Bear LEFT on Telegraph Road.
1.1	53.8	Continue on Telegraph Road through curve/corner. Road turns to gravel in about one-half mile.
1.0	54.8	Turn LEFT onto Waltz Road.
0.8	55.6	Outcrops along the road on the left are Stop 5. Buses will stop in the road.

STOP 5. DOE RUN SCHIST OF THE "GLENARM WISSAHICKON" with optional look at the Laurels schist

Leader: Gil Wiswall

OVERVIEW

The Doe Run and Laurels schists are subunits of the "Glenarm Wissahickon", the northern-most unit of the Wissahickon Formation west of the Rosemont Fault. They consist primarily of pelitic schist and are associated with the Embreeville thrust, a structure presumably formed during the Taconic orogeny in response to the accretion of the Wilmington Complex. The units are lithologically similar; they are distinguished on the basis of texture and metamorphic grade. Consequently, they are interpreted as sharing a common protolith.

In outcrop and hand sample, the Doe Run schist is silvery (weathered) to dark gray (fresh) schist dominated by medium-grained muscovite giving the rock a spangled appearance. Mineralogically, the rock consists of quartz-plagioclase-muscovite-biotite-garnet ± staurolite ± kyanite with abundant accessory tourmaline. Quartz and feldspar content varies and is locally present in sufficient quantity to make the rock psammitic. Garnet, staurolite, and kyanite range in size from a few millimeters to over a centimeter. Biotite is locally present. In localities close to the trace of the Embreeville thrust, sufficient secondary chlorite is present to impart a greenish cast to weathered surfaces. Concordant, centimeter-scale, discontinuous granitic pegmatite layers and quartz veins are present throughout the unit and are locally abundant. Dark gray metasandstone consisting primarily of quartz and plagioclase with minor biotite and muscovite are found in a few locations.

Microscopically, feldspar in the Doe Run schist is primarily plagioclase, with rare minor microcline. Tourmaline, epidote, and apatite are common accessory minerals. Retrogression becomes increasingly intense as the Embreeville thrust is approached. Staurolite and kyanite are replaced by mats of sericite. Chlorite is present in rims and pressure shadows around garnet in addition to replacing garnet and presumably biotite, although in most locations no relict biotite is present.

The Laurels schist is muscovite-chlorite schist that occurs in a narrow band parallel to and north of the trace of the Embreeville thrust west of PA Rte. 100. It is fine-grained, silvery- to grayish-green phyllitic schist dominated by muscovite and chlorite. Small, millimeter-scale garnets are common but staurolite and kyanite are absent. Locally, anhedral centimeter-scale garnets with abundant inclusions are observed. Tourmaline and magnetite are common accessory minerals. Large mats of quartz and sericite observed in one thin section may represent thoroughly retrograded staurolite porphyroblasts. Texturally, the unit is a button schist (Lister and Snoke, 1984); the

intersections of three distinct s-surfaces cause the rock to break into disk-shaped fragments. Based on the mineralogical similarity with the Doe Run schist, the Laurels schist is interpreted as highly strained and thoroughly retrograded Doe Run schist located within the Embreeville thrust zone. The Laurels schist has not been identified east of PA Rte. 100, a problem currently under investigation. Because the Laurels schist crops out poorly, this situation may be a function of the lack of outcrop and extensive development in this area. Alternatively, later deformation may have overprinted the textural characteristics diagnostic of the Laurels schist.

STOP DESCRIPTION

This outcrop was chosen because it is sufficient in size to accommodate the group safely; unfortunately it is not particularly representative of the Doe Run schist. The combination of weathering and development in this part of the southeast Pennsylvania Piedmont limits the number of options for field trip stops.

One of the rare metasandstone layers crops out at the south end of the outcrop. The rock is composed of medium grained quartz and subordinate feldspar with finely disseminated biotite and chlorite and accessory pyrite. The planar foliation is S_2 which is associated with top to the northwest movement along the Embreeville thrust.

The north end of the road cut exposes the Doe Run schist where it is more psammitic and finer grained than typical Doe Run schist. The rock consists of subequal amounts of quartz and feldspar with medium to fine grained muscovite, biotite, garnet, and chlorite. Fine accessory tourmaline is visible in hand sample, staurolite is visible in thin section. Discontinuous granitic pegmatite layers and quartz veins are moderately common. Two foliation surfaces are present. The dominant, shallow southeast-dipping surface is S_2. An older (S_1), more steeply southeast-dipping foliation is deformed by S_2 showing the top to the northwest displacement. The resultant fabric produces a wavy texture.

OPTIONAL STOP

The trace of the Embreeville thrust and an exposure of the Laurels schist occur north of the exposure of the Doe Run schist. If time permits, walk north for about 50 meters to a small quarry located on the hillside west of the road. The rock exposed in the quarry is the psammitic phase of the Doe Run schist viewed at the last outcrop. Note that S_2 is nearly penetrative and more planar. In addition, the granitic pegmatite veins are disaggregated into polycrystalline porphyroclasts. These features suggest an increase in the strain magnitude as the Embreeville thrust zone is approached.

About 100 meters farther north is an outcrop of typical Laurels schist exhibiting classic button texture. The rock is muscovite-chlorite schist with millimeter-scale garnets. From the road looking west, similar S_1/S_2 relations seen previously exhibit top to the northwest shearing associated with the emplacement of the Embreeville hanging wall. Viewing the north face of the outcrop toward the south, S_3 surfaces cut the subhorizontal S_1/S_2 fabric. Deflection of the older fabric indicates oblique slip composed of normal and dextral components. This younger deformation is presumably related to the late features viewed at the second stop tomorrow.

		Leave Stop 5 and head for “home”. Continue ahead on Waltz Road.
0.2	55.8	Turn RIGHT onto Sugars Bridge Road.
0.1	55.9	Turn RIGHT onto US 322. Stay on 322 East toward West Chester.
2.2	58.1	Turn LEFT onto East US 322 By-pass.
2.6	60.7	Merge up ramp on the right onto US 202 South.
2.9	63.6	Exit onto US 322 Business and make U-turn in Parkway Center, same as this morning.
0.5	64.1	Turn LEFT onto Stanton Avenue, then left into Holiday Inn parking lot.

INTRODUCTION TO DAY TWO

by
Howell Bosbyshell

INTRODUCTION

Today we will examine complexly deformed high grade metamorphic rocks in Delaware County, Pennsylvania, which record a long history of tectonic activity along the margin of the Laurentian craton. These rocks include gneiss of the Avondale massif, rock of uncertain affinity which may be considerably younger than the Precambrian age traditionally assigned to it; the Wilmington Complex, remnants of an Ordovician volcanic arc; and metasedimentary and metavolcanic rock of the Wissahickon Formation. Recent mapping (Plank *et al.*, 2000a: Schenk *et al.*, 2000; Bosbyshell, 2001), geochronology (Bosbyshell *et al.*, 2001; Aleinikoff *et al.*, 2001) and geochemical studies (Bosbyshell, 2001; Plank *et al.*, 2000b) place important new constraints on the tectonic evolution of the Central Appalachians. On this trip we will examine exposures of the Wilmington Complex, Wissahickon Formation, and Avondale massif which illustrate important lithologic, metamorphic, and deformational characteristics of these major units.

We will inspect two varieties of the Wissahickon Formation. One, informally referred to as Arc Wissahickon and considered to be part of the Mt. Cuba Wissahickon forearc accretionary complex (Plank and Schenk, this volume), will be seen at Stop 8. The other, referred to as Type Wissahickon, which is contiguous with and lithologically indistinguishable from the type-section Wissahickon Formation exposed along Wissahickon Creek in Philadelphia, will be seen at Stop 60. The intimate relationship between the Arc Wissahickon and the Wilmington Complex, and the reason for its inclusion in the Mt. Cuba forearc accretionary complex, is demonstrated by the presence of a boninitic dike within the Arc Wissahickon at the contact with the Wilmington Complex. This dike is described in the guidebook at Stop 7, but will not be seen.

The Arc Wissahickon differs from the Type Wissahickon in several ways, most notably in the lack of primary sedimentary bedding, the well defined interlayering of pelitic and psammitic rock which is characteristic of the Type Wissahickon farther to the east. At Stop 8, we will see that the Arc Wissahickon clearly contains portions of rock that contain more or less mica, i.e. there are pelitic and psammitic lithologies present, but recognizable bedding is rare.

In addition to the lack of identifiable bedding, the Arc Wissahickon apparently experienced a somewhat different metamorphic history than the Type Wissahickon. Monazite in two samples from pelitic gneiss near the Wilmington Complex contain euhedral cores that yield Ordovician ages (484 – 472 Ma; Bosbyshell, 2001). The euhedral nature of the cores suggests that they are not detrital in origin, but more likely formed during metamorphism. Since the age of the monazite cores is the same as the age of Wilmington Complex metaigneous rock, the most reasonable interpretation is that there was an episode of heating and monazite growth in the Arc Wissahickon in response to arc magmatism. This suggests that the original contact between these units was intrusive. The boninitic dike supports this interpretation. Monazite older than Silurian has not been identified in Type Wissahickon.

One additional difference between Type Wissahickon and Arc Wissahickon is the lack of significant amphibolite in the Arc Wissahickon. With the exception of the boninitic dike (only one exposure has been recognized) near the contact, amphibolite, which is quite common in the Type Wissahickon, is not present in the Arc Wissahickon.

Bosbyshell, H., 2004, Day two, *in* Blackmer, G. C., and Srogi, L., Marginalia – Magmatic arcs and continental margins in Delaware and southeastern Pennsylvania: Guidebook, 69th Annual Field Conference of Pennsylvania Geologists, West Chester, PA, p. 82-88

Limited exposure, complex deformation, and high grade metamorphism obscure stratigraphic relationships and may account for the relative paucity of recognizable primary sedimentary characteristics in the Arc Wissahickon. The limited exposure and deformation also make it exceedingly difficult to map the contact between the two units. Thus it may not be possible to formally designate Arc Wissahickon as a distinct member. Additional data, such as detrital zircon provenance and additional monazite geochronology, may contribute to resolving this problem.

TECTONIC HISTORY

Igneous activity, multistage deformation, and metamorphism in this portion of the Piedmont have long been considered to be the result of the formation of a volcanic-magmatic province, an island arc, during the early Paleozoic and its subsequent accretion to the Laurentian craton (Crawford and Crawford, 1980; Wagner and Srogi, 1987). Bosbyshell (2001) proposed a revised model which incorporates new geochronological constrains imposed by monazite (Bosbyshell, 2001) and zircon (Aleinikoff *et al.*, 2001) chemical and isotopic data. The stages in the model, presented as a pressure-temperature-deformation-time path (P-T-D-t) in figure 24 are (1) formation of the Wilmington Complex arc during the early Ordovician; (2) tectonic burial of volcanic and sedimentary rocks during middle to late Ordovician arc-continent collision; (3) low-pressure high-temperature metamorphism (M2) as a result of lithospheric thinning in the Silurian; (4) renewed convergence in the early Devonian which resulted in (5) middle Devonian intermediate-pressure metamorphism (M3); and finally (6) folding and the development of a widespread crenulation cleavage, possibly during the Mississippian. The relationship between deformation and metamorphism at the scale of a hypothetical Wissahickon Formation outcrop is represented in a schematic block diagram in figure 25.

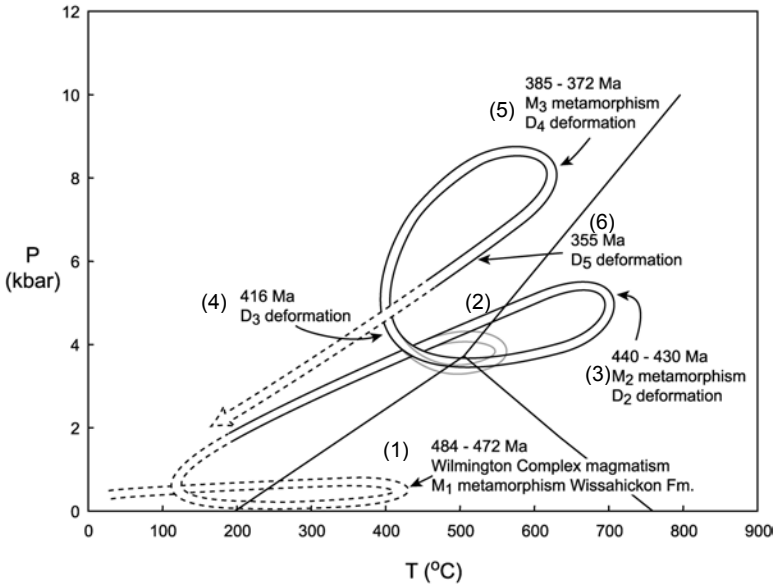

Figure 24. Pressure-temperature-deformation-time paths for the Wissahickon Formation. Black line for rocks along Chester Creek, nearest the Wilmington Complex, gray line for the Type Wissahickon along Crum Creek. The cooling path is constrained by an 40Ar/39Ar hornblende age of 359 ± 6 Ma (Sutter et al, 1980) and by Rb/Sr ages of muscovite (358 – 344 Ma) and biotite (270 – 257 Ma) (Kohn et al., 1993). See text for further details.

The model refines and extends earlier models in which the Wilmington Complex arc formed above an easterly dipping (present geographic coordinates) subduction zone (Crawford and Mark, 1982; Wagner and Srogi, 1987), but does not specifically address the different components of the Wissahickon Formation. The boninitic affinity of Wilmington Complex amphibolites (Bosbyshell, 2001; Plank *et al.* 2000b), and the observation that modern boninites are found primarily in fore-arc settings (Crawford *et al*., 1989), supports earlier models and is the strongest evidence to date for an arc origin for the Wilmington Complex. Previously, the interpretation of the Wilmington Complex as the remnant of a volcanic arc was based on the abundance and composition of igneous rock and orthogneiss and the steep geothermal gradient required by the intermediate pressure granulite facies metamorphism (Ward, 1959; Wagner and Srogi, 1987; Srogi, 1988). However, Wagner and Srogi

(1987) acknowledged that their data did not enable them to attribute Wilmington Complex magmatism to a unique tectonic setting.

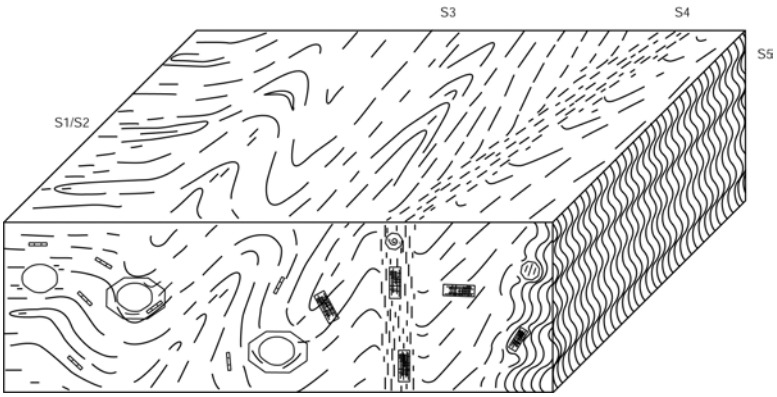

Figure 25. Schematic representation of sequence of deformation and metamorphism in Wissahickon Formation. Diagram is chronological from left to right. At left, S2 foliation and F2 isoclinal folds; M2 minerals garnet and sillimanite. Center, F3 folds and S3 foliation; M3 mineral growth, kyanite and garnet overgrowths are younger than F3 folding. To right, S4 shear zone synchronous with M3 metamorphism. At right, post M3, F5 crenulation with shallowly dipping axial planes, S5.

Exposures in Delaware County demonstrate that some portion of the Wissahickon Formation and the Wilmington Complex were contiguous during the early Ordovician. The similar age of monazite cores (484 – 472 Ma; Bosbyshell, 2001) in the Wissahickon Formation and igneous zircon in the Wilmington Complex (485 – 468 Ma; Aleinikoff *et al.*, 2001) suggests that the earliest metamorphism in the Wissahickon Formation, M1 (figure 24), was in response to heating by Wilmington Complex magmatism. Because porphyroblasts associated with this metamorphism have not been identified, the grade of M1 is unknown. Thus, this portion of the P-T-D-t path is dashed in figure 24. The presence of amphibolite dikes with boninitic affinity in both units near their contact and the observation that boninites are thought to form early in the evolution of an arc (Cameron *et al.*, 1979; Stern and Bloomer, 1992) support this interpretation. This evidence suggests that the original Wilmington Complex/Wissahickon Formation contact is intrusive.

The collision of the Wilmington Complex arc and the Laurentian margin is interpreted to have occurred during the middle to late Ordovician Taconic orogeny. The recognition of 480 Ma volcanic rocks in the Wilmington Complex (Aleinikoff *et al.*, 2001) requires burial of these units to depths corresponding to 4 – 6 kb pressure (Wagner and Srogi, 1987; Plank, 1989; Srogi *et al*., 1993) prior to high temperature metamorphism in the early Silurian. Some of the required crustal thickening could have been the result of burial by subsequent arc volcanism. However, given the considerable depth of burial required by the metamorphic data and the structural and biostratigraphic evidence for convergence in the foreland during the middle to late Ordovician (Faill, 1997a; Ganis *et al.*, 2001), significant tectonic thickening is indicated. This tectonic activity is the Taconic orogeny, the time of arc-continent collision. It is perhaps noteworthy that there is little evidence for metamorphic mineral growth at the time of collision. This suggests that the rocks followed a clockwise P-T path during M2, with heating and high-grade metamorphism following maximum burial (figure 24).

The Silurian M2, high-temperature low-pressure metamorphism in the Wissahickon Formation and moderate-pressure granulite facies metamorphism in the Wilmington Complex, is approximately the same age as magmatism in the Arden pluton (Aleinikoff *et al*., 2001) and therefore is interpreted to reflect the same thermal regime. Significant gabbro and gabbronorite in the Arden and Bringhurst plutons suggests that advection of mantle heat through mafic magmatism was important in establishing the steep geothermal gradient required by the metamorphic data (Wagner and Srogi, 1987). This thermal regime is interpreted to result from post-collisional thinning of the lithosphere resulting from either delamination of the down going slab (Sacks and Secor, 1990; Davies and von Blanckenburg, 1995) marking a shift in subduction polarity (Teng *et al.*, 2000), or subsequent backarc extension above a younger, west-dipping subduction zone. Late Ordovician and Silurian arc-related metaigneous rocks, found in settings consistent with west-dipping subduction,

are present to the north (Sevigny and Hanson, 1995; Karabinos *et al.*, 1998) and south of the study area (Hanan and Sinha, 1989; Horton *et al.*, 1999). Based on the E-MORB or backarc basin basalt (Plank *et al.*, 2000b) trace element geochemical characteristics of mafic igneous rocks in the Arden pluton, the backarc setting is the preferred interpretation.

A period of relative tectonic quiescence following M2 metamorphism is suggested by the sedimentary record in the Appalachian Basin (Faill, 1997b) and a hiatus of 25 – 30 Ma in metamorphic monazite growth. Early Devonian deformation, (D3, figure 24) marks the onset of renewed plate convergence, resulted in crustal thickening and middle Devonian Barrovian style metamorphism and intermediate pressure overprinting, M3. In the northern and southern Appalachians, middle Paleozoic orogenesis resulted from accretion of the peri-Gondwanan terranes, Avalonia and Carolina (e.g. Robinson *et al.*, 1998; Hibbard, 2000); however, rocks of peri-Gondwanan affinity are unknown in the Central Appalachians.

The final phase of deformation in the Wissahickon Formation produced folds with shallow north dipping axial planes with an associated crenulation cleavage in pelitic units, and some increment of deformation in shear zones. Monazite data suggest that this occurred during the Mississippian (~355 Ma), though due to the difficulty of measuring the low Pb content of monazite this young, these ages may not be reliable. The monazite ages are similar to 40Ar/39Ar cooling ages of hornblende in the study area (Sutter *et al.*, 1980), indicating temperatures at that time of 500 ±50 °C (McDougall and Harrison, 1988). If the timing is correct, then this deformation could be an early stage of the Alleghenian orogeny.

References (including references for Stops 6-10)

Aleinikoff, J. N., Schenck, W. S., Plank, M. O., Srogi, L., Armstrong, T. R., and Hodges, W., 2001, Morphology and SHRIMP U-Pb ages of zircon and monazite from high-grade rocks of the Wilmington Complex, Delaware: Geological Society of America Abstracts with Program, v. 33, p. 82.

Allan, J. F., and Gorton, M. P., 1992, Geochemistry of igneous rocks from Legs 127 and 128, Sea of Japan: Proceedings of the Ocean Drilling Program-Scientific Results, v. 127/128, p. 905-929.

Bascom, F., Clark, B., Darton, N. H., Kummel, H. B., Salisbury, R. D., Miller, B.L., and Knapp, g. N., 1909, Philadelphia folio, United States Geological Survey Geological Atlas of the U.S., Folio 162.

Beccaluva, L., and Serri, G., 1988, Boninitic and low-Ti subduction-related lavas from intraoceanic arc-backarc systems and low-Ti ophiolites: a reappraisal of their petrogenesis and original tectonic setting: Tectonophysics, v. 146, p. 291-315.

Bedard, J. H., Lauziere, K., Tremblay, A., and Sangster, A., 1998, Evidence for forearc seafloor-spreading from the Betts Cove ophiolite, Newfoundland: oceanic crust of boninitic affinity: Tectonophysics, v. 284, p. 233-245.

Bell, T. H., and Johnson, S. E., 1989, Porphyroblast inclusion trails: the key to orogensis: Journal of Metamorphic Geology, v. 7, p. 279-310.

Berg, T. M., Edmunds, W. E., Geyer, A. R., Glover, A. D., Hoskins, D. M., MacLachlin, D. B., Root, S. I., Sevon, W. D., and Socolow, A. A., 1980, Geologic map of Pennsylvania: Pennsylvania Topographic and Geologic Survey, Series 4, Map 1.

Berman, R. G., 1991 Thermobarometry using multiequilibrium calculations: a new technique with petrologic applications: Canadian Mineralogist, v. 29, 833-855.

Berman, R. G., and Aranovich, L. Y., 1996, Optimized standard state and mixing properties of minerals: I. Model calibration for olivine, orthopyroxene, cordiertie, garnet, and ilmenite in the system FeO-MgO-CaO-Al2O3-TiO2-SiO2: Contributions to Mineralogy and Petrology, v. 126, p. 1-24.

Berman, R. G., and Brown, T. H., 1997, TWQ2.02, Thermobarometry with equilibration state: Geological Survey of Canada, (www.gis.nrcan.gc.ca/twq.html).

Bloomer, S. H., 1987, Geochemical characteristics of boninite- and tholeiite-series volcanic rocks from the Mariana forearc and the role of an incompatible element-enriched fluid in arc petrogenesis: Geological Society of America Special Paper 215, p. 151-164.

Bloomer, S. H., and Hawkins, J. W., 1987, Petrology and geochemistry of boninite series volcanic rocks from the Mariana trench, Contributions to Mineralogy and Petrology, v. 97, p. 361-377.

Bosbyshell, H., 2001, Thermal evolution of a convergent orogen: Pressure–Temperature–Deformation–Time paths in the central Appalachian Piedmont of Pennsylvania and Delaware: [PhD. thesis]: Bryn Mawr College, Bryn Mawr, Pa., 233 p.

Bosbyshell, H., Sinha, A. K., Crawford, M. L., Fleming, P., Srogi, L., and Lutz, T., 1998, Thermal evolution of a convergent orogen: New U/Pb ages of monazite and zircon from the Central Appalachian Piedmont: Geological Society of America Abstracts with Programs, v. 30, p. 125.

Bosbyshell, H., Crawford, M. L., and Srogi, L., 1999, Distribution of overprinting metamorphic mineral assemblages in the Wissahickon Group, southeastern Pennsylvania, *in* Valentino, D. W., and Gates, A. E., eds., The Mid-Atlantic Piedmont: Tectonic Missing Link of the Appalachians: Boulder, Colorado, Geological Society of America Special Paper 330, p. 41-58.

Cameron, W. E., 1989, Contrasting boninite-tholeiite associations from New Caledonia *in* Crawford, A. J., ed., Boninites: London, Unwyn Hyman, p. 314-337.

Cameron, W. E., Nisbet, E. G., and Dietrich, V. J., 1979, Boninites, komatiites and ophiolitic basalts: Nature, v. 280, p. 550-553.

Cameron, W. E., McCulloch, M. T., and Walker, D. A., 1983, Boninite petrogenesis: chemical and Nd-Sr isotopic constraints: Earth and Planetary Science Letters, v. 65, p. 75-89.

Chakraborty, S., and Ganguly, J., 1992, Cation diffusion in aluminosilicate garnets: experimental determination in spessartine-almandine diffusion couples, evaluation of effective binary diffusion coefficients, and applications, Contributions to Mineralogy and Petrology, v. 111, p. 74-86.

Chatterjee, N. D., and Froese, F. E., 1975, A thermodynamic study of the pseudobinary join muscovite-paragonite in the system $KAlSi_3O_8$-$NaAlSi_3O_8$-Al_2O_3-SiO_2-H_2O: American Mineralogist, v. 60, p. 985-993.

Crawford, A. J., Beccaluva, L., and Serri, G., 1981, Tectono-magmatic evolution of the West Philippine-Mariana region and the origin of boninites: Earth and Planetary Science Letters, v. 54, p. 346-356.

Crawford, A. J., Falloon T. J., and Green, D. H., 1989, Classification, petrogenesis and tectonic setting of boninites, *in* Crawford, A. J., ed., Boninites: London, Unwyn Hyman, p. 1-49.

Crawford, M. L., and Crawford, W. A., 1980, Metamorphic and tectonic history of the Pennsylvania Piedmont: Journal of the Geological Society of London, v. 137, p. 311-320.

Crawford, M. L., and Mark, L. E., 1982, Evidence from metamorphic rocks for overthrusting. Pennsylvania Piedmont, U. S. A.: Canadian Mineralogist, v. 20, p. 333-347.

Crawford, M. L., and Mark, L. E., 1982, Evidence from metamorphic rocks for overthrusting. Pennsylvania Piedmont, U. S. A.: Canadian Mineralogist, v. 20, p. 333-347.

Davies, J. H., and von Blanckenburg, F., 1995, Slab breakoff: A model of lithosphere detachment and its test in the magmatism and deformation of collisional orogens, Earth and Planetary Science Letters, v. 129, p. 85-102.

Faill, R. T., 1997a, A Geologic history of the North-Central Appalachians. Part 1. Orogensis from the Mesoproterozoic through the Taconic orogeny: American Journal of Science, v. 297, pp. 551-619.

Faill, R. T., 1997b, A Geologic history of the North-Central Appalachians. Part 2: The Appalachian Basin from the Silurian through the Carboniferous: American Journal of Science, v. 297, pp. 729-761.

Fuhrman, M. L., and Lindsley, D. H., 1988, Ternary-feldspar modeling and thermometry: The American Mineralogist, 73, 201-216.

Ganis, G. R., Williams, S. H., and Repetski, J. E., 2001, New biostratigraphic information from the western part of the hamburg klippe, Pennsylvania, and its significance for interpreting the depositional and tectonic history of the klippe: Geological Society of America Bulletin, v. 113, p. 109-128.

Gordon, S. G., 1922, Mineralogy of Pennsylvania: Philadelphia Academy of Natural Science Special Publication 1.

Grauert, B., Crawford, M. L., and Wagner, M. E., 1973, U-Pb isotopic analysis of zircons from granulite and amphibolite facies rocks of the West Chester prong and the Avondale anticline, southeastern Pennsylvania: Carnegie Institution of Washington Yearbook, v. 72, p. 290-293.

Grauert, B., Wagner, M. E., and Crawford, M. L., 1974, Age and origin of amphibolite-facies rocks of the Avondale anticline (southeastern Pennsylvania) as derived from U-Pb iostopic studies on zircon: Yearbook of the Carnegie Institute of Washington, v. 73, p. 1000-1003.

Gribble, R. F., Stern, R. J., Newman, S., Bloomer, S. H., and O'Hearn, T., 1998, Chemical and isotopic composition of lavas from the northern Mariana Trough: implications for magma genesis in back-arc basins: Journal of Petrology, v. 39, p. 125-154.

Grove, T. L., Baker, M. B., and Kinzler, R. J., 1984, Coupled CaAl-NaSi diffusion in plagioclase feldspar: experiments and applications to cooling rate speedometry: Geochimica et Cosmochimica Acta, v. 48, p. 2113-2121.

Gust, D. A., Arculus, R. J., and Kersting, A. B., 1997, Aspects of magma sources and processes in the Honshu arc: The Canadian Mineralogist, v. 35, p. 347-365.

Hanan, B. B., and Sinha, A. K., 1989, Petrology and tectonic affinity of the Baltimore mafic complex, Maryland: in Mittwede, S. K., and Stoddard, E. F., eds., Ultramafic rocks of the Appalachian Piedmont: Geological Society of America Special Paper 231, p. 1-18.

Hess, D. F., 1981, Further data on andalusite and kyanite pseudomorphs after andalusite from Delaware County, Pennsylvania (P. I, Andalusite): Friends of Mineralogy, Pennsylvania Chapter, Newsletter, v. 9, p. 3-4.

Heyl, A. V., 1980, Pennsylvania News from Colorado: Friends of Mineralogy, Pennsylvania Chapter, Newsletter, v. 8, p. 4-5.
Hibbard, J., 2000, Docking Carolina: Mid-Paleozoic accretion in the southern Appalachians: Geology, v. 28, p. 127.
Hickey, R. L., and Frey, F. A., 1982, Geochemical characteristics of boninite series volcanics: implications for their source: Geochemica et Cosmochimica Acta, v. 46, p. 2099-2115.
Holdaway, M. J., 1971, Stability of andalusite and the aluminum silicate phase diagram: American Journal of Science, v. 271, p. 97-131.
Holdaway, M. J., Mukhopadhyay, B., Dyar, M. D., Guidotti, C. V., and Dutrow, B. L., 1997, Garnet-biotite geothermometry revised: New Margules parameters and a natural specimen data set from Maine: American Mineralogist, v. 82, p. 582-595.
Horton, J. W., Aleinikoff, J. N., Drake, A. A., Jr., Fanning, C. M., 1998, Significance of middle to late Ordovician volcanic-arc rocks in the Central Appalachian Piedmont, Maryland and Virginia: Geological Society of America Abstracts with Programs, v. 30, p. 125.
Irvine, T. N., and Baragar W. R. A., 1971, A guide to the Chemical Classification of the Common Volcanic Rocks: Canadian Journal of Earth Sciences, v. 8, p. 523-548.
Jenner, G. A., 1981, Geochemistry of high-Mg andesites from Cape Vogel, Papua New Guinea: Chemical Geology, v. 33, p. 307-332.
Johnson, L. E., and Fryer, P., 1990, The first evidence for MORB-like lavas from the outer Mariana forearc: geochemistry, petrography, and tectonic implications: Earth and Planetary Science Letters, v. 100, p. 304-316.
Karabinos, P., Samson, S. K., Hepburn, J. C., and Stoll, H. M., 1998, Taconian orogeny in the New England Appalachians: Collision between Laurentia and the Shelburne Falls arc: Geology, v. 26, p. 215-218.
Koziol, A. M.; and Newton, R. C., 1988, Grossular activity relationships in ternary garnets determined by reversed, displaced equilibrium experiments: Contributions to Mineralogy and Petrology, v. 103, p. 423-433.
LeBas, M.J., LeMaitre, R.W., Streckeisen, A., and Zanettin, B., 1986. A chemical classification of volcanic rocks based on the total alkali silica diagram: Journal of Petrology, v. 27, p. 745-750.
Loomis, T. P., Ganguly, J., and Elphick, S. C., 1985, Experimental determination of cation diffusivities in aluminosilicate garnets, Contributions to Mineralogy and Petrology, v. 90, p. 45-51.
McDougall, I., and Harrison, T. M., 1988, Geochronology and Thermochronology by the $^{40}Ar/^{39}Ar$ Method: Oxford University Press, New York, 212 p.
Means, W. D., 1999, Reversed structures and bounce structures: are the recognizable? Are they real?: Journal of Structural Geology, v. 21, p. 917-921.
Miyashiro, A., 1974, Volcanic rock series in island arcs and active continental margins: American Journal of Science, v. 274 p. 321-355.
Nichols, I. A., Whitford, D. J., Harris, K. L., and Taylor, S. R., 1980, Variation in the geochemistry of mantle sources for tholeiitic and calc-alkaline mafic magmas, western Sunda volcanic arc, Indonesia: Chemical Geology, v. 30, p. 177-199.
Plank, M. O., 1989, Metamorphism in the Wissahickon Formation of Delaware and adjacent areas of Maryland and Pennsylvania [M. A. thesis]: Newark, University of Delaware, 126 p.
Plank, M. O., Schenck, W. S., and Srogi, L., 2000a, Bedrock geology of the Piedmont of Delaware and adjacent Pennsylvania: Delaware Geological Survey Report of Investigations No. 59, 52p.
Plank, M. O., Srogi, L. A., Schenck, W.S., 2000b, Possible tectonic affinities of mafic units in the Pa-De Piedmont based on new geochemical data: Geological Society of America Abstracts with Programs, v. 32, p. A-66.
Robinson, P., Tucker, R. D., Bradley, D., Berry, H. N., Jr., and Osberg, P. H., 1998, Paleozoic orogens in New England, USA: GFF, v. 120, pp. 119-148.
Sacks, P. E., and Secor, D. T., 1990, Delamination in collisional orogens: Geology, v. 18, 999-1002.
Saunders, A., and Tarney, J, 1991, Back-arc basins, *in* Floyd, P. A., ed., Oceanic Basalts: Glasgow, Blackie and Son, Ltd., p. 219-263.
Schenck, W.S., Plank, M.O., and Srogi, L., 2000, Bedrock Geologic Map of the Piedmont of Delaware and Adjacent Pennsylvania: Delaware Geological Survey Geologic Map No. 10, Scale 1:36,000.
Sevigny, J. H., and Hanson, G. N., 1995, Late-Taconian and pre-Acadian history of the New England Appalachians of southwestern Connecticut: Geological Society of America Bulletin, v. 107, p. 487-498.
Smith, H., and Barriero, B., 1990, Monazite U-Pb dating of staurolite grade metamorphism in pelitic schists: Contributions to Mineralogy and Petrology, v. 105, pp. 602-615.
Spear, F. S., and Florence F. P., 1992, Thermobarometry in granulites: pitfalls and new approaches: Journal of Precambrian Research, v. 55, p. 209-241.
Srogi, L., 1988, The petrogenesis of the igneous and metamorphic rocks in the Wilmington Complex, Pennsylvania-Delaware Piedmont: unpublished Ph.D. thesis, University of Pennsylvania, 613 p.
Srogi, L., Wagner, M. E., and Lutz, T. M., 1993, Dehydration partial melting and disequilibrium in the granulite - facies Wilmington Complex, Pennsylvania-Delaware Piedmont: American Journal of Science, v. 293, p. 405-462.

Stern, R. J., and Bloomer, S. H., 1992, Subduction zone infancy: examples from the Eocene Izu-Bonin-Mariana and Jurassic California arcs: Geological Society of America Bulletin, v. 104, p. 1621-1636.
Stern, R. J., Ping-Nan Lin, Morris, J. D., Jackson, M. C., Fryer, P., Bloomer, S. H., and Ito, E., 1990, Enriched back-arc basin basalts from the northern Mariana Trough: implications for the magmatic evolution of back-arc basins: Chemical Geology, v. 100, p. 210-225.
Sun, S.-s and McDonough, W. F., 1989, Chemical and isotopic systematics of oceanic basalts: implications for mantle compositions and processes, *in* Saunders, A. D., and Norry, M. J., Magmatism in the Ocean Basins: Geological Society Special Publication No. 42, p. 313-345.
Sutter, J. F., Crawford, M. L., and Crawford, W. A., 1980, 40Ar/39Ar age spectra of coexisting hornblende and biotite from the Piedmont of SE Pennsylvania: Their bearing on the metamorphic and tectonic history: Geological society of America Abstracts with Programs, v. 12, p. 85.
Teng, L. S., Lee, C. T., Tsai, Y. B., and Hsiao, L-Y, 2000, Slab breakoff as a mechanism for flipping of subduction polarity in Taiwan: Geology, v. 28, p. 155-158.
Tracy, R. J., 1982, Compositional zoning and inclusions in metamorphic rocks: Reviews in Mineralogy, v. 10, p. 355-397.
Valentino, D. W., Valentino, R. W., and Hill, M. L., 1995, Paleozoic transcurrent conjugate shear zones in the Central Appalachian Piedmont of southeastern Pennsylvania: Journal of Geodynamics, v. 19, p. 303-324.
Valentino, D. W., and Gates, A. E., 1997, Ductile extensional deformation in the Central Appalachian Piedmont: Geological Society of America Abstracts with Programs, v. 29, p. 87.
Wagner, M. E., and Srogi, L., 1987, Early Paleozoic metamorphism at two crustal levels and a tectonic model for the Pennsylvania - Delaware Piedmont: Geological Society of America Bulletin, v. 99, p. 113-126.
Ward, R. F., 1959, Petrology and metamorphism of the Wilmington Complex, Delaware, Pennsylvania, and Maryland: Bulletin of the Geological Society of America, v. 70, p. 1425-1458.
Whitford, D. J., Nicholls, I. A., and Taylor, S. R., 1979, Spatial variations in the geochemistry of Quaternary lavas across the Sunda arc in Java and Bali: Contributions to Mineralogy and Petrology, v. 70, 341-356.
Wilson, M., 1989, Igneous Petrogenesis: Dordrecht, The Netherlands, Kluwer Academic Publishers, 466 p.
Winchester, J. A., and Floyd, P. A., 1977, Geochemical discrimination of different magma series and their differentiation products using immobile elements: Chemical Geology, v. 20, p. 325-343.
Wyckoff, D., 1952, Metamorphic facies in the Wissahickon Schist near Philadelphia, Pennsylvania: Geological Society of America Bulletin, v. 63, p. 25 - 58.
Yund, R. A., 1983, Diffusion in feldspars, *in* Ribbe, P. H., ed., Feldspar mineralogy: Reviews in Mineralogy, v. 2 , p. 203-222.

ROAD LOG AND STOP DESCRIPTIONS

DAY 2

Mileage		Description
Int.	Cum.	
0	0	Depart hotel parking lot. Turn RIGHT out of parking lot onto Stanton Avenue. Continue about 50 feet to stop sign. Since it is illegal to turn left here, we must turn right and then turn around. Turn RIGHT onto US 322 Business – High Street. Stay to the left; do NOT exit onto US 202 North. Then move to right lane.
0.2	0.2	First traffic light. Turn RIGHT into Parkway Center, make a U-turn, and return to the same traffic light. Get into left lane.
0.1	0.3	Turn LEFT onto 322 Business – High Street, which becomes US 202 South. Stay to the left; do NOT exit onto US 202 North.
1.7	2.0	Intersection of US 202 South and Rt. 926 (Street Road). Note house on the northwest corner (to right) made of serpentinite. This is the same serpentinite used for the external facing stone for many buildings in West Chester, West Chester University, and the University of Pennsylvania. This serpentinite is unusual; most in the area have too many closely-spaced fractures to be quarried for dimension stone. The quarry is located to the west along Rt. 926, and is now a private swim club.
3.1	5.1	Intersection of US 202 South with US 1 (Baltimore Pike; traffic light). Turn LEFT onto US 1 North (Baltimore Pike) – US 322 East.
1.1	6.2	US 322 East splits from US 1 North. Remain on US 1 North (Baltimore Pike).
1.0	7.2	Outcrop of mafic gneiss of the Avondale anticline (Precambrian age?) is visible on the left (northwest) side of US 1.
2.4	9.6	Wawa Corporate Headquarters on the right side of US 1.
0.4	10.0	Railroad bridge over US 1. One of the few on this line NOT damaged or destroyed by Hurricane Agnes (1972).
0.6	10.6	Wawa Dairy on the left side of US 1.
0.8	11.4	Intersection of US 1 North (Baltimore Pike) with Rt. 452 (traffic light). Turn RIGHT onto Rt. 452 South.
0.3	11.7	The old Riddle Farm is on the left, now the Riddlewood development. Mr. Riddle owned Man o' War and his progeny, War Admiral and Whirlaway. The streets of the development are named for his horses. The Lima Granite intrudes units of ultramafic rock beneath this development; contacts are exposed in Chrome Run, the creek that runs through Riddlewood.
0.3	12.0	Intersection of Rt. 452 South with Lenni Road (traffic light). Turn RIGHT onto Lenni Road.
0.9	12.9	Cross railroad tracks and make immediate RIGHT turn onto access road for Lenni

Technical Training Facility (owned and operated by Southeast Pennsylvania Transit Authority). Buses will park in area near Lenni Road. Walk down road to railroad tracks (we'll examine the rocks at the first cut on the return to the buses) and continue past building for about 10 minutes (heading away from Lenni Road) to next outcrops along railroad tracks. These rocks are mapped as Precambrian gneisses of the Avondale anticline, but contain Silurian zircons.

STOP 6. ROSEMONT SHEAR ZONE; SEPTA RAILROAD CUT, LENNI.
Leader: Howell Bosbyshell

Walk down road to railroad tracks of the currently inactive SEPTA Media-West Chester line and continue past the Lenni Technical Training Facility building and yard (heading away from Lenni Rd.) to outcrops along railroad tracks (we'll briefly examine the rocks in the cuts southeast of the training facility before returning to the buses). These rocks are within the Rosemont shear zone on the southeastern margin of the Avondale massif.

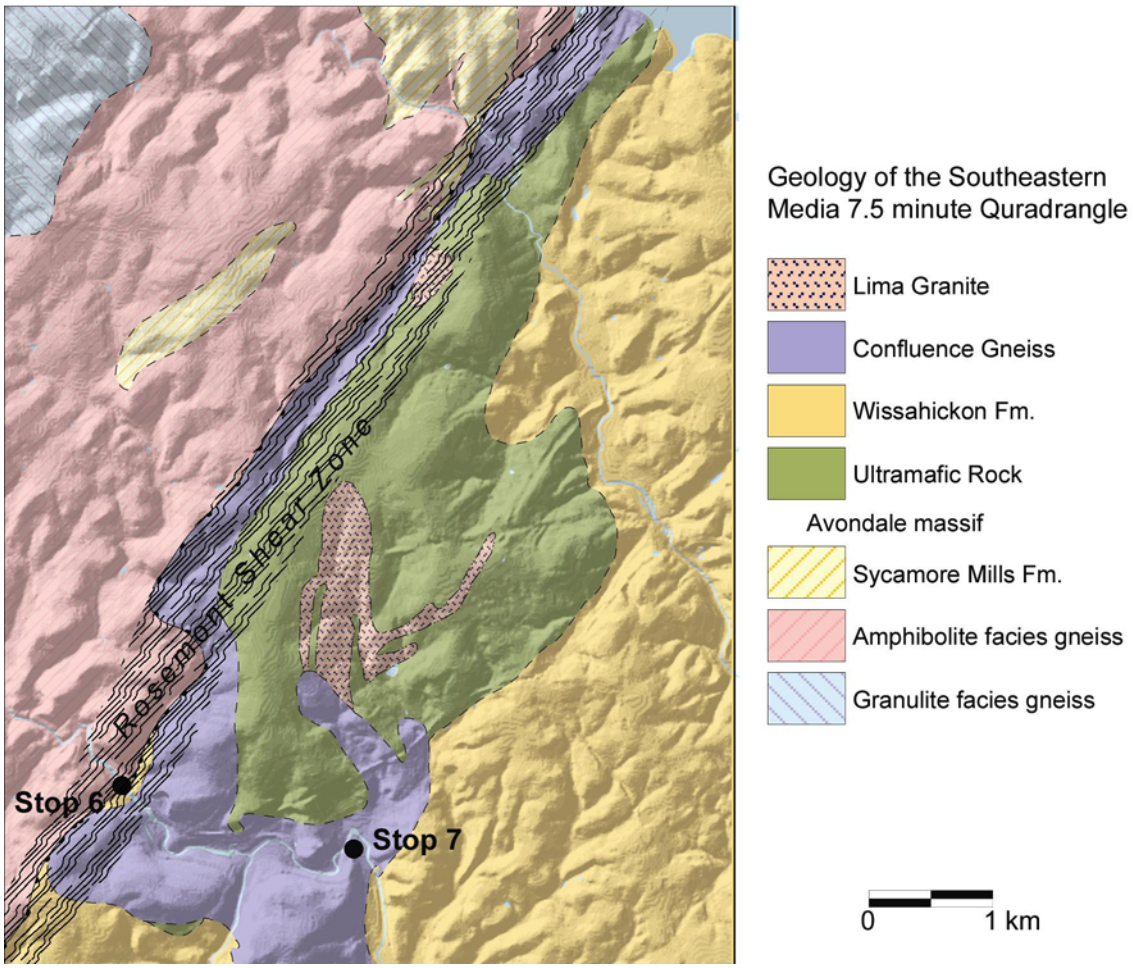

Figure 26. Geologic shaded-relief map of the area near the Rosemont shear zone in the southern Media quadrangle.

The Rosemont Shear Zone

This stop examines the Rosemont shear zone, the contact between rocks of the Avondale massif (Laurentia?) to the northwest and ultramafic rocks and orthogneiss of the Wilmington Complex and the Wissahickon Formation to the southeast. In the Media 7.5 minute quadrangle this contact is expressed as a well-defined topographic lineament along the western margin of the Lima

ultramafic body (figure 26). The Rosemont shear zone was originally mapped as a brittle fault (Armstrong, 1941; Weiss, 1949), but has since come to be regarded as a ductile shear zone (Valentino *et al*., 1995).

Numerous investigators have assessed the movement history and tectonic significance of the Rosemont shear zone along its length. Early workers (Armstrong, 1941; Weiss, 1949) describe the structure as a high angle reverse fault. Amenta (1974) and Tearpocke and Bischke (1980) also describe vertical motion and related movement in the Rosemont shear zone to the formation of the dominant fold set along Wissahickon Creek in Philadelphia. Tearpocke and Bischke (1980) suggested that the Rosemont is the root zone for northwest dipping nappe-style folds and possibly a suture zone, based on the presence of ultramafic rock along its trace. Valentino *et al*. (1995) described shallowly plunging lineations in the Rosemont shear zone and proposed that the most recent displacements were dextral strike-slip. Hager and Thompson (1975) and Valentino *et al*. (1995) also proposed that the Rosemont zone continues to the southwest along the western margin of the Wilmington Complex in Delaware. Bosbyshell (2001) concluded that the most recent ductile motion was vertical, with a dextral component. Rock on the southeast side, the Wilmington Complex and Wissahickon Formation, moved down and to the southeast relative to the Avondale massif. Electron microprobe monazite ages from pelitic mylonite at Stop 6 indicate that this motion is no older than Devonian (~388 Ma; Bosbyshell, 2001).

The most recent ductile deformation along the Rosemont Fault is preserved in outcrop scale and larger shear zones, which are characterized by mylonitic rock that experienced almost complete syn-tectonic recrystallization and under M3 metamorphic conditions. Just prior to reaching the first series of outcrops and railroad cuts, the railroad bed crosses a valley drained by an unnamed tributary to Chester Creek. This valley is marks the trace of the Rosemont Fault and here is underlain by a sliver of pelitic mylonite, assigned to the Wissahickon Formation. The contact between this pelite and Avondale gneiss is exposed in a very small outcrop in the stream. Pelitic rock is also exposed along the Rosemont Fault southwest of Stop 6 in an old quarry and road cut on Valley Brook Road (Pa. Route 261). In the Valley Brook Road cuts, much of the rock is migmatitic and is characterized by the M2 sillimanite-bearing, high temperature mineral assemblage. The generally shallow to moderately dipping foliation is cut by several meter wide vertical shear zones which also experienced complete recrystallization and contain the M3 assemblage. Similar shear zones are also present in the Confluence Gneiss and we will view several of these at Stop 7. Additional structural details will be discussed at Stop 7.

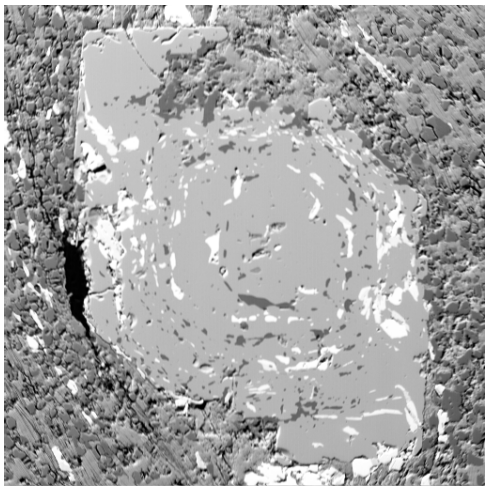

Figure 27. Back scattered electron image of syn-tectonic garnet neoblast in mylonite. Field of view = 0.46mm. Note extremely fine grain size of matrix, due to intense ductile deformation.

Metamorphism

Pelitic mylonite yields considerable data on the metamorphic conditions and timing of the most recent ductile motion in the shear zone. In high grade pelitic rocks the main Ca-bearing phases are garnet and plagioclase. The distribution of Ca in these minerals is controlled by the pressure sensitive reaction:

3 anorthite = grossular + 2 aluminosilicate + quartz.

This is the well known GASP geobarometer (e.g., Koziol and Newton, 1988), with the reaction proceeding to the right with increasing pressure. Garnet in mylonite occurs as small (100 - 500 μm) syn-tectonic neoblasts (figure 27) and as relict M2 porphyroclasts (figure 28). Variation in Ca content in garnet

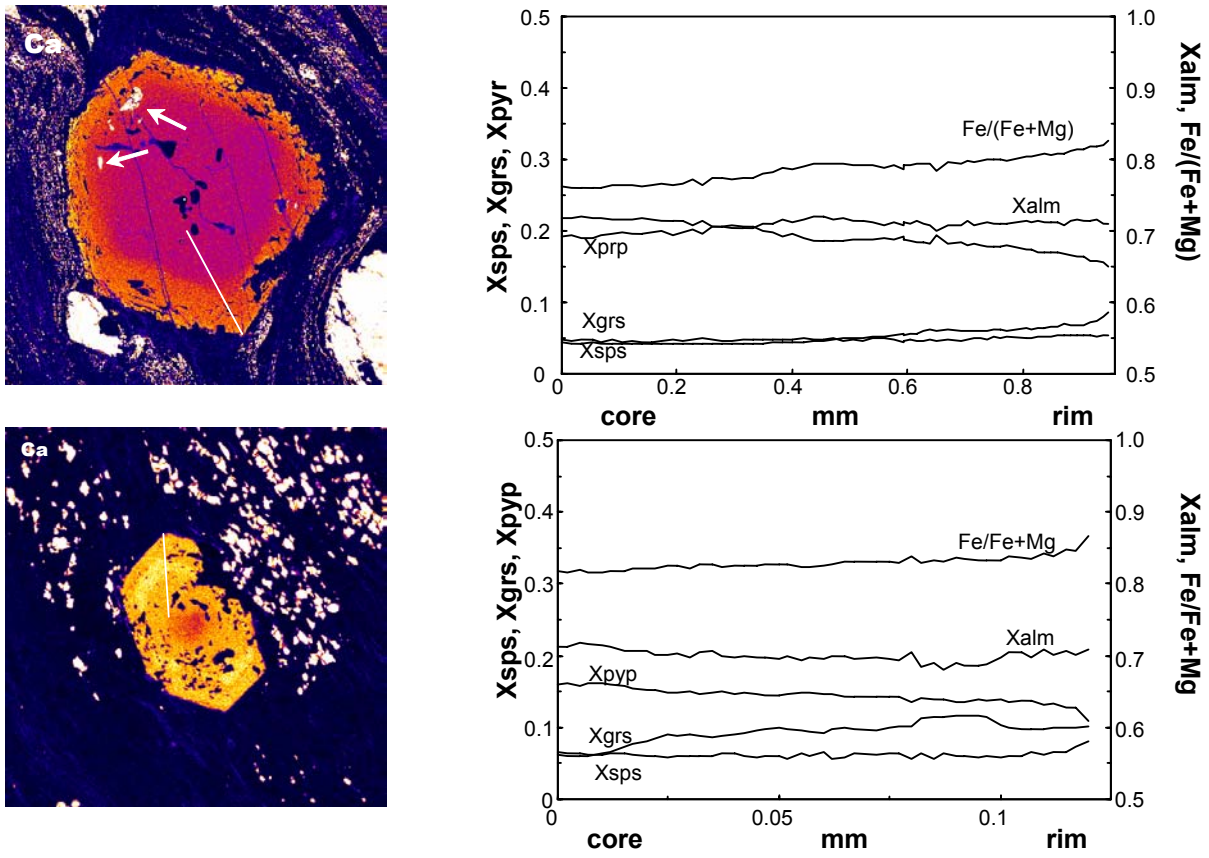

Figure 28. Ca X-ray composition maps and compositional zoning profiles of Wissahickon Formation garnet in the Rosemont shear zone. A, Relict M2 porphyroclast, field of view = 3.6mm. B, syn-tectonic neoblast, field of view = 0.51mm. White line is path of traverse; "hotter" color indicates greater concentration.

and plagioclase result from the difference in pressure between M2 and M3. Ca zoning in neoblasts is complex. Ca content is low in the small core, increases to a maximum zone, then decreases slightly at the rim (figure 28). The Ca content in the outer rims of the neoblastic garnet is approximately the same as the highest Ca content in the rim of larger garnet porphyroclasts (figure 28). Plagioclase exhibits a corresponding decrease in Ca content, from An_{44} in the core of M2 porphyroclasts, An_{39} in inclusions near the rim of garnet porphyroclasts (figure 28) to An_{37} in the recrystallized, fine grained mylonitic matrix.

Bosbyshell (2001) estimated pressure and temperature conditions using the garnet-aluminosilicate-plagioclase (GASP) geobarometer (Koziol and Newton, 1988) and garnet-biotite thermometry (Holdaway *et al*., 1997). The composition of garnet and plagioclase cores from samples outside shear zones were used in calculations to estimate M2 conditions, as these most likely approach the equilibrium composition at the time of maximum temperature. To minimize the effects on thermobarometric calculations of Fe–Mg diffusional exchange between garnet and biotite during cooling and retrogression, the composition of matrix biotite not in contact with garnet was used. The results of the calculations appear in figure 29. Calculations to estimate pressure-temperature conditions during M3 were performed on two shear zone samples, from an outcrop of Wissahickon Formation near Stop 7 and from the mylonite at Stop 6, using the composition of high Ca garnet rims (Stop 7 sample), and with the composition of the outer rim of the M_3 garnet neoblasts (Stop 6). The composition of fine-grained plagioclase and biotite in the mylonitic matrix of both samples was also used. In spite of differences in garnet and plagioclase composition between the

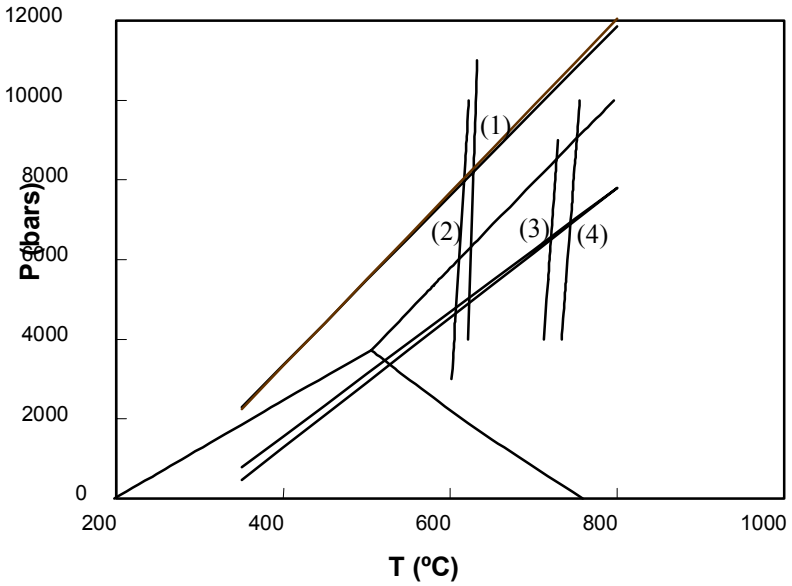

Figure 29. Results of thermobarometry near the Rosemont Fault. Curves with moderate slopes are the reaction 2 an = grs +2 ky + qtz (GASP), using the calibration of Koziol and Newton (1988); those with steep slopes are Fe-Mg exchange between garnet and biotite after Holdaway *et al*. (1997). Intersections 1 and 2 are from samples within S_4 shear zones (and give M3 conditions); intersections 3 and 4 are from outside shear zones (M2).

two samples, the results are quite similar (figure 29) and are in close agreement with other Chester Creek samples (Bosbyshell, 2001).

Monazite geochronology

Monazite from the pelitic mylonite at Stop 6 exhibits multi-stage growth zoning indicative of the complex metamorphic history described above (figure 30) (Bosbyshell, 2001). Nearly every monazite analyzed has an outer core that yields a Devonian age; the average of 24 analyses on five grains is 384 ± 6 Ma. Figure 31 shows a typical monazite grain from this sample. Monazite is typically elongate parallel to foliation. It is possible that deformation is younger than the monazite grains and the monazite rotated parallel to foliation during deformation. However, given the abundant evidence for syn-tectonic recrystallization, it is likely that monazite growth was synchronous with deformation. In either case, deformation can be no older than Devonian. Some grains exhibit narrow rims which yield Mississippian ages, but these are not considered reliable due to the low concentration of Pb in this part of the monazite.

Avondale Massif

Gneiss of the Avondale massif is exposed in the railroad cuts on the west side of the valley. This unit consists of medium to coarse grained, heterogeneous gneiss. The most common lithologies are of intermediate composition; however, both mafic and felsic rocks are present and interlayered at a scale too small to be depicted at typical map scale. Gneissic fabric is defined by aligned biotite and hornblende and by cm- to m-scale compositional layering, including migmatite leucosome. The intermediate gneiss consists of biotite, hornblende, plagioclase, garnet, quartz, and magnetite, with orthopyroxene, clinopyroxene, potassium feldspar, sphene, and/or epidote present at some locations. The relative abundance of the main minerals is variable; in some rocks the hornblende content exceeds that of biotite; garnet is the most abundant mineral in others. Mafic gneiss is foliated and lineated and consists primarily of hornblende and plagioclase with subordinate biotite, epidote, garnet, clinopyroxene, sphene, and/or quartz. Felsic gneiss is generally coarse grained and is composed of plagioclase, quartz, potassium feldspar (typically microcline), biotite, hornblende and garnet.

The Avondale massif was mapped as Precambrian Baltimore Gneiss by Bascom *et al.* (1909), though on the Philadelphia folio this particular location is shown as underlain by Wissahickon Gneiss. Following Bascom *et al.* (1909), the Avondale has since been regarded as basement gneiss, either Laurentia (Wagner and Srogi, 1987) or rifted microcontinental fragment (Faill, 1997a). Based on discordant zircon analyses (Grauert *et al.*, 1973; 1974), with a Proterozoic upper intercept and a Paleozoic lower intercept, metamorphism in the Avondale massif was thought

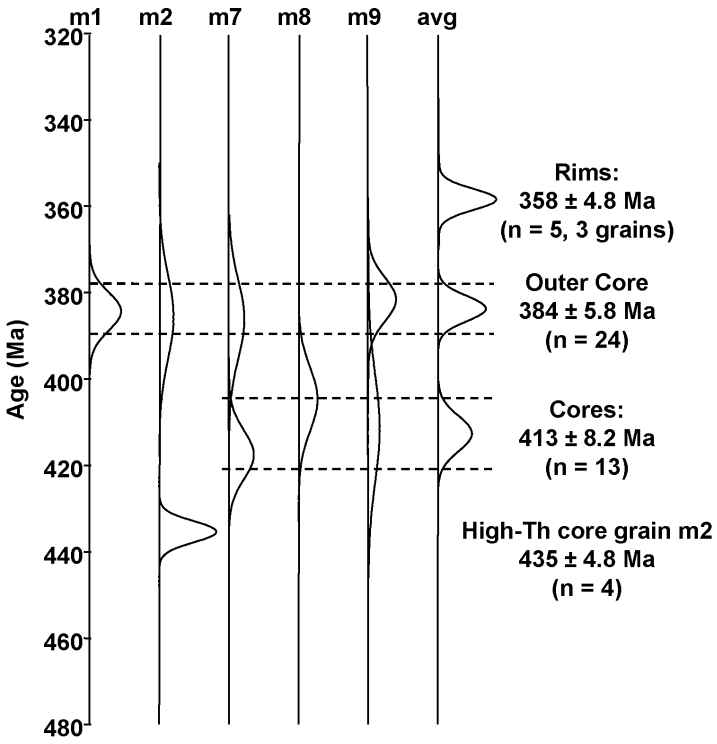

Figure 30. Wissahickon Formation mylonite at Stop 6. Electron microprobe chemical age results. The curves in this figure are normal distributions about the mean of multiple measurements within age domains of individual monazite grains, with 1σ equal to the standard error of the mean. Errors are reported at the 95% confidence level. Where multiple grains in a sample yield the same result, the reported age is the weighted mean of the ages from the individual grains. Errors associated with the weighted means were calculated using Isoplot/Ex (Ludwig, 1999) and are also reported at the 95% confidence level.

to be Grenvillian, with considerable Paleozoic overprinting. Recent geochronological data, from a sample collected in the railroad cut on the southwestern side of the railroad tracks, raises questions about this interpretation. Aleinikoff (unpublished data) describes a small, somewhat heterogeneous zircon population unlike typical Grenville rocks, which yield a Silurian age (420 ± 5Ma). The analyzed zircon was both equant and elongate in morphology and displayed oscillatory zoning indicative of igneous origin. However, given that only a single sample has been analyzed at present, and the small, heterogeneous zircon population it contained, it is not possible to draw significant conclusions at this time (John Aleinikoff, personal communication).

Walk back, southeast along the railroad tracks towards the buses. Stop briefly to examine the outcrops southeast of the training facility.

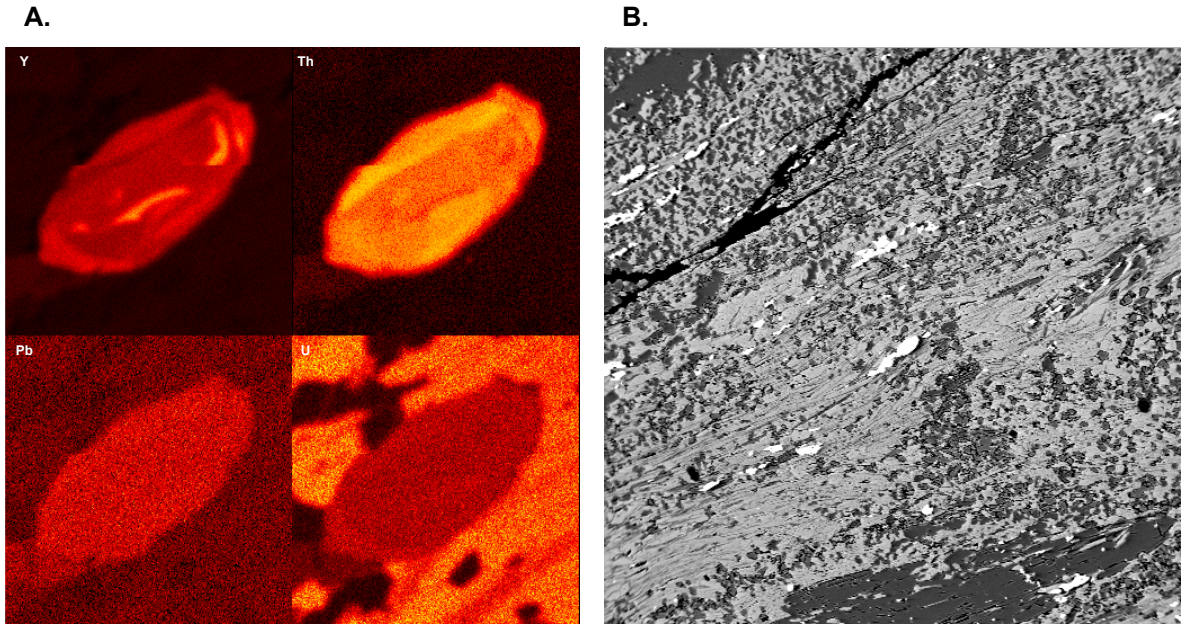

Figure 31. Monazite from pelitic mylonite. A, X-ray composition maps of monazite grain m1. FOV = 64μm. B, BSE image showing occurrence of this grain (arrow) parallel to mylonitic foliation.

Confluence Gneiss

The rocks in the outcrops southeast of the training facility and in the Lenni quarry (which we won't inspect today), are orthogneiss of the Confluence Gneiss, a unit considered to be part of the Wilmington Complex. The unit is so named because of the many outcrops that occur here, in the area near the confluence of the West and Main Branches of Chester Creek. We will discuss the Confluence Gneiss in detail at Stop 7.

		Return to the buses. Depart parking area at Stop 6 and turn LEFT onto Lenni Road.
0.9	13.8	Intersection of Lenni Road and Rt. 452. Sharp RIGHT turn onto Rt. 452.
0.8	14.6	Cross bridge over Chester Creek, enter Aston Township, and immediately turn RIGHT onto Mount Road.
0.1	14.7	Turn LEFT into the Novotni Brothers quarry. Buses will park here as we look at the rocks in the quarry.

STOP 7. CONFLUENCE GNEISS AT NOVOTNI BROTHERS PAVING COMPANY

Leader: Howell Bosbyshell

This stop (figure 32) examines an old quarry in the Confluence Gneiss, a unit considered to be part of the Wilmington Complex. The Confluence Gneiss is heterogeneous gneiss, consisting of hornblende plagioclase quartz biotite granofels, interlayered mafic, felsic, and intermediate orthogneiss, and several large amphibolite bodies (Bosbyshell, 2001). This unit is contiguous with the Brandywine Blue gneiss of the Wilmington Complex (Plank *et al*., 2000a), but shares many characteristics with the Rockford Park Gneiss (also part of the Wilmington Complex), including the scale of layering and the boninitic affinity of some mafic rocks. An Ordovician age is inferred from zircon ages of the Brandywine Blue Gneiss (476 ± 6 Ma) and Rockford Park Gneiss (476 ± 4 Ma) (Aleinikoff *et al*., 2001). Zircon from the Springton Tonalite, which crops out along the trend of the Rosemont Fault approximately 7 km from Stop 6, also yielded an identical Early Ordovician age, 476 ± 4 Ma (John Aleinikoff, unpublished data).

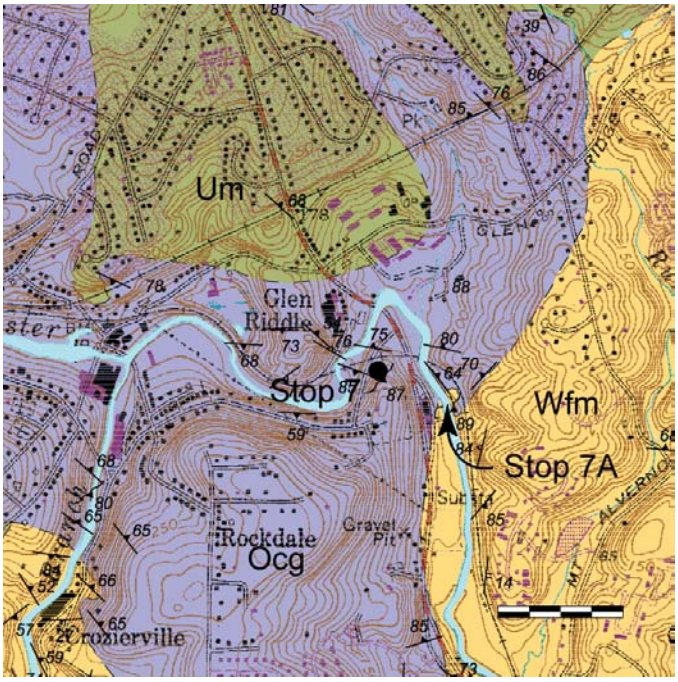

Figure 32. Geologic map of southern Media quadrangle showing location of Stop 7 and 7A. Scale bar is 400m. Ocg: Confluence Gneiss; Wfm: Wissahickon Formation; Um: ultramafic rock.

Geochemistry

Geochemically, the Confluence Gneiss is similar to modern volcanic arc rocks (figure 33). Intermediate gneiss resembles andesite or the intrusive equivalents, diorite, tonalite or granodiorite. Mafic layers are basaltic (figure 33.C, D), and some are geochemically similar to modern boninites (figures 33, 34), rocks that occur almost exclusively in fore arcs. Boninitic amphibolite layers are also present in the Wissahickon Formation, at the contact with the Confluence Gneiss in an outcrop

approximately 400m from Stop 6; these boninitic amphibolites are collectively referred to as the Confluence Dikes.

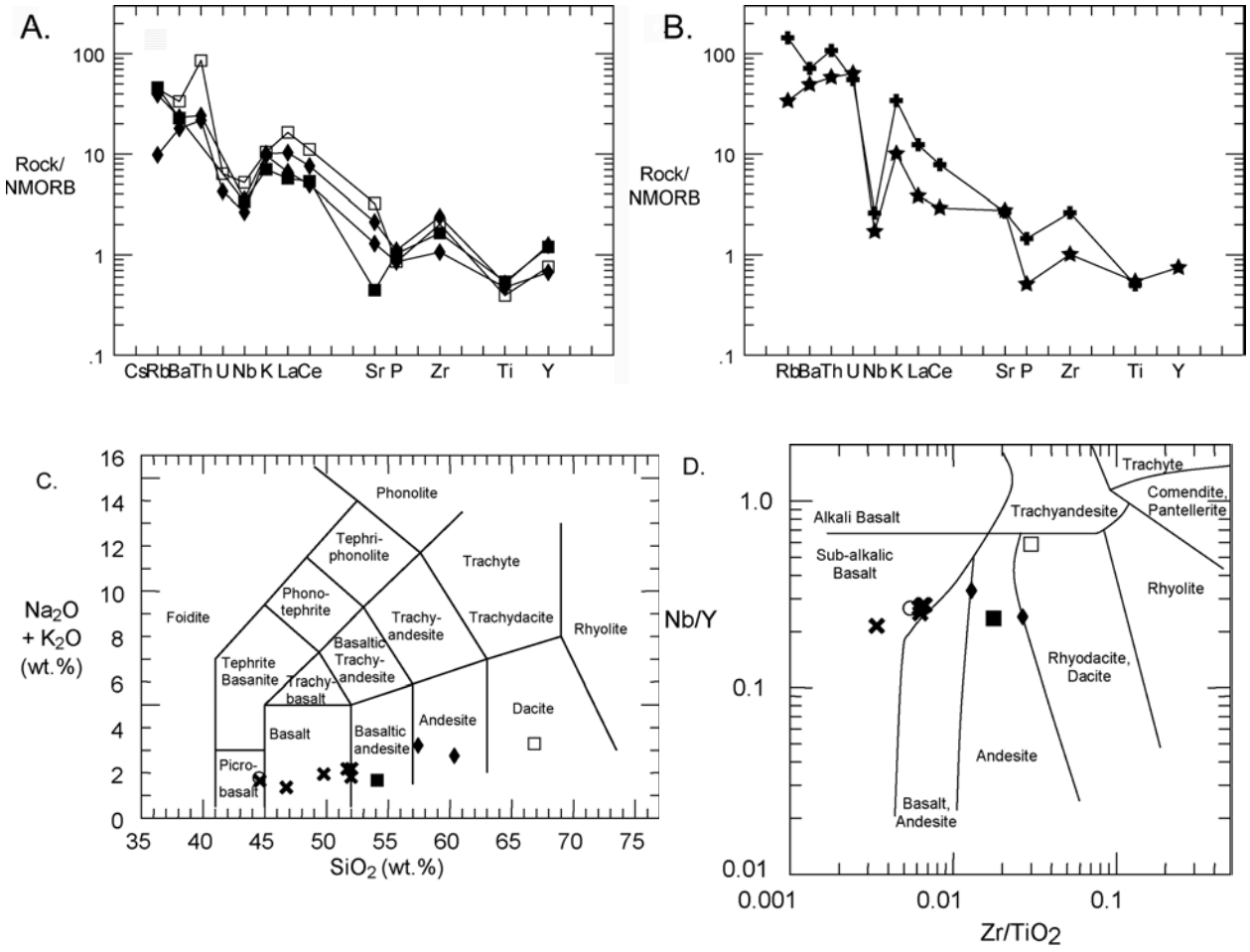

Figure 33. **A,** N-MORB normalized (after Sun and McDonough, 1989) trace element diagram illustrating range of composition of intermediate rocks. **B,** modern calcalkaline series volcanic arc rocks for comparison. Calcalkaline dacite, filled plus sign, Sunda arc (Whitford *et al*., 1979); calcalkaline andesite, filled star, Honshu arc (Gust *et al*., 1997). **C,** igneous rock classification diagram using total alkalis vs. silica after LeBas *et al*. (1986), with data from study area (Bosbyshell, 2001). **D,** igneous rock classification diagram using immobile trace elements (Winchester and Floyd, 1977) with data from study area. Diamonds, Confluence Gneiss: x's, Confluence dikes; open circle, open square, filled square, possibly related rocks from the Chester Park Gneiss (Stop 8).

Given the geochemical similarities that the Confluence dikes and Rockford Park Gneiss share with modern boninites, it is reasonable to infer that the mantle source and tectonic setting required to produce these basaltic magmas are similar to the source and tectonic setting of western Pacific boninites. Numerous authors have investigated boninite magma petrogenesis (Crawford *et al*., 1981; Jenner, 1981; Hickey and Frey, 1982; Cameron *et al*., 1983; Bloomer and Hawkins, 1987; Beccaluva and Serri, 1988; Crawford *et al*., 1989). They conclude that boninites are hydrous melts of previously melted mantle peridotite that has been metasomatically enriched in LREE and large ion lithophile elements prior to or during melting. The enriching component could be either fluid or melt derived from a subducting slab, melt from a less depleted, OIB-like mantle source, or both (Hickey and Frey, 1982; Cameron *et al*., 1983; Bloomer, 1987; Crawford *et al*., 1989).

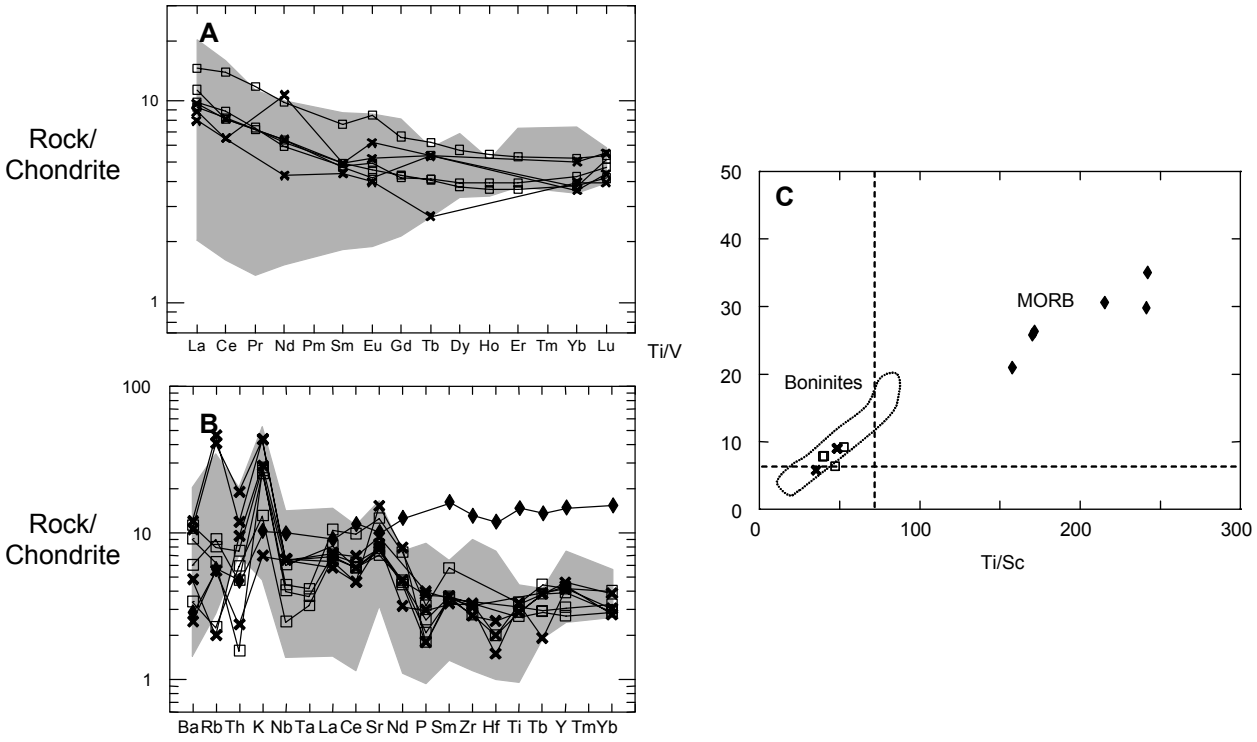

Figure 34. **A,** Chondrite normalized REE abundances in boninitic rocks, normalization factors after Sun and McDonough (1989). X's = Confluence dikes, open squares = Rockford Park Gneiss. Shaded area corresponds to REE abundance of western Pacific boninites with Mg # similar to study area rocks. **B,** Chondrite normalized abundances of trace elements in boninitic rocks, normalization factors after Thompson (1982). Symbols as in A, filled diamond = MORB, values after Pearce (1983), with the following exceptions: Th, La, Nd, Eu, from Bevins *et al*. (1984). **C.** Variation of incompatible/compatible element ratios, Ti/V and Ti/Sc, in Confluence dikes (X's), Rockford Park Gneiss (open squares), selected western Pacific boninites (dashed field), and MORB (diamonds). Dashed lines are chondrite values from Wood *et al*. (1979). MORB data are from Schilling *et al*. (1983), Boninite data from Jenner (1981), Hickey and Frey (1982), Bloomer (1987), Bloomer and Hawkins (1987), Cameron *et al*. (1983), Cameron (1989), and Falloon *et al*. (1989)..

The primary geodynamic constraint on the generation of boninitic magma is a steep geothermal gradient required to achieve sufficiently high temperatures to melt depleted peridotite at relatively shallow levels. Though it may be theoretically possible for these conditions to be met in zones of continental rifting or sea-floor spreading (Crawford *et al*., 1989), there is general agreement that recent boninites are the product of subduction-related magmatism. Several models have been advanced to explain the steep geothermal gradient including: (1) initiation of subduction (Cameron *et al*., 1979; Stern and Bloomer, 1992), (2) intra-arc rifting (Crawford *et al*., 1983; (3) subduction of an active spreading center (Cameron, 1989) and (4) sea-floor spreading in a forearc basin (Bedard *et al*., 1998).

The Wilmington Complex has long been considered to comprise the roots of a volcanic arc (Crawford and Crawford, 1980; Crawford and Mark, 1982; Wagner and Srogi, 1987). Though Wagner and Srogi (1987) preferred an arc interpretation, their geochemical results could not limit the igneous rocks there to an arc environment. The recognition of boninite-like magmas

(Bosbyshell, 2001; Plank *et al*. 2001), constrains the Wilmington Complex to a subduction-related tectonic setting.

Metamorphism

Unlike much of the Wilmington Complex, which experienced granulite facies metamorphism, the Confluence Gneiss contains mineral assemblages characteristic of the amphibolite facies: hornblende + plagioclase ± quartz ± biotite ± garnet ± epidote. Orthopyroxene is present in some rocks to the west of Stop 6 in outcrops along the West Branch of Chester Creek, suggesting that granulite facies conditions were achieved at least locally in the Confluence Gneiss. The age of metamorphism in the Confluence Gneiss has not been determined directly, but is inferred to be Silurian, based on zircon and monazite ages from other Wilmington Complex rocks (~428 Ma; Aleinikoff *et al*., 2001) and monazite ages from adjacent Wissahickon Formation (~438 Ma; Bosbyshell, 2001). Garnet is found in and adjacent to S4 shear zones, suggesting that garnet bearing assemblages may have formed during Devonian M3 metamorphism (Bosbyshell, 2001; Kellogg *et al*., 2001).

Structural geology

Multiple episodes of deformation are evident here. A large synform is visible on the NE-SW trending quarry face (parallel to Mount Rd.). This fold and the many related minor folds deform an older metamorphic foliation and so are part of at least the second episode of deformation to have affected these rocks. The dominant foliation here strikes approximately east-west and is parallel to the axial planes of these folds. Close inspection of the folds indicates that some degree of refolding has occurred, with the axial surface of the younger folds approximately parallel to that of the first. Whether this represents progressive deformation during a single deformation event or discreet deformation episodes cannot be determined. On the horizontal surface at the north end of the quarry wall doubly closed folds suggest sheath fold geometry. This may be the result of differential transport along axial surfaces during the refolding (figure 35).

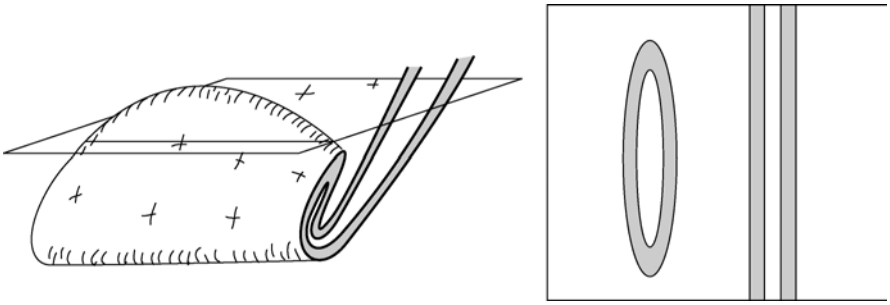

Figure 35. Sketch of possible style of refolding of folds at Stop 7 and resulting map pattern.

Several shear zones, which cross cut the fold set and dominant foliation described above, are visible in the other quarry wall (figure 36). Many similar shear zones occur along and near the trace of the Rosemont Fault. These shear zones strike approximately 030 and are parallel to the trace of the Rosemont Fault, the eastern margin of the Avondale massif and the boundary between arc-related rocks of the Wilmington Complex and Wissahickon Formation. The shear zones are characterized by a moderately to steeply plunging lineation defined by aligned hornblende crystals and sheath fold axes (figure 37A). Folded foliation at shear zone margins (figure 37B) and fabric asymmetry (figure 38) indicate east-side down motion with a dextral strike-slip component (Bosbyshell, 2001; Kellogg *et al*., 2001).

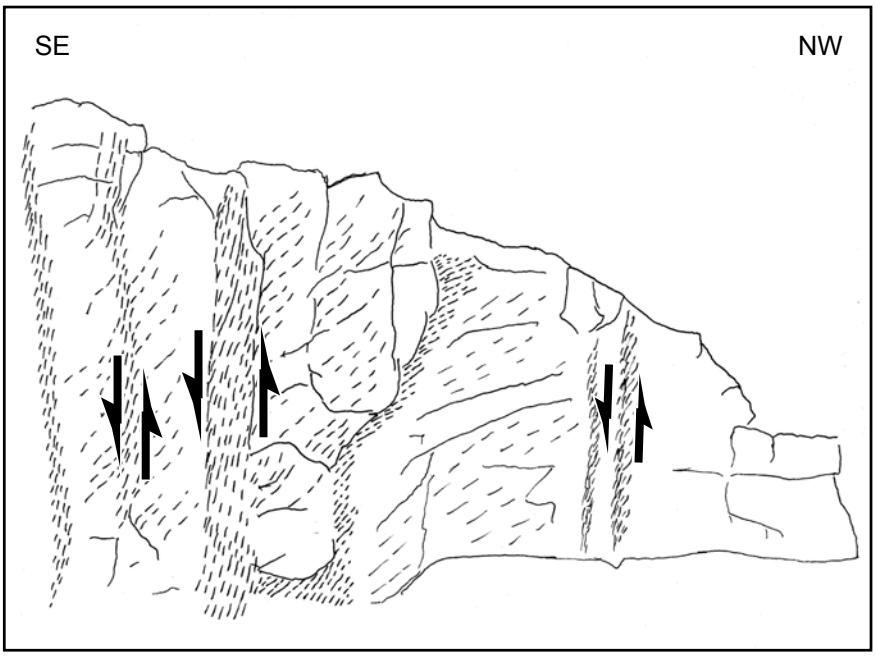

Figure 36. Sketch of shear zones in northeast facing quarry wall (Kellogg *et al*., 2001).

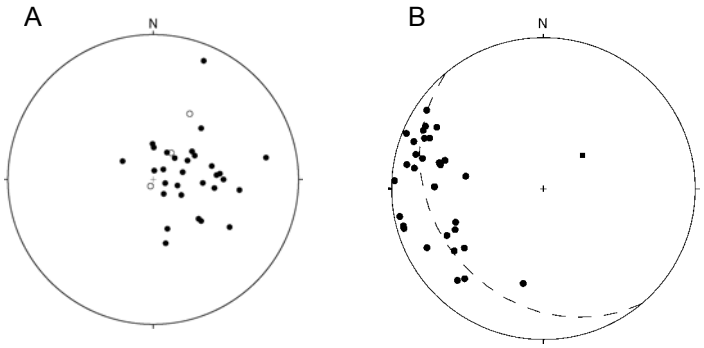

Figure 37. Equal area plots of structural elements at Stop 6. A, Filled circle, long dimension of hornblende grains; open circle, axes of sheath fold. B, π-diagram illustrating rotation of foliation at shear zones. Filled circle pole to foliation; dashed great circle, best-fit girdle; square, π-pole.

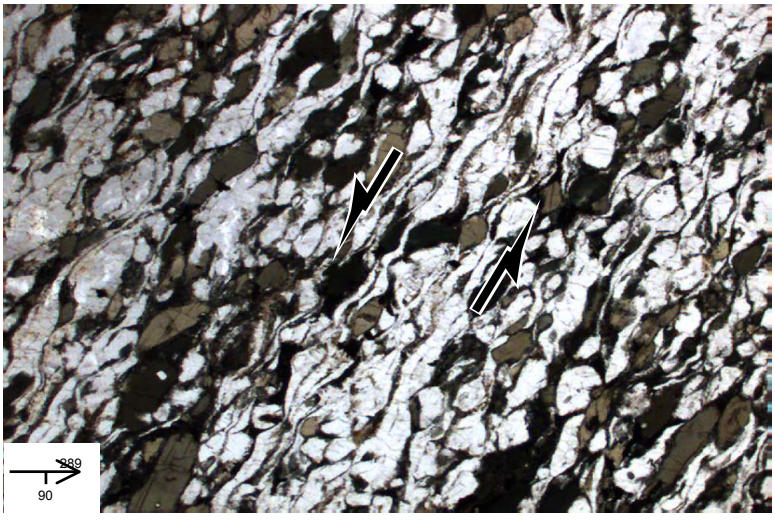

Figure 38. Photomicrograph of mylonitic rock in shear zone (Kellogg et al., 2001). Note orientation in lower left; fabric asymmetry indicates east-side down.

At first glance, the shear zones may appear to be brittle structures, due to intense weathering of the well defined, planar, shear zone foliation. However, petrographic analysis of shear zone mylonitic rock reveals microstructures in plagioclase feldspar, such as glide twinning, undulose extinction, deformation bands, subgrain formation and evidence for recrystallization via bulge nucleation, which are characteristic of deformation under amphibolite facies conditions. Similar shear zones in metapelitic rock contain kyanite, indicating that deformation was synchronous with M3 high pressure overprinting.

VIRTUAL STOP 7A.

The contact between the Confluence Gneiss and the Wissahickon Formation is exposed just across Chester Creek, approximately 400m from the Novotni Brothers facility. Unfortunately, this outcrop cannot accommodate a group of this size, so it is described here. If you have interest in visiting these exposures please note this is private property; obtain permission from King's Mill banquet facility before visiting these outcrops. The first railroad cut (figure 39) exposes Confluence Gneiss that we see here at Stop 7. Boninitic mafic layers, the Confluence Dikes, are also present here. The mafic layers are concordant with and stretched parallel to the dominant metamorphic foliation in the host rocks, thus they were present prior to the deformation that produced this foliation. In some places, notably a boulder on the side of the tracks opposite the cut, a thin layer of leucocratic rock, consisting of anhedral quartz, tabular plagioclase, and a small percentage of euhedral hornblende, is present along the margins of the mafic layers suggesting that some partial melting took place at the time of intrusion.

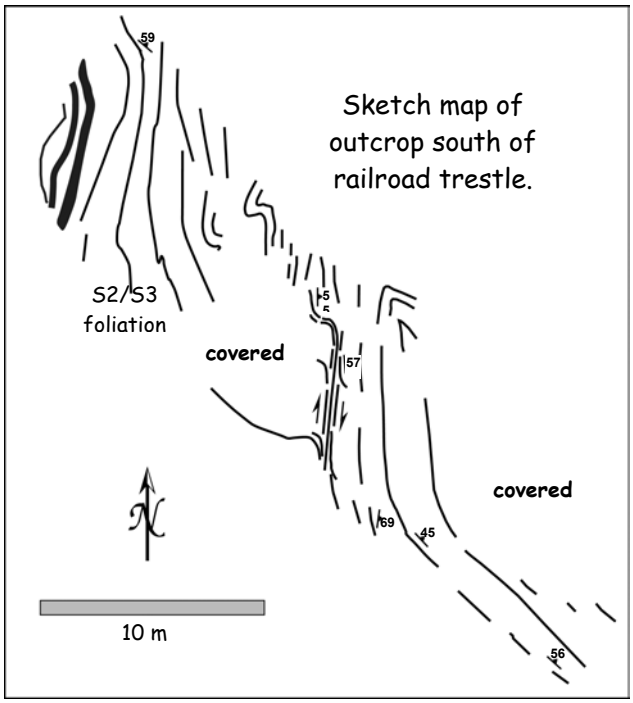

Figure 39. Sketch map of first outcrop at Virtual Stop 7A, showing location of boninitic dikes at NW end of outcrop and S4 shear zone near center of outcrop.

At the northwestern end of the next outcrop, (below tracks, just above creek level) is a small exposure of Confluence Gneiss. Though the contact is covered, pelitic gneiss of the Wissahickon Formation crops out just SE of this exposure (figure 40). The dominant metamorphic foliation in this rock is defined compositional layering of leucocratic, quartzo-feldspathic domains and micaceous domains consisting of aligned biotite and sillimanite, and garnet; an M2, high temperature-low pressure metamorphic mineral assemblage. Because this dominant foliation is parallel to the axial planes of isoclinal folds it is termed S2, a D2 structural element. S1 is the folded foliation in the hinge of the isoclinal folds. These folds are in turned folded by close to tight and locally isoclinal F3 folds; the axial planes of these folds are S3 (figure 41).

A thin (<1m thick) mafic layer is present near the northwest end and also in the center of the outcrop. This layer is identical in composition to the boninitic layers within the Confluence Gneiss.

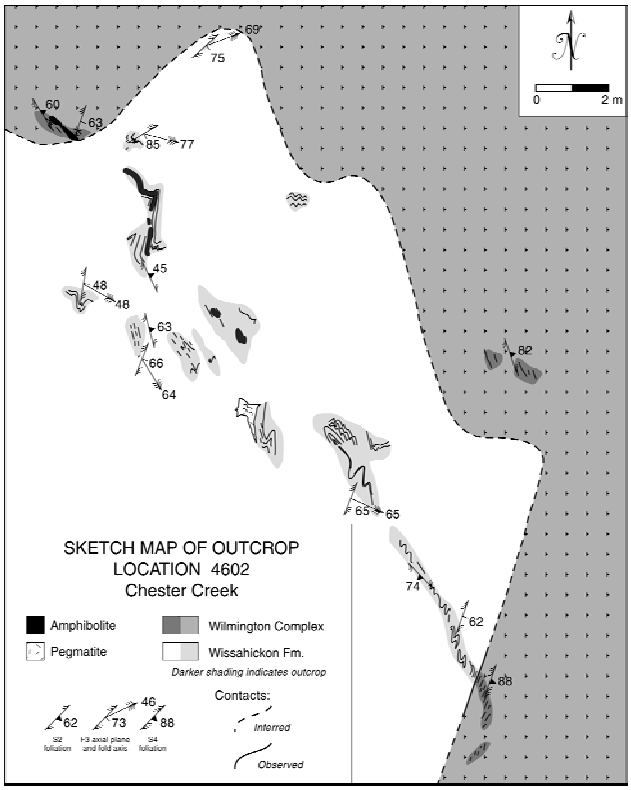

Figure 40. Sketch map of second series of outcrops at Stop 7A.

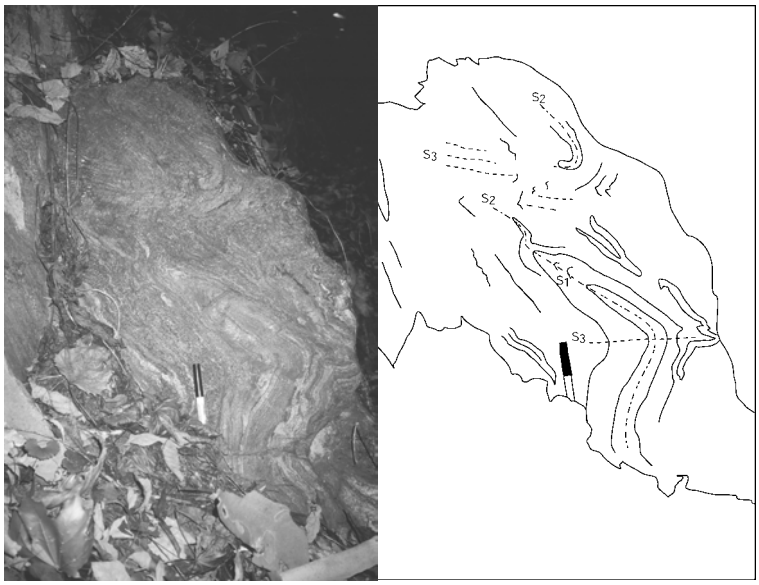

Figure 41. Photograph and sketch of Wissahickon Formation outcrop at King's Mill showing an F2 isoclinal fold refolded by F3. S1 is present in hinge of f2 isoclinal folds, S2 is parallel to F2 axial planes, S3 is parallel to F3 axial planes. Vertical face, view is towards the NE, cap of marker is approximately 5 cm long.

This mafic layer is concordant with and attenuated within the S2 foliation and folded by F3 folds, demonstrating that the dike can be no younger than the deformation responsible for the S2 foliation. Since the boninitic layers are present in both the Wilmington Complex and Wissahickon Formation, it follows that the contact between these units also predates this deformation. The boninitic layers have not been dated directly, but assuming they are the same age as the Rockford Park Gneiss (where geochemically similar boninitic rocks occur), then this contact can be no younger than the early Ordovician age (476 ± 4 Ma: Aleinikoff, *et al.*, 2001) of the Rockford Park Gneiss.

At the southeast end of the outcrop all the structures described above are deformed by a sub-vertical, northeast trending shear zone. This shear zone is similar in orientation and exhibits the same sense of motion as the shear zones at Stop 6 and all are thought to be the same generation of structures, D4 (figure 24), the shear zone foliation is S4. Most of the pelitic gneiss here contains the sillimanite-bearing M2, high temperature low-pressure mineral assemblage, but the shear zone contains the kyanite-bearing M3, higher pressure assemblage. The lighter colored rock on the southeast side of the shear zone is the Confluence gneiss, thus the shear zone folds the contact at this location. This is the only known exposure of the contact between the Wilmington Complex and Wissahickon Formation.

		Return to buses. Depart Novotni Bros. quarry. Turn RIGHT onto Mount Road.
0.1	14.8	Intersection of Mount Road with Rt. 452 (stop sign). Turn RIGHT onto Rt. 452 South.
0.2	15.0	Old mill on the left is now a banquet hall. Outcrop of Mt. Cuba Wissahickon and Wilmington Complex Gneiss with intrusive boninitic dike is located on hill behind the old mill.
0.5	15.5	Outcrops of Mt. Cuba Wissahickon on right side of Rt. 452.
0.5	16.0	The hill on the left side of Rt. 452 is underlain by anthophyllite-rich ultramafic rocks. Keep to left as you come up to a large intersection.
0.6	16.6	Five-points intersection of Rt. 452 South with Concord Road, Knowlton Road, and Pennell Road (traffic light). Turn the most extreme LEFT onto Knowlton Road.
0.6	17.2	Turn LEFT into the entrance for the Pyramid Materials. Look for the sign on the left side of Knowlton Road just before the quarry entrance. Proceed up lane onto quarry grounds and park.

STOP 8. ARC WISSAHICKON AT PYRAMID MATERIALS
Leader: Howell Bosbyshell

At Stop 8 (figure 42) we will examine the Arc Wissahickon, part of the Mt. Cuba forearc accretionary complex. Here the rock is pelitic and psammitic gneiss and is composed of biotite, garnet, sillimanite, plagioclase, orthoclase, and quartz, the high temperature-low pressure M_2 assemblage. Much of the rock is migmatite with abundant leucocratic segregations 1-2 cm thick with larger pegmatite lenses.

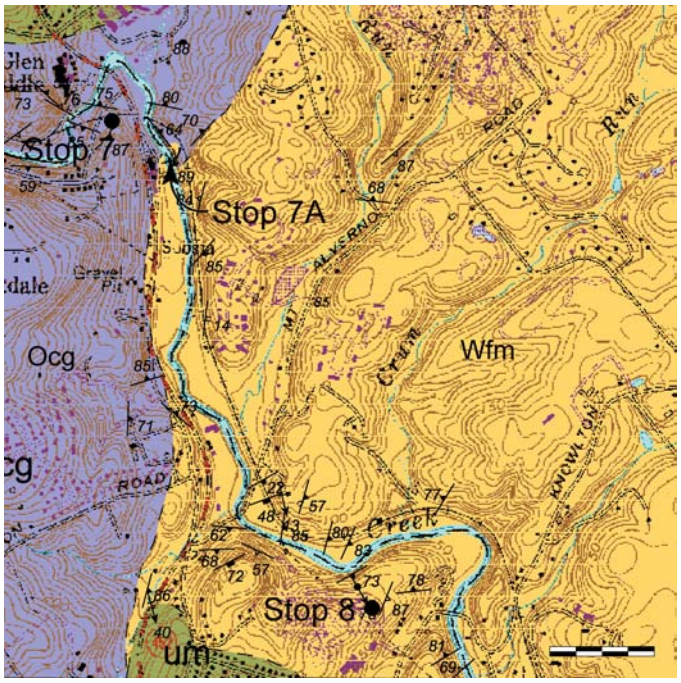

Figure 42. Geologic map of southern Media quadrangle showing location of Stop 8. Scale bar is 400m. Ocg: Confluence Gneiss; Wfm: Wissahickon Formation.

A pegmatitic leucocratic dike one to two meters thick, consisting mainly of plagioclase and quartz with minor biotite and xenocrystic garnet, was formerly exposed in the quarry. Boulders of this rock and a small exposure in one wall are still present. This dike is remarkable in that it contains small xenoliths of ultramafic rock consisting mostly of chlorite and talc.

Metamorphism

The rocks at Stop 8 contain the M2 high temperature-low pressure mineral assemblage sillimanite + biotite + orthoclase + quartz + plagioclase + garnet. Prismatic sillimanite up to several millimeters long occurs in addition to fibrolite. In a few samples intergrowths of pale green biotite (which contains virtually no Ti) and sillimanite or kyanite are present. These intergrowths are interpreted as pseudomorphs after cordierite, based on the very low Ti content of the biotite and the occurrence of similar intergrowths in partially replaced cordierite in the Marcus Hook quadrangle (Crawford and Mark 1982). Here, there is minor evidence for M3, higher pressure overprinting, though a few samples containing muscovite and kyanite can be found. An outcrop across Chester Creek (approximately 100m north of the quarry) and a much broader zone several hundred meters downstream from the quarry exhibit almost complete overprinting and contain the M3 assemblage muscovite + biotite + garnet + plagioclase + quartz + kyanite $\pm$ staurolite + ilmenite + magnetite.

The cores of garnet in samples from Pyramid Materials generally exhibit little zoning in major elements (figure 43). Porphyroblasts are characterized by a slight increase in almandine from core to rim, a corresponding decrease in pyrope (Mg component), and a complete lack of zoning in spessartine (Mn component). The core of this garnet shows no zoning in grossular (Ca-component), but does exhibit a narrow (<80 μm), somewhat irregular rim that shows a two- to three-fold increase in grossular and a decrease in pyrope (figure 43). Sillimanite inclusions are present where rims are best developed and grossular enrichment is most pronounced. The lack of zoning in major components, including grossular, in the interior garnet is interpreted to be the result of diffusion at high temperatures (Tracy, 1982; Spear and Florence, 1992), consistent with the high-temperature sillimanite-orthoclase assemblages. The grossular enriched rims are interpreted to have grown under the higher pressure conditions of M_3, as in the garnet porphyroblasts described above in pelitic mylonite from the Rosemont shear zone.

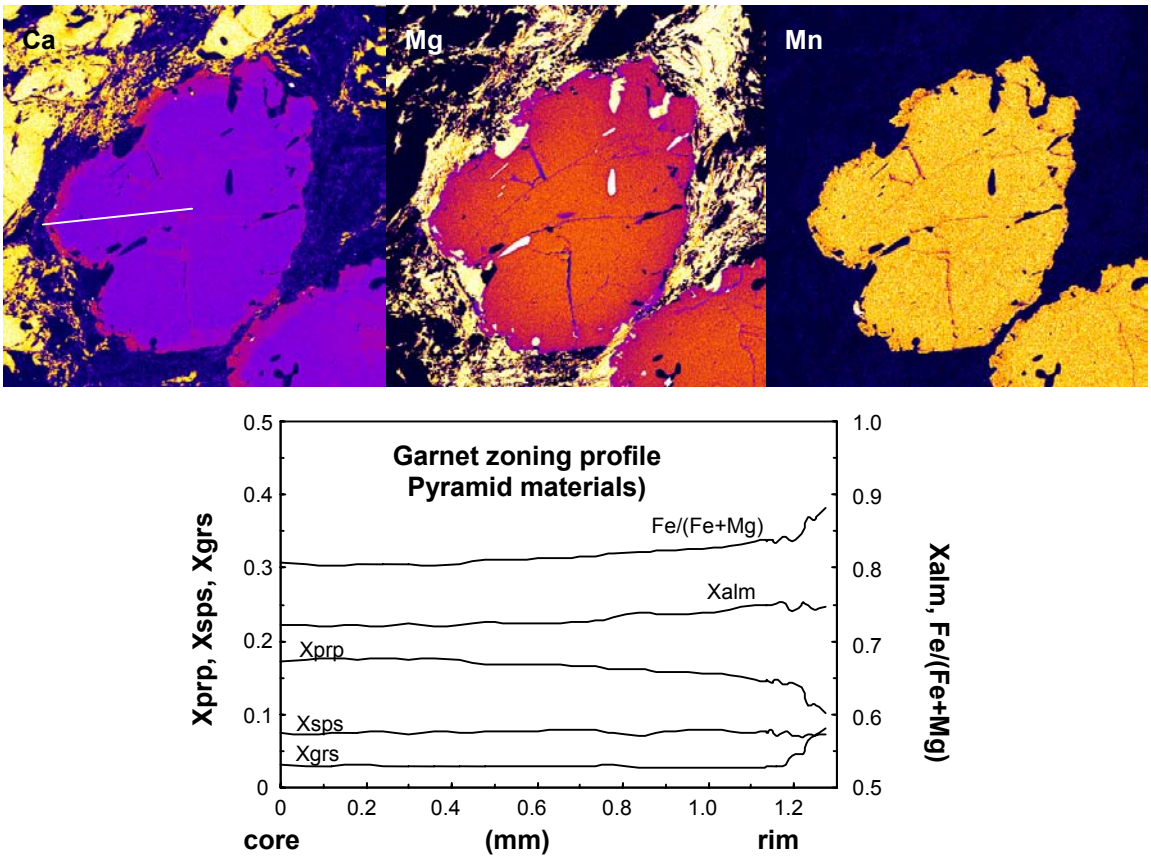

Figure 43. X-ray composition maps and zoning profiles from garnet in sample from Stop 8, which contains the muscovite absent M_2 assemblage sillimanite + biotite + garnet + orthoclase (+ quartz + plagioclase). Line in Ca map shows postion of zoning profile. Width of maps = 3.6 mm.

The major mineralogical constraints on pressure and temperature conditions during M2 are the sillimanite + orthoclase, muscovite absent assemblage and the relict presence of the low-pressure mineral cordierite. Precise temperature estimates cannot be made for the breakdown of muscovite in these rocks because the reaction is a function of water pressure at the time of metamorphism, which is not known. In figure 44, muscovite breakdown curves and curves for cordierite formation calculated for P_{H2O} = 1.0 and 0.5, using the composition of cordierite (Fe/(Fe+Mg) = 0.13) from locality 4 of Crawford and Mark (1982) are shown. These curves probably bracket the conditions actually experienced by these rocks. Migmatitic textures, if they are assumed to be the result of partial melting, suggest temperatures in excess of 650°C.

Thermobarometric calculations to determine the pressure and temperature conditions of M_2 are difficult, because most of the samples that have been analyzed contain at least some evidence for M_3 overprinting, implying disequilibrium among the relict phases. However, given the low diffusivity of Ca in both garnet (Loomis *et al*., 1985; Chakraborty and Ganguly, 1992) and plagioclase (Yund, 1983; Grove *et al*., 1984), the observations that garnet interiors are essentially unzoned in grossular, and that the interiors of plagioclase porphyroblasts are approximately homogeneous in composition on the scale of a thin section, suggest that the compositions of garnet and plagioclase cores reflect conditions of M_2 metamorphism and may be used for geobarometry. The selection of a suitable biotite composition for use in M_2 temperature determination is problematic. Matrix biotite and biotite inclusions in garnet differ in composition and the composition of both may have changed during M_3 and subsequent cooling. As noted, in the sample

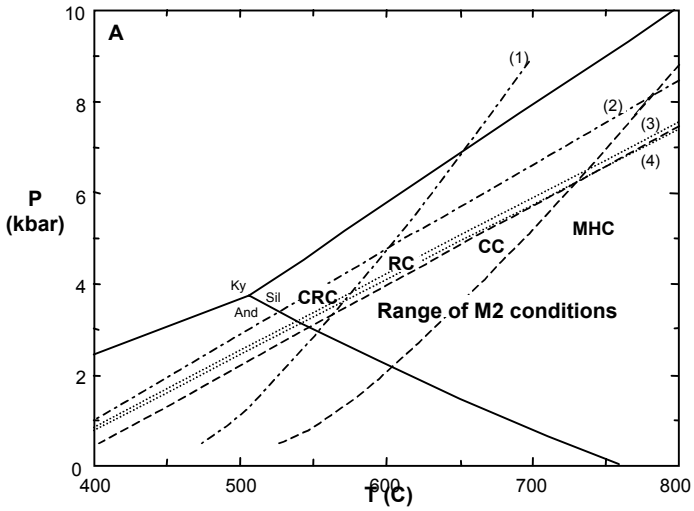

Figure 44. Estimates of M_2 conditions: reactions (1) and (3), muscovite + quartz = sillimanite + k-feldspar + H_2O; and (2) and (4), biotite + sillimanite = cordierite + k-feldspar + H_2O calculated with a_{H2O} = 0.5 (1 and 2, dash and dot) and 1.0 (3 and 4, dashed); unnumbered dotted lines, GASP (Koziol and Newton, 1988) curves calculated using the composition of garnet and plagioclase cores. The labels CRC (Crum Creek), RC (Ridley Creek), CC (Chester Creek), and MHC (Marcus Hook Creek) reflect M_2 P – T estimates at those locations. Reaction boundaries 1, 2, 3, and 4 were calculated using TWEEQU 2.02 (Berman, 1991) with the thermodynamic database of Berman (1988, 1990) with modifications described in Berman and Aranovich (1996) and default activity models for solid solution phases. These include: garnet, biotite, and cordierite, Berman and Aranovich (1996); plagioclase, Fuhrman & Lindsley (1988); and muscovite, Chatterjee & Froese (1975). Aluminum silicate curves are from Holdaway (1971).

from Pyramid Materials the unzoned interior of garnet (figure 43) indicates diffusional homogenization at high temperatures (Tracy, 1982; Spear and Florence, 1992), so it is likely that biotite inclusions equilibrated with garnet interiors at the time of maximum temperature during M2. However, a 15 to 20 μm diffusive halo is present in garnet surrounding included biotite that probably resulted from Fe-Mg exchange during cooling from peak temperatures. In this halo, Fe/(Fe+Mg) increases from 0.81 away from the biotite to a maximum value of 0.85 immediately adjacent to the inclusion. Calculations to estimate the magnitude of Fe-Mg exchange necessary to produce the halo in garnet indicate that the composition of the biotite inclusion was not significantly affected (Bosbyshell, 2001).

TWEEQU 2.02 (Berman, 1991; Berman and Brown, 1997) was used to test whether matrix or included biotite could have been in equilibrium with the M2 assemblage garnet + plagioclase + orthoclase + H_2O in the Pyramid sample. Reaction boundaries calculated using the composition of included biotite, garnet core, and plagioclase core, with the activity of H_2O = 0.79, intersect at a single point (figure 45), suggesting that the phases present equilibrated at approximately 4.6 kbar and 680°C. A similar result was obtained for a sample collected a few hundred meters downstream along Chester Creek. The positions of the GASP equilibria from these calculations are plotted in figure 44. When the calculation is performed using the composition of matrix biotite, with the same garnet and plagioclase, the curves are spread over a temperature range of 200°C and a pressure range of 3 kbar, indicating that minerals having this composition were not in chemical equilibrium.

Age of metamorphism. Monazite from samples of the "Arc Wissahickon" typically exhibits compositional zoning. In some cases this zoning also constitutes distinct age domains. As described above, the cores of monazite in two samples give Ordovician ages (484 – 472 Ma; Bosbyshell, 2001), essentially identical to the age of arc-building magmatism in the Wilmington Complex. M2 metamorphism is Silurian in age. Outside the small Ordovician cores, electron microprobe chemical ages in different samples range between 430 – 448 Ma (Bosbyshell, 2001). Thermal ionization mass

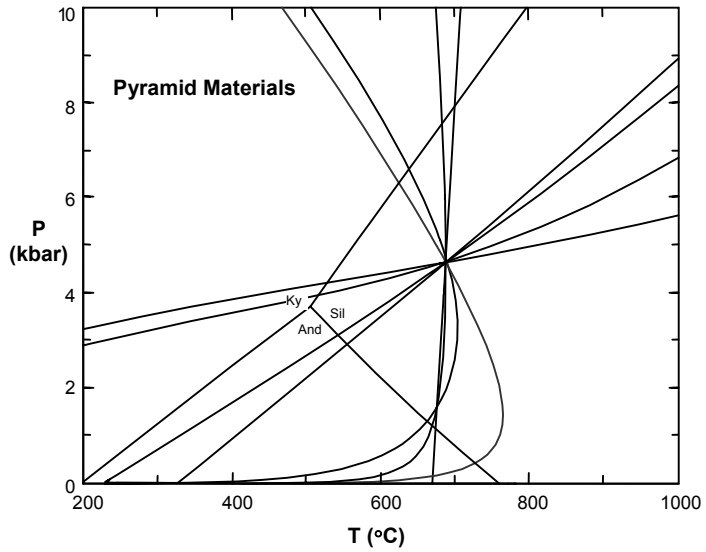

Figure 45. TWEEQU 2.02 plot for sample 1303 for the M_2 assemblage garnet + biotite + sillimanite + plagioclase + quartz + orthoclase. Calculated using the composition of garnet and plagioclase cores and biotite inclusion in garnet with $a_{H2O} = 0.79$; 3 independent reactions.

spectrometric (TIMS) isotopic analyses of monazite are discordant, yielding Silurian $^{206}Pb/^{207}Pb$ model ages that are somewhat younger than the microprobe chemical ages (~420 Ma). The difference between the chemical and isotopic ages is unresolved at present. The discordance in isotopic results is likely due to the presence of monazite crystals of different age within the analyzed sample and also the presence of different age domains within individual crystals.

Structural Geology

The dominant foliation at Pyramid Materials is S_2, the axial planar foliation to regional F_2 folds. F_2 folds are locally tight, but are mainly isoclinal, noncylindrical folds. At some locations along Chester Creek multiple F_2 hinges are present, but more commonly, F_2 hinges are transposed and isolated so that it is not possible to trace layering between successive hinges. In pelitic gneiss S_2 is defined by the parallel orientation of sillimanite needles and biotite. S_0 and S_1 are transposed in S_2, hence, in F_2 fold limbs, S_2 is also parallel to mm- to cm-scale layering of quartzo-feldspathic and micaceous domains and dm- to m-scale psammitic and pelitic lithological layering (figure 46). S_2 dips moderately to steeply throughout the region, but because F_2 folds and S_2 foliation have been affected by at least two subsequent episodes of deformation it is difficult to make any but the most general statements concerning their orientation.

F_3 folds deform the dominant S_2 foliation and predate kyanite grade M_3 metamorphism. Here along Chester Creek, F_3 folds are noncylindrical, close to tight and locally isoclinal (figure 47A, B, and C); in the east along Crum Creek (figure 47D), F_3 folds are tight to isoclinal. S_3 foliation is an axial-planar fabric in tight to isoclinal F_3 folds (figure 47A) and is also developed by shearing in the attenuated limbs of folds (figure 47A, B). F_3 folds are present at all scales of observation, including mm to cm wavelength crenulate folds (figure 48), m wavelength outcrop scale folds (figure 47) and larger wavelength map scale folds.

S_3 foliation is variably developed, ranging from incipient S_3, a widely spaced foliation with cleavage domains occupying a very small percentage of the rock (figure 48) to a closely spaced foliation comprising a significant portion of the rock (figure 47A). In limbs of isoclinal F_3 folds, the dominant foliation, folded S_2, is parallel to S_3, the axial plane, and is regarded as an S_2/S_3 composite

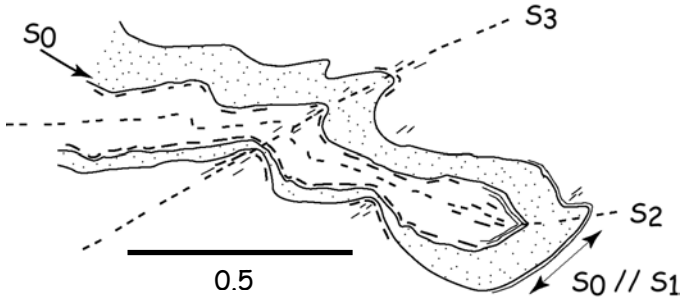

Figure 46. Field sketch of refolded F2 isocline showing relationships between different generations of foliation. Compositional layering is S0. In hinge of F2, S1 is parallel to S0; in limbs of F2, S0, S1, and S2 are parallel. Where F3 folds are tight to isoclinal, all older foliations approach parallelism with S3.

foliation (figure 47A, B). This is a continuous foliation in micaceous domains and a parallel spaced schistosity in more psammitic rocks.

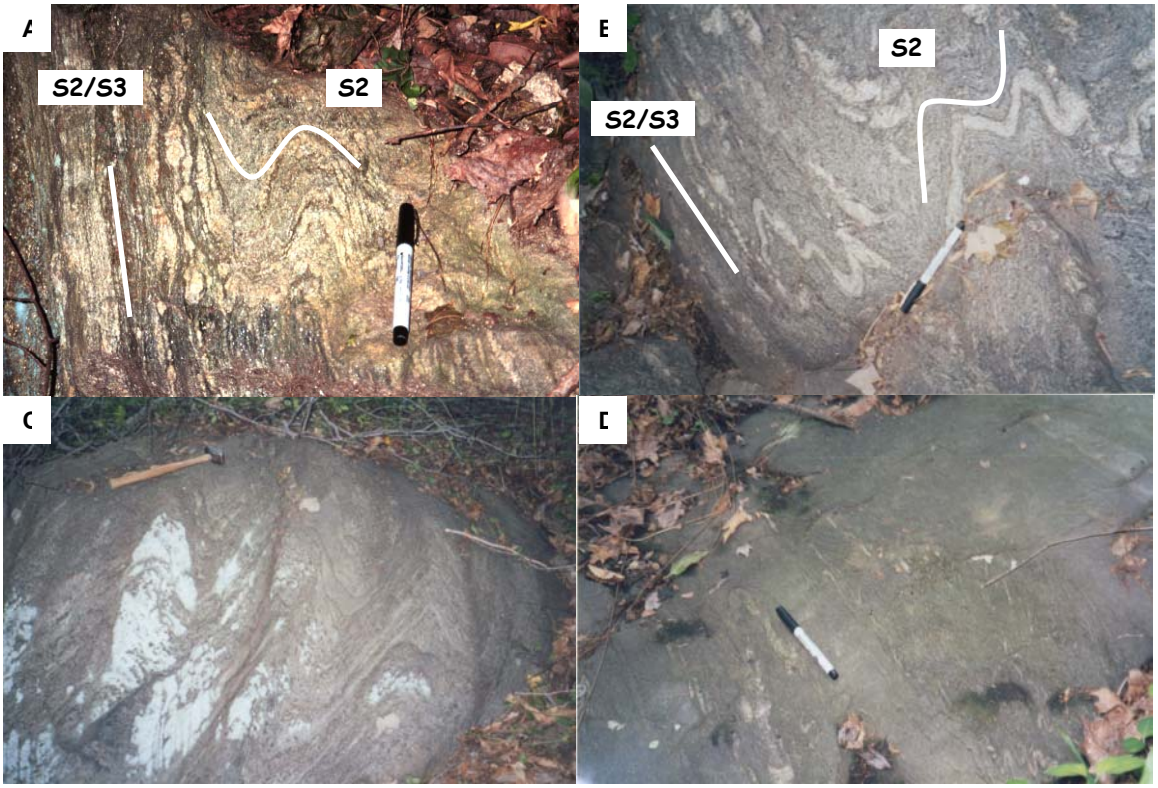

Figure 47. Photographs of F3 folds. A, F3 fold of S2 Chester Creek. Note limb of fold at left is parallel to axial plane, so that S2, the folded foliation, is parallel to the axial planar foliation, S3. Sub-horizontal outcrop surface, pen is approximately N-S. **B,** F_3 folds of S_2, Chester Creek. Sheared limb at left is parallel to S_3. Sub-horizontal outcrop surface, pen is approximately E-W. **C**, F3 folds of S2, Ridley Creek. Vertical outcrop surface, view is towards the north. **D**, Intrafolial F3 folds of pegmatite and quartz veins, bounded by S2/S3 foliation domains, Crum Creek on campus of Swarthmore College. Pen is approximately N-S.

Data from different scales of observation demonstrate that F3 folding is older than the intermediate pressure metamorphism (M_3). At the outcrop and map scales, S3 is rotated by shear zones (S4), described above, that are demonstrably syn-tectonic with respect to M_3 metamorphism.

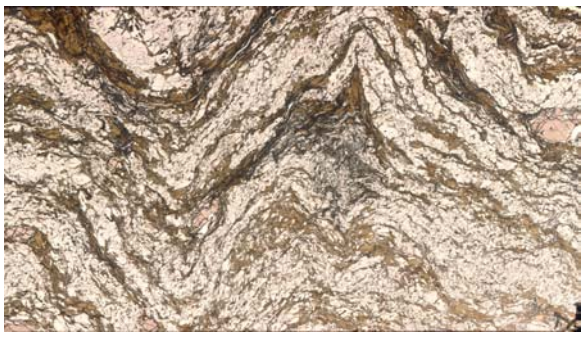

Figure 48. Photomicrograph of mm- to cm-scale F_3 folds of S_2, Chester Creek. Sub-horizontal section; N towards top of page. Long dimension of image is approximately 5.5 cm.

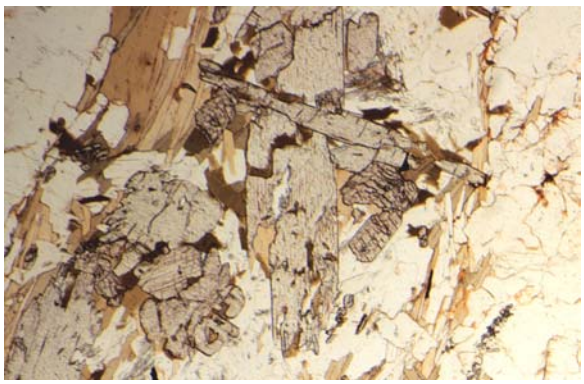

Figure 49. Photomicrograph illustrating relative timing of kyanite growth and F3 folding. Randomly oriented kyanite crosscuts biotite and muscovite that define S3.

That F_3 folding preceded M_3 is also apparent at the thin section scale. Figure 49 demonstrates cross-cutting relationships between M_3 phases, kyanite and fabric forming mica that parallel S_3.

At the Pyramid Materials quarry S_2 is subvertical and F_2 fold axes plunge steeply. F_3 folds, which deform S_2, are also characterized at this location by subvertical axial planes and fold axes. As a result the fold orientations, little folding is visible in the vertical quarry walls. Field trip participants are urged to inspect loose boulders to find what was once a horizontal surface which afford a view of the folding.

F3 folding may correspond to an early stage of convergence that ultimately resulted in crustal thickening and kyanite grade metamorphism, M3, metamorphism. S3 is generally steeply dipping suggesting that sub-horizontal shortening played an important role during D3. Though the present orientation of S3 is due in part to younger deformation, the strike of S3 is commonly sub-parallel to that of the Rosemont Fault in the study area. It is possible that the geometry of this contact influenced the geometry of D3 structural elements, although intense deformation in shear zones parallel to and along the trace of the Rosemont Fault is synchronous with M3, and therefore younger than D3.

LUNCH

		Depart Pyramid Quarry. Turn LEFT onto Knowlton Road. Bear right over bridge.
0.3	17.5	Creek Road branches off to the right from Knowlton Road. Bear RIGHT onto Creek Road. Note outcrops of Wissahickon on left side of Creek Road.
0.7	18.2	Intersection of Creek Road with Dutton Mill Road (stop sign). Cross Dutton Mill Road and continue on Creek Road. Note prominent folding in outcrops of Wissahickon on left side of Creek Road.
0.9	19.1	Intersection of Creek Road with Bridgewater Road (stop sign; Creek Road ends). Turn LEFT onto Bridgewater Road.
0.1	19.2	Intersection of Bridgewater Road with Brookhaven Road (traffic light). Turn LEFT onto Brookhaven Road.
0.8	20.0	Intersection of Brookhaven Road with Rt. 352 (traffic light). Cross Rt. 352 and continue on Brookhaven Road.
0.3	20.3	Cross Ridley Creek and immediately come to intersection of Brookhaven Road with Waterville Road (traffic light). Turn RIGHT onto Waterville Road.
0.6	20.9	Intersection of Waterville Road with Chester Park Drive (no stop sign or light). Turn RIGHT onto Chester Park Drive.
0.1	21.0	Pull into parking area near top of hill in Chester Park. Walk about 0.5 miles downhill along road to bridge (about 5 minutes). Just before bridge, examine large boulders along trail on the left. These are the Chester Park Gneiss (affectionately known as the Crack House Gneiss).

STOP 9. CHESTER PARK GNEISS IN CHESTER PARK

Leader: Howell Bosbyshell

Chester Park (figure 50), one of the oldest municipal parks in Delaware County, is owned and maintained by Chester City. It consists of 71 acres along the banks of Ridley Creek. The rock exposed in Chester Park is medium to coarse grained, quartzo-feldspathic biotite gneiss provisionally designated the Chester Park Gneiss. Some portions are sufficiently micaceous to be called schist. Garnet, fibrolitic sillimanite (replaced by kyanite blades at some locations) and cordierite are also present in more aluminous domains. Accessory minerals include Fe-Ti oxides, apatite, monazite, and zircon. Alkali feldspar is present only in pegmatite pods and lenses.

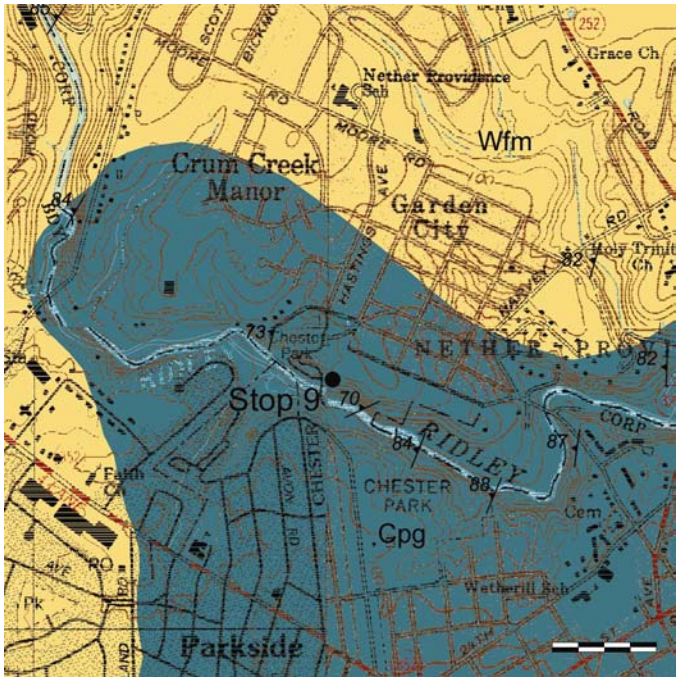

Figure 50. Geologic map of the corners of the Media, Lansdowne, Bridgeport, and Marcus Hook quadrangles showing location of Stop 9. Blue unit is the Chester Park Gneiss (Cpg), orange is Wissahickon Formation (Wfm). Scale bar is 400m.

This lithology can be mapped from southern Crum Creek south to Marcus Hook Creek, where it is host rock to the Arden pluton. Portions of the Chester Park Gneiss were originally mapped by Bascom et al., (1909) in the Philadelphia Folio as both Granitic Gneiss and Wissahickon Gneiss. Bascom et al.'s (1909) contacts were incorporated into the 1960 geologic map of Pennsylvania, but on the most recent state map (Berg et al., 1980) the area of granitic gneiss decreased and portions were mapped as pyroxene-bearing mafic gneiss of the Wilmington Complex.

The nature of the protolith of this unit is an area for discussion. The rock frequently has a massive appearance and contains enclaves (xenoliths?) that could suggest an intrusive igneous origin (figure 51). However, the aluminous character of some of the rock is consistent with a supra-crustal origin, as a sedimentary or possibly an altered volcanic rock. While compositional layering is present at some locations, it is generally not well developed. A zircon separate obtained from this

Figure 51. Photographs of Chester Park Gneiss showing inclusions which may be xenoliths, magmatic enclaves, or clasts.

rock for the purpose of determining an igneous crystallization age was morphologically heterogenous. Most grains were rounded and appeared to be detrital, supporting a sedimentary origin for the rock (John Aleinikoff, personal communication). This sample was deemed unsuitable for the purpose of obtaining a protolith age, and isotopic analysis was not carried out. Where best exposed, the contact between the Chester Park Gneiss and the Wissahickon Formation is highly tectonized; therefore contact relationships do not further illuminate the problem.

Structural Geology

In Chester Park the gneiss exhibits steeply dipping foliation that generally strikes north-south or slightly east of north. This is thought to be the regional S3 foliation. F3 folds, to which the dominant foliation is axial planar, are common in outcrops farther downstream where Ridley Creek flows under Chestnut Parkway. Folds visible in large boulders and outcrops (?) near the parking area are younger folds. Since much of the rock here is not in place, the orientation of these folds is not known. Similar folds are present in outcrop about 100 m downstream, where Chester Park abuts the Taylor Arboretum. There the dominant NE striking foliation is folded by a steep E-W fabric. This is a fairly uncommon orientation for late folds, but the style of folding is similar to F5 folds that we will see in the Wissahickon Formation at Stop 10.

		Return to buses via road or follow trail uphill through woods (follow pavers in soil). Depart Chester Park. Turn RIGHT onto Chester Parkway (continuation of Waterville Road). Chester Parkway becomes Chestnut Street.
0.8	21.8	Intersection of Chestnut Street. with Providence Avenue. – Rt. 320 (second traffic light). Cross Providence Avenue. – Rt. 320 and continue on Chestnut Street.
0.1	21.9	Intersection of Chestnut Street. with 22nd Street. (traffic light). Turn LEFT onto 22nd Street. Continue through one traffic light.
0.4	22.3	Behind the shopping center on right side can be seen the contact between the Chester Park Gneiss and the Wissahickon. Move into left lane.
0.5	22.8	Entrance for I-476 North. Turn LEFT onto ramp for I-476 North (I- 476 is also called “the Blue Route”). Note outcrops of granitic rock on the right side of I-476, correlated with the Springfield Granodiorite.
2.5	25.3	EXIT from I-476 (right side) at Exit 3, Media-Swarthmore. Move into right lane on exit ramp.
0.3	25.6	End of ramp and intersection with US 1 (Baltimore Pike; traffic light). Turn RIGHT onto US 1 (Baltimore Pike) and immediately get into LEFT LANE.
0.2	25.8	After bridge make the first LEFT onto Papermill Road, entrance to Smedley Park. Be careful as you come to the railroad tracks: this is an active commuter rail line.
0.3	26.1	Cross railroad tracks and pull into parking area. Disembark from buses. From picnic parking area, follow road (moving away from US 1), and cross Crum Creek. Continue across the open field, which was the site of a paper mill that was cleaned up as a Superfund project. After the field, bear right and climb the outcrop in the woods. Follow the trail to the old quarry next to the creek in Type Wissahickon. About 15 minutes walking time. Return by same trail to buses in parking area.

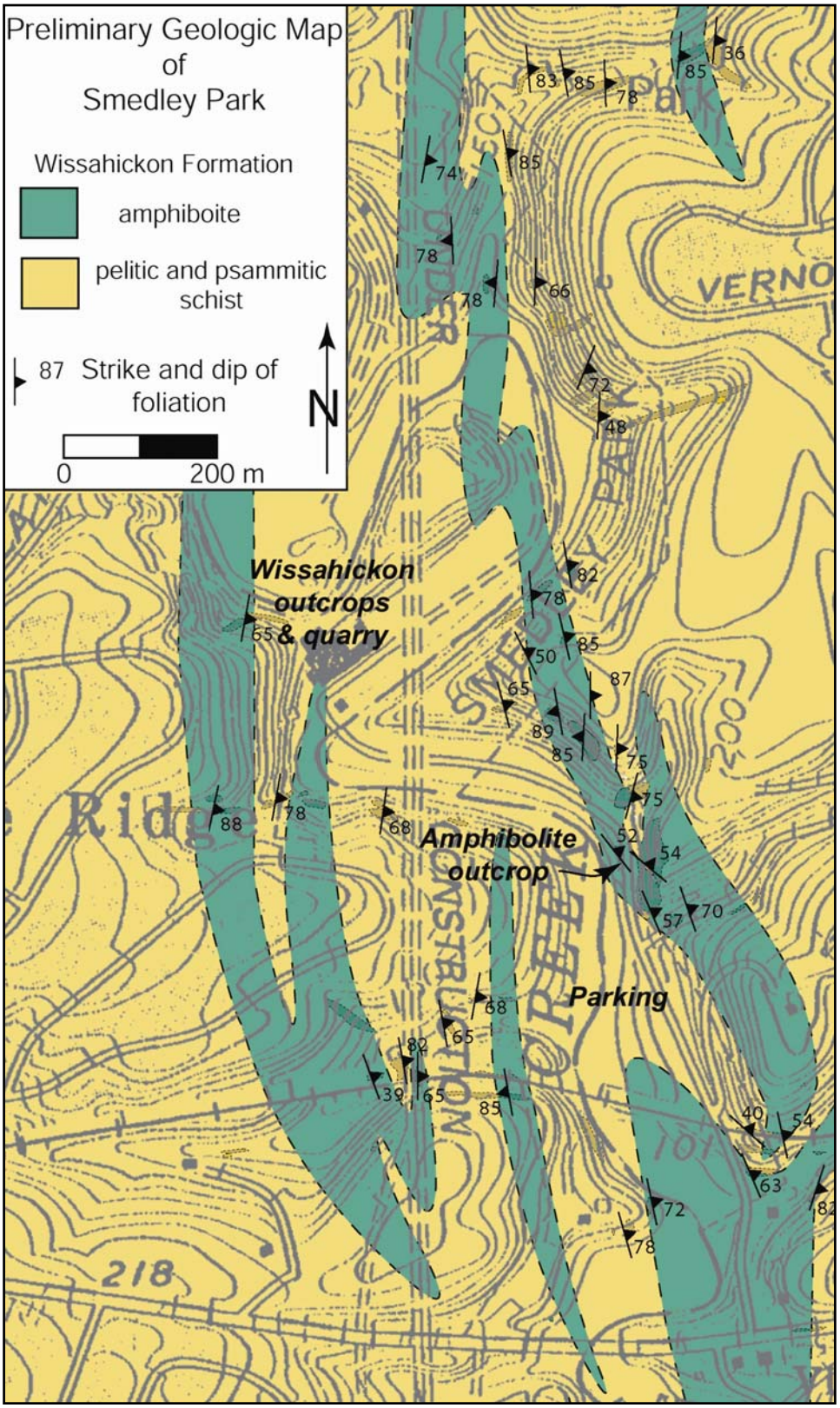

Figure 52. Geologic map of Smedley Park showing location of outcrops. Note that the Blue Route (I-476) is dashed on this map.

STOP 10. WISSAHICKON FORMATION IN SMEDLEY PARK
Leader: Howell Bosbyshell

Smedley Park is one of four major parks in the Delaware County Park system. Crum Creek flows through the 120 acres of the park, as does I-476, locally known as the Blue Route. The park was the site of an old paper mill, a former Super Fund site where remediation measures were completed in the 1990's.

Smedley Park (figure 52) is underlain by the Wissahickon Formation, *sensu stricto,* or Type Wissahickon, which consists of pelitic and psammitic schist with interlayered quartzite and rare, thin coticule layers. Here, these rocks occur with abundant amphibolite, with back-arc basin (BABB) geochemistry, and thin (< 1 m) layers of an unusual garbenschist-like, hornblende epidote quartz plagioclase garnet granofels and gneiss. Pelitic schist is medium to coarse grained and is composed of quartz, biotite, muscovite, plagioclase, garnet, staurolite, and kyanite. Sillimanite is present as very fine acicular inclusions in garnet and muscovite.

Smedley Park Amphibolite

The first outcrops one encounters walking north along Paper Mill Road from the parking area expose the Smedley Park amphibolite. The Smedley Park amphibolite occurs over a large area in the western Lansdowne quadrangle, extending from the Coastal Plain on lap to the Rosemont Fault, a distance of greater than 10 km. This amphibolite is concordant with layering in Wissahickon Formation metasedimentary rocks; although limited exposure and intense deformation make it difficult to determine the thickness of individual layers. Map relationships indicate an outcrop width of greater than 20m in many locations. The areal extent of the amphibolite, its chemical homogeneity, and apparent concordant contacts with adjacent metasediments suggest that this unit originated as lava flows or sills. The contact between amphibolite and a quartzite layer is well exposed in the outcrop along Paper Mill Rd. Was this originally a depositional or intrusive contact?

The Smedley Park Amphibolite is medium grained, granoblastic gneiss containing hornblende, plagioclase, titanite, epidote, Fe-Ti oxides, and some quartz. Locally, plagioclase grains contain cores that exhibit concentric, oscillatory zoning, which may be a relict igneous texture. Foliation is defined by preferred orientation of hornblende and mm scale compositional layering of hornblende- and plagioclase-rich domains.

Geochemistry. All samples of the Smedley Park amphibolite are basaltic (figure 53) and are classified as tholeiitic on both the AFM diagram of Irvine and Baragar (1971) and the FeO/MgO vs. SiO2 diagram of Miyashiro (1974). The Smedley Park amphibolite plots in the MORB or volcanic-arc basalt fields on discrimination diagrams based on immobile trace elements (Bosbyshell, 2001). Trace element composition is consistent with the tholeiitic characterization seen in major elements (Bosbyshell, 2001).

On chondrite normalized REE diagrams (figure 54A), Smedley Park amphibolite is enriched in LREE and exhibits a flat pattern from middle to HREE (La/Sm_{CN} = 1.8 – 2.0, Sm/Lu_{CN} = 1.1 – 1.3). A small negative Eu anomaly (Eu/Eu* = 0.87 –0.90) is present. REE abundances are similar to transitional or E- MORB and back-arc basin basalt (BABB) but are near the upper limit of values found in island arc basalts. Overall, the shape of the REE pattern for the Smedley Park amphibolites most closely resembles BABB (Bosbyshell, 2001).

The Smedley Park amphibolite shows enrichment in incompatible to moderately incompatible elements with respect to N-MORB, and least incompatible trace element abundances that are similar to or slightly greater than N-MORB (figure 54B). As with REE, the overall shape and slope of the trace element pattern is most similar to BABB (Figure 54B), but enrichment in the

most incompatible elements and a negative Nb anomaly ($Nb/Nb^*_{avg.} = 0.42$) are also characteristic of island arc basalt.

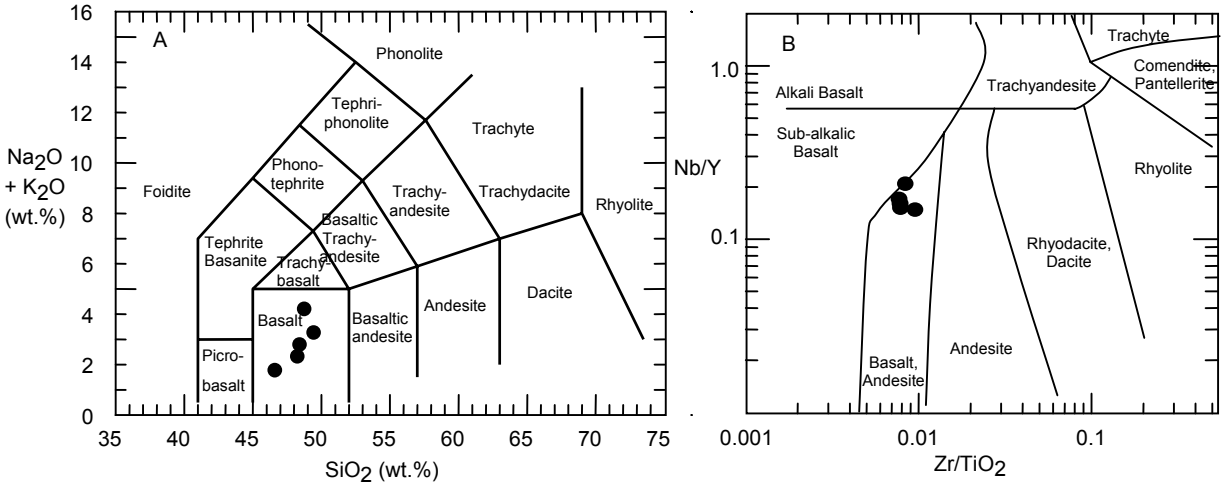

Figure 53. Geochemical classification of Smedley Park Amphibolite. A, igneous rock classification diagram using total alkalis vs. silica after LeBas *et al*. (1986). B, igneous rock classification diagram using immobile trace elements (Winchester and Floyd, 1977).

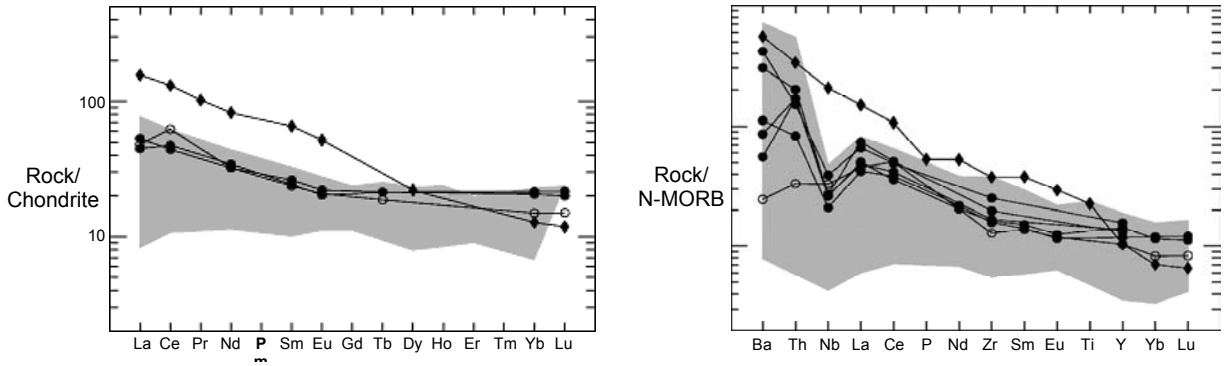

Figure 54. A. Chondrite normalized REE diagram comparing Smedley Park amphibolites (filled circles) and BR372 (open circles) with back-arc basin basalt (BABB) B. N-MORB normalized trace element diagram comparing Smedley Park amphibolite with back arc basin basalt. Shaded area in A and B represents data from Cameron, 1989; Allan and Gorton, 1992; Gribble *et al*., 1996; Gribble *et al*., 1998; Saunders and Tarney, 1991. Filled diamonds are ocean island basalt for comparison (Sun and McDonough, 1989). BR372 is an amphibolite layer in the Chester Park Gneiss.

Tectonic setting. The trace element geochemical characteristics of the Smedley Park amphibolite, enrichment in LREE and other incompatible trace elements and a negative Nb anomaly, are characteristic of volcanic-arc related magmatism. However, although similarly enriched basalt is found in some arcs (e.g. the Sunda arc, Whitford *et al*., 1979; Nichols *et al*., 1980), the overall abundance of incompatible trace elements including HREE in the Smedley Park amphibolite is greater than in most basalt found in volcanic arcs. Basalt with very similar composition to the Smedley Park amphibolite has been recovered from the Yamato Basin in the Sea of Japan (Allan and Gorton, 1992) and similar, though slightly less enriched, basalt also occurs in the Mariana Trough (Johnson and Fryer, 1990; Stern *et al*., 1990, Gribble *et al*., 1998). It is widely recognized that the composition of back-arc basin basalt ranges from magmas that are virtually indistinguishable from those erupted in an arc, where basin rifting is youngest, through MORB, where the basin is more mature and a spreading ridge is developed (Wilson, 1989; Cameron, 1989; Saunders and Tarney, 1991; Gribble *et al*., 1998). Thus, the Smedley Park amphibolite appears to be arc-related, but it

cannot be assigned to a unique tectonic setting based on geochemistry alone. Its chemical composition most closely resembles basalt recovered from back-arc basins.

Wissahickon Formation

Continue walking north on Paper Mill Rd., ford Crum Creek and follow the trail across an open field (the former site of the paper mill) and up a small rise to outcrops of Wissahickon Formation and continue to follow trail into an old quarry. The quarry and nearby outcrops afford a view of the pelitic and psammitic lithologies that characterize the Wissahickon Formation along Crum Creek and east to the type section.

Metamorphism. The Type Wissahickon at Smedley Park contains kyanite- and staurolite-bearing metamorphic mineral assemblages characteristic of M3, intermediate pressure metamorphism. Elsewhere along Crum Creek, the Type Wissahickon is unique in Southeastern Pennsylvania due to the presence of andalusite and pseudomorphs after andalusite (consisting mostly of kyanite and muscovite) (Gordon, 1922; Wyckoff, 1952; Heyl, 1980; Hess, 1981; Crawford and Mark, 1982). The andalusite is thought to be the result of the Silurian, M2, high temperature-low pressure metamorphic episode (Crawford and Mark, 1982; Bosbyshell et. al., 1999). Unfortunately, pseudomorphs after andalusite are not present in Smedley Park, but can be seen in outcrops 1-2 km south of the park, in exposures on the campus of Swarthmore College.

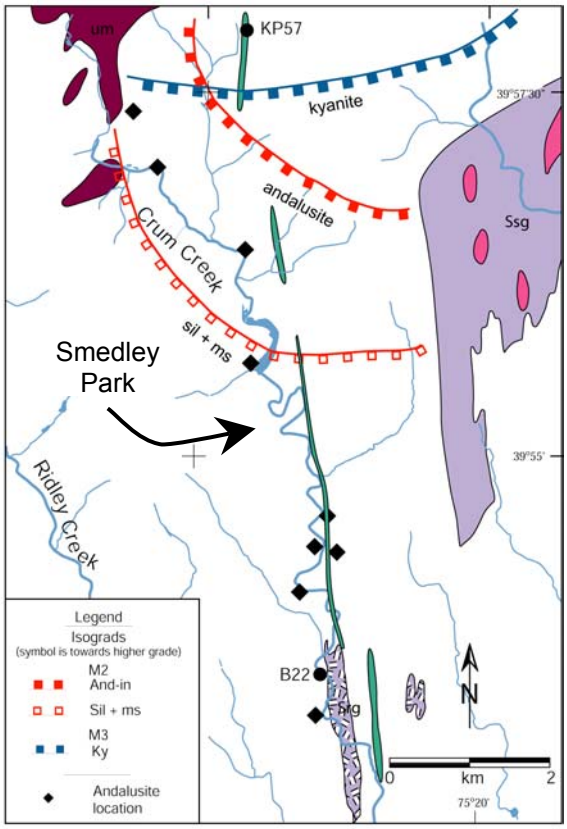

Figure 55. Isograd map of the Crum Creek area, showing andalusite locations (Wycock, 1952) and locations mentioned in text. Ssg, Springfield Granodiorite; Srg, Ridley Park granite; um, ultramafic rock; unpatterned is Type Wissahickon, green unit is Smedley Park Amphibolite

Figure 55 is an isograd map of the Crum Creek transect. Relict M2 assemblages define a low pressure metamorphic field gradient. Andalusite, or much more commonly pseudomorphs after andalusite (locations are from Wyckoff, 1952), occurs throughout the transect, but in the southern portion, sillimanite is present as inclusions in garnet and muscovite and less commonly as a relict matrix phase. Sillimanite is not present north of the isograd labeled sil + ms in the central portion and there is scant evidence for M2 porphyroblast growth in the north (Bosbyshell, 2001). The existence of this relict metamorphic field gradient is supported by petrographic analysis, garnet zoning profiles, field relationships, and monazite geochronology.

Figure 56A shows x-ray composition maps of garnet which illustrate the two stage metamorphic history. The garnet is from sample B22 (figure 55), collected about 1 km south of the Swarthmore campus, towards the southern end of the transect. This sample contains the kyanite-bearing M3 assemblage, but sillimanite inclusions are present in some garnet crystals. The small euhedral core which is particularly evident in the Ca map is interpreted to have grown during M2, while the high Ca overgrowth formed during M3 overprinting. Note that the core (figure 56), though less than 0.5mm diameter, preserves subtle growth zoning. This indicates that metamorphic conditions, though hot enough to grow sillimanite, they were not sufficient in temperature or duration to permit intracrystaline diffusion to homogenize even this small core. This is in marked

contrast to garnet in the Arc Wissahickon seen at Stop 8, where considerably larger garnet porphyroblasts show no internal zoning.

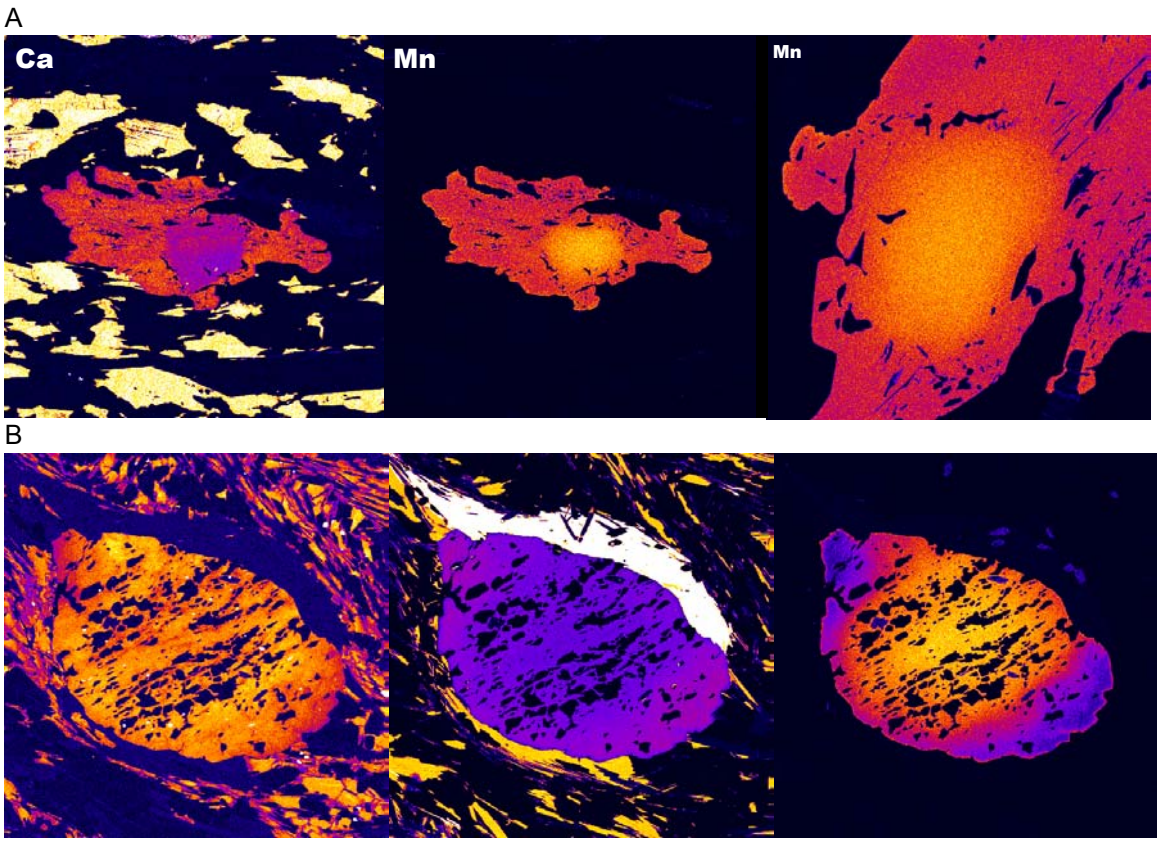

Figure 56. **A**. X-ray composition maps of garnet from sample B22, showing zoning indicative of the two-stage metamorphic history. The Mn map at right is a close-up of the center image (rotated clockwise 90º). Field of view in left and center images = 2.0 mm; Mn map at left = 0.67 mm. **B.** X-ray composition maps of garnet from sample KP57, showing simple growth zoning indicative of a single growth episode. Note that the included fabric forms a pair of crenulation hinges, at a high angle to the crenulation in the external foliation. Field of view = 3.1 mm.

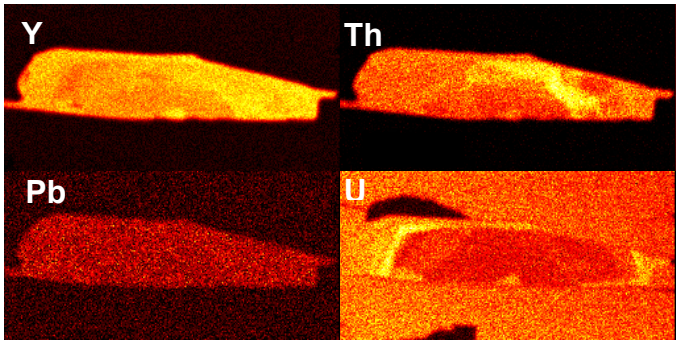

Figure 57. X-ray composition maps of monazite from sample B22. Zoning comprises two age domains, an early Silurian core, and the high U rim which gives a late Silurian age. Field of view = 110 μm.

Garnet in sample B22 is also significantly different from that in a sample from the northern end of the transect (KP57, figure 55). KP57 is on the lower grade side of the M3 kyanite isograd and is also north of reported M2 andalusite locations. The rock contains staurolite, in addition to garnet, biotite, muscovite, quartz and plagioclase feldspar. Mn content in garnet from this sample (figure 56B) decreases from core to rim (when graphed this is the classic "bell-shaped" zoning profile), a zoning pattern that is characteristic of partitioning of Mn in garnet during a single growth episode, M3.

Monazite geochronology also highlights the difference in metamorphism from south to north along Crum Creek. Monazite from sample B22 is typically zoned, with high U overgrowths on all grains and contains distinct age domains (figure 57). The Silurian age, 431 ± 7.5 Ma, is interpreted as the time of M2 metamorphism in this sample. High U overgrowths yield a late Silurian age, 416 ± 9.6 Ma. The rims are elongate parallel to foliation and constrain the timing of deformation (see section on structural geology below). Monazite in KP57, though zoned, does not contain distinct age domains and yields a Devonian age, 377 ± 3.3 Ma, indistinguishable from $^{207}Pb/^{206}Pb$ model ages of discordant TIMS results from Wissahickon Creek (Bosbyshell et al., 1998).

The similar lithologic characteristics of metasedimentary rock and the presence of the concordant Smedley Park amphibolite along the entire length of the transect, indicate that metamorphic differences from north to south occur within the same unit, as opposed to resulting form tectonic juxtaposition of rocks with different metamorphic histories. Many studies suggest that initial monazite growth occurs in metapelitic rocks under approximately the same conditions as initial garnet growth (e.g., Smith and Barreiro, 1990; Kingsbury, et al., 1993). This implies that much of the Type Wissahickon remained at lower greenschist conditions throughout the early Paleozoic. This distinguishes the Type Wissahickon from Arc Wissahickon, which contains early Ordovician monazite, suggesting a period of metamorphism related to Wilmington Complex arc magmatism.

Bosbyshell (2001) proposed that the low pressure metamorphic field gradient in the Wissahickon Formation was the result of Silurian emplacement of the Arden plutonic suite, implying that the spatial distribution of these units has remained largely unchanged since that time. However, recent zircon geochronology (John Aleinikoff, unpublished data) demonstrates that the Springfield Granodiorite, which intrudes the Wissahickon Formation a few kilometers to the east of Crum Creek transect (figure 55) is also a Silurian (427 ± 3 Ma) pluton. Andalusite and sillimanite grade metamorphism in the Type Wissahickon along Crum Creek could be related to emplacement of the Springfield Granodiorite. Thus, the metamorphic history of the Type Wissahickon and the Wilmington Complex does not exclude some degree of post-Silurian tectonic juxtaposition of these units.

The similar age of the Arden and Springfield plutons and high temperature-low pressure metamorphism suggests that there was an elevated geothermal gradient in the Silurian lithosphere that was regional in extent. This thermal regime is interpreted to result from thinning of the lithosphere resulting from either slab delamination (Sacks and Secor, 1990; Davies and von Blanckenburg, 1995) marking a shift in subduction polarity (Teng *et al.*, 2000), or subsequent backarc extension above a younger, west-dipping subduction zone.

Structural Geology. The dominant foliation in the rocks exposed in Smedley Park and along much of Crum Creek typically dips very steeply and strikes approximately north-south. In most places the foliation is concordant with compositional layering in the Wissahickon Formation. This foliation is the regional S2/S3 composite foliation. Figure 58 shows a microfiche image of sample B22; the uppermost garnet is the garnet shown in figure 56A, above. The inclusion trails in garnet are essentially parallel to the external foliation, but wrap around the small, euhedral, relatively inclusion-free garnet cores present in the uppermost garnet (figure 56) and in the rotated garnet in

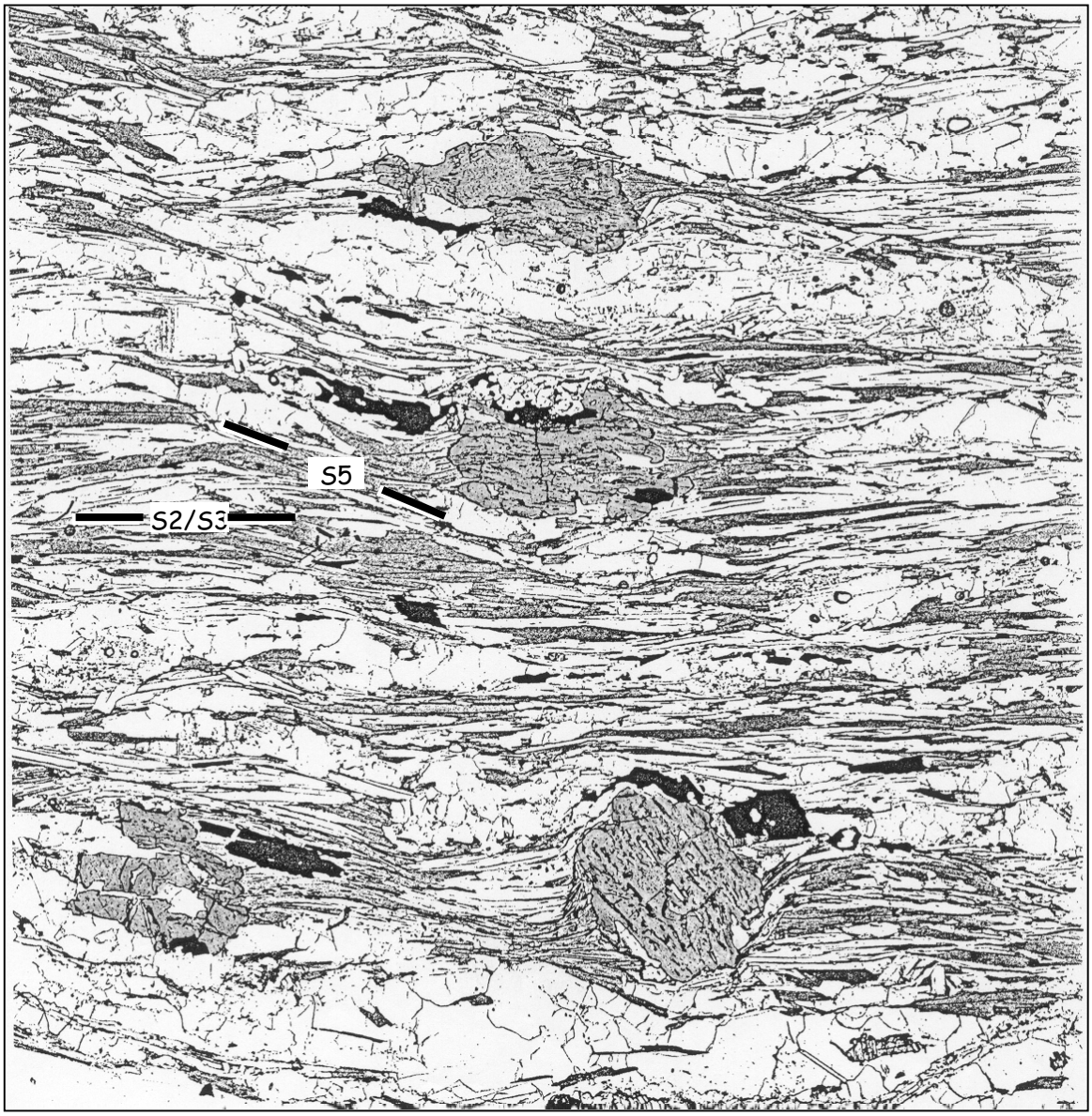

Figure 58. Microfiche image of sample B22, Crum Creek. Note that inclusion trails in garnet are parallel to the external foliation. Small, relatively inclusion free M_2 cores are present in the uppermost garnet and in the rotated garnet in the lower right (see figure 56A). The plane of the thin section does not appear to penetrate the core of the central garnet. See text for details.

the lower right. The sequence of metamorphism and deformation that can be deduced is (1) growth of garnet cores during M2, (2) deformation to produce the dominant E-W (in page view) foliation, (3) growth of garnet during M3 followed by (4) additional deformation, resulting in NW-SE foliation (again, in page view) and garnet rotation. The lack of curvature of the included fabric in the rotated garnet demonstrates that rotation is post-garnet growth. The relative timing of deformation that produced the dominant foliation, post-M2, but pre-M3, is the same as that for F3 folding described at Stop 8. Thus, this foliation is interpreted as the S2/S3 composite. Transposed isoclinal folds which occur in a few places along the Crum Creek transect (figure 47D, above), but which are relatively uncommon in Smedley Park are thought to be the same generation as F3 folds described above. The high-U rims on monazite in this sample are elongate parallel to the S2/S3 foliation (figure 57). Thus, deformation that produced this foliation can be no younger than the 416 Ma age of these rims; *i.e.*, the monazite is either syn- or post-tectonic with regard to this foliation.

The S3 foliation and F3 folds are in turn folded by younger deformation, which is seen throughout Smedley Park as open folds and a pervasive crenulation. This deformation is demonstrably younger than M3, kyanite grade metamorphism, which is synchronous with deformation in shear zones (S4) described at Stops 6 and 7. Thus this episode of folding is termed F5. F5 folds are open to close, parallel (class 1B to 1C, Ramsay, 1967), noncylindrical folds with round hinges, and are associated with a variably developed axial planar foliation and crenulation cleavage. F_5 folds generally have shallow to moderately dipping axial planes, S_5 (figure 59) and occur at all scales of observation from mm-scale crenulations, minor folds at the centimeter (figure 60) to decimeter scale, outcrop scale folds with wavelengths up to several meters, through map scale warps of older structures. D_5 folded older micas against the grossular enriched rims of M3 garnet (figure 60); indicating this deformation is younger than the intermediate pressure M_3 metamorphism. In places recrystallized muscovite and biotite are oriented parallel to S_5, indicating that the metamorphic conditions during D_5 were no lower than greenschist facies.

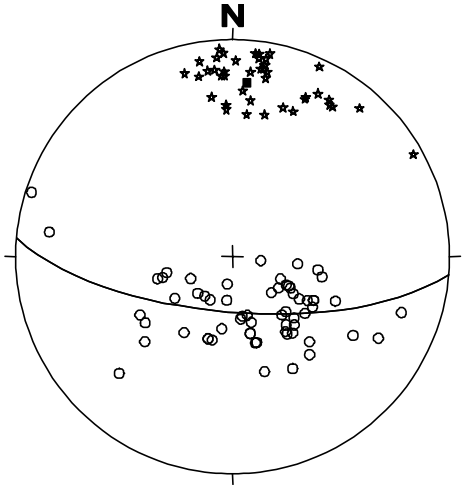

Figure 59. π–diagram of poles to S_5, Crum Creek transect. Open circles, poles to F5 axial planes, S_5, (n = 62); stars, F_5 fold axes (n = 41); solid square, F_5 π-pole; great circle, best-fit girdle. Plot includes data of Busé *et al*., 1997.

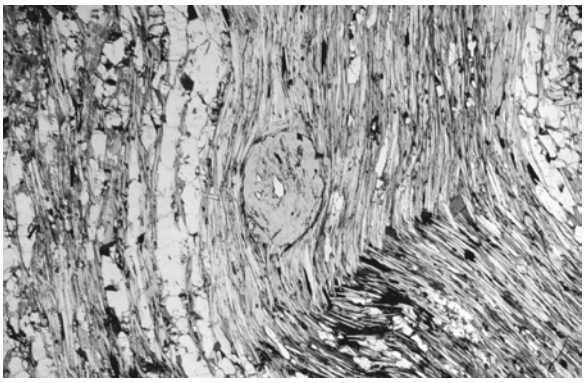

Figure 60. Photomicrograph of sample from Smedley Park. F_5 folding caused mica grains to "wrap" M3 garnet, demonstrating that D_5 is younger than M_3.

Folds with shallowly dipping axial surfaces could develop in either a compressive stress regime, as a result of thrust related shearing, or in an extensional environment resulting from orogen scale gravitational instability (Bell and Johnson, 1989), where the principle compressive stress ($\sigma 1$) is sub-vertical. A third model was proposed by Means (1999), who suggested that sub-horizontal foliations could form where $\sigma 1$ is sub-horizontal if the product of $\sigma 1$ and the horizontal rate of shortening is less than the product of $\sigma 3$ and the vertical rate of shortening. Presently available data are insufficient to distinguish between the Bell and Johnson (1989) and Means (1999) models. There is no evidence in the field area that F5 folds are thrust related; such folds would likely be associated with well-developed shear fabrics and show consistent asymmetry. Valentino and Gates (1997) described late stage box folds and associated shallowly dipping conjugate cleavage in the region and suggested that these formed during late Alleghanian gravitational collapse.

Return to buses. Depart parking lot. Cross railroad tracks and continue to end of Papermill Road.

0.2	26.3	Intersection of Papermill Road with US 1 (Baltimore Pike; stop sign). Traffic on US 1 is controlled by light and will clear. Turn RIGHT onto US 1 South (Baltimore Pike). Stay to the right.
0.2	26.5	Bear RIGHT onto the ramp to enter I-476 North.
1.0	27.5	Outcrops of Smedley Park amphibolite on right side of I-476 North.
0.4	27.9	EXIT from I-476 North (right side) at Exit 5, Lima-Springfield. Stay to left on exit ramp. At end of ramp (first traffic light) go straight.
0.4	28.3	Second traffic light, turn LEFT onto US 1 South (Media bypass) toward Lima. After left turn, continue through one more traffic light and then Merge onto US 1 South (Media bypass).
0.5	28.8	Outcrop of Wissahickon at bridge on right side of US 1 South.
3.1	31.9	Merge onto US 1 South (Baltimore Pike), which comes in from the left. Immediately move out of far right lane; do NOT exit onto Rt. 352.
0.4	32.3	Granite Run Mall is on the right side of US 1 South. This was formerly a quarry in the Lima Granite, which intruded ultramafic units. Outcrops of the ultramafic rocks can be seen in the sides of the parking lot.
6.3	38.6	Intersection of US 1 South (Baltimore Pike) with US 202 (traffic light). Turn RIGHT onto US 202 North.
4.6	43.2	Holiday Inn on right side of US 202 North. Turn RIGHT from US 202 North onto Stanton Avenue. Turn LEFT into parking lot for Holiday Inn. END OF DAY 2.

HAVE A SAFE TRIP HOME. SEE YOU NEXT YEAR AT THE OTHER END OF THE STATE.

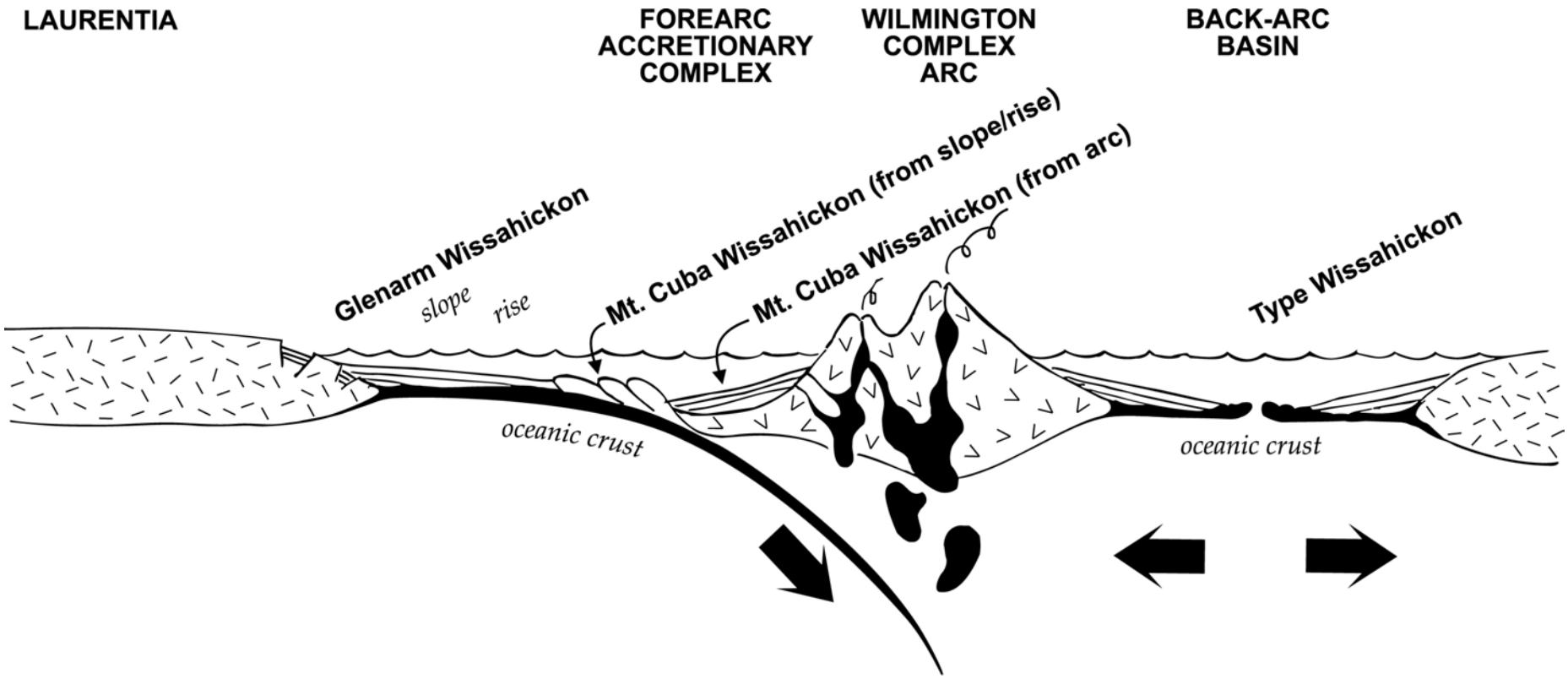

Conceptual cross-section (not to scale) showing depositional and tectonic environments of the Type Wissahickon, Glenarm Wissahickon, and Mt. Cuba Wissahickon sometime during the Ordovician.